Faculty of Science & Engineering

Department of Imaging and Applied Physics

Characterization and Development of Flax Fibre Reinforced Geopolymer Nanocomposites

Hasan Suliman Assaedi

This thesis is presented for the degree of

Doctor of Philosophy

of

Curtin University

April 2017

DECLARATION

To the best of my knowledge, this project does not contain materials previously published by other persons except where due acknowledgement has been done. This thesis contains no material which has been accepted for the award of any other degree or diploma in any university.

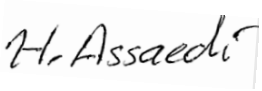

14-April-2017

Abstract

Geopolymer cement is a green alternative to the cement technologies currently employed in the construction sector. The weaknesses of geopolymer matrices to date have largely been consequences of the poor mechanical properties and brittle nature of such matrices. A key to increasing the application of geopolymer concrete is to improve its toughness and flexural strength. At least two approaches exist to improve such mechanical properties. One way is to reinforce the geopolymer with fibres to create a fibre-reinforced composite. Another way is to improve the microstructural and physical matrix properties by incorporating nanoparticles into the paste of geopolymer.

To date, the most frequently employed reinforcements of geopolymers have been glass, carbon and other fibres of synthetic nature. Inherent problems with synthetic fibres include the economic and environmental costs of the materials. The latter is particularly salient in a time where climate change receives increasing attention internationally. In light of the issues with synthetic fibres and their composites, there has been a renewed interest in the use of natural fibre-reinforcement. Natural fibre composites are lower cost and have lower density. Natural fibres also add a feature of being recyclable, thus promoting renewability while still maintaining strong mechanical properties. Natural fibres are also non-toxic to humans and the environment. For these reasons, and others, natural fibre has become an increasingly common reinforcing filler used in the construction, building and automotive manufacturing sectors. However, to date, the interfacial bond between the geopolymer matrix and the natural fibre is still moderately weak. In addition, the degradation of natural fibres in the high alkaline matrices of geopolymer can adversely affect the durability and the mechanical performance of geopolymer composites.

The current project attempts a more novel approach to provide solutions to the recognised issues associated with natural fibre geopolymer composites. The solutions involved using a combination of nanoparticles and flax fibres. Observations made using the combination revealed improvements in the mechanical, thermal and

physical properties. There were also recorded improvements in the microstructure and an increase in durability of the natural fibre composites. The project used class F fly-ash geopolymer as the matrix for three types of composite materials. Firstly, eco-composites were created by reinforcing geopolymer with flax fabrics. Secondly, nanocomposites were produced by reinforcing geopolymer with nanoclay and nanosilica. Thirdly, eco-nanocomposites were created by reinforcing geopolymer with both flax fabrics and nanoparticles.

The microstructures of nanocomposites and flax fibre reinforced geopolymer nanocomposites were investigated using scanning electron microscopy (SEM), Fourier transform infrared spectroscopy (FTIR), quantitative X-ray diffraction analysis (QXDA) with Rietveld refinement by MAUD software, X-ray diffraction, energy dispersive spectroscopy (EDS), quantitative energy dispersive spectroscopy (QEDS), thermogravimetric analysis (TGA) and differential thermogravimetry (DTG).

The beginning part of the investigation started with determining the mechanical properties and thermal behaviour of flax fabric reinforced geopolymer composites. Geopolymer matrices were reinforced with 2.4, 3.0 and 4.1 wt.% of flax fabric in a number of layers and tested for their mechanical properties, namely, flexural strength, modulus, hardness, compressive strength and fracture toughness. Results of each mechanical property showed improvement as the flax fibre content was increased, thus suggesting superior mechanical properties when compared to the pure geopolymer matrix. At elevated temperature, the thermal behaviour of the composites exhibited a significant degradation in the flax fibres at 300 °C.

Then the effect of nanoclay addition on the mechanical, microstructural and thermal properties of fly ash-geopolymer was investigated. The nanoclay particles were added to support the geopolymer paste at loadings of 1.0%, 2.0%, and 3.0% by weight, and then all samples were tested after 4 weeks. Results showed that the mechanical properties of geopolymer nanocomposites improved with the addition of nanoclay. It was observed that the loading of 2.0 wt.% nanoclay decreased the porosity but increased the resistance of geopolymer samples to water absorption considerably. The optimum 2.0 wt.% nanoclay exhibited higher flexural and

compressive strengths together with increased flexural modulus and hardness. Outcomes of microstructural analysis suggested that nanoclay acted as a nano-filler to enhance the microstructure. Besides, nanoclay worked as an activator to facilitate the geopolymer reaction. In addition, TGA tests showed that geopolymer nanocomposites exhibited an improvement in thermal stability when compared to the pure geopolymer.

The effect of nanosilica (NS) particles on physical and mechanical characterisation of geopolymer pastes was also investigated. Different loadings of nanosilica at 0.5, 1.0, 2.0, and 3.0 wt.% were studied. The nanoparticles were mixed with geopolymer in two methods; dry and wet-mixing method. Comparison was made between mechanical dry-mixing of nanosilica with fly-ash powders, and wet-mixing of nanosilica in alkaline solutions. Each sample had been stored at ambient temperature for 4 weeks prior to testing. The method of mixing was found to control the way the nanoparticle disperse, and thus to change the mechanical and physical properties of the resulted nanocomposites in both cases. The Si:Al ratios were found to increase with additional nanosilica particles in each sample; however, the ratios differed depending on the mixing approach. The whole amount of silica was observed to be completely dissolved in the process of wet mixing, giving a high Si:Al ratio. While in the case of dry-mixing process, portions of nanosilica particles did not fully dissolve, but played a void-filler role in the geopolymer paste. Results of the study indicated that the addition of nanosilica particles using both preparation methods improved the microstructure and increased the flexural and compressive strengths of geopolymer nanocomposites. However, samples prepared by the dry-mix method showed better properties when compared to wet-mixed geopolymer samples.

The geopolymer matrices were subsequently reinforced using a combination of flax fabrics (FF) and nanoclay particles. The nanoclay particles were added to geopolymer matrices at loadings of 1.0%, 2.0%, and 3.0% by weight. The FF-reinforced geopolymer nanocomposites were synthesised and their physical and mechanical properties were tested after 4 weeks. The loading of 2.0 wt.% nanoclay was shown to exhibit enhanced density, reduced porosity and improved flexural strength and toughness. The microstructural investigation indicated that nanoclay

acted as an activator to facilitate the process of geopolymerization to produce higher amounts of geopolymer gel. This action helped to enhance the adhesion between geopolymer matrix and flax fibres, thus improving the mechanical behaviour of geopolymer nanocomposites reinforced with flax fabrics.

The effect of nanosilica on properties of flax fabric reinforced geopolymer composites were also studied. Geopolymer pastes were loaded with nanosilica at loadings of 0.5, 1.0, 2.0 and 3.0 wt.%. Ten layers of flax fabric were utilized and the total amount of flax fibres in each specimen was about 4.1 wt.%. When compared to the flax fabric reinforced geopolymer composite, the incorporation of 1.0 wt.% dry-mixed nanosilica resulted in reduced the porosity and water absorption, but the density and flexural toughness of the samples were increased.

Finally, the effects of nanoclay and nanosilica on the durability of geopolymer nanocomposites and flax fabric reinforced geopolymer nanocomposites were investigated. The durability tests were conducted after the samples were stored at ambient temperature for 32 weeks. The influence of nanoparticles on the durability of the composites was studied in terms of their flexural strength and toughness, stress-midspan deflection and microstructurial examination. In the case of geopolymer nanocomposites, further improvement was observed in the mechanical properties of the pure geopolymer and geopolymer nanocomposites. The reason for the observed improvements is attributed to a slow reaction between free silica and alumina in an environment with sodium ions during aging. In contrast, all FF-geopolymer nanocomposites exhibited a reduction in their flexural properties after the ageing period of 32 weeks. The results showed that flax fibres in all composites suffered from damage and degradation. However, nanoclay and nanosilica had effectively mitigated the rate of degradation in the flax fibre. The degradation resistance and durability of the flax fibre showed enhanced performance as a result of nanoparticle dispersion within the geopolymer matrices. The optimum loadings of nanoclay and nanosilica particles were 2.0 wt.% and 1.0 wt.%, respectively. Results of SEM examination suggested that flax fibres within the geopolymer composites experienced a higher rate of degradation than flax fabric-reinforced geopolymer nanocomposites. In brief, the addition of nanoclay and nanosilica has a great

potential to improve the durability of flax fabric reinforced geopolymer nanocomposites.

Acknowledgements

I would like to express my sincere gratitude to my principal supervisor, Professor Jim Low of the Department of Physics and Astronomy at Curtin University, for his constant support, professional guidance, kindness and invaluable help in all aspects of the project. His patience and availability to answer my queries and explain problems any time has been extremely helpful during the period of the research. His comments, constructive criticisms, suggestions and encouragement have been of great value to me, and the work was only possible through such contribution. I also want to express my appreciation to Dr Faiz Shaikh of the Department of Civil Engineering at Curtin University, for his kind support and his valuable suggestions and comments during my research.

I am also grateful to Dr Brendan McGann, Post-graduate Coordinator of the Department of Applied Physics, who provided me with essential information for carrying out the research.

My sincere gratitude is expressed to Ms Elaine Miller of John de Laeter Centre, Curtin University for her kind assistance with SEM imaging. I would like to acknowledge Ms Veronica Avery and Ms Kelly Merigot of John de Laeter Centre, Curtin University, and Mr. Andrew Chan from the Departments of Chemical Engineering, Curtin University for their laboratory assistance.

I wish to express my deep thanks to all my colleagues, in particular, Faisal Assaq, Thamer Alomayri, Les Vickers, Jeong Hun Ha, Xinh Le, Ahmed Hakamy, and Hani Albetran, for their friendship and emotional support.

I am entirely indebted to my family and in particular my parents, my mother Nora Assaedi and my late father Suliman Assaedi. Words are not enough to express my gratitude and appreciation, without their encouragement, guidance and sacrifices; I have been fortunate to have some measures of success in my life. Finally, very special and sincere gratitude is offered to my wife Eman Alhujuri for her constant patience, understanding and encouragement throughout my research.

List of Publications Included as Part of the Thesis

ASSAEDI, H., ALOMAYRI, T., SHAIKH, F. U. A. & LOW, I.-M. 2015. Characterisation of mechanical and thermal properties in flax fabric reinforced geopolymer composites. *Journal of Advanced Ceramics,* 4, 272-281.

ASSAEDI, H., SHAIKH, F. U. A. & LOW, I. M. 2015. Effect of nano-clay on mechanical and thermal properties of geopolymer. *Journal of Asian Ceramic Societies*, 4, 19-28.

ASSAEDI, H., SHAIKH, F. U. A. & LOW, I. M. 2016. Characterizations of flax fabric reinforced nanoclay-geopolymer composites. *Composites Part B: Engineering*, 95, 412-422.

ASSAEDI, H., SHAIKH, F. U. A. & LOW, I. M. 2016. Influence of mixing methods of nano silica on the microstructural and mechanical properties of flax fabric reinforced geopolymer composites. *Construction and Building Materials*, 123, 541-552.

ASSAEDI, H., SHAIKH, F. U. A. & LOW, I. M. 2017. Effect of nanoclay on durability and mechanical properties of flax fabric reinforced geopolymer composites. *Journal of Asian Ceramic Societies*, *5(1)*, pp.62-70.

Statement of Contribution of Others

Hasan Assaedi's input into this study and the associated papers include the execution of all the experimental work as well as a dominant contribution to the intellectual input involved in the project. As is almost always the case in the physical sciences, other scientists made contributions to the work that were significant enough to warrant co-authorship on the resulting journal articles. These are specified below

Prof. I.M. Low, provided project supervision and manuscript editing.

Dr. F.U.A. Shaikh, provided project supervision and manuscript editing.

Dr. T. Al-Omayri provided technical assistance during the preparation and testing of geopolymer composite samples.

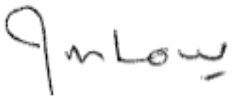

Hasan Assaedi Prof. It-Meng (Jim) Low

List of Papers and Presentations by the Candidate Relevant to the Thesis

---

Journal Papers:

ALOMAYRI, T., **ASSAEDI, H.**, SHAIKH, F. U. A. and LOW, I. M. 2014. Effect of water absorption on the mechanical properties of cotton fabric-reinforced geopolymer composites. *Journal of Asian Ceramic Societies,* 2, 223-230.

Conference Papers and Oral Presentations

ASSAEDI, H., ALOMAYRI, T., SHAIKH, F.U.A. and LOW, I.M. 2014. Synthesis and mechanical properties of flax fabric reinforced geopolymer composites, *3rd Biennial Conference of the Combined Australian Materials Societies (CAMS14),* Sydney, Australia, 26-28 November 2014.

ASSAEDI, H., SHAIKH, F.U.A. and LOW, I.M. 2015. Utilization of nanoclay to reinforce flax fabric-geopolymer composites. *17th International Conference on Materials Engineering and Technology (ICMET),* Melbourne, Australia, 13th Dec 2015, 6 pages.

ASSAEDI, H., SHAIKH, F.U.A. and LOW, I.M. 2015. Characteristics of nanosilica-geopolymer nanocomposites and mixing effect. *17th International Conference on Materials Engineering and Technology (ICMET),* Melbourne, Australia, 13th Dec 2015, 6 pages.

Book-Chapters:

ASSAEDI, H., ALOMAYRI, T. and LOW, I.M. 2017. Advances in geopolymer composites with natural reinforcement, Chapter 19 in *Advances in Ceramic matrix Composites - Second Edition*, (Ed. I.M. Low). Elsevier, *In Press*.

Table of Contents

List of Figures

List of Tables

List of Abbreviations

ASTM	American Society for Testing and Materials
EDS	Energy Dispersive X-ray Spectroscopy
FF	Flax fibres
FTIR	Fourier Transform Infrared Spectroscopy
GC	Geopolymer Composites
MPa	Mega Pascals
NC	Nanoclay
NS	Nanosilica
OPC	Ordinary Portland Cement
QEDS	Quantitative Energy Dispersive X-ray Spectrometer
QXDA	Quantitative X-ray Diffraction Analysis
SEM	Scanning Electron Microscopy
TGA	Thermogravimetric Analysis
DTG	Differential Thermogravimetry
wt. %	Weight precent
XRD	X-ray Diffraction
XRF	X-ray Fluorescence Spectroscopy

1 INTRODUCTION

1.1 Background

Inorganic aluminosilicate Portland cements remain a popular choice in construction due to their superior mechanical properties and comparative low costs. However, the high amounts of greenhouse emissions from cement-based materials and cement production have become an increasing concern. Due to a demand for more eco-friendly solutions, alternative materials have become an important topic. One promising green material is geopolymer, which is another form of aluminosilicate inorganic material. Geopolymers may be synthesized by activating a solid aluminosilicate source using alkaline solutions. At present, they are gaining extensive attention due to their potential as high performance and eco-friendly alternative for ordinary Portland cements in many applications (McLellan *et al.*, 2011, Pacheco-Torgal *et al.*, 2012) . Geopolymers have good mechanical properties, durability, flame and acid resistance. Additionally, the curing and hardening cycles may take place at room temperatures. The material can be prepared with 80-90% less carbon dioxide emission when compared to Portland cement (Barbosa *et al.*, 2000, Li *et al.*, 2004, Duxson *et al.*, 2007a, Pernica *et al.*, 2010).

However, geopolymers tend to become brittle and fail when stressed as in most ceramics. A typical value of compressive strength for geopolymers is approximately 45 MPa (Kriven *et al.*, 2003), which is as good as the strength of ordinary Portland cements. However, geopolymers have a much lower flexural strength when compared to ordinary Portland cement pastes (Kriven *et al.*, 2003, Duxson *et al.*, 2007b, Lin *et al.*, 2008). Improving the fracture properties would significantly increase the applications for geopolymers. Dispersing inorganic or organic fibres within these matrices could improve the flexural properties of geopolymers. Inorganic fibres such as carbon, basalt or glass fibres have been used as a reinforcement of geopolymers (Hung *et al.*, 2008, Yunsheng *et al.*, 2008, Rill *et al.*, 2010, Silva and Thaumaturgo, 2003, Zhao *et al.*, 2007). However the processes required to source such fibres are typically environmental unfriendly and expensive.

Natural fibre reinforced composites are again attracting interest as a solution for the above-mentioned problems (Zeng *et al.*, 2005).

Natural fibres that can be used for reinforcement include bamboo, cotton, coir, flax, hemp, jute, kenaf, pineapple, straw, and switch grass (Dweib *et al.*, 2004, Tanobe *et al.*, 2005, Pickering, 2008, Wambua *et al.*, 2003). Natural fibres are believed to be increasingly used due to their low density, low cost, renewable, recyclable, and acceptable mechanical properties such as flexibility, strength and modulus (Low *et al.*, 1995, Low *et al.*, 2007b). New environmental regulations to support global sustainability, environmental awareness and concerns of society have presented a motivation for the development of more environmental friendly materials. Natural fibres are non-toxic and can assist in a healthier and safer world because they are safe during handling (Satyanarayana *et al.*, 1990, Bessadok *et al.*, 2007).

However, natural fibres in alkali-based matrices still have obstacles to overcome. Long-term durability of composites containing natural fibres is still an issue. Natural fibres are degraded and damaged when they are in contact with high-alkaline matrices. Consequently, the mechanical performance and durability of these composites are adversely affected (Hakamy *et al.*, 2016, Aly *et al.*, 2011b, Yan and Chouw, 2015). Gram investigated this problem and indicated that the mechanism of degradation can be attributed to the decomposition of hemicellulose and linen which leads to splitting of natural fibres to form micro-fibrils (Gram, 1983). Observations under SEM showed that jute fibres extracted from cement matrices were heavily split-up and degraded, thus causing the tensile strength of the composites to be reduced by 76% (Velpari *et al.*, 1980).

Nanoparticles may offer the solution to the issue of fibre degradation. Effect of nanoclay particles on the durability of flax fibre reinforced composites was studied on 28 days and after 50 wet/dry cycles by Aly and co-workers (Aly *et al.*, 2011b). The samples were loaded with 2.5 wt.% of nanoclay particles and they displayed a lower deterioration rate in flexural strength when compared to control samples. Hakamy and coworkers also discovered that the additions of nanoclay and calcined nanoclay helped to improve the physical and mechanical properties in cement

matrices while improving the durability in composites reinforced with hemp fabric in wet-dry cycles (Hakamy *et al.*, 2013a, Hakamy *et al.*, 2015b).

Nanotechnology has become popular in geopolymer and cement research, particularly in the production of nanocomposites with superior mechanical properties (Shaikh and Supit, 2014, Qing *et al.*, 2007, Nazari and Sanjayan, 2015). A number of nanomaterials have become part of geopolymer studies. For example, it has been found that silica and alumina nanoparticles are able to reduce the porosity and water absorption for geopolymer materials (Nazari and Sanjayan, 2015). In another study (Phoo-ngernkham *et al.*, 2014), nano-alumina and nano-silica particles have been incorporated in geopolymer pastes giving them superior mechanical performance. The nanoparticles are not only acting as fillers, but also enhancing the geopolymeric reaction. Additional report on the effect of carbon nanotubes (CNT) in fly-ash-based geopolymer has shown an improvement in the mechanical and electrical properties of geopolymer nanocomposites when compared to pure geopolymer (Saafi *et al.*, 2013). Wei *et al.* reported the properties of cement/nanoclay composites, where the nanoparticles helped to reduce the porosity of cement matrices, as well as to improve the strength of cement paste during the pozzolanic effects (Wei and Meyer, 2014). Farzadnia *et al.* (Farzadnia *et al.*, 2013) reported that the addition of 3.0 wt.% halloysite nanoclay to cement matrices improved the compressive strength by up to 24%, when compared to control samples. Supit and Shaikh (2014b) reported that addition of 1.0 wt.% nano-$CaCO_3$ helped to improve the compressive strength in mortar and concrete.

The incorporation of nanoclay and nanosilica in flax fibre reinforced geopolymer composites is expected to reduce the alkalinity of geopolymer matrices as sodium hydroxide is consumed during the activated geopolymeric reaction. As a result, the durability of flax fibres in the composite can be improved. In addition, the microstructure of the geopolymeric material can be enhanced due to the void-filling effect of nanoparticles. Besides, the geopolymer adhesive bond between the flax fibres and the geopolymer matrix is expected to be improved due to the resultant geopolymer gel. Consequently, a geopolymeric composite with superior mechanical

performance can be expected after the incorporation of both flax fibres and nanoparticles.

In this project, a novel technique for producing flax fabric-reinforced geopolymer nanocomposites has been proposed and investigated. Geopolymer matrices were modified using nanoparticles with the aim of improving the durability and degradation resistance of flax fibres in flax fabric reinforced geopolymer composites. Nanoparticles were used as an additive to geopolymer pastes at varying ratios. Flax fibres were also utilized to reinforce the geopolymer nano-matrices. The aim of the current study was to evaluate the effect of different loadings of nanoclay and nanosilica on physical and mechanical properties of geopolymer matrices and flax fabric reinforced geopolymer composites. The durability of flax fabric reinforced geopolymer composites and nanocomposites has been discussed in terms of flexural performance obtained at 4 and 32 weeks. The microstructures of nanocomposites and flax fabric geopolymer nanocomposites were also investigated using scanning electron microscopy (SEM), X-ray diffraction, quantitative, X-ray diffraction analysis (QXDA) with Rietveld refinement, Fourier transform infrared spectroscopy (FTIR), energy dispersive spectroscopy (EDS), quantitative energy dispersive X-ray spectrometer (QEDS), thermogravimetric analysis (TGA) and differential thermogravimetry (DTG).

1.2 Project Significance

There has been limited or no research on using both natural fibres and nanoparticles as hybrid reinforcement in geopolymer composites. In the current project, nanoclay and nanosilica were incorporated into geopolymer matrices as fillers at varying loadings to form nanocomposites, and flax fabrics as reinforcement to fabricate geopolymer nanocomposites. Flax fibre geopolymer composites are considered a sustainable alternative to their synthetic fibre counterparts because they are greener, biodegradable, and lower in cost. However, the interfacial bonding between flax fibres and geopolymer matrices is relatively weak. Moreover, the alkalinity of geopolymers could adversely affect the durability of flax fibres embedded within the composites. This could consequently influence the mechanical performance of the

composites. The incorporation of nanoclay and nanosilica in flax fibre-reinforced geopolymer composites is expected to activate the geopolymerization reaction and reduce the alkalinity of geopolymer matrices, which can help to improve the durability of flax fibres in the composite and the physical properties of geopolymer matrices such as density and porosity through denser -packing and voids-filling.

It is highly expected that the outcomes of the current study will provide useful data includes microstructural, physical and mechanical properties of geopolymer composites for material researchers and industry-users relevant to geopolymer technology. It is also expected that the conclusions obtained will aid the development, and use of environmentally friendly composites.

1.3 Project Objectives

The main aim of the current research was to design novel geopolymer nanocomposites that are reinforced with nanoparticles and flax fibres, as well as to achieve optimum physical and mechanical properties. The specific objectives of the project were as follows:

- To study the effect of flax fabric reinforcement on the mechanical and thermal properties of geopolymer composites.
- To develop a better understanding of the relationships between the microstructural and mechanical properties of flax fabric reinforced geopolymer composites.
- To evaluate the effect of nanoclay and nanosilica on the physical and mechanical properties of geopolymer matrices.
- To determine the optimum content of nanoclay and nanosilica in geopolymer matrices and in flax fabric reinforced geopolymer composites.

- To investigate the influence of mixing method of nanosilica on the microstructural, physical and mechanical properties of geopolymer matrices.

- To investigate the effect of nanoclay and nanosilica on the microstructure of geopolymer matrices, and interfaces between the flax fabric and geopolymer matrix.

- To elucidate the fundamental mechanisms of superior microstructural, physical and mechanical properties achieved for flax fibre-reinforced geopolymer nanocomposites.

- To evaluate the influence of nanoclay and nanosilica on the short- to medium-term durability of flax fabric-reinforced geopolymer composites.

1.4 Research Plan

In order to address the objectives of the research project, the following investigation tasks were conducted:

- Fabrication of geopolymer composites by reinforcing geopolymer with multiple layers of flax fabrics.

- Fabrication of nanoclay-geopolymer nanocomposites and nanosilica-geopolymer nanocomposites using different preparation approaches.

- Fabrication of flax fabric reinforced nanoclay-geopolymer composites and flax fabric reinforced nanosilica-geopolymer composites.

- Investigation of the influence of flax fabric and nanoparticles on physical and mechanical properties of geopolymer composites.

- Examinations of fracture surfaces and failure mechanisms in flax fabric reinforced geopolymer composites and nanocomposites using scanning electron microscopy (SEM).

- Investigation of the influence of different mixing procedures of nanosilica particles on the physical and mechanical properties of the resultant geopolymer nanocomposites, and FF-reinforced geopolymer composites.

- Characterization of geopolymer composites and nanoparticles dispersion, morphology and microstructure by scanning electron microscopy (SEM), X-ray diffraction (QRD), quantitative X-ray diffraction analysis (QXDA), quantitative energy dispersive X-ray spectrometer (QEDS), Fourier transform infrared spectroscopy (FTIR), thermogravimetric analysis (TGA) and differential thermogravimetric (DTG).

- Investigation of the effect of high alkalinity environment of geopolymer on the mechanical properties, durability, fibre-matrix interfaces and fibre degradation of geopolymer composites and nanocomposites.

2 LITERATURE REVIEW

2.1 Natural Fibres

2.1.1 Overview

Fibres are referred to as a material that is made of continuous filaments or elongated pieces, which resemble lengths of thread. Fibre may be spun to create filaments, string and rope. Fibres may be found in two types, natural and synthetic. Natural fibres are classified according to their source (Zhu *et al.*, 2013, Bavan and Kumar, 2010):

- Plant or vegetable fibres may be obtained from vegetables and plants. Different parts of plant may be used to make fibres including fruit, leaves, seeds and stems. Plant fibres may be created from seeds as observed in cotton and kapok. Fibre-sheaves in dicotyledonous plants and vessel sheaves in monocotyledon plants such as flax, ramie, jute and hemp along with hard fibres like sisal, coir and henequen can be used to create fibres. Plant fibres can also be grouped as wood (soft and hard wood) and non-wood fibres.
- Animal (protein) fibres refer to materials derived from animals. Animal fibres may be classified by hairs such as wool, fur as in angora and secretions such as silk.
- Mineral fibres refer to a more hazardous form of fibres such as asbestos and basalt.

A classification of most commonly employed fibres is given in Figure 1. Natural fibres include a wide range of animal, plant and mineral fibres. Within the composites community, natural fibres refer to wood and agro-based bast, seed, stem and leaf fibres. The fibres are found to contribute in the structural performance of each composite. When natural fibres are used to reinforce ceramic and cementitious materials, performance is significantly improved (Clemons and Caufield, 2005).

Plant fibres, are classified according to the part of the plant (Azwa *et al.*, 2013, Bismarck *et al.*, 2005):

- Bast fibres (bundles) are obtained from the inner bark of phloem or bast stems of dicotyledonous plants. Examples are flax, hemp, jute, ramie and kenaf.
- Leaf fibres which run lengthwise in leaves of monocotyledonous plants found in abaca, sisal and banana. Leaf fibres are also denoted as hard fibres used in reinforcing agents to make plastics.
- Seed and fruit hairs are fibres from seed-hairs and flosses found in plants like cotton, coir and kapok.
- Wood fibres are derived from the xylem of angiosperm for hard wood and gymnosperm for soft wood. Examples of wood fibres may come from yellow poplar, maple, pine or spruce trees.
- Grass and reeds: Cellulose fibres are retrieved from the stems of monocotyledonous plants. For example, bamboo and sugar cane are used to create cellulose fibres for reinforcing plastics.

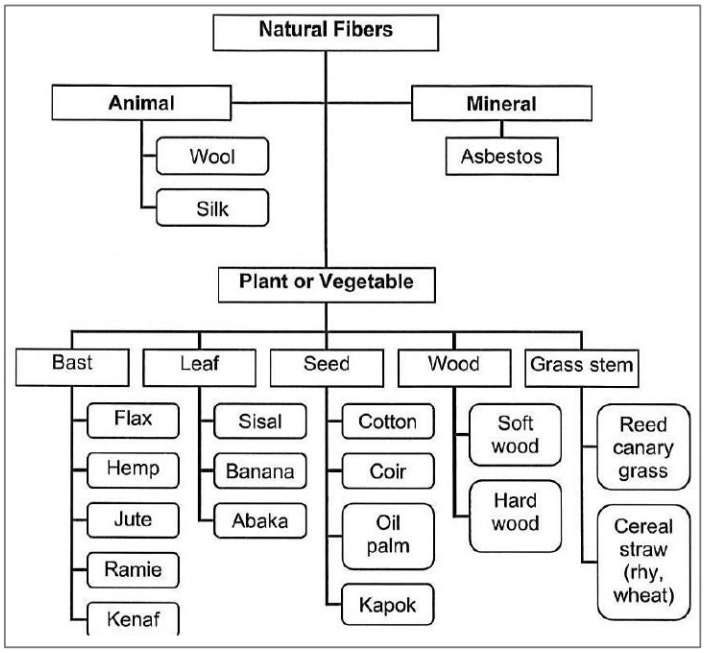

Figure 1: Classification of natural fibres based on their origin *(Zhu et al., 2013).*

Natural fibre composites were used for many years; however, interests in them waned on the advent of materials created with synthetic fibres such as glass and carbon. Nevertheless, there has been a re-emergence of interest in natural fibres. Currently, academics research have increased interest in composites reinforced using natural fibres (Pickering *et al.*, 2016, Mohanty *et al.*, 2002). A number of natural fibres are available to be used as reinforcement materials. Natural fibres have long cells with thick walls that add stiffness and strength. Three types of polymer cells build the plant fibres, cellulose, lignin and matrix polysaccharides (found in pectin and hemicelluloses). Pectin and hemicelluloses are connected to cellulose and lignin found in the cell walls of plant fibres. Cellulose in fibres plays a positive role in the improvement of their strength and durability (Alix *et al.*, 2008, Fowler *et al.*, 2006).

The most common plant fibres used in fabricating composite materials are fibres taken from flax, jute, hemp, kenaf or sisal due to their properties and availability. Their similar morphology properties imply similar functions when they are used in composite materials (Pickering *et al.*, 2016, Mohanty *et al.*, 2002, Holbery and Houston, 2006, Ashori, 2008).

2.1.2 Advantages and Limitations of Plant Fibres

There are four listed reasons why the application of natural fibres is an attractive alternative to synthetic fibres (Ashori, 2008, John and Thomas, 2008, Pimenta and Pinho, 2011, Williams and Wool, 2000).

- High specific properties: The cellulose found in natural fibres has lower density. Besides they are relatively stiff and strong. Their specific properties are comparable to fibres from glass.
- Health advantages: The use of natural fibres diminishes possible health problems faced by workers during processing the composites. Natural fibres are not causing some of the concerns that lead to the development of major health concerns such as skin irritations and lung cancer. The concern of a possible link between glass fibres and lung cancer has justified the use of alternative natural products.
- Recyclability: In light of the current “green” movements around the world,

natural fibre composites have found popularity due to their ability to be recyclable. However, there has been much confusion regarding the recyclable issue. In the process of mechanical recycling, natural fibres are unable to demonstrate a clear advantage when compared to the use of glass fibres. Flax fibres face a possible thermal degradation during the processing steps. However, one definite advantage found in flax fibre composites compared to glass fibre composites is that they could be burned via thermal recycling. During the thermal recycling process, flax fibres do not leave large amounts of slag. Nonetheless, natural fibres have developed the image as being a "green" product.

- Price: Natural fibres used for reinforced composites aim to replace synthetic fibre composites. Depending upon the required property of the fibre for a specific material, natural fibres are typically cheaper than glass fibres.

Although natural fibres have advantages, there are two negative characteristics. First, they are highly hydrophilic in nature, which influence their durability when used as reinforcement. Second, their properties are highly variable which make the prediction of resultant composite properties rather difficult (Dhakal *et al.*, 2007, Dittenber and GangaRao, 2012).

2.1.3 Chemical Compositions of Plant

The chemical structure of natural fibres fluctuates significantly depending on the source and processing variables. Nevertheless, its identification is possible through common features. Natural fibres can be found to be three-dimensional, complex polymer composed of cellulose, hemicellulose, lignin and pectin. The chemical compositions of a number of plant-fibres are presented in Figure 2 (Azwa *et al.*, 2013, Thygesen *et al.*, 2005, Mwaikambo and Ansell, 2002).

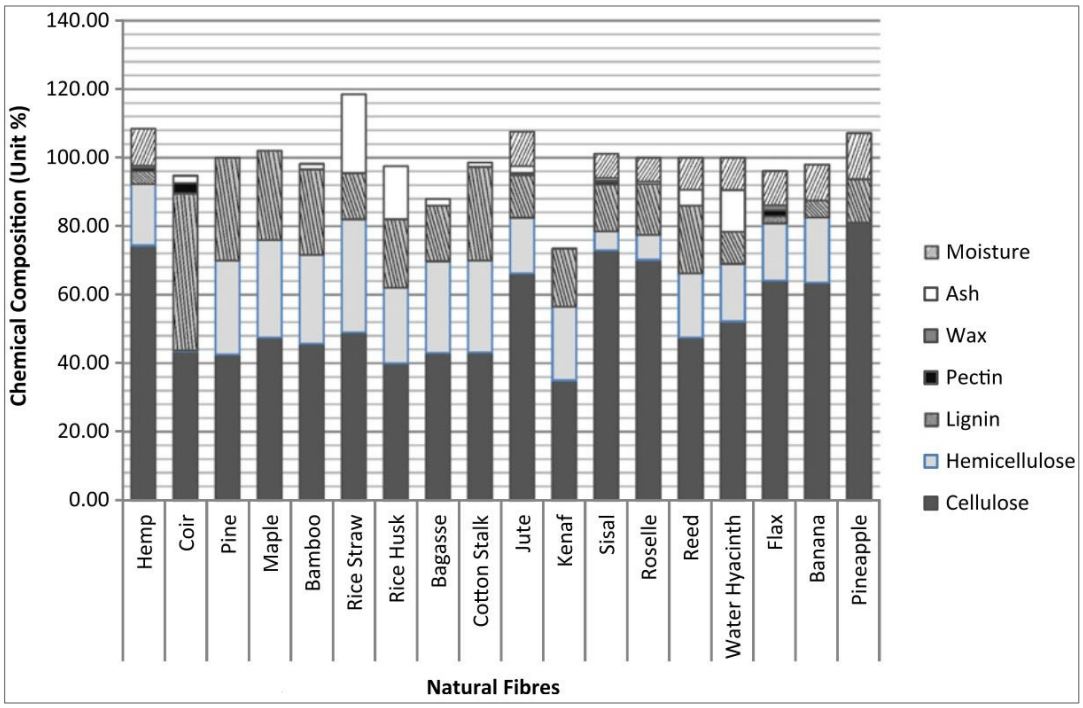

Figure 2:Chemical composition of different plant fibres *(Azwa et al., 2013).*

It can be observed that the main components in the cell walls are cellulose, hemicelluloses, lignin and pectin. However, pectin is commonly known as the main binder.

- Cellulose

Cellulose is known to form a major component of natural plant fibres. Cellulose is a crystalline linear molecule without branching. It is the major contributor to the strength, stiffness and stability to natural plant fibres. It also has reasonable resistance to hydrolysis even though chemical treatment could result in degradation of cellulose (Summerscales *et al.*, 2010). Cellulose is a hydrophilic polymer which contains D-anhydroglucose, represented as the formula $C_6H_{11}O_5$. Repeating glucose units are connected by 1,4-β-D glycosidic bonds. Each single glucose molecule bonds to its neighbour by 1 and 4 carbon atoms as seen in Figure 3-a (Mohanty *et al.*, 2005, John and Thomas, 2008). Each repeated unit is comprised of three separate hydroxyl groups. The hydroxyl groups and hydrogen bonds influence the crystalline packing, thus the physical properties of cellulose materials (Bismarck *et al.*, 2005). The degree of polymerization found in cellulose molecules is approximately 10,000.

Cellulose molecules are found in micro-fibrils with their diameters varying between 10 nm to 20 nm (Rösler *et al.*, 2007).

The cellulose fibril has an estimated diameter of 3.5 nm and is made up of 40 molecules (Vincent, 1990). The cellulose fibrils may be moved into a bigger fibril ranging between 20-25 nm diameters. Adjacent cellulose chains form hydrogen bonds, which lead to partially crystalline areas like micelles. These crystalline areas form a much stronger molecular structural within the cell walls (John *et al.*, 2010).

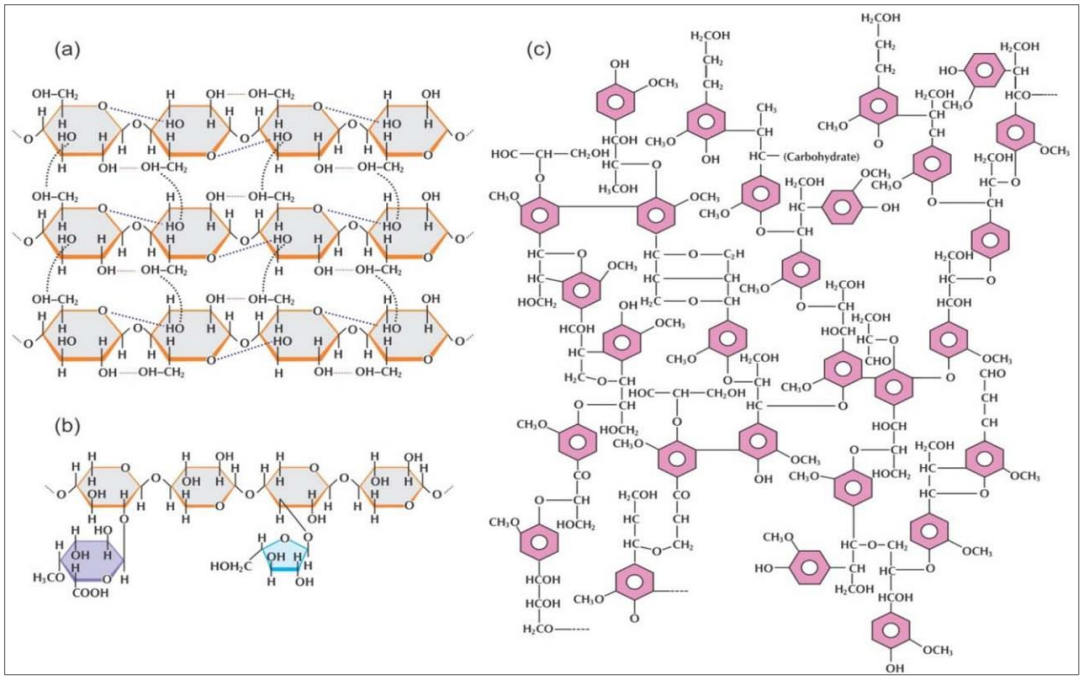

Figure 3: Chemical structure of: (a) cellulose, (b) hemicellulose and (c) lignin (Akhtar *et al.*, 2015).

- Hemicellulose

Hemicelluloses refer to the lower molecular weight polysaccharides which are found in glucose copolymers, mannose, glucuronic acid, arabinose, in addition to xylose (van Hazendonk *et al.*, 1996). It creates a random, amorphous branch or a nonlinear structure that imparts lower strength (Figure 3-b). The hemicellulose is different from cellulose by three aspects (Bledzki and Gassan, 1999, van Hazendonk *et al.*, 1996). First, the degree of polymerization in cellulose is found to be 10 to 100 times greater than hemicellulose. Secondly, hemicellulose includes a number of units of sugar whereas cellulose containing only units of 1,4-β-D glucopyranose. Finally, a

large amount of chain branching is found in hemicellulose, while cellulose is only a linear polymer.

- Lignin

Lignin is an amorphous polymer with a cross linking network consisting of hydroxy bonded with methoxy phenyl-propane units (Pettersen, 1984). The chemical structure depends on the source of origin. Lignin is less polar when compared to cellulose. It is considered a chemical glue inside and between fibres (Lee *et al.*, 2009). The chemical structure of lignin is shown in Figure 3-c.

Lignin is created through a non-reversible of water dehydration from sugar or xylose to make aromatic structures. A process of lignification is when the plant grows up causing a mechanical constancy found in the plant. When lignin becomes rigid, it breaks away from lumen surfaces and the porous wall regions, retaining strength and permeability that helps to transfer water. Lignin is resistant to attack by a number of micro-organisms. The aromatic rings prevent anaerobic processes when the aerobic breakdown of lignin becomes slow. The mechanical properties of lignin are weaker when compared to cellulose (Bledzki and Gassan, 1999).

- Pectin

Pectins are complex polysaccharides in which the primary chains contain glucuronic acid (modified polymers) and rhamnose. The side chains are rich in arabinose, rhamnose, and galactose sugars. The chains are cross linked with calcium ions to improve the structural integrity within the pectin areas. Lignin, hemicelluloses and pectins work together as a matrix or adhesive, which hold the cellulose molecular structure together in natural composite fibres (Lilholt and Lawther, 2000). Pectin is also water soluble after partial neutralization using an alkali or ammonium hydroxide (Bledzki and Gassan, 1999).

- Waxes

Plant fibres are also shown to contain various amounts of extraneous components which include low molecular weight organic components and inorganic components

such as ashes. Although the organic components are low in quantity, they can influence the colour, decay and odour resistance significantly (Pettersen, 1984). The waxy materials are made of water, soluble alcohols and acids such as palmitic, oleaginous and stearic acids (Bledzki and Gassan, 1999).

2.1.4 Physical and Mechanical Properties of Plant Fibres

The physical and mechanical performance of natural fibres may differ widely according to environments and growing seasons of their plants. Natural fibres show a maximum density of about 1.5 g/cm^3. Wood fibres, for example, are hollow and have a lower density in the normal state and becomes denser during processing. However, the maximum density of natural fibres is less than the synthetic glass fibres. The low density of natural fibres is an attractive feature for use as a reinforcement in applications where weight is important such as in automotive or naval. Table 1 shows physical and mechanical properties of various plant fibres as compared to E-glass and carbon fibres (Célino *et al.*, 2013).

Table 1: Physical and mechanical properties of various fibres (Célino *et al.*, 2013).

Fiber	Density	Young's modulus (GPa)	Tensile strength (MPa)	Elongation at break (%)
Flax	1.54	27.5–85	345–2000	1–4
Ramie	1.5–1.56	27–128	400–1000	1.2–3.8
Hemp	1.47	17–70	368–800	1.6
Jute	1.44	10–30	393–773	1.5–1.8
Sisal	1.45–1.5	9–22	350–700	2–7
Coconut	1.15	4–6	131–175	15–40
Cotton	1.5–1.6	5.5–12.6	287–597	7–8
Nettle	1.51	24.5–87	560–1600	2.1–2.5
Kenaf	1.2	14–53	240–930	1.6
Bamboo	0.6–1.1	11–17	140–230	–
E-glass	2.5	70	2000–3500	2.5
Carbone	1.4	230–240	4000	1.4–1.8

Cellulose modulus was estimated using XRD to be about 140 GPa (Vincent, 1990). The high modulus in cellulose is because of its chemical structure consisting of

covalent bonds and hydrogen bonds. If hydrogen bonds are absent, a decrease in the modulus by factor of eight is predicted. Vincent (1990) measured the modulus values of up to 100 GPa in dry flax fibres, and approximately 80 GPa in wet flax. It is believed that water and humidity reduces the modulus of the natural fibres when measured experimentally. When water begins to penetrate within the amorphous areas of the cellulose, stiffness may decrease sharply by between 2 to 4 times as the contribution of hydrogen-bonding is gradually removed from the material.

Although studies have shown that the mechanical performances found in plant fibres are good, synthetic fibres have shown to have better capabilities. Densities of plant fibres are considerably lower when compared to synthesis fibres as well. The variability range in most plant fibres is considerably wider when compared to other synthetic fibres. These variances are due to differences found in the fibre's structures. However, for a fibre to be successful as reinforcement, a balance of reinforcing ability with low density, and low cost are important factors to be considered.

In addition, fibres dimensions and aspect ratio are essential factor to consider. Fibres aspect ratio (l_c/d) is defined as the minimum (critical) length to diameter of the short fibre. It can be calculated using the following relation:

$$l_c / d = \sigma / 2\tau_c \tag{2.1}$$

Where σ is the peak tensile strength of the fibre and τ_c is the interfacial bond strength between the fibre and reinforced matrix.

Fibres must be chosen with length more than the critical length l_c to be successful in reinforcement, shorter fibres are considered as ineffective for reinforcement due to the inability of transferring the stress (Callister, 1991).

2.2 Geopolymers

2.2.1 Overview

The use of cementitious materials is central to the construction industry. Ordinary Portland Cement (OPC) remains the most commonly applied cementitious material in the construction sector. In manufacturing OPC, however, large amounts of resources are used such as energy and natural materials. It takes approximately 1.5 tons of natural materials to produce an estimated 1 ton of OPC. Another concern is that the use of OPC contributes to adverse environmental consequences. Studies show that a huge amount of greenhouse gases is released into the atmosphere during production. The process of creating one ton of OPC releases an estimated 1 ton of CO_2 into the atmosphere. According to the researchers, 6 - 7 percent of the total CO_2 emitted worldwide originates from the cement industry (Davidovits, 1994a, Chen *et al.*, 2014, Shaikh, 2013). Besides the potential environmental concerns linked to the production of OPC, the substance also has drawbacks in relation to its resistance to chemicals and its limited mechanical strength in a number of applications (Chen *et al.*, 2014).

Geopolymers, also known as inorganic polymers, have attracted attention as a potential alternative for OPC in the construction industry. Geopolymer provides an alternative form of cementitious material that is produced from a rich source of aluminosilicates. Chemically, aluminosilicates produce a reaction when an alkaline solution is applied with either ambient or slightly elevated temperatures. The types of raw materials that are used in the production of geopolymers are readily obtainable from natural sources (Shaikh, 2013, Liew *et al.*, 2016).

An abundant supply of by-products is available for the production of geopolymers and these include industry of by-products, volcanic ash or meta-kaolin. The by-products that may be used include furnace slag, fly-ash or mine tailings. The industrial by-products produced by a number of industries has become a problem due to the difficulty in their disposal. Geopolymers may provide a solution for disposal while providing more enhanced performance when compared to the traditional form

of OPC. However, there are additional benefits above the reduction of greenhouse gases and waste materials. The advantages for the use of geopolymers include using a material which is fire and acid resistant, hazardous materials and toxins can be immobilized, rapid curing and adherence to a number of aggregates (Part *et al.*, 2015, Chen *et al.*, 2014).

2.2.2 Geopolymer Molecular Model and Chemical Reaction

Davidovits first coined the term "geopolymer". The term was first used to refer to aluminosilicate polymers that had an amorphous microstructure. Davidovits recommended the chemical designator for geopolymer made of aluminosilicates as polysialate (Davidovits). Sialate is represented as the abbreviation in silicon-oxo-aluminate when the alkali is sodium (Na^+) or potassium (K^+). Polysiliate is referred to as chain and ring polymers. Polysiliates are polymer molecules containing chains of Si and Al ions in four fold coordination linked with oxygen (Davidovits, 1994b). The empirical formula of geopolymer molecules is written as:

$$Mn(-(SiO_2)_z-AlO_2)_n, wH_2O \qquad (2.2)$$

M represents the cation, *n* represents the degree of polycondesation and z is equal to 1, 2, 3 and higher. Geopolymer molecules are molecules with amorphous to semi-crystalline aluminosilicates structures. They can be classified according to the ratio of (Si:Al) to polysialate, polysilate-siloxo and polysialate-disiloxo as shown in Figure 4 (Davidovits, 2008).

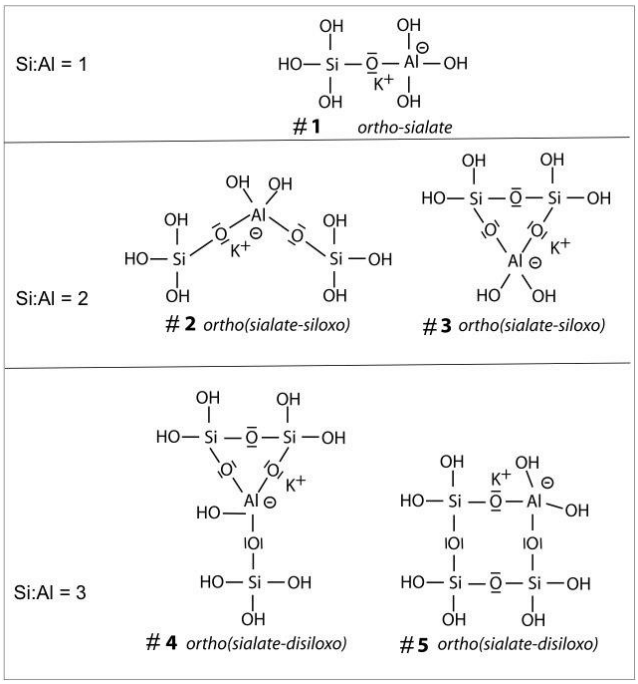

Figure 4: Molecular structure of geopolymers (Davidovits, 2008).

A simplified model of the reaction process in geopolymer was offered by Duxson (2007). The significant part of the processes starts when the aluminosilicate dissolves as it is exposed to a highly alkaline solution (see Figure. 5). Once the aluminosilicate is exposed to an alkaline environment, the dissolution process begins immediately, resulting in breaking of the covalent bonds that connect aluminium, silicon and oxygen molecules. The molecules then polymerize into a structured gel for a short period. The results reveal a three-dimensional chain polymeric structure that is made from Si-O-Al-O bonds. The structured gel is formed when the oligomers create a network during the aqueous phase by releasing water through condensing and dissolution process. The newly formed gel will reorganize from gel 1 to gel 2 as more water is released. Finally, polymerization through a stage of condensation occurs (Duxson *et al.*, 2007a).

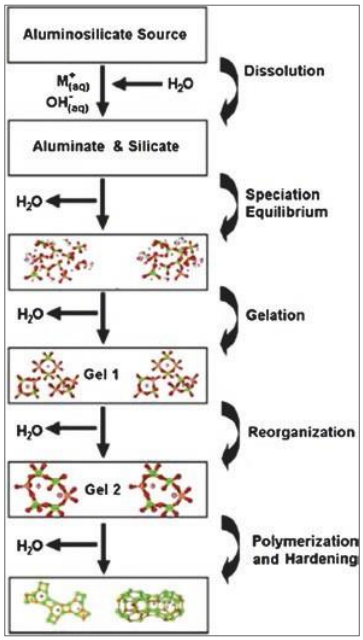

Figure 5: Geopolymer molecular reaction model *(Duxson et al., 2007a).*

Another model was proposed by Fernandez-Jimenez *et al.* (2005) who proposed a framework for dissolution of particles of fly-ash in an alkaline environment. The research findings revealed that the pH level set by the activator system had a high influence on the rate of dissolution and activation of fly-ash. A graphical model (Figure 6) shows the details proposed by Fernandez-Jimenez *et al.* (2005). In this model, the fly-ash particle starts the dissolution process as a visible part of the particle's shell begins to dissolve (Figure 6a). The details shown in Figure 6 (b) reveal the sphere of fly-ash undergoing a bi-directional attack created by the alkaline liquid. The dissolution process will continue as the alkaline liquid penetrates the interior of the sphere and begins to create the dissolution process from the inside out. The process causes the formation of aluminosilicate gel, a product of the process, in and on the sphere of fly-ash. The gel that forms in larger fly-ash spheres is able to block the penetration of the alkaline liquid. The blocked alkaline material is then unable to penetrate further reaction on smaller particles and is observable when the dissolution process is complete as shown in Figure 6 (e). The size of fly-ash particles and variations in pH levels cause a uniform dissolution in the gel. In Figure 6 (c), a fly-ash particle is observed to be incompletely dissolved. In Figure 6 (d), a typical fly-ash geopolymer shows a range of undissolved particles in the geopolymer gel (Fernández-Jiménez *et al.*, 2005).

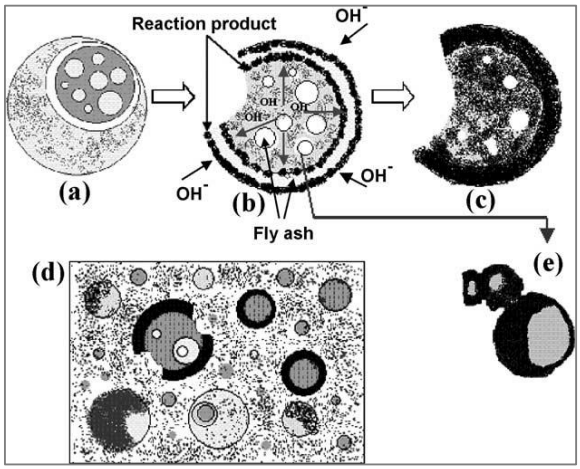

Figure 6: A model describing fly-ash particle activated by alkali (Fernández-Jiménez *et al.*, 2005)

2.2.3 Geopolymer Synthesis

Geopolymers are made up of two parts. The first part includes materials that provide a reactive aluminosilicate solid (raw materials), similar to what is found in fly-ash or metakaolin. The second part is the solution that activates the alkaline reaction of either alkali metal hydroxide or silicate (see Figure 7).

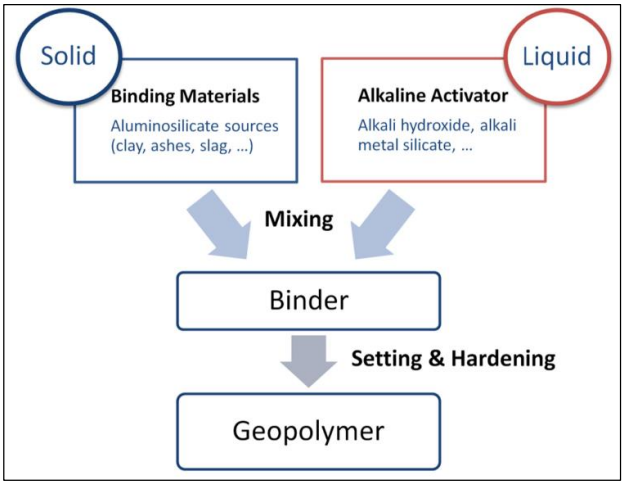

Figure 7: Geopolymer formation from aluminosilicate solids and alkaline activator solutions (Liew *et al.*, 2016).

2.2.3.1 Sources of Aluminosilicate

An aluminosilicate is a raw material which is used to make geopolymers. The

selection of raw materials is a very important step to achieve the desired level of performance from geopolymers (Liew *et al.*, 2016). Aluminosilicates are chosen for the process because they are rich in alumina (Al_2O_3) and silica (SiO_2). Alumina and silica are an abundant resource found inside the earth's crust.

The aluminosilicate source materials, however, are preferred to be in a reactive phase as only the reactive phase is able to contribute in geopolymerisatoin process (Cioffi *et al.*, 2003). The best raw materials to use in the manufacturing of geopolymers are those rated high in silica and alumina while in amorphous form (Williams *et al.*, 2011). The polymerization reaction greatly depends on the quality of the raw materials used in the process. The quality of the materials is important as the structural properties of geopolymers depend on their purity.

Minerals and industrial by-products as essential constituent materials for producing geopolymers have been widely studied. For example, metakaolin has been studied extensively as a source material of geopolymers (Palomo *et al.*, 1999a, Perera *et al.*, 2005, Duxson *et al.*, 2007b, He *et al.*, 2012, Williams *et al.*, 2011). Investigations into low-calcium fly-ash as a material showed a number of potentials (Bakharev, 2006, Bakharev, 2005, Jun and Oh, 2015). A number of studies are also available on the results of using natural Al and Si minerals (Xu and Van Deventer, 2000). Other research has suggested using a combination of calcined as well as non-calcined minerals (Xu and Van Deventer, 2002). Researchers have also proposed using a combination of metakaolin and fly-ash (Van Jaarsveld *et al.*, 2002). Materials such as combining rice husk-ash (Detphan and Chindaprasirt, 2009) and furnace slag (Cheng and Chiu, 2003, Islam *et al.*, 2014) have also been offered as alternatives to be used in the production of geopolymers. Each of these materials contain high amounts of reactive and amorphous alumina and silica.

- Metakaolin

In the early years of studying raw materials to create geopolymers, metakaolin was a commonly investigated material (Davidovits, 1991). However, in recent years, fly-ash has become the most popular raw material as the application focus has altered towards constructions. Metakaolin is obtained through a process known as calcination or the dehydroxylation when kaolin clay is heated to temperatures

ranging from 600 to 800 °C (Ferone *et al.*, 2013, Kong *et al.*, 2007). The process removes the chemically bonded molecules of the water and the octahedral coordinated aluminium. The octahedral coordinated aluminium is discovered within the kaolin in a four to five fold configuration (Palomo *et al.*, 1999a).

- Volcanic-ash

Volcanic-ash has also been studied for use as a raw material to make geopolymers. Volcanic-ash is made up of minerals, rocks and small volcanic fragments of glass created through the volcanic process. Volcanic-ash contains high amounts of silica and alumina. However, the content of crystalline phases was found to be high in the volcanic ash, so the ash has been mixed with other aluminosilicates sources such as metakaolin and fly-ash in order to produce better geopolymers (Tchakoute Kouamo *et al.*, 2013).

- Rice husk-ash

As the title suggests, rice husk-ash is made from burning rice husks. When rice husks are burned, the lignin and cellulose are consumed by the heat and leave behind a substance rich in silica ash. Rice husk-ash (RHA) is found to contain high amounts of amorphous silica. The amorphous silica is a highly porous convex structure. The material is found to be a successful silica additive in the production of geopolymers (He *et al.*, 2013, Rattanasak *et al.*, 2010, Bohlooli *et al.*, 2012, Detphan and Chindaprasirt, 2009).

- Fly-ash

Fly-ash refers to the raw material derived from the industrial by-product made from generating power through the combustion of coal. When coal is burned within a combustion chamber, ash begins to form on the bottom of the chamber (bottom ash) and fine particles rise up the flue with the hot gases. The fine particles which rise with the hot gas are collected by filtration devices such as electrostatic precipitators prior to reaching the chimney.

According to the Standard Specification for Coal Fly-ash and Raw or Calcined Natural Pozzolan for use in Concrete or the ASTM C 618-15, fly-ash can be

classified into three types. Each type is based upon the major chemical substance (see Table 2). The purity of SiO_2, Al_2O_3 and Fe_2O_3 must meet the standard requirements such as 70 percent in class N and class F. Class C requires a minimum amount of SiO_2, Al_2O_3 and Fe_2O_3 to be between 50 and 70 percent.

Table 2: The chemical requirements of fly ash according to ASTM C618-15.

Requirements		Class	
	N	F	C
Silicon dioxide (SiO_2) plus aluminum oxide (Al_2O_3) plus iron oxide (Fe_2O_3), min, %	70.0	70.0	50.0
Sulfur trioxide (SO_3), max, %	4.0	5.0	5.0
Moisture content, max, %	3.0	3.0	3.0
Loss on ignition, max, %	10.0	6.0	6.0

The amounts of incombustible material and the types of coal determine the fly-ash chemical composition after the combustion process. Bituminous and anthracite coals produce Class F fly-ash while Class C is formed through burning lignitic and sub-bituminous coal. Specifications of calcium contents are not stated from each class. However, the calcium content of Class C fly-ash is expressed as calcium oxide (CaO), which is found to be higher than Class F. Class F fly-ash is found to contain pozzolanic properties, while Class C contains both cementitious and pozzolanic properties.

Over the last decade, new research has focused on creating fly-ash geopolymers with lower amounts of calcium (Palomo *et al.*, 1999b, Duxson *et al.*, 2007a). Generally, Class F fly-ash with low-calcium is considered the preferred material when compared to Class C fly-ash with higher levels of calcium. The presence of high calcium content may interfere with the polymerization process by altering the microstructure (Gourley, 2003, Shaikh, 2013). However, fly-ash contains high levels of CaO which produces geopolymers with greater compressive strength. The increase of compressive strength occurs because of the development of compounds such as calcium-aluminate-hydrate (Van Jaarsveld and Van Deventer, 1999).

Fly-ash from coal is considered a variable material in terms of the physical and chemical properties of the fly-ash particles. The reactivity and the chemistry of fly-ash particles depends on variables such as the source coal, the pre and post-combustion conditions (Kutchko and Kim, 2006). However, research revealed that a classified fly-ash from a given source locations exhibits some constancy over a period of time. The phase composition of fly-ash changes depending on the power plants the material is sourced from. The sourced fly-ash will react in similar fashion as long as there are no changes to coal source or burning conditions. Fly-ash's bulk chemical composition may be quantitatively determined using X-ray fluorescence (XRF). Table 3 and Table 4 show the chemical compositions and estimated particle sizes of five types of Australian fly-ash, respectively (Gunasekara *et al.*, 2014).

Table 3: Chemical compositions of fly-ash collected from five different locations in Australia *(Gunasekara et al., 2014).*

Fly-ash Type	by weight (%)										
	SiO_2	Al_2O_3	Fe_2O_3	CaO	K_2O	TiO_2	P_2O_5	MgO	Na_2O	SO_3	LOI
Gladstone (GFA)	50.82	29.89	10.26	3.24	0.58	2.05	1.61	0.80	0.00	0.28	0.43
Port Augusta (PAFA)	49.97	31.45	3.22	5.03	1.87	2.54	1.77	1.54	1.85	0.33	0.51
Collie (CFA)	52.67	29.60	11.27	0.94	0.65	1.83	1.13	0.72	0.00	0.48	0.63
Mount Piper (MPFA)	65.18	25.30	1.90	0.63	3.65	1.53	1.21	0.00	0.00	0.23	1.30
Tarong (TFA)	73.12	21.50	1.36	0.29	0.63	1.84	1.06	0.00	0.00	0.00	1.16

Table 4: Particle size distributions of fly-ash collected from five different locations in Australia *(Gunasekara et al., 2014).*

FA Type	Passing (%)										Surface Area (m^2/kg)
	10μm	20μm	30μm	40μm	45μm	50μm	60μm	70μm	80μm	90μm	
GFA	43.1	61.9	73.2	79.8	82.7	85.3	89.6	91.2	92.6	93.8	2003
PAFA	46.7	62.1	71.4	77.4	80.9	82.9	87.9	90.1	92.1	93.8	2161
CFA	40.9	54.6	62.7	67.7	70.0	72.3	76.7	79.0	81.3	83.6	1934
MPFA	36.0	57.1	69.9	77.4	80.7	83.8	89.0	91.2	93.0	94.6	1555
TFA	43.0	63.0	73.6	79.3	81.8	84.2	88.3	90.2	91.9	93.4	1766

Fly-ash is primarily amorphous. Besides the amorphous content, class F fly-ash has crystalline phases made from quartz, magnetite, mullite and hematite (Rattanasak and Chindaprasirt, 2009, Lee and van Deventer, 2002, Rickard *et al.*, 2011). The crystalline content within fly-ash is unreactive through the alkali activation process and do not dissolve during geopolymerization. However, the crystalline content may

still affect the properties of the geopolymer.

X-ray diffraction (XRD) is used to determine the phase composition of fly-ash. Diffractometer and search-phase software can be used in the lab to perform qualitative analysis of data. An internal standard such as fluorite (CaF_2) is usually mixed with fly-ash powder before analysis in order to determine the amorphous and crystalline contents quantitatively. XRD quantitative analysis is usually conducted using Rietveld refinement modeling (Williams *et al.*, 2011, Rickard *et al.*, 2011). Chen-Tan *et al.* analysed Colie fly-ash quantitatively and concluded that the only content that is reactive in fly-ash is the amorphous aluminosilicates during the geopolymerisation reaction (Chen-Tan *et al.*, 2009). Therefore, to define the reactivity of any fly-ash type, phase composition analysis must be conducted. Table 5 shows the phase composition of fly-ash collected from three different resources as presented by Rickard *et al.* (2011).

Table 5: Phase composition of three different class-F fly-ash *(Rickard et al., 2011).*

Phase	Formula	Collie FA(wt.%)	Eraring FA(wt.%)	Tarong FA(wt.%)
Amorphous content		54.00 (45)	62.74 (31)	50.82 (28)
Mullite (ICSD 66452) Mullite (ICSD 66449)	$Al_{4.56}Si_{1.44}O_{9.72}$ $Al_{4.59}Si_{1.41}O_{9.7}$	15.80 (18)	20.88 (14)	25.1 (11)
Quartz low (ICSD 83849)	SiO_2	11.14 (18)	8.08 (16)	10.31 (14)
Quartz low Primary (ICSD 83849)	SiO_2	15.05 (21)	6.81 (14)	13.77 (13)
Magnetite (ICSD 43001)	Fe_3O_4	2.51 (83)	1.491 (52)	
Hematite (ICSD 88417)	Fe_2O_3	1.50 (64)		

2.2.3.2 Activator Solution

Alkaline solutions are necessary to activate the source materials in each geopolymerisation process. Sodium hydroxide (NaOH) is used most often as an alkali activator when combined with sodium silicate (Na_2SiO_3). Another alkali activator is potassium hydroxide (KOH) with potassium silicate (K_2SiO_3). A singular activator may also be functional in geopolymeric reaction. For example, successful research has shown synthesizing geopolymer using a single sodium hydroxide

activator with rice husk-ash and red mud (He *et al.*, 2013).

The type and concentration of each alkali activator is a main factor in geopolymerization process (Komljenović *et al.*, 2010). Five different types of alkali activators have been identified by the researchers. The first alkali activator used in the research was calcium hydroxide ($Ca(OH)_2$). The second activator used was sodium hydroxide (NaOH). A mixture of sodium hydroxide and sodium carbonate (Na_2CO_3) was also used. Potassium hydroxide (KOH) and sodium silicate (Na_2SiO_3) were also examined as useful alkali activators. A number of different concentrations were examined to create fly-ash geopolymers. The curing conditions were fixed to accurately study the effect of alkali activators on the mechanical properties of geopolymers. Sodium silicate showed the strongest compressive strength over each of the tested alkali activators (see Figure.8). The next strongest was calcium hydroxide, followed by sodium hydroxide, then sodium hydroxide combined with sodium carbonate, and finally potassium hydroxide. The activation potential of potassium hydroxide was low when compared to sodium hydroxide; this difference was attributed to the size difference of sodium and potassium ions. The study also concluded that the optimum value of sodium silicate modulus was estimated to be 1.5 (see Figure.8). It was therefore suggested that higher levels than the standard modulus may result in a loss in compressive strength of the matrices. The study also revealed that compressive strength values depended greatly on the concentration of alkali activators. Higher compressive strength results have been obtained with higher concentrations of all types of activators.

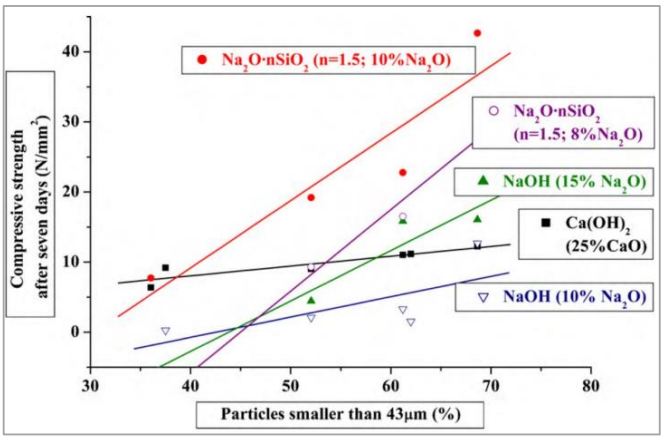

Figure 8: Compressive strength of geopolymers as activated using different alkali solution. n=represents the modulus SiO_2/Na_2O (Komljenović *et al.*, 2010).

Geopolymerization is a process that greatly depends on the use of alkaline solutions. Strong alkaline solutions are needed to increase the surface hydrolysis of aluminosilicate particles (Hu *et al.*, 2009). The alkali concentration is an important factor when dissolving Si and A1 during the geopolymerisation process; the amount of ions leached in the process is mostly dependent on the concentration of the alkali activator. Research suggests that enhancement in compressive strength can be achieved by increasing the concentration of alkali activators (Somna *et al.*, 2011, Ahmari and Zhang, 2012, Gorhan and Kurklu, 2014, Yusuf *et al.*, 2014, Hanjitsuwan *et al.*, 2014).

2.2.4 Microstructural Properties of Geopolymers

The phase composition of geopolymers is typically assessed with x-ray diffraction (XRD). XRD phase patterns of geopolymers commonly show both crystalline and amorphous phases. Amorphous phase is found at a broad peak of 2θ= 20˚-30˚. Crystalline may be identified as sharp peaks. Crystalline phases can be found in both sources of aluminosilicates and geopolymers, which imply that the crystalline contents do not react during the geopolymerization process. Diffraction patterns of three different geopolymer mortars are presented in Figure 9. Mullite and quartz are found in geopolymer samples of crystalline fly-ash bases. XRD pattern research has shown a 7° shift in the broad peak of amorphous silica in the geopolymer process. The study concluded that the silicate phase in geopolymerisation processes was highly chaotic (Rattanasak and Chindaprasirt, 2009).

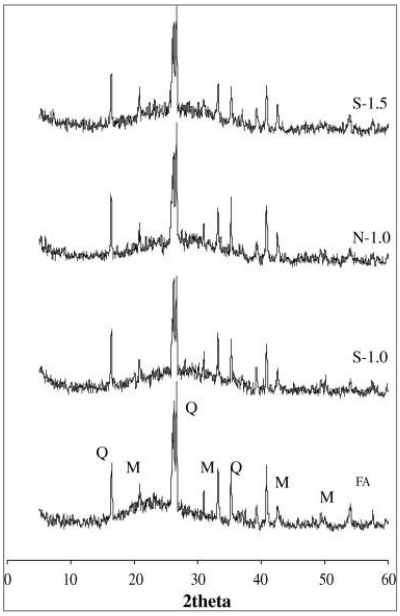

Figure 9: XRD patterns of fly-ash and geopolymer pastes Q: quartz, M: mullite (Rattanasak and Chindaprasirt, 2009).

Fourier Transform Infrared Spectroscopy (FTIR) is currently being used by researchers to analyse the reaction products of geopolymer materials (Rees *et al.*, 2008, Perná *et al.*, 2014, Phair and Van Deventer, 2002, Gao *et al.*, 2014). FTIR patterns provide molecular data of the chemical bonds found in geopolymers as each compound presents a different vibration. Different wavelengths and different intensities provide information of molecular bond formations in geopolymer pastes. Thus, FTIR techniques may give evidence of effective geopolymerization reactions.

An example of FTIR spectra of fly-ash based geopolymers can be observed in Figure. 10. Features of the FTIR spectra can be distinguished by the bands at ~1000 cm^{-1}. The band is a representation of a Si–O–Si tetrahedron which is a typical band in geopolymers (Chindaprasirt *et al.*, 2009, Arioz *et al.*, 2013, Gao *et al.*, 2014). Therefore, some researchers used the highest and the area under the peak Si–O–Si vibration as indicator to the degree of geopolymerisation (Chindaprasirt *et al.*, 2009, ul Haq *et al.*, 2014). Based on shape and location of the Si–O–Si band, Chindaprasirt *et al.* (2009) argued that the concentration of alkaline solution is one of the main factors in geopolymerization. The molecular band Si–O–Al may also be lowered in frequency during polycondensation process as a result of alternating the Si–O and Al–O bonds (Lee and van Deventer, 2002). Bands at approximately at 3450 cm^{-1}

were observed to be for O–H stretching, while 1650–1600 cm^{-1} was ascribed to O–H bending (Zaharaki *et al.*, 2010, Rattanasak and Chindaprasirt, 2009).

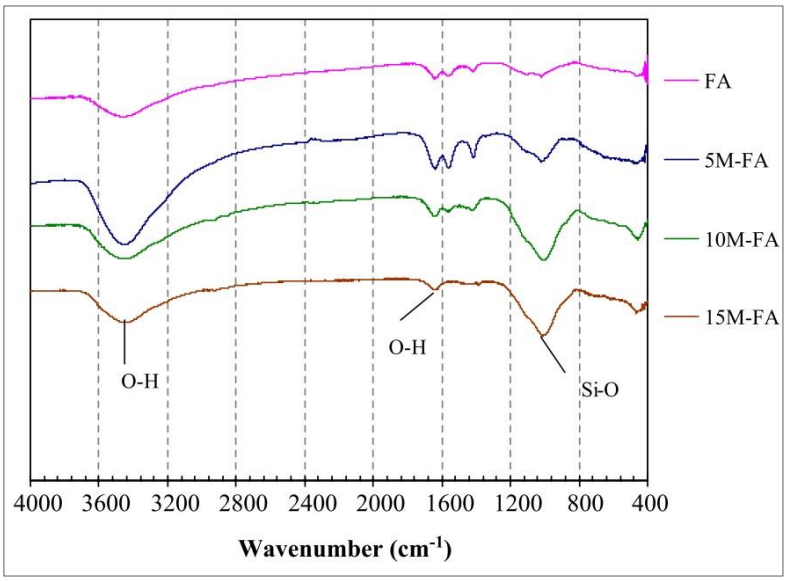

Figure 10: FTIR spectra of fly-ash geopolymers created using various concentrations of NaOH (Chindaprasirt *et al.*, 2009).

Scanning electron microscopy (SEM) may also be used to examine geopolymer's microstructure and precursors. Microstructures of geopolymers are usually examined using SEM to provide an image of defects, cracks, morphology, porosity and reactions of aggregates. A typical SEM image of the microstructure of fly-ash based geopolymer can be seen in Figure 11. It is common to find unreacted particles within the geopolymer gel. A geopolymer with developed dissolution reaction has high proportions of gel when compared to unreacted fly-ash particles (Kriven *et al.*, 2003). Pores and micro-cracks are commonly found in geopolymer matrices as well.

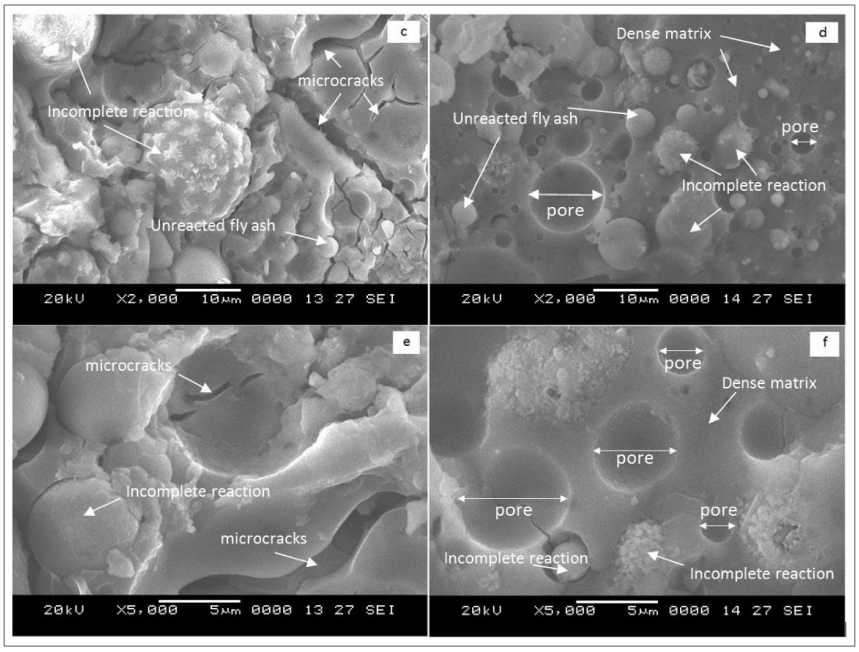

Figure 11: A typical microstructure of fly-ash based geopolymers showing geopolymer matrices, unreacted fly-ash particles, pores and micro-cracks (Abdullah *et al.*, 2012).

2.2.5 Thermal Properties of Geopolymers

The thermodynamic processes of geopolymers are typically measured using differential thermal analysis (DTA), differential thermogravimetry (DTG), and thermogravimetric analysis (TGA). Each technique assists in gathering information on phase stability and thermodynamic properties of materials (ul Haq *et al.*, 2014, Kong and Sanjayan, 2010, Li *et al.*, 2012, Duxson *et al.*, 2007b). To study thermal stability and eliminate oxidation reaction, nitrogen or argon may be used as an inert atmosphere. Strong thermal resistance has been discovered in geopolymers, where such resistance may be used for industrial or domestic insulation.

The curves in Figure 12 represent common TGA, DTG and DTA features in fly-ash based geopolymer as observed by Li *et al.* (2012). Above ambient temperatures, the mass loss as the dehydration of water begins is found to be proportional to the amount of initial water in the sample. Evaporation is found to continue until the majority of water is evaporated at 250°C, (Kong and Sanjayan, 2010). The peak of water lost was recorded at 120°C as shown in the DTG curve. The mass loss stabilizes when exposed to higher temperatures. Typical small changes are found at

over 600°C. The thermodynamics of geopolymer is studied using DTA as a function of temperature. A rise in the DTA cure corresponds to the exothermic process while a decline shows endothermic processes at a certain temperature. The endothermic process includes the dehydration effect as the system losses energy to water vapour. Another endothermic reaction is when the mineral phases change as they draw energy from the system to change the phase. Both crystal destruction and dihydroxylation are exothermic processes (ul Haq *et al.*, 2014, Zivica *et al.*, 2014).

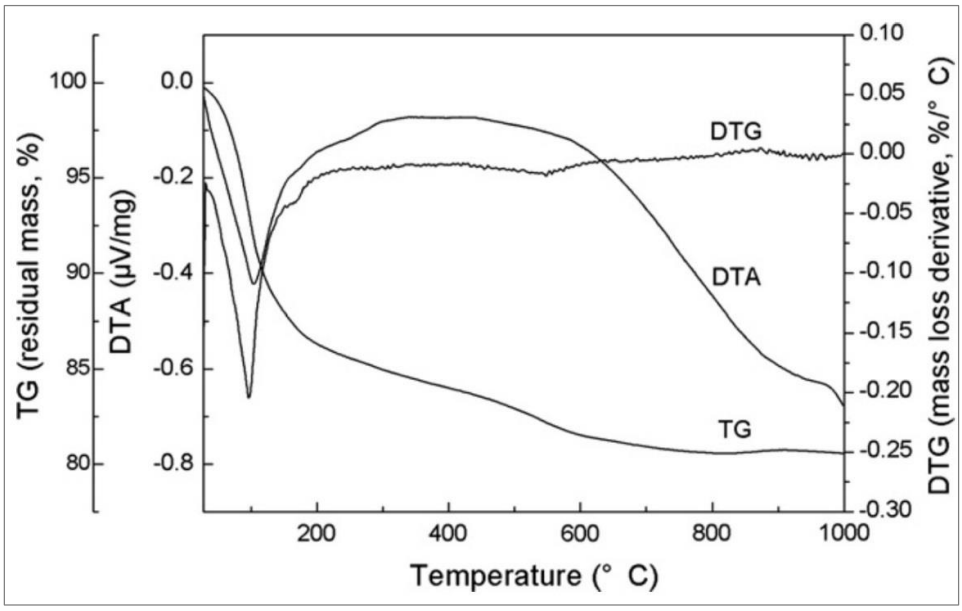

Figure 12: TGA, DTG and DTA of fly ash geopolymer paste (Li *et al.*, 2012).

Due to their thermal properties, the automotive and construction industry has discovered a number of uses for geopolymers (Liefke, 1999). Liefke (1999) suggests the use of foamed geopolymer for insulation in a number of areas. One characteristic in geopolymer that is studied extensively is its thermal conductivity. Thermal conductivity is affected by different parameters such as the material density, porosity, chemical composition and fillers. Materials that are low in density and high in porosity are applicable to be a good insulator, as the air that filled the microstructural voids has low conductivity. Kamseu *et al.* (2012) illustrates the effects the porosity on the thermal conductivity of geopolymer samples in Figure 13. Thermal conductivity of geopolymer was observed as being influenced by porosity. Furthermore, it may be assumed that higher thermal conductivity may be gained in denser geopolymers that possess higher compressive strength as shown in Figure 14.

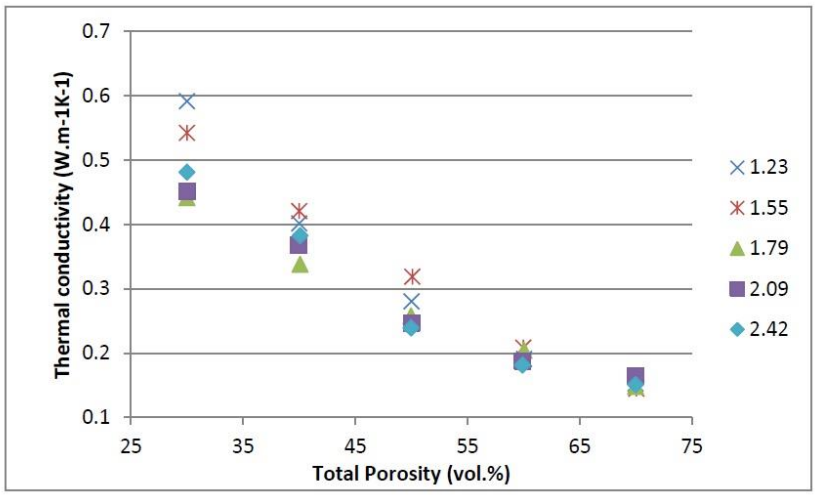

Figure 13: The inverse relationship between porosity and thermal conductivity of geopolymers (Kamseu *et al.*, 2012).

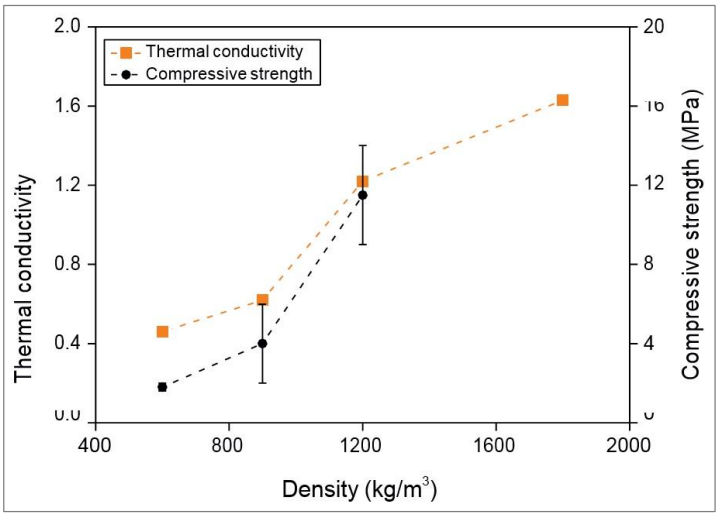

Figure 14: The thermal conductivity, density and compressive strength of metakaolin-based geopolymers shows steady relationship (Zhang *et al.*, 2014).

2.2.6 Mechanical Properties of Geopolymers

The mechanical properties of geopolymers are variable. Such properties are dependent on each geopolymer's relative amounts of aluminium, alkali, silicon, and water. Solid to liquid ratio or amount of amorphous Al_2O_3:SiO_2 and Si:Al are significant binder variables. Ratios including silicon and aluminium are important as they directly affect the molecular network of geopolymer. Another important factor in the quality of geopolymer formation is curing conditions; this includes some sub-factors such as curing temperatures and duration of curing. This section presents the

mechanical properties of geopolymers with consideration of their variable factors.

2.2.6.1 Effect of Activator Settings on Mechanical Properties of Geopolymers

Alkali concentration is important in geopolymer production. The concentration of alkali activator solutions impacts on the mechanical properties of geopolymer samples. Features of concern when using alkaline solutions is when sodium silicate is combined with sodium hydroxide. Ratios between sodium silicate and sodium hydroxide (Na_2SiO_3:NaOH) are essential to the geopolymerization process. By changing sodium silicate to sodium hydroxide ratio, the strength and the economy aspects of geopolymers can be optimized (Yusuf *et al.*, 2015). Additionally, the effect of the activator modulus (Ms) should also be studied. Ms is defined as the mass ratio from silicon dioxide (SiO_2) to sodium oxide (Na_2O). This section will outline the observed effects of alkali concentration, Na_2SiO_3:NaOH and Ms in relation to the mechanical strength of geopolymers.

Alkali solutions promote and speed up the geopolymerzation process. The concentration of alkali depends greatly on the ion numbers and pH levels. By increasing the concentration of sodium hydroxide, the strength of metakaolin geopolymer is increased (Alonso and Palomo, 2001, Mishra *et al.*, 2008). However, a number of researchers believe high levels of alkalinity are unfavourable to the strength of geopolymers. The increased strength observed when increasing concentration in sodium hydroxide showed a sharp decrease after reaching optimum levels. Sodium hydroxide may reduce leaching Si and A1 ions from the aluminosilicate at high concentrations. This may lead to premature precipitation in geopolymer gel and a reduction in mechanical strength of the material (He *et al.*, 2013)

In a study using fly-ash and rice husk-ash as a source aluminosilicate material, the greatest strength value was obtained when a concentration of 12M sodium hydroxide as alkaline solution was used (Nazari *et al.*, 2011). Khale and Chaudhary (2007) studied the relationship between geopolymers pH and their strength. They found that samples of pH 14 were over 50 times higher strength when compared to samples with pH 12. Their review concluded that pH range of between 13-14 is

considered to be ideal in the creation of geopolymer that is high in mechanical strength (Khale and Chaudhary, 2007). In another study, it has been shown that a solution with higher caustic alkalinity causes more successful dissolution of raw aluminosilicates and activates higher amounts of alumina and silica, which consequently increased geopolymer gel and the strength of matrices (He *et al.*, 2012).

The compressive strength of fly-ash-geopolymer in terms of sodium hydroxide concentration while cured at the ambient temperature was reported by Somna *et al.* (Somna *et al.*, 2011). The concentration of sodium hydroxide was changed between 4.5 and 16.5 M. A rapid improvement in compressive strength was observed when the concentration increased to 14 M (Figure 15). The observed increased strength was due to the high leaching of alumina and silica species. However, the compressive strength of samples prepared with sodium hydroxide concentrations at 16.5 M appeared to decrease. The excess of hydroxide ions caused precipitation in the aluminosilicate gel, which resulted in lower strength geopolymers (Somna *et al.*, 2011).

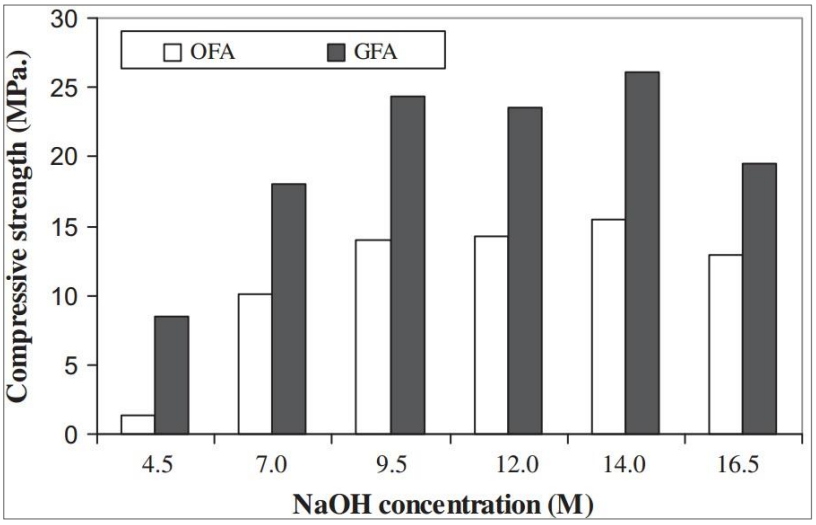

Figure 15: Compressive strength of geopolymers in terms of NaOH concentrations (Somna *et al.*, 2011).

A study presented by Gorhan and Kurklu (2013) examined the compressive strength of fly-ash geopolymer with different sodium hydroxide concentrations over a 7 day experiment. All samples were thermally cured for 2, 5 and 24 hours at 65°C and

85°C. Concentrations of 3, 6 and 9 M of sodium hydroxide was used in the preparation of samples. The ideal sodium hydroxide concentration for the greatest compressive strength was 6 M that achieved 21.3 MPa and 22MPa for samples cured at 65°C and 85°C, respectively, for 24 hours (Figure 16). This optimal concentration gave an alkaline environment to dissolute the source material without hindering the polycondensation process. The concentration of 3 M is considered to be too low and unable to stimulate strong reactions while the high concentration at 9 M caused premature coagulation in silica leading to a weaker geopolymers (Gorhan and Kurklu, 2014).

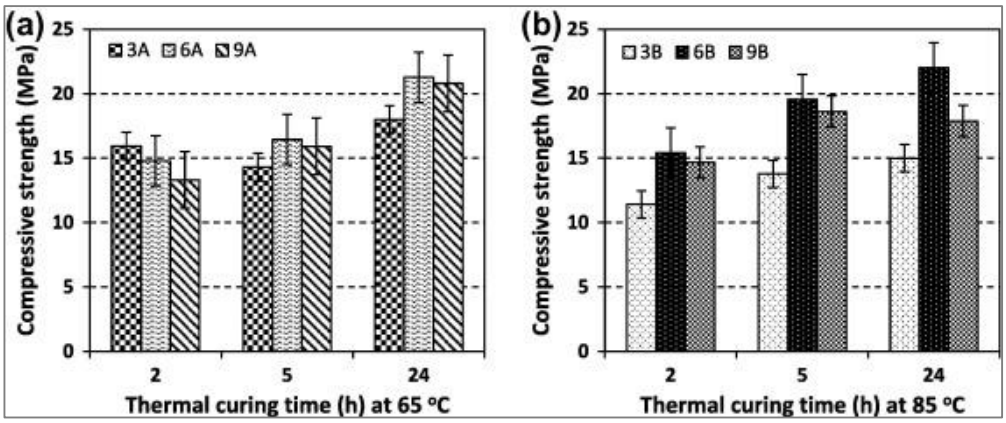

Figure 16: Compressive strength of geopolymers in terms of curing time (h) and NaOH concentration (M) (Gorhan and Kurklu, 2014).

Ahmari and Zhang (2012) studied the mechanical performance of geopolymers created from copper mine tailings and sodium hydroxide. The concentrations of sodium hydroxide varied between 10 and 15M. The variations were used to understand the effect of sodium hydroxide concentration on the compressive strength of geopolymers. The compressive strength results indicated that samples with 15 M concentration were higher in strength than that of 10 M. The variation in strength was found to be caused by the higher sodium hydroxide-to-aluminosilicate ratio which caused, in turn, higher Na:Si and Na:Al (Ahmari and Zhang, 2012).

When creating geopolymers, it is important to pay attention to the ideal ratios of sodium silicate to sodium hydroxide solutions Na_2SiO_3:NaOH. Sodium hydroxide solution becomes a dissolvent while the sodium silicate becomes a binder during the reaction. Ridtirud *et al.* (2011) found that the optimum ratio of Na_2SiO_3:NaOH in

fly-ash based geopolymers was 1.5. Ratios studied were 0.33, 0.67, 1.0, 1.5 and 3.0. The highest compressive strength recorded was 45.0 MPa in the case of Na_2SiO_3:NaOH=1.5. The increase in strength was attributed to the sodium content where Na^+ ions are critical to geopolymer formation to provide charge balancing ions during the reaction process. However, excessive silicate throughout the reaction process caused a reduction in strength (see Figure 17) as the additional amount of silicate caused a delay in water evaporation, as well as causing an interference in geopolymerisation (Ridtirud *et al.*, 2011).

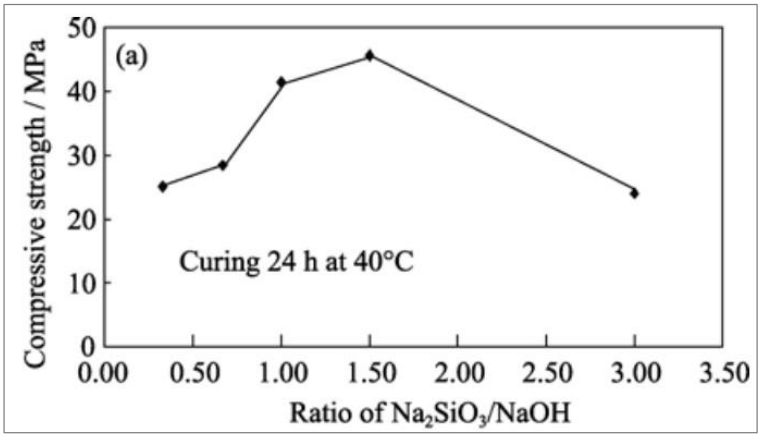

Figure 17: Compressive strength of geopolymers in terms of Na_2SiO_3/NaOH ratios(Ridtirud *et al.*, 2011).

Sathonsaowaphak *et al.* (2009) reported the effect of liquid alkaline:ash ratio, Na_2SiO_3:NaOH ratio and sodium hydroxide concentration on the compressive strength of bottom ash geopolymers. It was found that a liquid alkaline:ash ratio of 0.4209–0.709, a Na_2SiO_3:NaOH ratio of 0.67–1.5 and a sodium hydroxide concentration of 10 M respectively, led to superior compressive strength and ideal workability in geopolymer samples. 10M sodium hydroxide was important, since sodium hydroxide solution improves the dissolution of silica and alumina's species, and sodium ions act as charge balancing (Sathonsaowaphak *et al.*, 2009).

Salih *et al.* (2014) found that in the case of geopolymer produced using palm oil fuel ash, the optimum Na_2SiO_3:NaOH ratio was 2.5 and the optimum solid:liquid ratio was 1.32 for maximum compressive strength (see Figure 18). The researchers found that solid:liquid ratios of less than 1.32 led to a higher presence of voids which adversely affected compressive strength. Similarly, Na_2SiO_3:NaOH ratios higher

than 2.5 led to excessive amounts of sodium silicate which hindered the geopolymerization reaction.

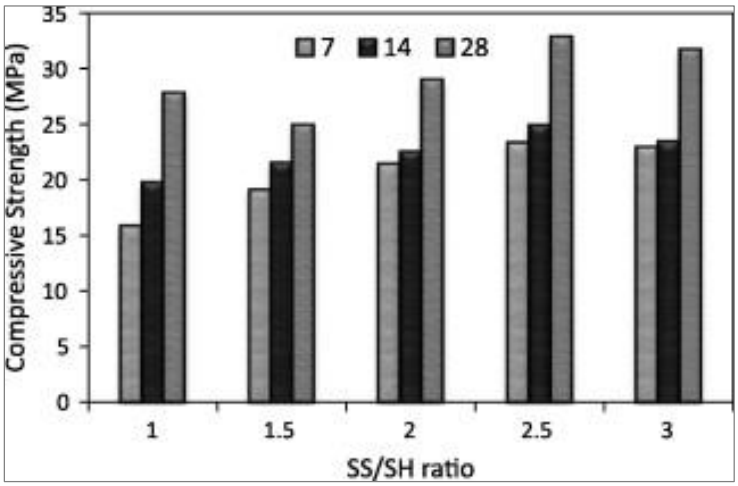

Figure 18: Compressive strengths of geopolymers with solid: liquid ratio=1.32 at 7, 14, and 28 days (SS/SH= Na_2SiO_3: NaOH) (Salih *et al.*, 2014).

Sukmak *et al.* (2013) investigated the influence of liquid:fly-ash and Na_2SiO_3:NaOH ratios on the development of compressive strength of geopolymers created using clay and fly-ash as aluminosilicate source materials. Liquid:fly-ash ratios applied were 0.4, 0.5, 0.6 and 0.7, and the Na_2SiO_3:NaOH applied ranged between 0.4 and 2.3. The outcome was that liquid:fly-ash ratios <0.3 and >0.8 failed to be suitable for clay-fly-ash geopolymers due to null strength. The optimum values of liquid:fly-ash and Na_2SiO_3:NaOH were 0.6 and 0.7, respectively (see Figure 19). This result was lower than the optimum ratio in the case of fly-ash-based geopolymers. This could be attributed to the fact that clay has a higher tendency to absorb the cations and is likely to absorb added sodium hydroxide. The greatest compressive strength achieved was ~15 MPa at 90 days of curing (Sukmak *et al.*, 2013).

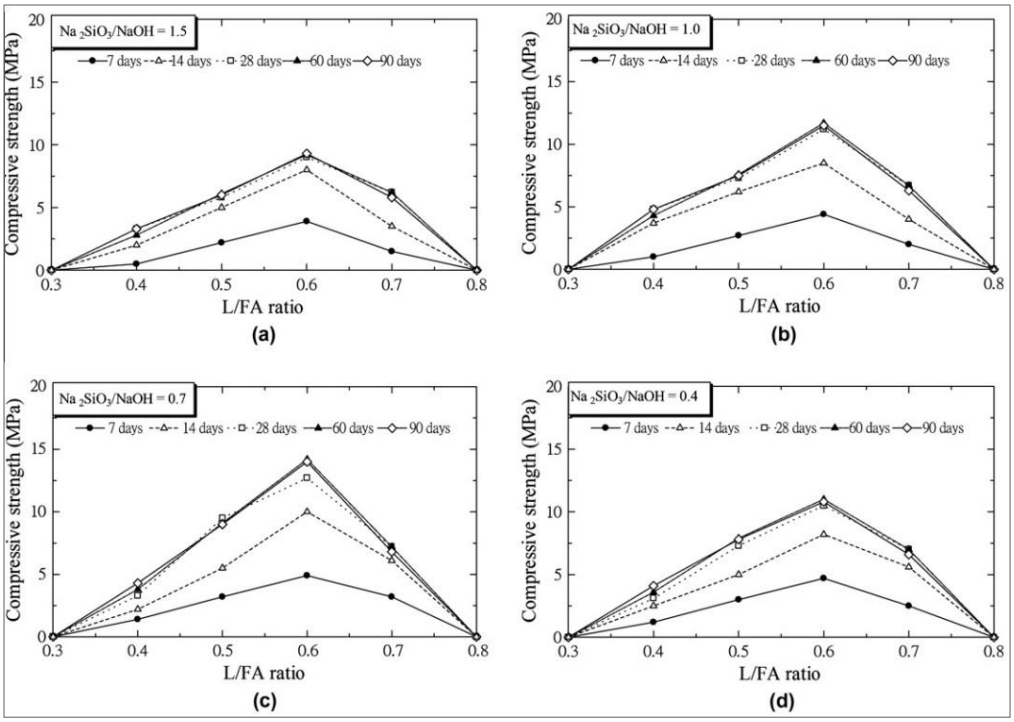

Figure 19: Compressive strength results of clay/fly-ash geopolymer samples cured at 75 °C for 48 hours with various liquid: fly-ash and Na_2SiO_3/NaOH ratios (Sukmak *et al.*, 2013).

Activator modulus (Ms) is a variable that can determine the soluble silicate amount used in geopolymers. It controls the dissolution rate as well as the gelation and polycondensation throughout the chemical reaction of geopolymer. Thus, it impacts on the ultimate strength development of geopolymer material. A suitable Ms must be designed and chosen depending on the chemical composition of the raw aluminosilicate materials. Law *et al.* (2014) reported that 1.0 is an optimum Ms for fly-ash geopolymers, and any subsequent increase fails to result in compressive strength increase. It was suggested that greater than 1.0 Ms, all particles of fly-ash had dissolved or that there was an absence of further dissolution of each fly-ash particle (Law *et al.*, 2014). Yusuf *et al.* (2014) reported that the influence of activator modulus Ms on the strength of samples produced from ground steel slag and palm oil fuel ash was small. In their study, compressive strengths obtained were 69.1 MPa and 65.0 MPa using a modulus of 0.915 and 1.635, respectively (Yusuf *et al.*, 2015).

Komljenovic *et al.* (2010) investigated the influence of Ms on the mechanical properties of fly-ash geopolymers. With increasing sodium silicate activator

modulus, the ratio Si:Al of the reaction products increased, and Na:Si and Na:Al decreased. Based on the results of compressive strength, the researchers found that greater compressive strength was associated with greater modulus values, and greater Si:Al ratio of geopolymers (Komljenović *et al.*, 2010).

Guo *et al.* (2010) investigated the influence of activator modulus and alkali activator content (Na_2O %) on the compressive strength of fly-ash based geopolymers. Combinations of Na_2SiO_3 and NaOH were applied as activator. The alkali activator's modulus was increased from 1.0 to 2.0 and alkali activator content ranged from 5.0% to 15%. The alkali activator content was found to be dependent on the mass quantity of Na_2O to fly-ash. Silica-alkali modulus and alkali activator content were found to be critical in the strength development of geopolymers. The content of alkali activator (Na_2O %) and the optimum modulus were recorded as 10% and 1.5% respectively. This produced compressive strength values that were recorded to be 22.6 at 3 days, 34.5 at 7 days and 59.3 MPa at 28 days when the samples were cured at ambient temperature (see Figure 20) (Guo *et al.*, 2010).

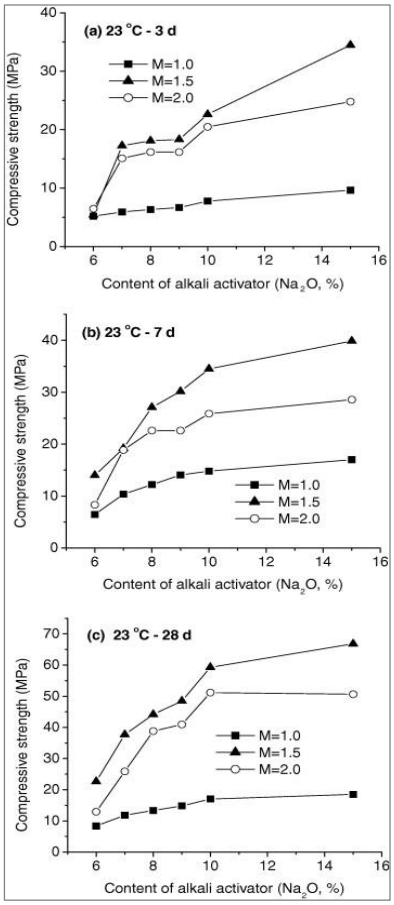

Figure 20: The effects of activator modulus (M) and content of alkali activator (Na_2O%) on the compressive strength of geopolymers cured at room temperature of 23°C for 3, 7, and 28 d (Guo *et al.*, 2010).

The previous studies investigated factors that are relevant to the activator and procedure of geopolymer preparation. However, most of the aluminosilicate contents involved in the geopolymeric reaction is derived from the source material. It is necessary to determine the amorphous contents of the source aluminosilicate materials since they have an essential role in forming geopolymers.

2.2.6.2 Effect of Molar Ratios on Mechanical Properties of Geopolymers

The sodium content in a geopolymer system is mainly provided by sodium hydroxide and sodium silicate solutions. The aluminosilicate sources and sodium silicate collectively are responsible for the silicon content while the aluminosilicates alone are responsible for the aluminium content in geopolymers. Sodium hydroxide and sodium silicate liquids as well as free water that were added during the mixing

process are responsible for the water content. Furthermore, the various different mixing parameters and ratios i.e. the solid:liquid ratio, Na_2SiO_3:NaOH ratio and the NaOH concentration are responsible for the differences in molar and atomic ratios in a geopolymer system. Nevertheless, the quantity in which each component is used in a geopolymerization reaction extensively depends on the reactive phases or the reactivity of aluminosilicates. It is quite common in the published studies to figure out the molar ratios of geopolymers such as Si:Al by considering the chemical composition of the precursor materials. However, this may be inaccurate since the crystalline aluminosilicate phases are unreactive during the geopolymer reaction. The actual molar ratios in geopolymer gel can be determined experimentally for only the amorphous phase using quantitative XRD analysis (Rickard *et al.*, 2011, Rickard *et al.*, 2015), quantitative EDS analysis (Rowles and O'Connor, 2003) or both techniques (Williams *et al.*, 2011).

Varying the atomic ratios leads to changes on the preparation setting of geopolymers, and thus their mechanical strength. The effective Si:Al ratios affect the dissolution as well as the hydrolysis and the polycondensation process of geopolymers. Furthermore, raising the ratios of SiO_2:Al_2O_3 can improve the mechanical properties of the geopolymer (Davidovits, 2008). The content of silica is also seen to have a great influence on the mechanical properties of geopolymers. Also, the alumina content of the geopolymer controls its setting. This can be one of the reasons for the increase in the dissolution of aluminosilicates in high concentration of Si content in the geopolymerization reaction (Dimas *et al.*, 2009, Palomo *et al.*, 1999b).

Rowles and O'Connor (2003) examined the impact of the ratios Na:Al and Si:Al on the compressive strength of metakaolin geopolymers activated by sodium silicate and sodium hydroxide. They discovered that varying both ratios seemed to have a considerable impact on the measured compressive strength of geopolymer. Figure 21 is a contour graph showing the compressive strength values for geopolymers in terms of the ratios Na:Al and Si:Al as presented by the authors. The optimum strength (53.1 MPa) was obtained by preparing geopolymers with a ratio of 1.29 in Na:Al and 2.50 with Si:Al. Furthermore, it was also recorded that the ratios were based on the source material measurement rather than the geopolymer gel. Since the entire

metakaolin did not react, the actual ratio of Na:Al and Si:Al of the geopolymer gel produced would not have been the same as the calculated ones. Amongst the amorphous geopolymer gel, unreacted aluminosilicates remain as a secondary phase (Rowles and O'Connor, 2003).

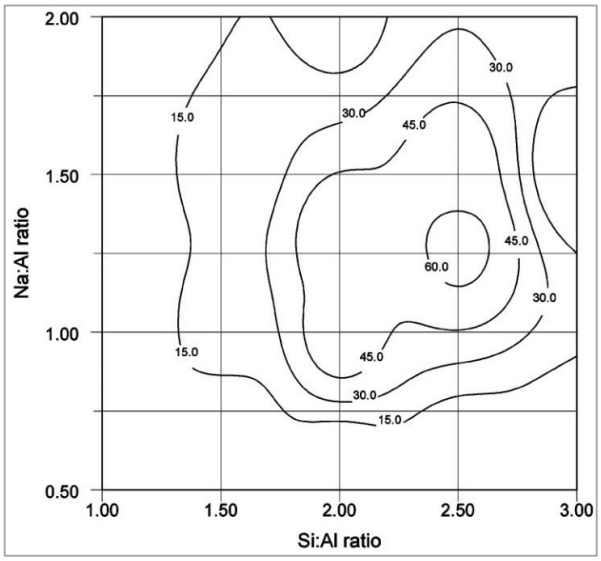

Figure 21: Compressive strength contours for metkaolin based geopolymers in terms of the ratios Na:Al and Si:Al (Rowles and O'Connor, 2003).

The degree of geopolymerization of the dissolved species is controlled by the SiO_2:Na_2O molar ratio. A rise in the content of Na_2O was seen as a responsible factor in improving the strength gained in the geopolymers, an increase in the setting rate, as well as a significant reduction of cracking in the final product (Xu and Van Deventer, 2002).

Gao *et. al* (2014) investigated the influence of SiO_2:Na_2O ratio on metakaolin based geopolymers. On the basis of the results obtained by the experiment, it was seen that the setting time of the metakaolin-based geopolymer increased with the SiO_2:Na_2O ratio due to the viscous property of the sodium silicate. When the ratio of SiO_2:Na_2O in geopolymers was recorded as 1.50, the sample showed less porosity, and thus better compressive strength (Gao *et al.*, 2014). In yet another study carried out by Soleimani *et al.* (2012), metakaolin geopolymer was manufactured with different Na_2O:SiO_2 activator ratios ranging between 0.3 and 1.1, and cured at room temperature for 1 and 4 weeks. According to this study, when the sample's ratio of Na_2O:SiO_2 was raised up to 0.6, the strength of the samples increased and reached 32

MPa after 4 weeks of curing (Soleimani *et al.*, 2012).

The compressive strength of geopolymers can also be improved by optimizing the SiO_2:Al_2O_3 ratio. One way of optimization is to combine two different aluminosilicate source materials in order to adjust the ratio (He *et al.*, 2013, Yan and Sagoe-Crentsil, 2012). Nazari *et al.*(2011) proposed a new and innovative way to alter the chemical composition of the resulting geopolymer by mixing recycling husk bark-ash, a high silica source, with fly-ash. Various concentrations of NaOH i.e. 4, 8 and 12 M as well as sodium silicate were used as chemical activators for the purpose of stabilizing the mix. Here, the ratio of Na_2SiO_3:NaOH and the chemical activator to solid source material was fixed at 2.5 and 0.4. Husk bark-ash was loaded to the mix at varying amounts (20, 30 and 40 wt. %). Following that, the samples were left for 24 hour for pre-curing, and then they were exposed to oven curing at 80°C for at least 36 hours. In the end, the authors concluded that a rise was observed in the compressive strength of the blended husk bark-ash and fly-ash geopolymer at almost every single fly-ash replacement level. Furthermore, samples with fly-ash replacement of 30% and any concentration of sodium hydroxide solutions showed the greatest values of compressive strength among the various geopolymer matrices being studied. The strength values of all mixes were found to range somewhere between 20 and 30 MPa (Nazari *et al.*, 2011).

The alkalinity of alkali reactant solution can be expressed in the form of Na_2O:H_2O. It has been reported that even though Na_2O:H_2O does not affect or alter the nature of the final product, the ratio holds considerable importance (Rahier *et al.*, 1997). It has been observed that an increase in Na_2O:H_2O ratio can be held responsible for enhanced dissolution ability as well as the mechanical strength development within the various clay-based geopolymers (Xu and Van Deventer, 2000) According to Latella *et al.* (2008), the low content of water (H_2O:Na molar ratio less than 5.5) was responsible for cracks formation in the sample after 10 days of curing. Furthermore, higher amounts of porosities were seen developing in geopolymers with the molar ratio H_2O:Na=6. However, when the molar ratio equals to 5.5, the geopolymer matrices gained the highest bulk density among other samples. Table 6 shows the bulk density and open porosity of metakaolin geopolymer samples in terms of

H_2O:Na molar ratio as tested on the 7th day after preparation. (Latella *et al.*, 2008).

Table 6: Open porosity and bulk density values in terms of the molar ratio H_2O:Na for metakaolin based geopolymers.

H_2O/Na molar ratio	Open porosity (%)	Bulk density (g/cm3)
2	6	1.85
4	12	1.64
4.5	16	1.55
5.5	20	1.57
6	30	1.30

2.2.6.3 Effect of Water Content on Mechanical Properties of Geopolymers

When it comes to the alkali activation reaction, the process of geopolymerization typically includes a reaction between the dissolved species of alumina and silica. This chemical reaction takes place in a highly alkaline environment. In a geopolymer system, water simply provides a medium of transportation between the dissolved alumina and silica ions (Yunsheng *et al.*, 2010). Furthermore, water can also give workability to the freshly prepared pastes since it does not contribute to the reaction directly (Chindaprasirt *et al.*, 2007, Jansen and Christiansen, 2015).

Still, the addition of water during the formation of the geopolymer is always seen with concern, since it is seen to be responsible for the dilution of alkalinity of the system as well as the transportation of ions away from the reaction zone (Barbosa *et al.*, 2000, Zuhua *et al.*, 2009). Since the entire reaction is a water releasing process, it may thwart the process of geopolymerization (Davidovits, 2008). According to Rahier *et al.* (2007), either too high or too low concentration of water content in the reaction can be held responsible for decreasing the geopolymerization process. The amount of OH^- ions is affected by the water content in the geopolymeric reaction, which in turn affects the efficiency of the chemical reaction (Rahier *et al.*, 2007).

Apart from it all, water is seen to have a direct effect especially on the open porosity as well as the density of the geopolymer matrices. More often than not, higher level of water results in an increase in the total porosity of the geopolymer (Zhao *et al.*,

2009, Lizcano *et al.*, 2012, Latella *et al.*, 2008). This causes a decrease in the mechanical strength of geopolymer matrices. Figure 22 shows Young's modulus (E) and cold crushing strength (CCS) versus porosity of four meta-kaolin-based geopolymer matrices as obtained by Latella *et al.*(2008). The porosity of all samples is seen to be inversely proportional to the strength.

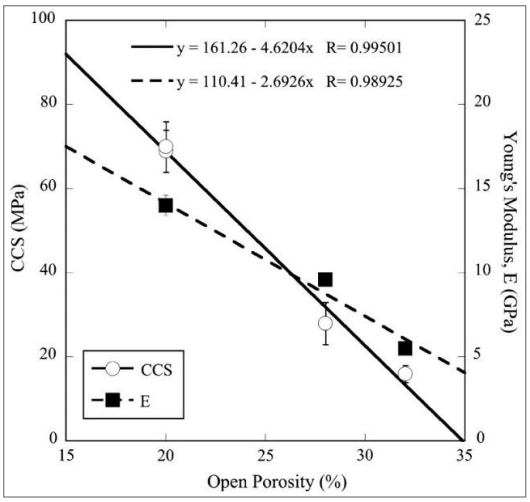

Figure 22: The inverse relationship between open porosity and both cold crushing strength (CCS) and Young's modulus (E) for geopolymer (Latella *et al.*, 2008).

Geopolymer's water content, as Ahmari and Zhang (2010) and others found, significantly affects its performance and mechanical strength. In particular, they looked at how initial water contents affected UCS (or unconfined compressive strength) in copper mine-tailing geopolymer. More specifically, they created their geopolymer samples at 6 different water content levels between 8% (the lowest) and 18% (the highest), each separated by 2% water content. The initial water contens was calculated as the ratio (by mass) between water in sodium hydroxide activating solutions and solid contents in the mixture. Those geopolymer pastes were then placed inside steel molds, whereby they were compressed until a saturation state was achieved. The samples were then tested after one week. Results showed that as the initial water content increased, UCS increased in all geopolymer samples (Figure 23). Samples exhibited UCS of 33.7 MPa were prepared with an initial water content of 18% (and 0.2 foaming pressure). Such improvement in the mechanical performance of geopolymers was ascribed to the role of water plays as liquid medium during geopolymerization (Ahmari and Zhang, 2012). Similar results were

also observed in other experimental study by Zhao and cowarkers (2009). Compressed autoclave bricks of alkali-activated material and low-level silicon tailings (both slag and fly-ash) reached peak strength of 16.0 MPa at water percentages ranging between 6.5 and 8.0 wt%. Higher amounts of water content, however, resulted in decreased compressive strength (Zhao *et al.*, 2009).

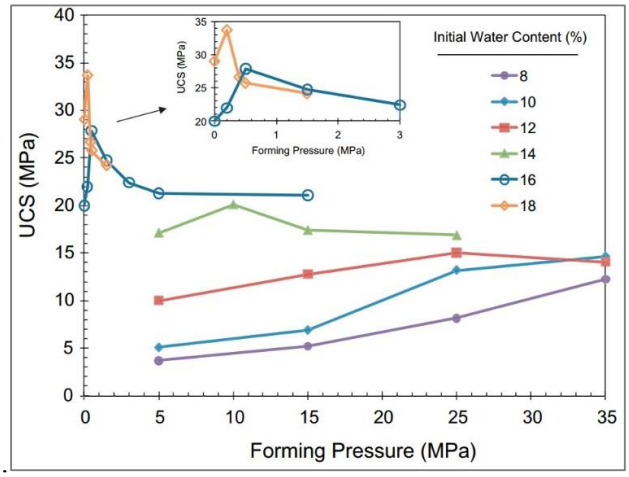

Figure 23: Unconfined compressive strength versus forming pressure for geopolymers prepared at different initial water contents (Ahmari and Zhang, 2012).

Water dependency is also determined by other mixing parameters related to the raw materials and alkali activator in use such as solid:liquid ratio, alkali concentration, as well as alkaline reactant ratios. Komljenovic *et al.* (2010) noted potentially significant effect in water:fly-ash ratios on geopolymers strength, depending on the type of activator used. In general, the geopolymer's compressive strength increased with decreased water:fly-ash ratios. In potassium hydroxide activated geopolymers, however, the geopolymers displayed lower strength at low water:fly-ash ratios. This can be attributed to the low activation potential in the case of potassium hydroxide when compared to other activators (Komljenović *et al.*, 2010).

Also noteworthy is how source material fineness affects water demand. For instance, metakaolin requires higher liquid demands compared to fly-ash, due to differing particle shapes. Metakaolin's shape is that of structured layers, whereas fly-ash particles are spherical. As the layered structure limits particle mobility during mixing, it is consequently less workable, and metakaolin geopolymers require lower solid:liquid ratios when compared to fly-ash for homogeneous mixing. According to

Kong *et al.* (2007), the ideal solid:liquid ratios for fly-ash and metakaolin geopolymers were 3.0 and 0.80, respectively. Beyond aforementioned ratios, pastes were found to lose workability in both cases (Kong *et al.*, 2007).

2.2.6.4 Effect of Curing Conditions on Mechanical Properties of Geopolymers

Better durability and mechanical performance require suitable curing temperatures (Komnitsas and Zaharaki, 2007). Heat increases reaction rates by accelerating dissolution from aluminosilicates into alumina and silica species, and thus facilitating polycondensation and geopolymer paste hardening (Alonso and Palomo, 2001, Sathonsaowaphak *et al.*, 2009, Kong *et al.*, 2008). Thus, heat is required to initiate the geopolymerization reaction by surpassing the reaction's thermal activation point. Evidently, if temperatures are very high, or the exposure time is too long, the process can also cause a weakening in the material strength (Pangdaeng *et al.*, 2015).

As a result, many attempts to study varied curing temperatures ranging from room temperature to 120 ° for geopolymerization reactions have been reported (Giasuddin *et al.*, 2013, Aydin and Baradan, 2012, Ahmari *et al.*, 2012, Ridtirud *et al.*, 2011, De Vargas *et al.*, 2011, Bakharev, 2006, Mishra *et al.*, 2008).

Palomo *et al.* (1999) reported that geopolymer matrices when cured for 24 h at 85°C gained much greater compressive strength than when cured at 65°C. However, if the curing time extended to more than 24 h, increased strength was much less (Palomo *et al.*, 1999b). Other research found that curing metakaolin geopolymers at ambient temperatures proved unfeasible, though increased temperatures (40°C through 100°C) resulted in strength gains after curing 1-3 days. However, curing for longer durations or at higher temperatures caused the samples to fail later (Heah *et al.*, 2011). Also, Rovnanik (2010) noted that when metakaolin-based geopolymers were cured at higher temperatures (40-80°C), they showed deterioration of their compressive strengths after 28 days as compared to samples cured at ambient or even slightly decreased temperatures (see Figure 24) (Rovnaník, 2010).

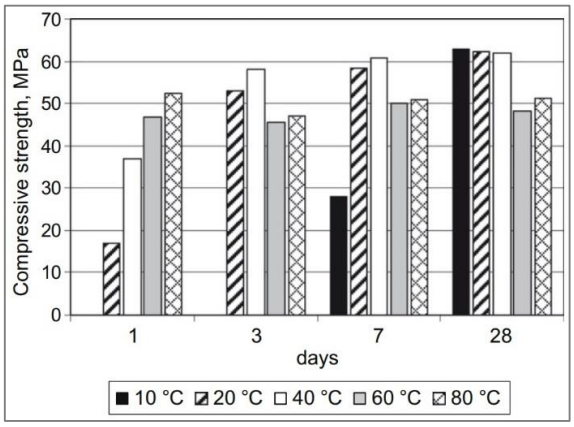

Figure 24: Development of compressive in geopolymers cured at 10, 20, 40, 60 and 80 °C over a period of 1, 3, 7, and 28 days (Rovnaník, 2010).

Another experimental investigation found that 90°C is the best curing temperature that produced the greatest unconfined compressive strengths in geopolymer. Moreover, temperatures higher than 90°C resulted in a significant reduction in the unconfined compressive strengths. Too high of a curing temperature results in rapid polycondensation, as well as excessive geopolymeric gel formation, which hinders unreacted alumina and silica dissolution. Additionally, excessively high temperatures cause pore solutions to rapidly evaporate, which can lead to incomplete geopolymerizations (Ahmari and Zhang, 2012). Another similar study found higher curing temperatures (in this case, 60°C) resulted in rapid strength development in the early curing stages of geopolymers– the first 28 days (Figure 25). However, after 28 days of curing, further strength development proved negligible (Ridtirud *et al.*, 2011).

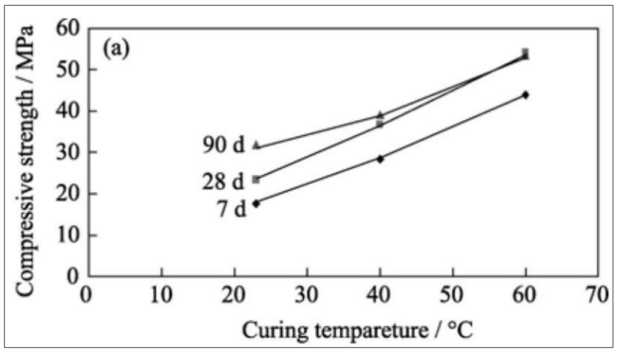

Figure 25: Development of compressive in geopolymers cured at various temperatures over a period of 7, 28 and 90 days (Ridtirud *et al.*, 2011).

According to Rovnanik (2010), high curing temperatures can result in the development of large pores which affects the strength of geopolymers negatively. At temperatures of 60°C and 80°C, samples showed high strength; but with a reduction of strength after 4 weeks. On the other hand, geopolymers exposed to temperatures of 20°C or 40°C show an increase in strength up to 4 weeks of testing (Rovnaník, 2010). However, if the geopolymers were cured in water with say 20°C, low strength would be obtained. This implication is believed to be as a result of leaching of dissolved species out from geopolymer's surfaces (Zuhua *et al.*, 2009).

Also, high temperature curing would certainly raise the tendency of geopolymer matrices to be cracked. The inclination to cracking in geopolymers is ascribed to the rapid loss of water and reduction of the open porosity (Perera *et al.*, 2007). The rapid evaporation of mixing water eliminates the development of the desired strength. Therefore, it is often recommended to seal the samples of geopolymers at surfaces exposed during curing. A small amount of structural water should be held in the system to prevent cracking (Khalil and Merz, 1994, Van Jaarsveld *et al.*, 2002). Zuhua *et al.*, (2009) pointed out that water traveling and liberated to the surface of the calcined kaolin-based geopolymers through capillary action will result in the reduction of the structural water even in a sealed environment (Zuhua *et al.*, 2009).

Pre-curing of geopolymer pastes before being exposed to the regular curing has been proven to further augment their strength (Kani and Allahverdi, 2009, Perera *et al.*, 2007, Kim and Kim, 2013). This pre-curing process is necessary for the consistent development of strength during the entire period, and good strength at early stages can be obtained. Additionally, it lowers the porosity of geopolymer's matrix, and thus more water can be retained within the paste (Perera *et al.*, 2007). Kim and Kim suggested that the process of pre-curing at 75°C for 3h and then 4 weeks curing at room temperature produces high strength (51.06 MPa) metakaolin geopolymers (Kim and Kim, 2013).

Nazari *et al.*, (2011) examined the impact of curing temperature on the compressive strength of geopolymers produced from a combination of fly-ash and rice husk ash. A 24 hour pre-curing time was conducted before casting to increase the consistency of the polymeric products prior to the heat being applied. Once the period of pre-

curing was completed, the samples of geopolymers were exposed to temperatures ranging from 50°C to 90°C for 36 hours. Based on the outcome from the inclusive developed strength, the maximum curing temperature of the entire mixtures at 1 and 4 weeks of curing was 80°C. Additionally, the compressive strength of samples decreased after curing temperatures and time of curing were increased. This is because elevated curing temperatures can destroy the granular structural of the geopolymers. Elevated temperatures in curing also led to a contraction of the geopolymer gel and shrinkage of the matrices (Nazari *et al.*, 2011). A method to reduce high temperature curing time of high calcium fly-ash was proposed by Chindaprasirt *et al.*(2013). The outcome was that by exposing the specimens to microwave heating of 5 minutes combined with traditional oven treatment for 6 hours at 60°C, the compressive strength achieved was higher when compared to the specimens cured for 24 hours at 60°C with no microwave curing (Chindaprasirt *et al.*, 2013).

2.2.7 Behaviour of Geopolymer Matrices at Elevated Temperatures

In recent years, many investigations into the resistance of geopolymer concretes to high temperatures have been conducted. One of the necessities for safety when designing construction materials is the aptitude to hold against high temperatures, which can result in spall due to increased fragility and reduced permeability. The effect of high temperatures on the geopolymer produced using metakaolin and fly-ash in varied proportion of mixtures has been presented by Kong *et al.* (2007). The strength of fly-ash-based geopolymer became firmer after it was exposed to elevated temperatures (800°C). On the other hand, the strength of the subsequent metakaolin geopolymer decreased after a similar exposure. The study revealed that the fly-ash based geopolymers have numerous small pores that enabled moisture escape during heating, therefore leading to less damage on the geopolymer matrix. However, metakaolin geopolymers do not have similar microstructure. The strength development in fly-ash geopolymers during heating is also ascribed to the sintering reaction of unreacted fly-ash particles (Kong *et al.*, 2007).

Kong and Sanjayan (2010) in a different study carried out an investigation into the

effect of high temperatures on geopolymer pastes made from fly-ash. Different experimental parameters such as aggregate sizing, aggregate type, specimen size and super plasticizer type have been examined. The study identified specimen size and aggregate size as two primary factors governing the geopolymer's behavior at elevated temperature (800°C). As can be seen in Figure 26, the results showed that aggregate sizes with size greater than 10mm produced greater performance in strength in the geopolymer concrete at increased temperatures. Furthermore, the reduction in mechanical strength at increased temperatures was due to the thermal mismatch between the aggregates and the geopolymer matrices (Kong and Sanjayan, 2010).

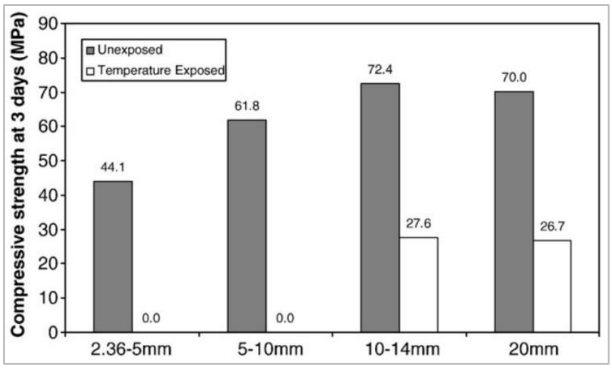

Figure 26: Effect of exposed temperature (800°C) and aggregate size on the compressive strength of geopolymer (Kong and Sanjayan, 2010).

Another observation was made by Bakharev (2006) suggested that the thermal stability of class- F fly ash geopolymers made using sodium activators was not high, and considerable variations in the microstructure were observed. At temperatures of about 800°C, the strength of the concrete decreased as a result of increased average pore size where the amorphous structures were substituted with crystalline Na-feldspars. The opposite effect happened when the potassium silicate was used as an activator as it remained mostly amorphous to 1200°C. When firing geopolymer materials, the average pore size was decreased and improvements were observed on the compressive strength of geopolymers. In a different study, the effect of fired temperature on class-F fly-ash based geopolymers activated using sodium and potassium silicate has been reported. When exposing the material to increasing temperature ranging from 800°C to 1200°C, high shrinkages with increased changes in compressive strength were reported (Bakharev, 2006).

2.3 Fibre Reinforced Geopolymer Composites

2.3.1 Overview on Composite Materials

A composite material consists of at least two constituent materials which interact macroscopically. Composite materials are made up of: (a) a reinforcing material, such as fillers, particles, fibres, and fabrics, and (b) a matrix such as ceramics, metals, and polymers. The matrix material holds the reinforcement material so that a designed shape is achieved, and the reinforcement material enhances its properties.

A fibre-reinforced composite (FRC) is a composite made up of fibres and a matrix. In FRCs, the fibres and matrix will retain their respective physical and mechanical identities. They are able to achieve properties that are unobtainable outside of fibre-matrix combination. The fibres act as load-carrying members that provide FRCs with their strength. The matrix maintains the fibres in the desired orientation and provides protection for them from external damage.

Fibres, synthetic and natural, are used in a range of matrices, such as ceramic-based, polymer-based, and metal-based matrices. However, there are unique advantages of using synthetic fibres over natural and vice versa. In general, composites reinforced with synthetic fibres will demonstrate superior mechanical performance than those fabricated with natural fibres due to the high mechanical strength of synthetic fibres. Synthetic fibres; however, are expensive in economic and environmental terms.

Applications of FRCs are widely used in the building and construction industry as well as in aerospace and sporting equipment. FRCs have been widely commercialized for the industrial and manufacturing sectors due to their mechanical properties such as strength and stiffness (Agarwal *et al.*, 2006).

In FRCs, continuous and discontinuous fibres can be used. Continuous fibres, also known as long fibres, are used in a dispersed phase to form what is known as a continuous fibre reinforced composites. Effective transfer of applied load is typically transferred to the long fibres or fabric sheets without obstacles. On the other hand, discontinuous fibres tend to be poor stress bearers when compared to long fibres. By

definition, discontinuous fibres are shorter and offer less strength to the resultant composites when compared to the option of continuous fibres. The shorter the fibre, the lower the stress it will bear (Callister, 1991). In short fibre reinforcement, an effective transfer of load will occur when the individual fibre lengths is optimal. Such length will occur when each discontinuous fibre is short enough to avoid entangling itself or other discontinuous fibres, but long enough to maintain a fibrous nature.

2.3.2 Parameters Influencing the Properties of Fibre Reinforced Composites

The resultant reinforcement imparted by short or long fibres in the composites is governed by parameters that include fibres chemical properties, the preparation procedure and fibre-matrix interfacial adhesion (Bentur and Mindess, 2007, Balaguru and Shah, 1992, Aldousiri *et al.*, 2013, Silva *et al.*, 2011).

2.3.2.1 Properties of the Fibres

Synthetic fibres such as glass fibres generally have higher strength and stiffness than natural fibres. Although the specific properties of natural fibres can be comparable or higher than that of glass fibres due to their lower density. In plant fibres, superior mechanical strength can be attained in fibres containing higher amounts of cellulose and aligned micro-fibrils in the fibre direction. This is more likely to take place in bast fibres such as flax, jute and hemp (Pickering *et al.*, 2016). Properties of natural fibres differ significantly according to their chemical compositions and microstructures, which depend on the fibre type, growing and harvesting environments and preparation processes (Bos *et al.*, 2002, Pickering *et al.*, 2007).

2.3.2.2 Preparation Procedure of the Fibres-Reinforced Composites

The experimental procedures of incorporating fibres in the matrices influences significantly the mechanical performance of the resultant composite. Some of the factors to take into consideration prior preparation includes the fibres volume (content), the fibres dispersion, mixing process and fibres orientation in the matrices.

Fibre volume fraction is an essential parameter that significantly impacts the mechanical properties of composite materials. Generally, when fibres are incorporated into a matrix, the resultant composite exhibits higher mechanical strength. This is due to the high capacity of fibres to load the stress applied on the composites. Nevertheless, incorporating fibres does not lead to enhanced properties for unlimited volume fractions. An optimum concentration of fibres when the composite exhibits the highest strength must be considered. Once the optimal content of fibres is achieved, additional fibres are expected to lead to a reduction in the strength. This is due to the insufficient resin material to bond with fibres, which could result in agglomerated fibres being forced inside the composite, and therefore weaker composites (Alomayri and Low, 2013, Bibo and Hogg, 1996, Curvelo *et al.*, 2001)

One of the main concerns in incorporating short fibres within the resin matrix is their uniform distribution. Bad dispersion might lead to the fibre agglomerations during mixing, which will produce fibre-rich regions and matrix-rich regions. Both fibre-rich regions and matrix regions are vulnerable to brittleness and micro cracking (Balaguru and Shah, 1992, Bentur and Mindess, 2007, Taib, 1998). Alomayri *et al.* (2013) studied the effect of adding short cotton fibres on the mechanical properties of geopolymer composites. The authors found that cotton fibres improved the mechanical performance of the composites only modestly. When the fibres agglomerated within the geopolymer matrix (Figure 27), a reduction in the strength was observed (Alomayri *et al.*, 2013a).

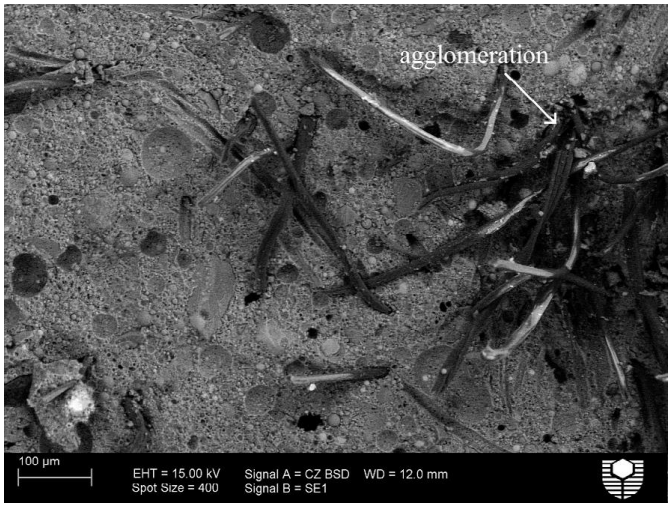

Figure 27: SEM showing agglomeration of short fibres in geopolymer matrix (Alomayri *et al.*, 2013a).

To avoid this condition and to achieve highest strength, fibres must be dispersed homogeneously throughout the matrix during mixing process. In general, there are two mixing procedures to incorporate short fibres into the resin matrices, wet and dry mixing methods. In the wet-mixing procedure, short fibres are mixed with liquid components first (water, solutions) and then dry materials are added to the mixture. In the dry-mixing procedure, short fibres are mixed with dry materials for few minutes first and then the water and liquid solutions are added during further mixing (Balaguru and Shah, 1992, Bentur and Mindess, 2007).

Another critical factor to consider during designing the composites is the orientation of fibres within the matrix. It is an important factor because the fibres alignment with regard to the loading axis controls the way of transferring the stress from the matrix to the fibres (De and White, 1996, Aldousiri *et al.*, 2013). Continuous fibres (fabrics) can be aligned either vertically or horizontally with respect to the loading axis (Figure 28). The maximum mechanical strength can be attained when fabrics oriented horizontally to the applied force. However, composites with fabrics directed vertically to the applied load during the flexural strength test showed lower results since the applied load decomposes and detaches fabrics layers from the composites. Figure 29 shows the flexural stress–strain curves of geopolymer composites reinforced with cotton fabric as tested in horizontal (Figure29-a) and vertical (Figure 29-b) orientations. It can be seen that samples laid horizontally exhibited higher

strain, while the vertically aligned samples showed catastrophic fracture behaviour (Alomayri *et al.*, 2014a).

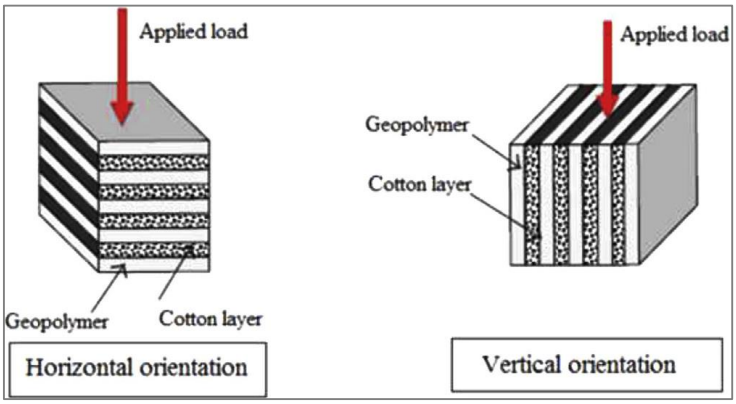

Figure 28: Schematic representation of the composites orientation to the applied force (Alomayri *et al.*, 2014a).

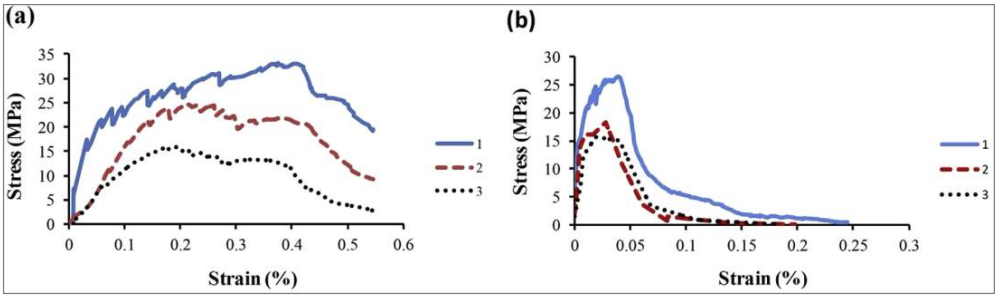

Figure 29: Stress/strain behaviour of geopolymer composites reinforced with various volume content of cotton fabric as oriented (a) horizontally and (b) vertically to the applied force on the flexural test (Alomayri *et al.*, 2014a).

The rule of mixture concept estimates the elastic modulus of a composite by taking into account the volume fraction of both the matrix and the fibres, and the direction of the applied load. When a composite is exposed to a load that is parallel to the fibres direction, the elastic modules of the composite E_c is given by (Callister, 1991):

$$E_c = E_m(1 - V_f) + E_f \mathrm{V_f} \tag{2.3}$$

Nevertheless, when the load is applied vertically to the fibres, the elastic modulus of the composite is estimated by the equation (Callister, 1991):

$$E_c = \frac{E_m E_f}{(1-V_f)E_f + V_f E_m} \quad (2.4)$$

Where E_m and E_f are moduli of matrix and continuous fibres, respectively. While V_m and V_f are volume fractions of matrix and continuous fibres, respectively.

2.3.2.3 Fibre-Matrix Adhesion

The fibre-matrix adhesion is an important factor that determines the mechanical performance of composites. On the subject of natural fibres, a number of researchers reported that plant fibres exhibit relatively weak adhesion bonding when combined with cementitious materials. The existence of chemical contents such as wax in plant fibres tends to decrease fibre-matrix interface. Studies have shown that treating plant fibres by chemical processes or coating fibres with polymer such as epoxy have marginally enhanced the adhesion bonding strength with matrices. Accordingly, the mechanical performance of composites reinforced with treated plant fibres is slightly improved (Sedan *et al.*, 2008, Pacheco-Torgal and Jalali, 2011, Hakamy *et al.*, 2016, Bledzki *et al.*, 1996, Bledzki and Gassan, 1999).

2.3.3 Synthetic Fibres Reinforced-Geopolymer Composites

Mechanical performance of geopolymer matrices varies widely depending on the chemical composition and nature of aluminosilicate material, alkali activator and preparation process. However, geopolymers, like other ceramics, are generally brittle in nature (Pan and Sanjayan, 2010, Pan *et al.*, 2011). A composite material of geopolymer with fibre or fabric reinforcement will extend the application of geopolymers in various industries. Many researchers have studied the effect of fibres on the mechanical properties of geopolymer composites (Lembo *et al.*, 2014). For example, Puertas *et al.* (2003) studied the flexural and compressive strength of polypropylene fibre-reinforced mortars formed by adding slag, fly-ash, and slag/fly-ash at concentrations of 0%, 0.5% and 1.0% by mortar volume. The researchers determined compressive strength at day 2 and/or day 28. Table 7 presents the results of flexural and compressive strength of all composites as tested at day 2 and day 28. These researchers found that adding polypropylene fibre at 0.5% and 1.0%

concentration to slag-based geopolymer composites had no impact; at least no significant impact on compressive strength were measured at either day 2 or day 28. Additionally, they found that raising the concentration of polypropylene fibre in fly-ash-based geopolymer composite from 0%, to 0.5% and to 1.0% led to an increase in compressive strength by day 2 but an unexplained reduction in compressive strength by day 28. Slag/fly-ash-based geopolymer composites with polypropylene-fibre content increased from 0.5% to 1.0% were found to increase compressive strength marginally at days 2 and 28 (Puertas *et al.*, 2003). The study only investigated the durability of samples for up to 28 days. Clearly, further study on the effect of longer periods is necessary to gain more useful information that is vital for use in the building industry.

Table 7: Flexural and compressive strengths of geopolymer composites as tested at day 2 and day 28 (Puertas *et al.*, 2003).

Mortars	Fibre (%)	2 days		28 days	
		Flexural (MPa)	Compression (MPa)	Flexural (MPa)	Compression (MPa)
Slag	0	7.2	59.5	7.8	89.5
	0.5	6.5	60.1	7.6	90.0
	1	6.4	59.0	6.7	79.0
Fly-ash	0	3.9	24.5	6.8	39.4
	0.5	4.5	33.9	6.1	35.8
	1	4.9	34.3	5.5	26.9
Fly-ash/slag	0	3.6	11.8	4.6	30.0
	0.5	3.4	13.5	4.8	31.2
	1	2.9	13.6	4.8	30.1
Cement	0	6.3	39.1	7.8	53.0
	0.5	5.8	35.5	7.5	48.2
	1	5.4	38.9	7.4	47.6

In a study by Zhang *et al.* (2009), compressive strengths in reinforced composite and non-reinforced composite were compared while using fly-ash and kaolin in geopolymer preparation. They stated that after adding polypropylene-fibre of 0.5 wt.%, the overall compressive strength increased. The increase was observed to be 67.8% on day 1 and at 19.5% on day 3. Although, when the content of polypropylene was over 0.5 wt. %, the rate of improvement in compressive strength decreased. The authors discovered a major improvement on the first and third day of test. Additional proportions equalling 0.25, 50 and 0.75 wt.% were also studied. The authors found

that the flexural strength of the composites improved as the fibres contents increased (Zhang *et al.*, 2009). These results are in contrast with the earlier results presented by Puertas *et al.* (2003) where the additional polypropylene fibres did not improve the composite's flexural strength on the 2nd and 28th test days. The poor performance observed by Puertas and coworkers may be attributed to inferior workability because of added polypropylene fibres within the geopolymer paste (Shaikh, 2013).

Yunsheng *et al.* (2006) studied the effect of increased amount of polyvinyl alcohol fibres on the impact strength of metakaolin-geopolymer composites. The strongest impact strength was found within the non-reinforced mortar at 450N. The pure material was found to have a short internal displacement at 0.84 mm due to the brittleness and susceptibility to failure after exceeding the peak load. The study reported a transformation from brittleness to ductility once polyvinyl alcohol fibres were increased to 2.0% by volume. The impact curve exceeded the peak load exhibiting a strain-hardening performance and showing ductility. The authors found that the peak load was 429.6N and displacement was about 2.5mm. When the peak load amount is exceeded, bearing capacity decreased until a displacement of 7.5 mm is reached. The impact performance of geopolymer composites is presented in Figure 30. The researchers reported that with an additional 10 wt.% of fly-ash, the absorbed energy increased from 1833 mJ to 2108 mJ (15% improvement). However, greater concentrations above 30% fly-ash presented a reduction in the impact resistance, and at 50 wt.% the reduction begins to change significantly, with stiffness and impact strength showing some enhancement. Yunsheng *et al.* (2006) reported that geopolymer with 50% fly-ash showed an increase in toughness and stiffness, by 28.7% and 39.1%, respectively, but a decrease in impact strength by 37.4% when compared to composites not using fly-ash (Yunsheng *et al.*, 2006). Hitherto, the researchers have presented the optimum replacement amount of fly-ash, but the ideal content of polyvinyl alcohol fibre has not been specified in the study. It is critically important to determine the optimum addition of fibres since the workability and physical properties of the pastes vary with varying the source materials. Accordingly the ideal content of each type of fibres needed to design the composites achieving the highest mechanical properties will vary.

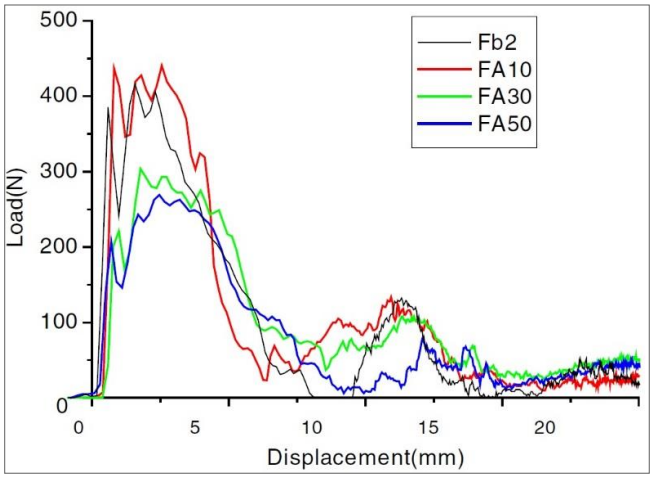

Figure 30: Impact curves of geopolymer composites with various contents of fly-ash(Yunsheng *et al.*, 2006).

Natali *et al.* (2011) presented a research on the flexural strength in metakaolin/slag-geopolymer composites reinforced with E-glass, polyvinyl-alcohol (PVA), high tenacity carbon (HT) and polyvinyl-chloride (PVC). Improvements were observed in the flexural strength when adding PVA, HT carbon, E-glass, and PVC. The study concluded that each fibre type has led to a satisfactory bridging effect during the flexural tests. Additional 1.0 wt.% of the above-mentioned fibres to geopolymer composites increased the flexural strength between 30% and 70%. The authors found that PVC and carbon fibres provided the best improvement in preventing post-crack behaviour (Natali *et al.*, 2011). The reinforcements gave composites the greatest ductility at the first crack load. Table 8 and Figure 31 present toughness indices and load-deflection curves for the geopolymer composites, respectively.

Table 8: Resilience and toughness indices for geopolymer composites (Natali *et al.*, 2011).

Samples	Resilience* [J/cm^2]	Toughness Indices		
		I_5	I_{10}	I_{20}
GS	2.2	1.0	1.0	0
FcGS	3.1	4.6	6.5	8
FgGS	2.2	1.7	1.9	2.0
FpvaGS	2.6	3.1	3.4	3.5
FpvcGS	2.4	2.0	3.2	4.9

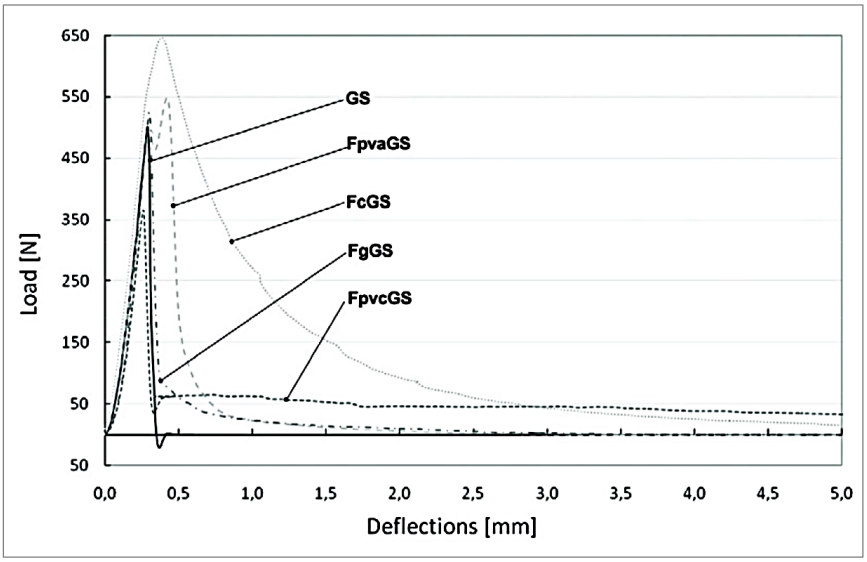

Figure 31: Load-deflection curves of geopolymer composites (Natali *et al.*, 2011).

Lin *et al.* (2009) also presented a study on the flexural strength of carbon fibre reinforced geopolymers composites. A solution of K_2SiO_3 was used as alkali activator and metakaolin as raw aluminosilicates material. Composites were synthesized by varying the amounts of carbon fibres (3.5, 4.5, 6 and 7.5 wt.%). Table 9 presents the results of density and mechanical properties for all samples. The composite's density increased with increasing fibre content due to the high density of carbon fibres. As the carbon-fibre volume fraction increased from 3.5% to 4.5%, the flexural strength of composites also increased. At volume fraction 4.5%, the flexural strength of geopolymer composite improved approximately by 475% when compared to the control sample. The addition of 6.0 and 7.5% of carbon fibres caused the strength to be reduced as shown in Figure 32. Lin *et al.* (2009) argued that the reduction may be due to the damage in the fibres, as high pressures formed shear stress in the fibre/matrix interface region (Lin *et al.*, 2009).

Table 9: density and mechanical results of all samples (Lin *et al.*, 2009).

Materials	Density (g/cm^3)	Flexural strength (MPa)	Work of fracture (J/m^2)	Young's modulus (GPa)
Geopolymer	1·42	16·8 ± 0·7	54·2 ± 4·6	8·61 ± 0·43
3·5 vol.% C_f/geopolymer	1·42	91·3 ± 1·3	6435·3 ± 319·9	4·74 ± 0·63
4·5 vol.% C_f/geopolymer	1·49	96·6 ± 4·9	5915·2 ± 151·2	12·04 ± 0·45
6 vol.% C_f/geopolymer	1·56	87·4 ± 4·5	3926·3 ± 116·2	20·46 ± 1·61
7·5 vol.% C_f/geopolymer	1·67	42·0 ± 6·1	805·7 ± 49·9	17·77 ± 0·78

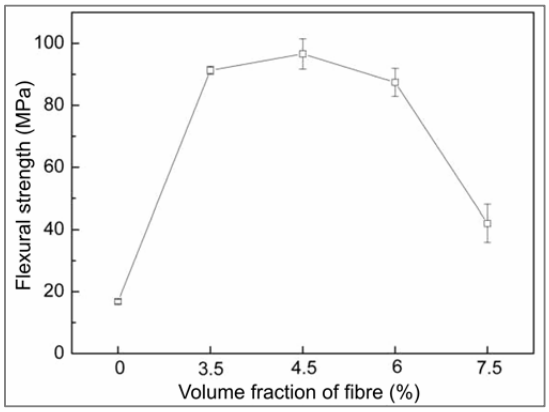

Figure 32: Flexural strength results of geopolymer composites as a function of fibres content (Lin *et al.*, 2009).

Li and Xu (2009) observed the impact strength, deformation and energy absorption in geopolymer matrices which have been reinforced with basalt fibres. The research suggested that basalt fibre-reinforced samples showed high dependency on the strain rate. That means that the impact strength improved as the strain increased. The basalt fibre reinforcement greatly enhanced energy absorption and deformation in concrete. The optimal loading for maximum energy absorption was suggested to be 0.3% volume fraction (Li and Xu, 2009).

2.3.4 Natural Fibres Reinforced-Geopolymer Composites

Hitherto, several studies have investigated the effect of natural fibres on the mechanical performance of geopolymer composites. Natural fibres have the ability to overcome the issue of geopolymer brittleness and increase its ductility. Alzeer and MacKenzie (2013) researched flexural strength in metakaolin-based composites by adding 4.0 to 10% content of unidirectional flax fibres. The composites showed improved flexural strength from 6.0 MPa to 70 MPa after adding 10% of reinforcing fibres (Alzeer and MacKenzie, 2013). Figure 33 shows the stress-strain curves for the control matrix and geopolymer composites containing various loadings of flax fibres.

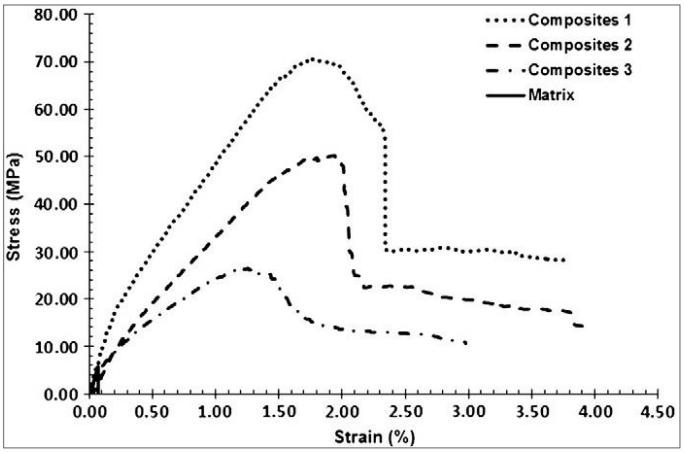

Figure 33: Stress-strain curve in control matrix and geopolymer composite containing various contents of flax fibres (Alzeer and MacKenzie, 2013).

The same authors presented a study in the mechanical performance of kaolinite-clay geopolymer composites reinforced with Merino wool and carpet wool (Figure 34). The wool fibre surface was given a chemical treatment to enhance reinforcing and alkali resistance properties. Table 10 shows the results of mechanical tests of all samples. The research found that unreinforced matrices exhibit brittle failure. However, the addition of the carpet wool that had been chemically-treated presented an increase in the averaged flexural strength by 50% and significant improvements in failure properties (Alzeer and MacKenzie, 2012).

Table 10: Results of mechanical tests of geopolymer control sample and geopolymer composites reinforced with 5% of various types of wool fibres (Alzeer and MacKenzie, 2012).

Fibre	Average fibre Content (wt. %)	Ultimate flexural strength (MPa)	Peak load (N)	Elastic modulus (GPa)
Merino wool	5	8.2 ± 1.5	25.4 ± 5.1	5.9 ± 0.5
Cleaned Merino wool	5	9.1 ± 0.6	27.8 ± 2.3	10.2 ± 1.3
Treated Merino wool	5	8.2 ± 0.8	25.0 ± 2.3	8.3 ± 1.1
Carpet wool	5	8.1 ± 2.3	19.8 ± 2.1	9.0 ± 1.9
Cleaned carpet wool	5	8.1 ± 1.5	25.8 ± 4.7	8.7 ± 2.0
Treated carpet wool	5	8.7 ± 0.5	26.6 ± 1.5	9.4 ± 0.6
Geopolymer matrix	0	5.8 ± 1.8	17.1 ± 6.0	9.6 ± 0.7

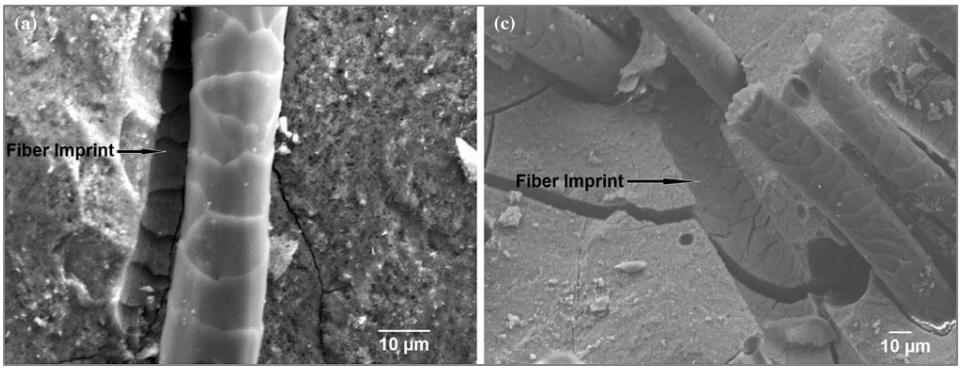

Figure 34: SEM images showing broken geopolymer composite that was reinforced with: (left) carpet wool, and (right) Merino wool (Alzeer and MacKenzie, 2012).

Alomayri *et al.* (2013) presented their findings on mechanical and fracture performance of class-F fly-ash geopolymer which has been reinforced with short cotton fibres. The study showed that mechanical properties could be improved using cotton fibres in geopolymer composites. However, the study confirmed that increasing fibre contents caused a reduction of the composite's densities and an increase in porosities. Besides, agglomeration and poor dispersion of cotton fibres were observed when high content of the fibres were incorporated, causing a reduction on the mechanical strength of geopolymer composites. The researchers concluded that the optimum flexural strength and fracture toughness was reached when fibre content used was 0.5 wt. % (Alomayri *et al.*, 2013a, Alomayri and Low, 2013). Figures 35 and 36 present the density and flexural strength of these geopolymer composites.

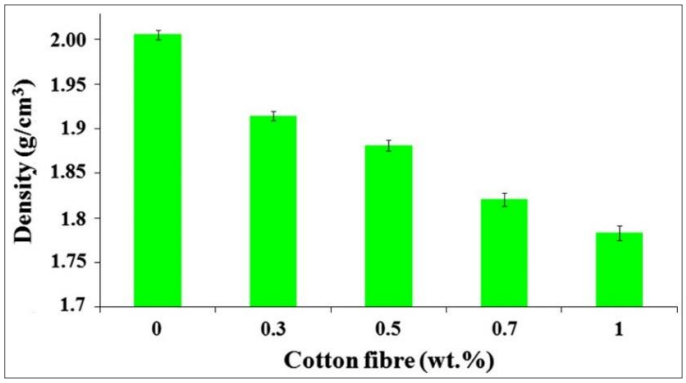

Figure 35: Density of geopolymer composites as a function of cotton fibre content (Alomayri *et al.*, 2013a).

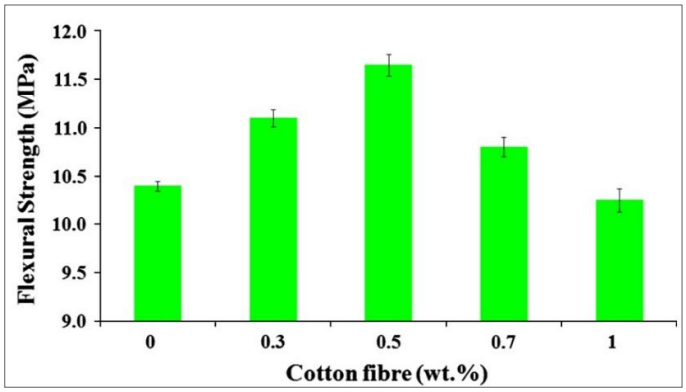

Figure 36: Flexural strength of geopolymer composites as a function of cotton fibre content (Alomayri *et al.*, 2013a).

The same authors suggested that in order to solve the problem of fibres agglomeration, geopolymer may be reinforced with cotton fabrics instead of short cotton fibres. Therefore, they reinforced fly ash geopolymer matrices with different layers of woven cotton fabrics (3.6, 4.5, 6.2 and 8.3 wt.%) using the lay-up technique. Results showed that mechanical properties were improved when cotton fabric contents are increased. Mechanical strength of geopolymer composites that were reinforced with fabrics gave superior results when compared to those reinforced with short cotton fibres (Alomayri *et al.*, 2014b). Figure 37 shows the improvement in flexural strength when the content of cotton fabric was increased. This study is comparable to the study presented by Alzeer and Mackenzie (2013) in the case of geopolymer reinforced with unidirectional flax fibres. In both of these investigations the flexural strength increased with increasing fibre contents without reaching an optimum amount of the natural fibres.

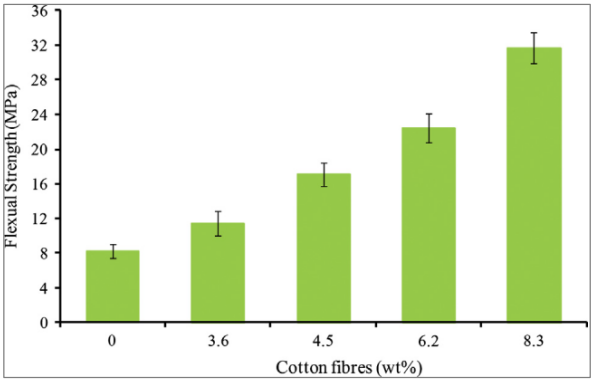

Figure 37: Flexural strength of geopolymer composites as a function of fibre content (Alomayri *et al.*, 2014b).

Korniejenko *et al.* (2016) studied the mechanical properties when reinforcing fly ash geopolymers with short natural fibres. The short fibres used were cotton, sisal, raffia and coconut. The study analysed the influence on mechanical performance when adding a variety of natural fibres to geopolymer composites. The study included the results of both flexural and compressive strength tests. The test verified that the mechanical properties of composites reinforced with cotton, sisal and coir fibres were improved. However, composites reinforced with raffia were found to be poor in its mechanical performance. It is speculated that this result was due to the fibre size and characteristics. Tables 11-12 provide a summarized version of the study's outcomes (Korniejenko *et al.*, 2016). While this study presented an interesting comparison showing the mechanical strength results of composites containing different types of natural fibres, it does not show the ductile behaviour of each composite during the flexural experiments. This can be given by presenting the stress-strain or load-mid-span deflection curves. Those curves can provide important information such as peak-loading points, strains and the toughness of each composite.

Table 11: Compressive strength values of the natural fibres- reinforced geopolymer composites at 28 days (Korniejenko *et al.*, 2016).

Sample	MPa	Standard deviation of recorded values of strengths
Geopolymer (matrix)	24.78	1.89
Geopolymer with coir fibers (1%)	31.36	10.10
Geopolymer with cotton fibers (1%)	28.42	5.30
Geopolymer with raffia fibers (1%)	13.66	1.71
Geopolymer with sisal fibers (1%)	25.16	3.43

Table 12: Flexural strength values of the natural fibres- reinforced geopolymer composites at 28 days (Korniejenko *et al.*, 2016).

Sample	MPa	Standard deviation of recorded values of strengths
Geopolymer (matrix)	5.55	0.72
Geopolymer with coir fibers (1%)	5.25	0.57
Geopolymer with cotton fibers (1%)	5.85	0.78
Geopolymer with raffia fibers (1%)	3.05	0.35
Geopolymer with sisal fibers (1%)	5.90	0.14

Al Bakri *et al.* (2013) provided a study on the compressive strength of fly-ash-geopolymer that has been reinforced with wood fibres. In sample preparation, the fly-ash was activated using 2.5 ratio of Na_2SiO_3:NaOH, and short-wood fibres were introduced into the mixture with loadings ranging between 10 wt.% and 50 wt.%. The results showed that an increase of wood fibre content caused a decrease in compressive strength of the composites at the 7th and 14th day. It is theorized that the result is due to wood-fibre acting as a filler in the matrix. Reduction is due to an increased surface areas of filler materials that bond to the geopolymer matrix which created a decrease in geopolymer's surface area (Al Bakri *et al.*, 2013). Figure 38 shows the compressive strength of the samples as a function of the fibres content at 7 and 14 days. However, this study lacked control geopolymer samples for comparison. Additionally, it is necessity to investigate the compressive strength of composites containing fibres less than 10 wt.% in order to find an optimum loading for achieving the maximum compressive strength.

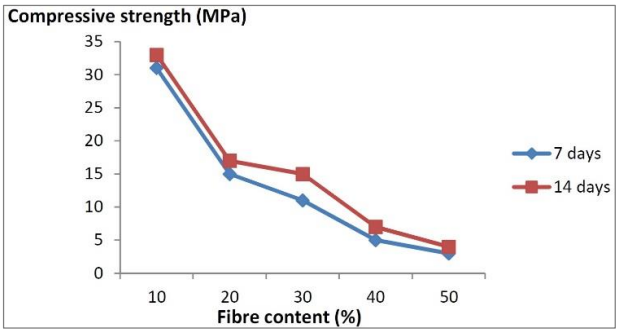

Figure 38: Compressive strength of wood fibre reinforced geopolymer composites as tested at 7 and 14 days (Al Bakri *et al.*, 2013).

Chen *et al.* (2014) investigated the flexural strength of sweet sorghum reinforced

geopolymer composites. The research found that the strength increased with fibre content up to 2.0 wt.%. However, when fibre exceeds 2.0%, the toughness, tensile and flexural strength decreased as shown in Figure 39. They concluded that 2.0 wt.% in sweet sorghum fibre is the effective amount which allows stronger loads to be distributed throughout the composite and delays the growth of micro-cracks, increasing flexural strength. However, going beyond 2.0 wt% caused poor workability, and a disproportional dispersion of the fibres causing air bubbles to become entrapped. The weakness caused concentrations of stress and a reduction of the composite's flexural strength (Chen *et al.*, 2014).

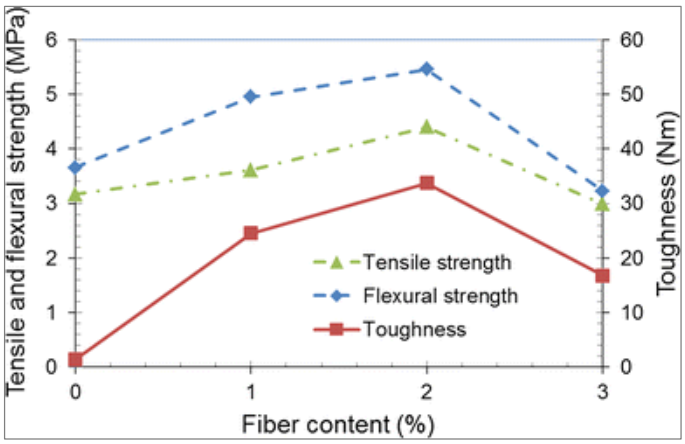

Figure 39: Splitting tensile strength, flexural strength and toughness values of geopolymer composites in terms of fibre content (Chen *et al.*, 2014).

Correia *et al.* (2013) provided an investigation on the compressive and impact properties of geopolymer composites reinforced using plant fibres. The researchers used 3.0 vol% of pineapple leaf fibres (PALF) and sisal fibres for the metakaolin-based geopolymer composites. The findings showed that pineapple leaf fibres and sisal fibres imparted an improvement in the compressive and impact strengths. The strength of the geopolymer composites with added sisal fibres was observed to be higher than pineapple leaf fibres (Correia *et al.*, 2013). Figures 40 and 41 present the compressive and impact strengths of the control sample and composites.

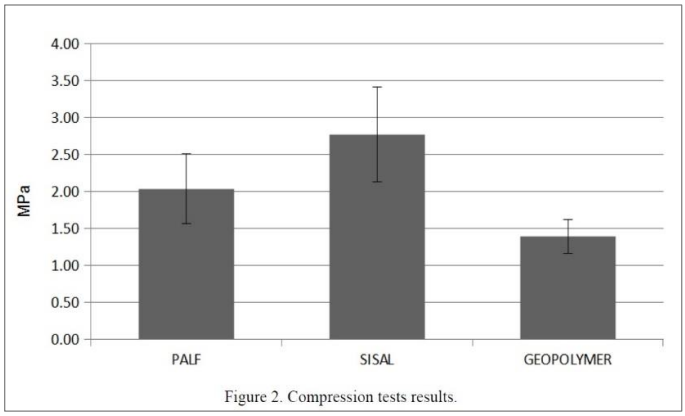

Figure 40: Compressive strength of geopolymer composites and the control sample (Correia *et al.*, 2013).

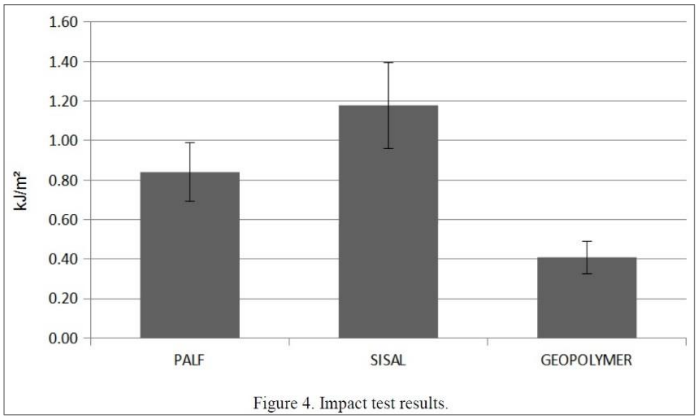

Figure 41: Impact strength of geopolymer composites and the control sample (Correia *et al.*, 2013).

2.3.5 Durability of Natural Fibre Reinforced Composites

Durability of natural fibres in composites is their capability to resist the degradation processes either by external damage such as chloride and alkali attack or internal damage such as compatibility between fibres and the resin matrices (Mohr *et al.*, 2005, Walker *et al.*, 2014, Gram, 1983, Santos *et al.*, 2015, Wei and Meyer, 2015). Geopolymers are generally high alkali matrices. Therefore, there are concerns in incorporating plant fibres in alkali-based pastes. The main concern is regarding the long-term durability of natural fibre reinforced composites. Natural fibres can be degraded and damaged in a high-alkaline environment; thereby adversely affecting the mechanical performance and durability of the composites (Hakamy *et al.*, 2016,

Aly *et al.*, 2011b, Yan and Chouw, 2015). Natural fibre degradations in alkaline environments was studied in early 1980's (Gram, 1983). The degradation mechanism was described as the decomposition of hemicellulose and linen which leads to the splitting of natural fibres into micro-fibrils as shown in Figure. 42. This effect has been observed using SEM in the case of jute fibres in cement matrix, where the natural fibres split-up and fibrillised resulting in reduction in the tensile strength of jute fibres by 76% (Velpari *et al.*, 1980). To reduce the degradation impact of natural fibres in alkaline matrices, nanoparticles can play an important role. The effect of nanoclay particles on the durability of flax fibres reinforced cement composites at 28 days and after 50 wet/dry cycles has been examined by Aly and coworkers (Aly *et al.*, 2011b). Figure 43 shows SEM images of flax fibres being removed from cement composites before and after aging. Samples loaded with 2.5 wt.% nanoclay particles showed lower deterioration in the flexural strength when compared to its counterpart control samples. This was attributed to the effect of nanoclay particles in decreasing the degradation of flax fibres. However, there is no known published research discussing the durability of geopolymer composites reinforced with natural fibres, or the deterioration of cellulose fibres in geopolymer matrices.

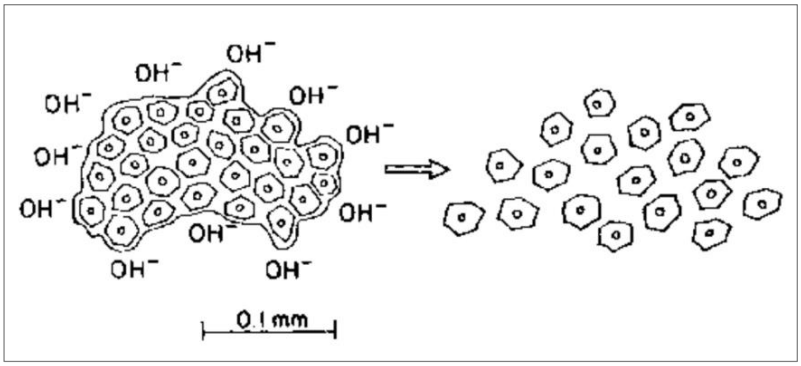

Figure 42: Scheme showing the degradation of plant fibres in alkali environment (Gram, 1983).

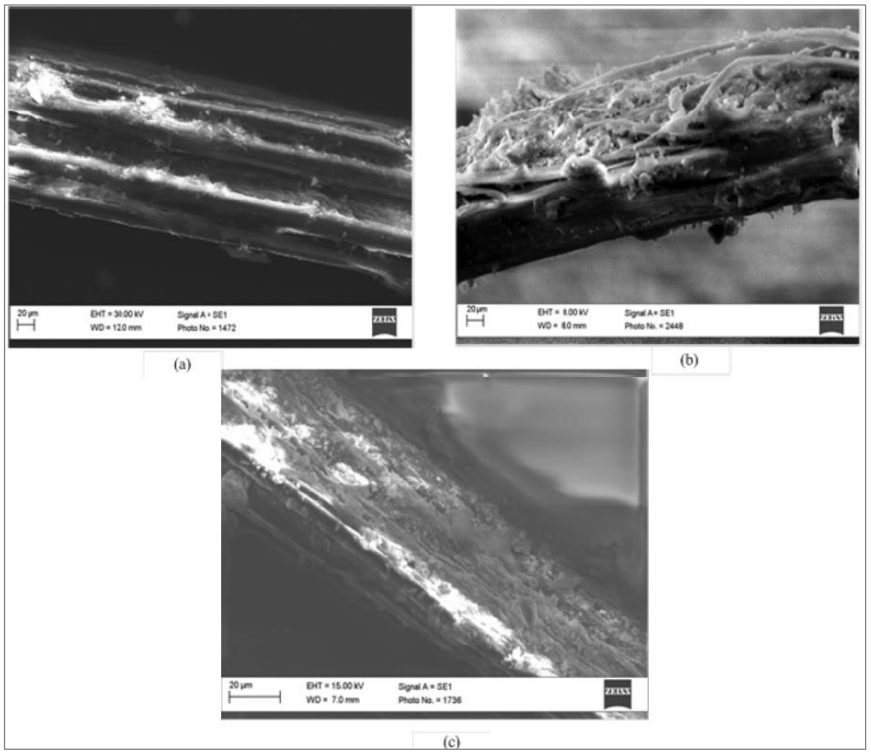

Figure 43: SEM images showing flax fibre in geopolymer: (a) before ageing, (b) after aging (c) flax fibre extracted from geopolymer with the addition of nanoclay after aging (Aly *et al.*, 2011b).

2.4 Nanoparticle Reinforced Composites

Nanomaterials, especially nanoparticles, have gained increasing attention for use in concrete within the field of construction material research. Nanoparticles are found to improve the mechanical strength of cementitious materials (Mohamed, 2016, Nazari and Sanjayan, 2015, Rong *et al.*, 2015). As the size of nanoparticles decreases, the specific surface area of the particles increases leading to increased chemical reactivity. As a result, nano-engineered concrete demonstrates higher strength than those demonstrated by high performance concrete or conventional concrete. Figure 44 provides the specific sizes of various particles used within the field of construction material research and within the industry itself (Sanchez and Sobolev, 2010). This section discusses the influence of incorporating nanoparticles in cement and geopolymers.

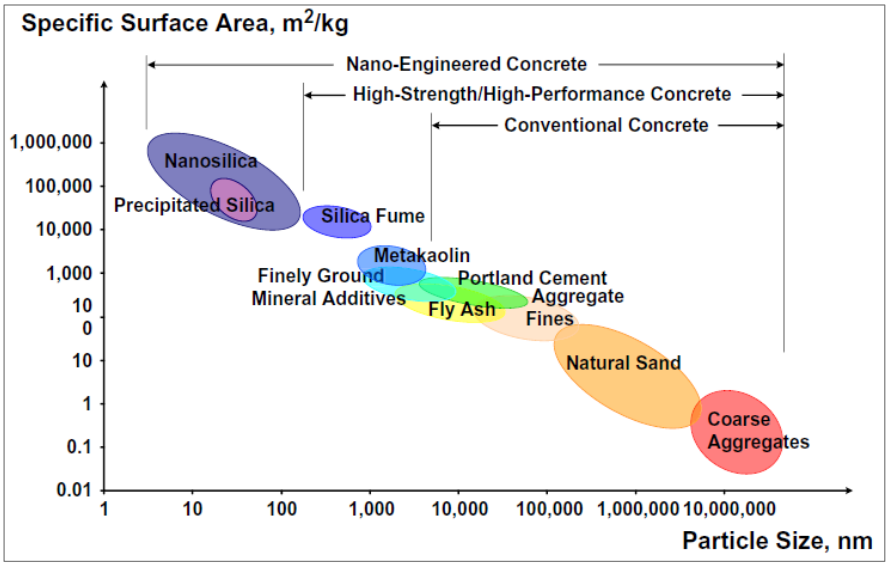

Figure 44: Specific surface areas and sizes of some chosen particles used in cementitious materials (Sanchez and Sobolev, 2010).

2.4.1 Nanoclay Reinforced-Cements

Nanoclay is a broad class of naturally occurring inorganic minerals. Montmorillonite platelets are one of the most commonly used nanoclays for reinforcing polymer materials. Over the last two decades, polymer-nanoclay nanocomposites have received significant attention in manufacturing and applications (Hussain *et al.*, 2006, Alamri *et al.*, 2012). Polymer-nanoclay composites have superior physical and mechanical properties (Alamri *et al.*, 2012, Lai *et al.*, 2014). Studies have been carried out using nanoclay for reinforcing construction and building materials (Chang *et al.*, 2007, Hakamy *et al.*, 2015a, He and Shi, 2008, Wei and Meyer, 2014). There are different types of commercial nanoclay platelets. Notable examples are nano-halloysite, Cloisite 30B and nano-kaolin (Chang *et al.*, 2007, Morsy and Aglan, 2007). As a type of pozzolanic material with a nanosize feature, nanoclay was found to increase the density of the cement matrices, and improve their mechanical and thermal properties (Morsy *et al.*, 2009, Hakamy *et al.*, 2013b, Farzadnia *et al.*, 2013, Quanji *et al.*, 2014).

In a different study, Aly *et al.* (2011a) used the same nanoclay particles (Cloisite 30B) as a reinforcement to the waste-glass powder and cement mortars. Portland

cement was partially substituted by different ratios of waste-glass powder ranging between 5.0 and 50 wt.% (by cement weight) and 2.5 wt.% of nanoclay (by cement weight), and then each sample was tested at 28 days. The samples containing nanoclay demonstrated a higher mechanical strength when compared to other samples. The compressive and flexural strength of samples containing nanoclay was found to have improvement by 28% and 33% respectively when compared to the controls (Figures 45-46). The enhancement was attributed to the multifunctional effect of the nanoclay particles that includes both physical filler effect, and chemical pozzolanic effect.

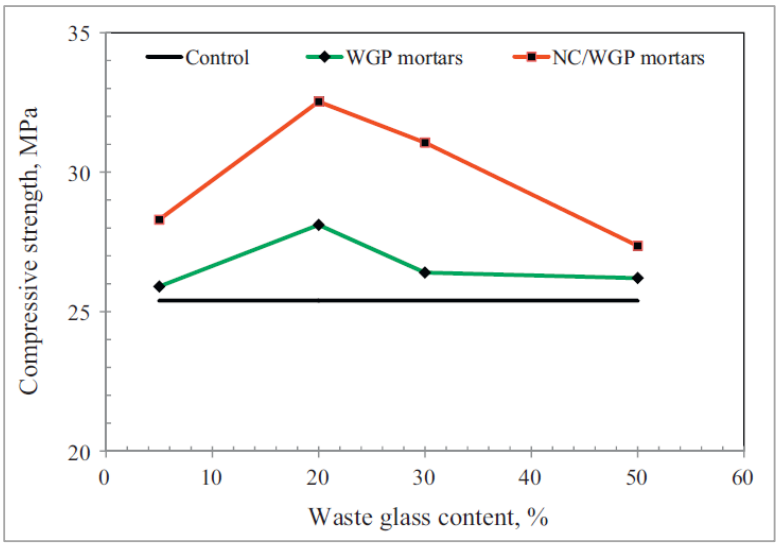

Figure 45: Compressive strength results of samples, WGP: waste glass powder, NC: nanoclay, (Aly *et al.*, 2011a).

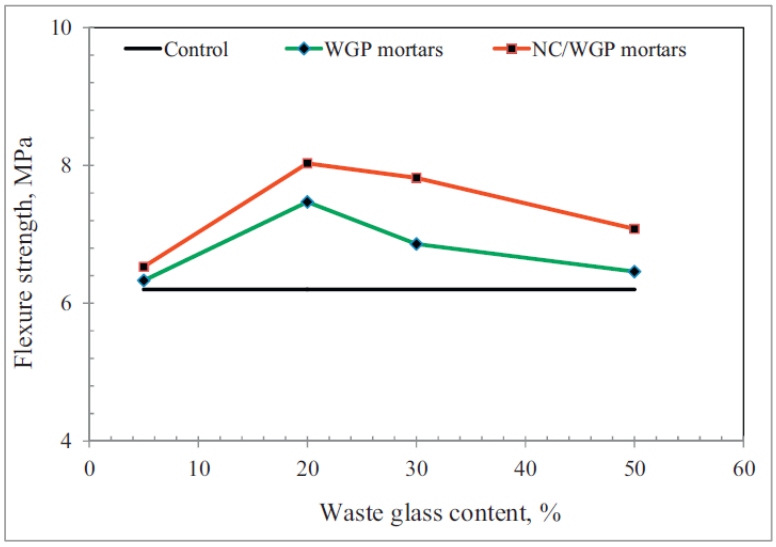

Figure 46: Flexural strength results of samples, WGP: waste glass powder, NC: nanoclay,(Aly *et al.*, 2011a).

The influence of nanoclay on the mechanical strength of cementitious materials has been investigated extensively over past few years. The influence of nanoclay (Cloisite 30B) on the indirect tensile strength of cement paste at 1 and 4 weeks was studied. Portland white cement was partially substituted by 2.0 and 4.0 wt.% Cloisite 30B nanoclay. Indirect tensile strength of cement nanocomposites loaded with 2.0 wt.% nanoclay was found to be 25% higher than the control sample when tested at 28 days (Figure 47). However, loading of further nanoclay particles caused a reduction in the nanocomposite strength due to the agglomeration and poor diffusion of the nanoparticles (Morsy and Aglan, 2007).

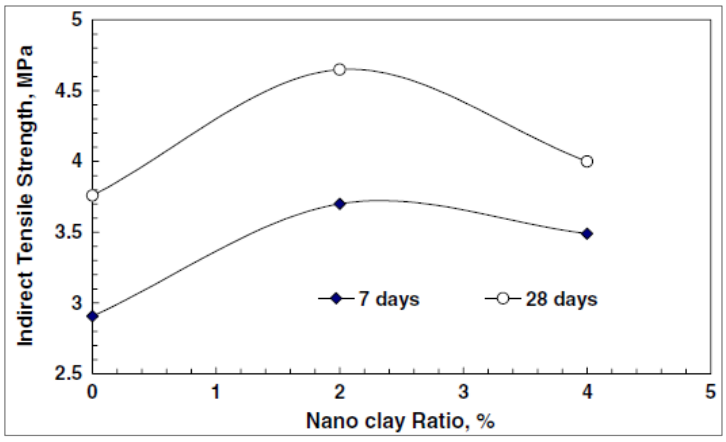

Figure 47: Indirect tensile strengths of control sample and nanocomposites containing 2.0 and 4.0 wt.% at 7 and 28 days (Morsy and Aglan, 2007) .

In another study, Chang *et al.* (2007) investigated the effect of nanoclay on the microstructure and strength of cement matrix. OPC was partially substituted by nanoclay particles at ratios ranging between 0.2 and 0.8 wt. %. The curing durations were 7, 14, 28 and 56 days. The effect of nanoclay on compressive strength and permeability coefficients of the samples at various loadings and curing ages are shown in Figure 48. It can be seen that 0.6 wt.% and 0.4 wt.% nanoclay were the optimum contents in terms of the compressive strength and permeability coefficients respectively at all ages when compared to their control samples. Its strength increased by 13.2 % and the permeability coefficients decreased by 50.0% when compared to the pure matrix. These authors concluded that the development in the strength and microstructure of samples was because of the effectiveness of nanoclay particles in supporting the pozzolanic reaction, as well as filling the micro-holes in the matrices, which produces denser cement matrices (Chang *et al.*, 2007).

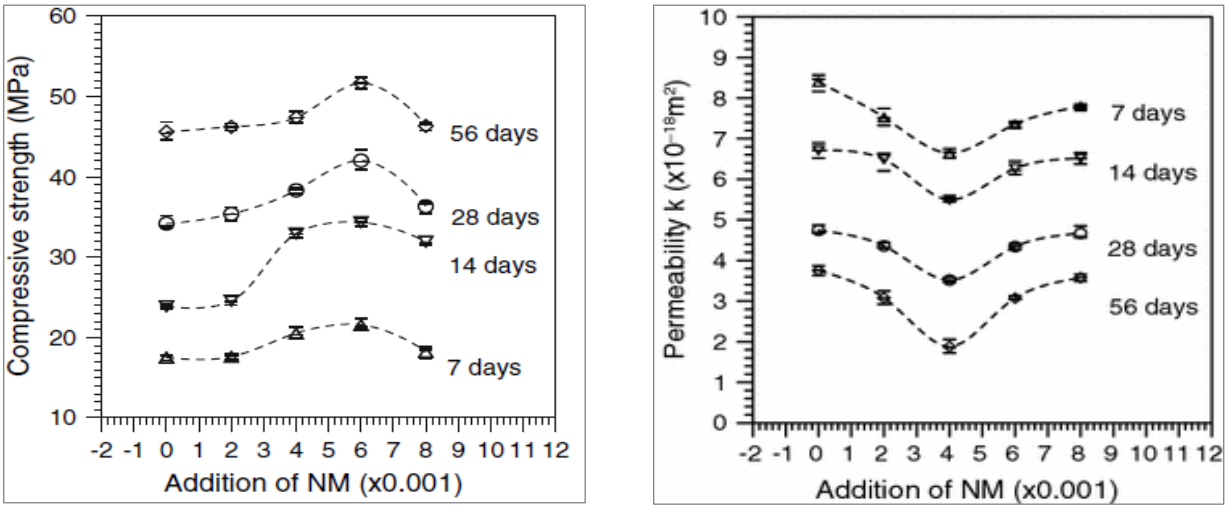

Figure 48: Compressive strength and permeability coefficients of control cement paste, cement nanocomposites at different ages and additions of nanoclay particles (Chang *et al.*, 2007).

The influence of nanoclay (halloysite) on the compressive strength and physical properties of cement matrices was reported by Farzadnia *et al.* (2013). Cement powder was partially substituted by 1.0, 2.0 and 3.0 wt.% nanoclay particles and 5.0 wt.% of silica fume, and then tested at 7 and 28 days. It was found that the loading of 3.0 wt.% nanoclay improved the compressive strength at 28 days by up to 24% over the control paste. Figures 49 and 50 show the compressive strengths and stress-strain

curves of the samples. The pure sample showed more brittle behaviour when compared to the nanocomposites due to high porosity. It was concluded that the improvement of strength could be ascribed to three reasons. First, the pore filling effect led to denser matrices than the control paste as shown in SEM micrograph of Figure 51. Second, the activation of the pozzolanic chemical reaction by virtue of high surface area of the nanoparticles, and finally because of crosslinking effect which bridge the micro-cracks in the matrices. As these researchers showed in the study that the compressive strength of cement mortars increased with increasing the amount of nanoclay, however, the optimum amount of nanoclay required has not been identified. Contents higher than 3.0 wt.% must be utilized in cement mortars in order to specify the maximum compressive strength achieved.

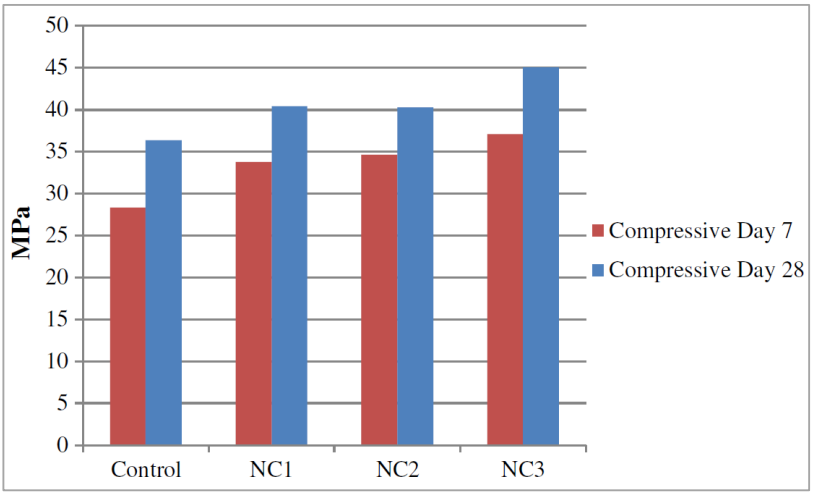

Figure 49: Compressive strengths of control composites and nanocomposites (Farzadnia *et al.*, 2013).

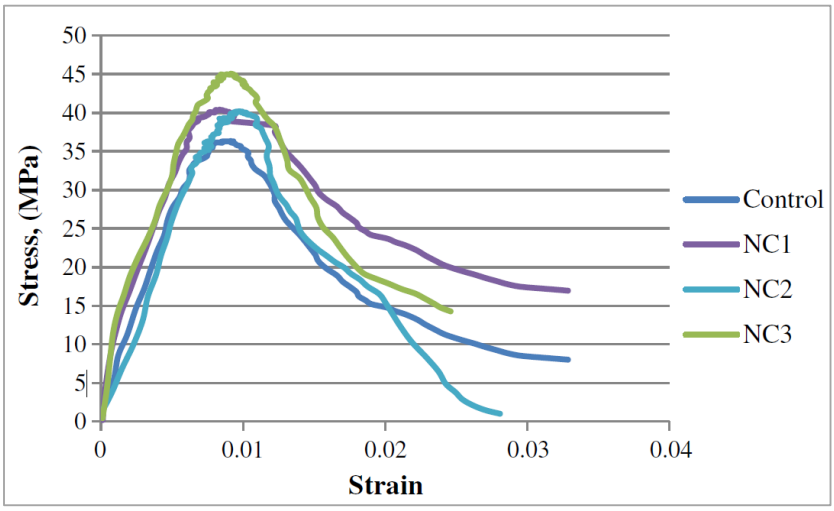

Figure 50: Stress-strain curves of all samples Farzadnia *et al.* (2013).

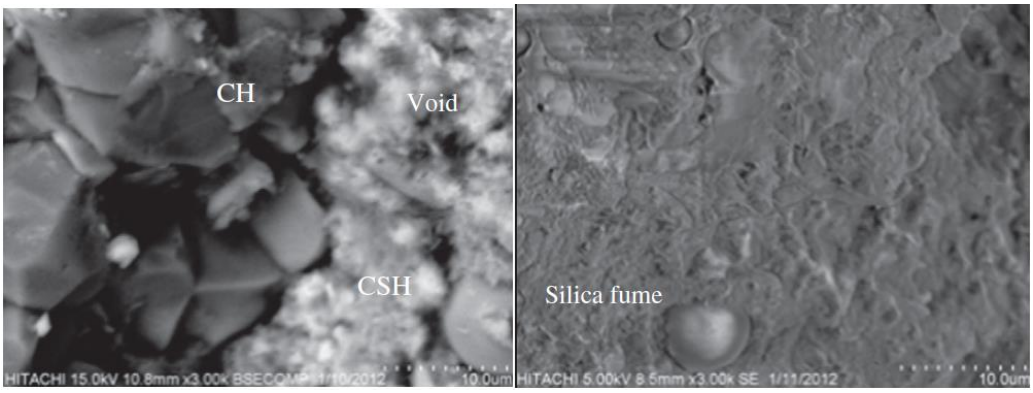

Figure 51: SEM for control and the sample incorporated with 2.0 wt. % NC at 28th day; (left image: control paste, right image: NC-2) Farzadnia *et al.* (2013).

In another study, Wei and Meyer (2014) considered the effect of fractional replacement of cement by a mixture of nanoclay and metakaolin on the microstructure and mechanical properties of cement composites reinforced with sisal fibres. Portland cement was initially replaced by 10, 30 and 50 wt.% of metakaolin, and then metakaolin was replaced with 1.0, 2.0 and 3.0 wt.% of nanoclay. The compressive strengths of pure sample and nanocomposites at 1, 7, 14 and 28 days are presented in Figure 52. The results of this investigation revealed that the highest strength was attained by nanocomposites with 28.0 wt.% metakaolin and 2.0 wt.% nanoclay. Compared to the control mortar, the highest strength was 18.48 % improvement at 28 days. This improvement in the compressive strength and microstructure of the nanocomposite was attributed to the filler effect and the

enhanced pozzolanic reaction, which helped to improve the interfacial bond strength between sisal fibres and nanocomposites. Figure 53 (a-b) show contour curves for the bond strength between sisal fibres and nanocomposites, and the pull-out energy. The composites with the optimum addition of nanoclay showed the highest bond strength with the natural fibres. The authors also investigated the flexural strength and flexural toughness of the fibre-reinforced nanocomposites. The pair found that nanoparticles played an important role in improving the first crack strength, flexural strength and post-crack toughness of the composites (Figure 54).

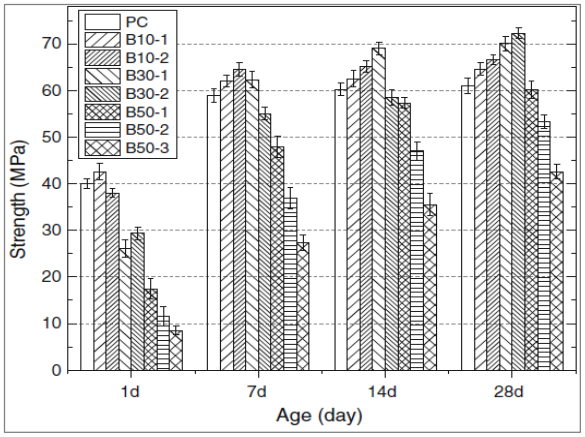

Figure 52: Compressive strengths of pure sample and nanocomposites at 1, 7, 14 and 28 days (Wei and Meyer, 2014).

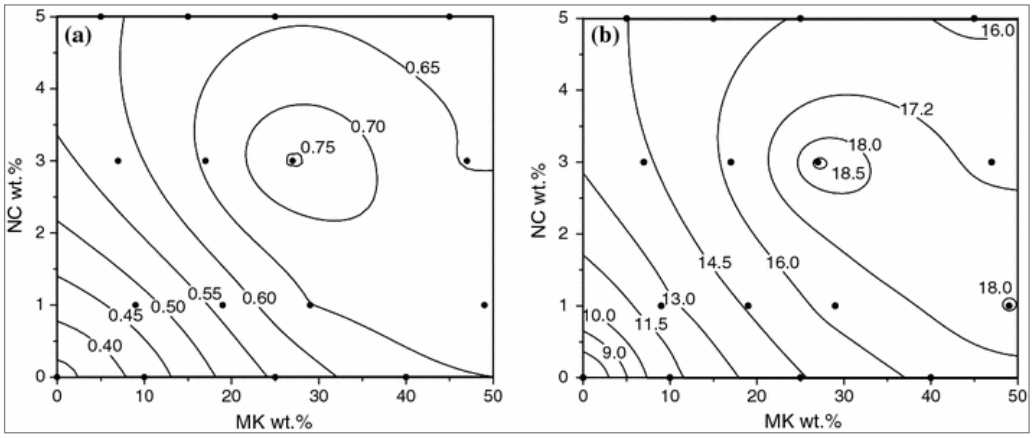

Figure 53: Contour curves show: (a) Bond strength between sisal fibres and cement matrices (in MPa), (b) Energy of pulling out the fibres (in N.mm) (Wei and Meyer, 2014).

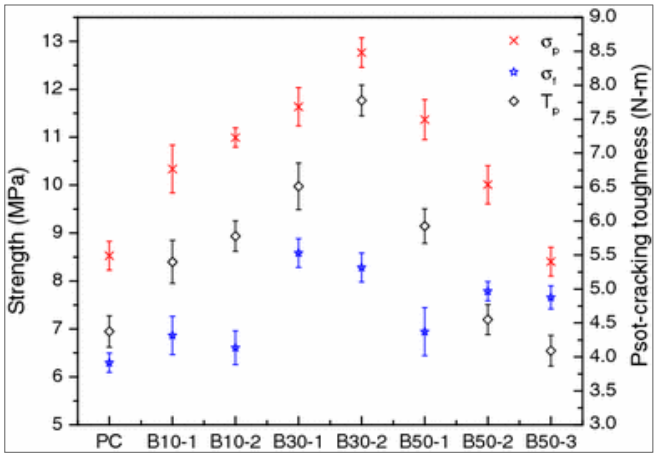

Figure 54: Results of flexural strength and post crack toughness of the cement composites in terms of metakaolin and nanoclay contents, where, σ_p : first crack strength (in MPa), σ_f : flexural strength of post crack (in MPa), and T_p :the post cracking toughness (in N.m) (Wei and Meyer, 2014).

Hosseini *et al.* (2014) investigated the effect of incorporating various nanoparticle types including nanoclay in cement matrices on the microstructure and mechanical strength at different ages (7, 28 and 90 days). Portland cement was partially substituted with 1.0 wt.% nanoclay. Compressive and flexural strengths of the nanocomposite, when compared with that of the control composite, improved across all time durations due to the effective filler and chemical influence of nanoclay. At 28 day for instance, an improvement of 12.5 and 30% was recorded in their compressive and flexural strengths respectively.

Hakamy *et al.* (2014) studied the mechanical properties of nanoclay-cement composites. The authors fabricated the nanocomposites by partially replacing the Portland cement with nanoclay at 1.0, 2.0 and 3.0 wt.%. The samples were tested at 56 days. It was found that nanoclay at 1.0 wt.% was the optimum ratio for improving a wide range of properties of the nanocomposites. Nanocomposite with 1.0 wt.% nanoclay exhibited a reduction in porosity of 20.6%, a reduction in water absorption by 23.5%, and an increase in density of 4%. It was determined that this improvement in the physical structure of nanocomposites had led to an improvement in the mechanical properties. The results revealed that the compressive strength of nanocomposites improved by 31%, flexural strength by 32%, fracture toughness by 31%, impact strength by 29% and Rockwell hardness by 24% when compared to the pure cement sample (Hakamy *et al.*, 2013a, Hakamy *et al.*, 2014).

In a further study, the same authors investigated the influence of calcined nanoclay (Cloisite 30B) on the physical and mechanical properties of cement nanocomposites. At 900°C, the nanoclay particles were found to undergo transformation into an amorphous state, as can be seen in Figure 55. The transformation increased the reactivity of the nanoparticles, and produced higher amounts of calcium-silica-hydrate (CSH) gel. The ideal content of calcined nanoclay was reported as 1.0 wt.%. At such a ratio, the resultant nanocomposites exhibited a decrease in porosity by 31.2%, a decrease in water absorption by 34%, and an increase in density by 9.7%. Addition of 1.0 wt.% calcined nanoclay dramatically enhanced the mechanical properties of the nanocomposite through increasing its compressive strength by 40% (Figure 56), its flexural strength by about 43%, its fracture toughness by about 40%, and its impact strength by about 34%, when compared to the control cement samples (Hakamy *et al.*, 2015a).

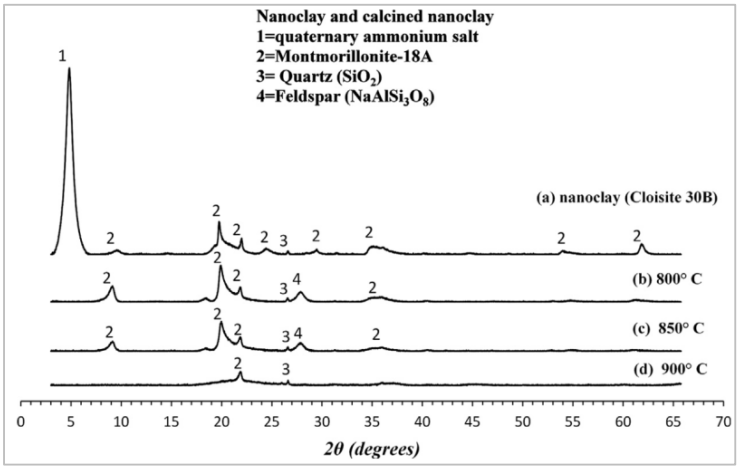

Figure 55: XRD patterns of nanoclay (Cloisite 30B) and calcined nanoclay (Cloisite 30B) at various temperatures (Hakamy *et al.*, 2015a).

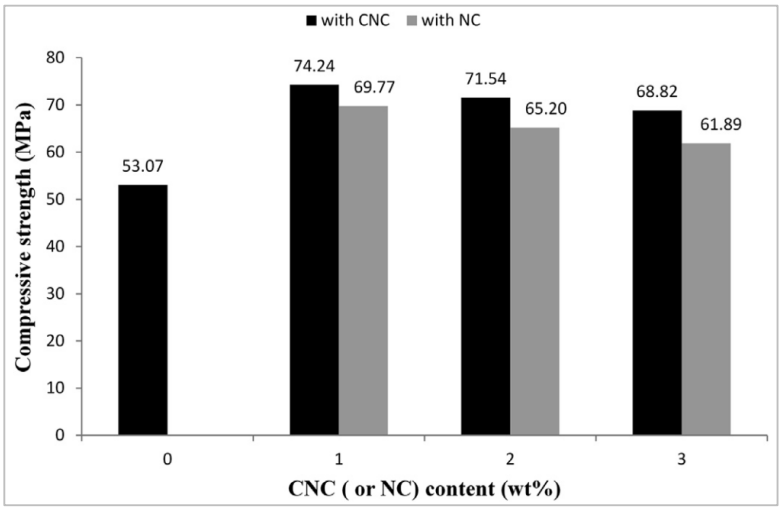

Figure 56: Compressive strength in terms of nanoclay and calcined nanoclay content in the samples (Hakamy *et al.*, 2015a).

2.4.2 Nanosilica Reinforced-Cements

Nanosilica (NS), also known as silicon dioxide nanoparticles, is the most commonly used nano-particles in the concrete research for the purpose of enhancing the physical, mechanical strength and durability of cement matrices due to its reactivity and ability to play a pore filling effect (Shaikh *et al.*, 2014, Hanus and Harris, 2013, Senff *et al.*, 2013, Singh *et al.*, 2013, Jo *et al.*, 2007, Givi *et al.*, 2010, Supit and Shaikh, 2014).

Singh *et al.* (2014) studied the effects of silica-fume and nanosilica, in powdered and colloidal form on the mechanical properties of cement pastes. Powdered nanosilica was produced using the sol gel process and then compared with the commonly used colloidal nanosilica. The three types of silica particles, colloidal, powdered nanosilica and silica fume, at 3.0 wt. % were mixed with cement mortar to evaluate the strength of the resulted matrices. The researchers found an improvement in compressive strength of 27, 37 and 19% in the case of colloidal, powdered nanosilica and silica fume, respectively (Figure 57). XRD and SEM tests showed that powdered and colloidal nanosilica are amorphous in nature; however, the powdered nanosilica particles are not agglomerated, although agglomeration has been observed in colloidal nanosilica (see Figures 58-59).

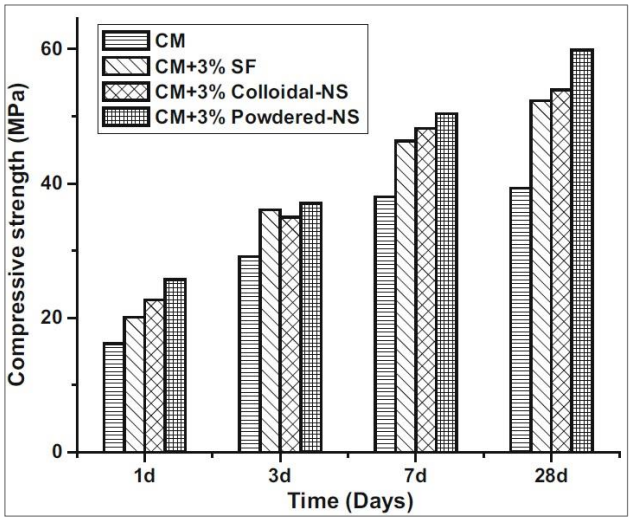

Figure 57: Compressive strength results of cement samples with the silica in various forms; SF: silica fume, NS: nanosilica (Singh *et al.*, 2015).

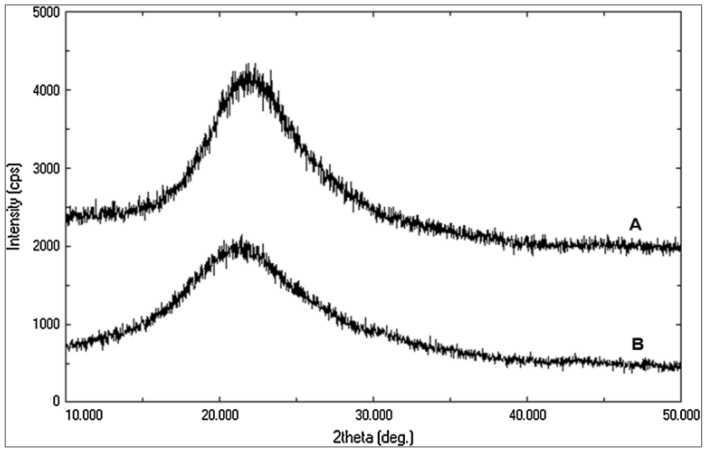

Figure 58: XRD patterns of A: colloidal nanosilica, and B: powdered nanosilica particles (Singh *et al.*, 2015).

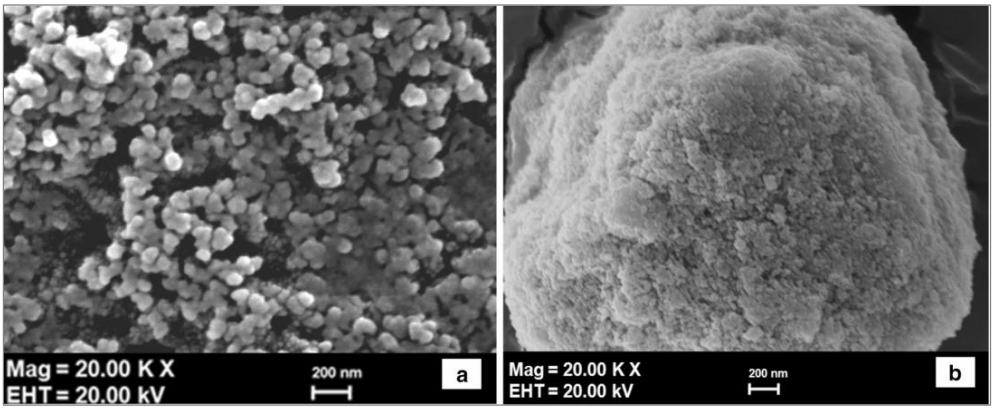

Figure 59: SEM micrographs of: a: powdered nanosilica, b: colloidal nanosilica particles.

In a similar study, Jo and coworkers (Jo *et al.*, 2007) investigated the compressive strength of cement mortars mixed with varying concentrations of silica-fume and nanosilica. The effectiveness of the pozzolanic reaction was found to be related to the total surface area offered for reaction. Silica-fume particles have an average particle size of 0.1 μm and surface area of 20 m^2/g, while nanosilica particles have a much smaller particle size (i.e. 20 nm), giving a surface area of 60 m^2/g. Figure 60 shows the SEM micrographs of their silica-fume and nanosilica particles. The experimental results (see Table 13) indicated that the nanosilica particles were more efficient in improving strength than silica fume. The compressive strength results showed that pastes containing nanosilica were superior to the mortars with silica-fume at 7 and 28 days (Jo *et al.*, 2007). The results of SEM revealed that nanoparticles act as an activator by promoting the pozzolanic reaction quality, and as a filler in improving the microstructure.

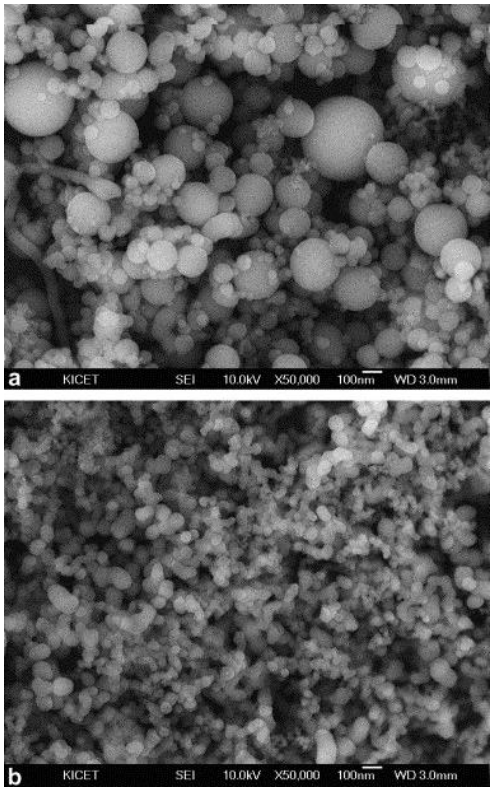

Figure 60: SEM images of: (a) silica-fume and (b) nanosilica particles (Jo *et al.*, 2007).

Table 13: Compressive strength results of cement matrices with various contents of silica-fume (SF) and nanosilica (NS) particles at 7 and 28 days (Jo *et al.*, 2007).

	7 days	28 days
OPC	18.3	25.6
SF5	22.5	35.1
SF10	24.7	37.4
SF15	26.1	38.0
NS3	39.5	54.3
NS6	46.1	61.9
NS10	49.3	68.2
NS12	50.7	68.8

Li (2004) investigated the mechanical strength of high-volume-fly-ash concrete with nanosilica particles across different time periods. A cement paste concrete was prepared as a control sample, and compared with both high-volume-fly-ash concrete and high-volume-fly-ash concrete containing nanosilica (4.0 wt. %). The concrete samples were examined at different ages starting from 1 day up to 1 year. The results of compressive strength against time (Figure 61) showed that nanosilica played a role in increasing the compressive strength of concrete at initial and late stages. The

concrete samples containing nanosilica were able to rapidly attain and maintain high strength over prolonged time (Li, 2004).

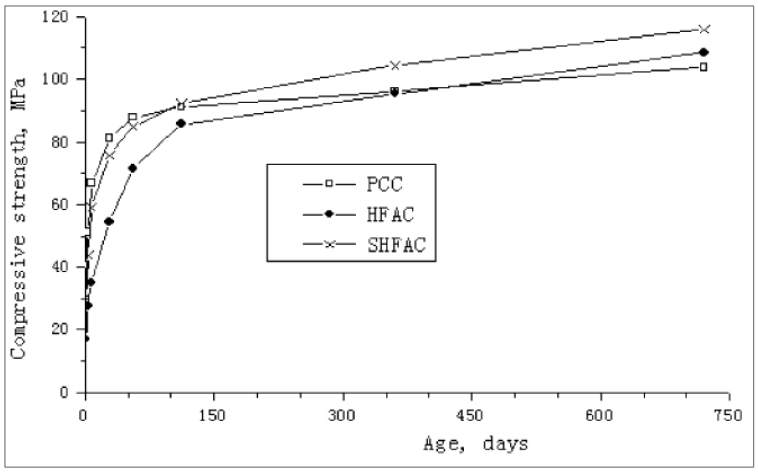

Figure 61: Growth of the compressive strength with time; PCC: cement control sample, HFAC: high-volume-fly-ash concrete and SHFAC: high-volume-fly-ash concrete with nanosilica (Li, 2004).

Qing *et al.* (2007) investigated the influence of nanosilica addition on the strength of cement-based concrete as compared to cement based concrete with silica-fume addition (Qing *et al.*, 2007). Portland cement powder was substituted with silica-fume at 2.0, 3.0 and 5.0 wt.% and nanosilica at 1.0, 2.0, 3.0, 5.0 wt.%. The contents of water and superplasticizer were fixed for all samples. Nanosilica or silica-fume was dry-mixed with cement powder in the sample preparation process. The authors reported that compressive strength of nanosilica-incorporated concrete was higher than that with the same content of silica fume. At 28 days, compressive strength of the concrete specimen increased by 25% and 20% in the case of 5.0 wt.% nanosilica and 5.0 wt.% silica-fume respectively when compared to the control cement paste (see Table 14). The superior results of nanosilica over silica-fume as an additive was attributed to the great surface area of the nanoparticles, leading to greater pozzolanic activity. Besides, nanosilica performs as a filler for the micro-voids existed in cement matrices, which in turn decreases the amount of water that occupied in the voids of the composites (Qing *et al.*, 2007). The authors provided useful outcomes regarding the comparison between the effect of nanosilica and silica fume in concrete, but they did not determine an optimum contents of the nanosilica particles that achieved a maximum strength. The compressive strength improved linearly with the amount of nanosilica in the mixture, and it may be useful to investigate samples with contents

of the nanoparticles greater than 5.0 wt.%.

Table 14: Contents and compresssieve strength results of all samples at 1,2,28 and 60 days (Qing *et al.*, 2007).

Sample	Mix proportion in mass					Compressive strength (MPa) (%)			
	C	NS	SF	W	SM	1d	3d	28d	60d
CO	100	0	0	22	2.5	48.9 (100)	61.1 (100)	79.2 (100)	94.9 (100)
A1	99	1	0	22	2.5	49.2 (101)	71.6 (117)	94.7 (120)	101.6 (107)
A2	98	2	0	22	2.5	49.8 (102)	72.6 (119)	95.8 (121)	102.5 (108)
A3	97	3	0	22	2.5	52.0 (106)	82.2 (135)	97.6 (123)	105.8 (111)
A5	95	5	0	22	2.5	53.0 (108)	86.1 (141)	98.8 (125)	108.8 (115)
B2	98	0	2	22	2.5	47.5 (97)	61.0 (100)	84.2 (106)	101.5 (107)
B3	97	0	3	22	2.5	47.3 (97)	60.4 (99)	92.0 (116)	104.3 (110)
B5	95	0	5	22	2.5	47.0 (96)	60.0 (98)	95.3 (120)	106.9 (113)

2.4.3 Nanoparticle Reinforced-Geopolymers

The incorporation of nanoparticles to geopolymers is a relatively novel field. To date, research has focused on the addition of nanosilica and nanoalumina to geopolymer pastes with the aim to improving their mechanical properties (Nazari and Sanjayan, 2015, Phoo-ngernkham *et al.*, 2014).

The effect of nanosilica and nanoalumina addition on the physical and mechanical properties of high-calcium-fly-ash geopolymers was investigated by Phoo-ngernkham *et al.* (2014). Nanoparticles at 1.0%, 2.0%, and 3.0% by weight were mixed with fly-ash. The geopolymer parameters were fixed for all samples, namely, NaOH concentration was 10 molars, Na_2SiO_3:NaOH ratio was 2.0, the liquid:binder ratio was 0.60; and samples were cured at room temperature. Mechanical tests were conducted at 7, 28 and 90 days.

The research outcomes indicated that the addition of nanosilica to fly-ash resulted in a reduction of initial and final time of setting when compared to the setting time of the control sample. In contrast, the addition of nanoalumina resulted in a very minor reduction in setting time. The setting time of all samples can be seen in Figure 62. The reduction in setting time by nanosilica was attributed to a rapid activation rate with the freely existing Ca ions in the high-calcium-fly-ash, which produced higher

amounts of calcium-silicate-hydrate gel.

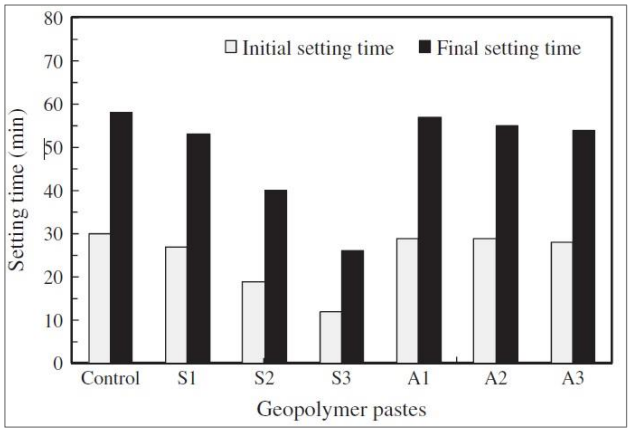

Figure 62: Setting time of geopolymer mixtures; where S: nanosilica and A:nanoalumina (Phoo-ngernkham *et al.*, 2014) .

XRD and SEM showed that 1.0 to 2.0 wt.% loading of any type of nanoparticles improved the physical structures, and produced denser geopolymer nanocomposites. Consequently, an improvement in both compressive and flexural strengths was observed. The results revealed that the addition of nanosilica and nanoalumina, regardless of the amount, increased to the strength of the nanocomposites when compared to the control sample. The compressive and flexural strength results are presented in Table 15. This improvement was attributed to the development of further calcium-aluminosilicate-hydrate, calcium-silicate-hydrate and geopolymer gel in the geopolymer pastes. Also, the addition of both nanosilica and nanoalumina was found to enhance the shear bond between geopolymer and concrete. However, a further addition of the nanoparticles at 3.0% led to a slight reduction in the mechanical strength of the resultant samples. These authors also presented a linear relation connecting the square root of compressive strength with the flexural results of geopolymer samples (Figure 63).

Table 15: Results of compressive and flexural strengths of all samples (Phoo-ngernkham *et al.*, 2014).

Mix	Compressive strength (MPa)			Flexural strength (MPa)		
	7 days	28 days	90 days	7 days	28 days	90 days
Control	16.8	29.6	39.4	1.83	3.66	4.13
S1	20.2	35.3	51.3	1.89	5.12	6.41
S2	24.1	31.8	51.8	2.13	4.89	5.98
S3	23.1	29.7	48.1	2.10	4.31	5.23
A1	21.8	36.2	56.4	2.22	4.63	5.67
A2	23.2	37.1	50.0	2.36	4.95	5.92
A3	23.3	31.4	46.1	2.14	4.49	5.26

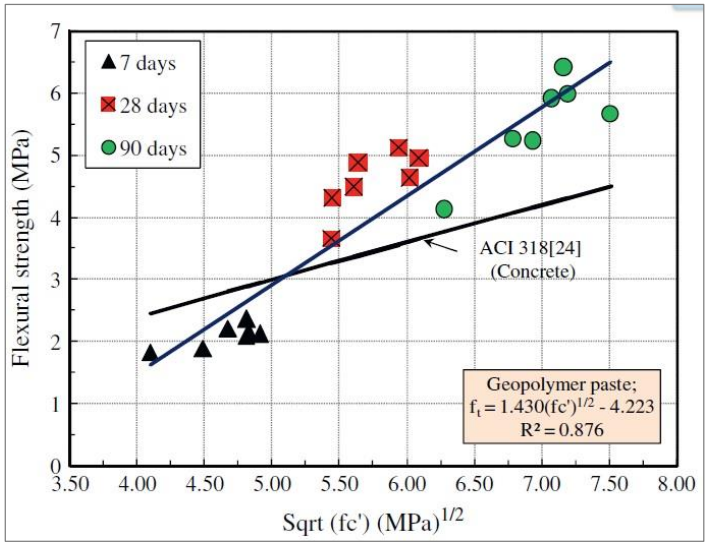

Figure 63: The square root of compressive strength related linearly with the flexural strength of geopolymers (Phoo-ngernkham *et al.*, 2014) .

The effect of loading various amounts of nanosilica on fly-ash based geopolymer was studied by Adak *et al.* (2014). The nanocomposites were synthesized using different colloidal nanosilica ratios (4, 6, 8 and 10% by fly-ash weight), and different activator concentrations (8, 10 and 12 M) and cured at ambient temperature. The control sample was a cement matrix prepared using OPC and sand. All samples were tested at 3, 7 and 28 days

Results showed that regardless of the content of nanosilica, compressive strength of geopolymer matrices increased when the alkali concentration increased, attributable to the greater activation rate. Nevertheless, the addition of nanosilica in the fly-ash based geopolymer pastes by up to 6.0% of fly-ash resulted in the highest strength among all samples (Figure 64). Adding nanosilica beyond 6.0% was found to result

in a decrease in compressive strength at all ages. Results of flexural strength showed similar trend. Figure 65 shows the flexural strength of control sample, geopolymers without nanosilica and geopolymer nanocomposites containing 6.0% nanosilica at different molar concentration. Samples activated using high molar concentration (12M), and incorporating 6.0% nanosilica exhibited 62% increase in flexural strength over the control. While samples activated by the same activator without nanosilica showed only 35% increase. The authors concluded that the addition of 6.0% nanosilica has provided an optimum 28 days strength without any heat curing for activation (Adak *et al.*, 2014).

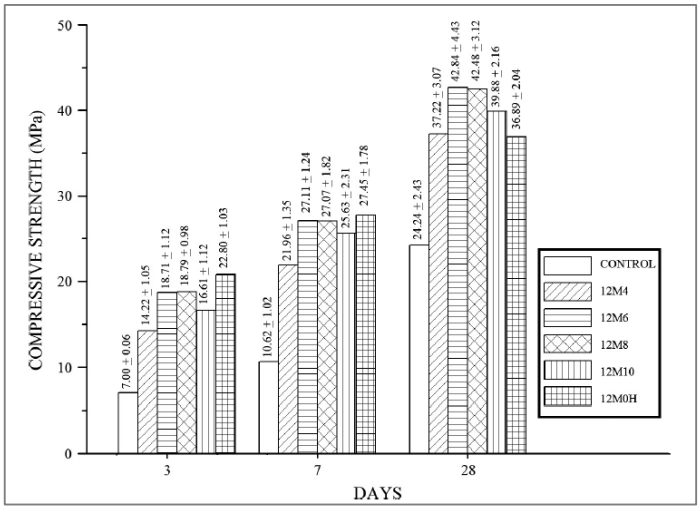

Figure 64: Compressive strength of cement control mortar sample, geopolymer nanocomposites with molar concentration of 12 (M) at 3, 7 and 28 days (Adak *et al.*, 2014).

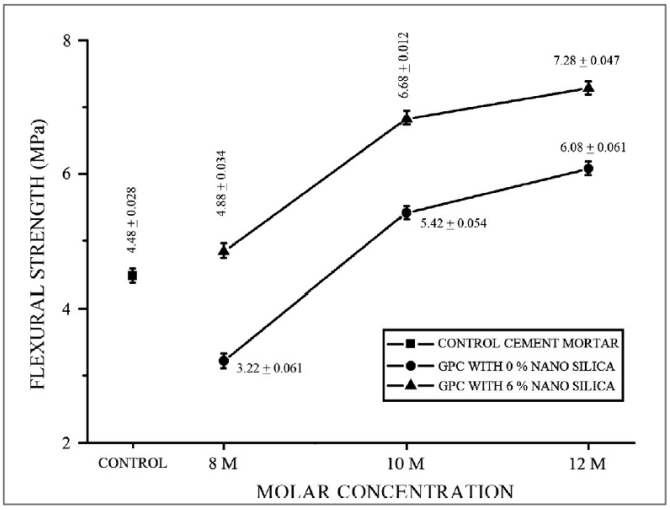

Figure 65: Flexural strength of control sample, geopolymers without nanosilica and geopolymer nanocomposites containing 6.0% nanosilica at different molar concertation(Adak *et al.*, 2014).

Comparable results are reported for geopolymer synthesized using a combination of rice-husk-ash (93.0%) and fly-ash (3.0%) with different amounts of nanosilica and nanoalumina (1.0, 2.0, 3.0% by weight) activated at different NaOH concentration, and oven cured at 25, 70 and 90 ˚C for 2.0, 4.0 and 8.0 hours (Riahi and Nazari, 2012).

The results of the investigation indicated that 3.0 wt.% nanosilica particles resulted in the achievement of highest strength. While nanoalumina particles had no influence on the compressive strength, the researchers attributed this to the crystalline nature of nanoalumina which could not contribute efficiently in improving the strength (Riahi and Nazari, 2012).

3 PUBLICATIONS FORMING PART OF THE THESIS

3.1 Characterisation of mechanical and thermal properties in flax fabric reinforced geopolymer composites

Assaedi, H., Alomayri, T., Shaikh, F.U. and Low, I.M., 2015. Characterisation of mechanical and thermal properties in flax fabric reinforced geopolymer composites. *Journal of Advanced Ceramics*, *4*(4), pp.272-281.

Journal of Advanced Ceramics
2015, **4**(4): 272–281
DOI: 10.1007/s40145-015-0161-1

ISSN 2226-4108
CN 10-1154/TQ

Research Article

Characterisation of mechanical and thermal properties in flax fabric reinforced geopolymer composites

Hasan ASSAEDI[a], Thamer ALOMAYRI[a], Faiz U. A. SHAIKH[b], It-Meng LOW[a,c,*]

[a]*Department of Imaging & Applied Physics*, *Curtin University*, *GPO Box U1987*, *Perth*, *WA 6845*, *Australia*
[b]*Department of Civil Engineering*, *Curtin University*, *GPO Box U1987*, *Perth*, *WA 6845*, *Australia*
[c]*Department of Engineering*, *Curtin College*, *Building 205*, *Curtin University Bentley Campus*, *Kent Street*, *Perth*, *Western Australia 6102*, *Australia*

Received: February 19, 2015; Revised: June 17, 2015; Accepted: June 18, 2015

Abstract: This paper presents the mechanical and thermal properties of flax fabric reinforced fly ash based geopolymer composites. Geopolymer composites reinforced with 2.4, 3.0 and 4.1 wt% woven flax fabric in various layers were fabricated using a hand lay-up technique and tested for mechanical properties such as flexural strength, flexural modulus, compressive strength, hardness, and fracture toughness. All mechanical properties were improved by increasing the flax fibre contents, and showed superior mechanical properties over a pure geopolymer matrix. Fourier transform infrared spectroscopy (FTIR) and scanning electron microscopy (SEM) studies were carried out to evaluate the composition and fracture surfaces of geopolymer and geopolymer/flax composites. The thermal behaviour of composites was studied by thermogravimetric analysis (TGA) and the results showed significant degradation of flax fibres at 300 ℃.

Keywords: geopolymer composites; flax fibre; mechanical properties; thermal properties

1 Introduction

Ordinary Portland cements are used in many construction applications because of their good mechanical and durability properties. However, the greenhouse emissions caused by cement based materials have made it necessary to find an eco-friendly alternative. A new group of promising construction material is geopolymer, first introduced and named by Davidovits in 1989, exhibiting good mechanical performance, durability, and fire and acid resistance. It can be cured and hardened at room temperature with 80%–90% fewer CO_2 emissions than Portland cement [1–5].

Despite their desirable characteristics, geopolymer matrices suffer from brittle failure under applied force and demonstrate low flexural strength ranging between 1.7 and 16.8 MPa [6,7]. Improving their flexural and tensile strengths will significantly increase the application of these materials in the construction and building industries; and this may be accomplished by dispersing inorganic or organic fibres throughout the matrices. Hitherto, the most common fibre reinforcements used in geopolymer composites are based on carbon, basalt, and glass fibres [8–12], but concerns over the environment and non-biodegradability have made renewed interest recently in replacing the synthetic fibres used in geopolymer or other brittle matrices with natural plant

* Corresponding author.
E-mail: j.low@curtin.edu.au

fibres. These include flax, hemp, jute, pineapple, straw, switch grass, kenaf, coir, and bamboo [13,14]. These plant fibres cost less, have low density, and display good mechanical properties when compared with industrial fibres [15]. For example, natural fibres have lower densities than synthetic fibres generally, with many almost 30%–50% less dense than their synthetic counterparts [16]. They are also renewable, recyclable, and biodegradable, and demonstrate excellent mechanical characteristics like flexibility, high specific strength, and high specific modulus [17,18]. For example, wood-derived cellulose can be used for toughening epoxy and other polymers [19–22], and bamboo fibres improve the flexural strength of concrete [23]; the same desirable effect has been observed in wood fibre reinforced concrete [24]. Cotton fabrics also enhance the strength and toughness of geopolymer [25], and wool and flax fibres have been successfully used to reinforce geopolymer composites, with improvements in mechanical and fracture properties [26,27]. However, no study so far has reported the mechanical properties of flax fabric (FF) reinforced fly ash based geopolymer composites despite their advantages of cheapness, ready availability, lack of toxicity, biodegradability, and good tensile strength. The present report describes the development and mechanical properties of new environmentally friendly geopolymer composites reinforced with the readily-available natural flax fibres of Australia, to produce materials with excellent flexural strength and graceful failure properties.

This study considers the viability of developing a green composite material that uses fly ash geopolymer as the matrix and FF as the reinforcement. Fourier transform infrared spectroscopy (FTIR), scanning electron microscopy (SEM), and thermogravimetric analysis (TGA) are used to investigate the morphology, microstructure, failure mechanisms, and thermal behaviour of geopolymer/flax composites. The effect of different FF contents of 2.4, 3.0, and 4.1 wt% on mechanical properties of the composites such as flexural strength, flexural modulus, compressive strength, hardness, and fracture toughness is also presented in this paper.

2 Experimental procedures

2. 1 Materials

Flax fabric shown in Fig. 1, supplied by Pure Linen Australia, was used as reinforcement in the fabrication of geopolymer composites. The structure and physical properties of the flax fabric are shown in Table 1. Low calcium fly ash (ASTM class F) collected from the Eraring power station in New South Wales, Australia, was used as the source material for the geopolymer matrix. The chemical composition of fly ash is shown in Table 2. The alkaline activator for geopolymerisation was a combination of sodium hydroxide and sodium silicate grade D solution. Sodium hydroxide flakes of 98% purity were used to prepare the solution. The chemical composition of sodium silicate used was 14.7% Na_2O, 29.4% SiO_2, and 55.9% water by mass.

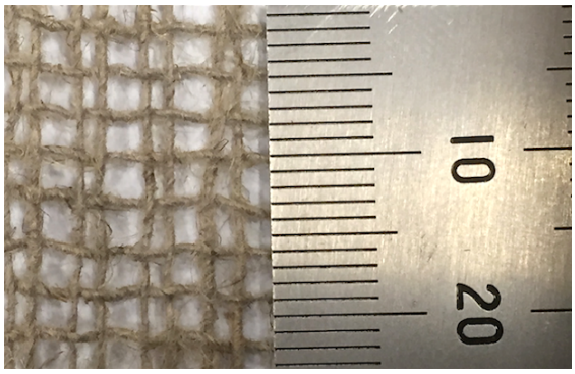

Fig. 1 Structure of the flax fabric.

To prepare the geopolymer composites, an alkaline solution to fly ash ratio of 0.75 was used, and the ratio of sodium silicate solution to sodium hydroxide solution was fixed at 2.5. The concentration of sodium hydroxide solution was 8 M, and was prepared and combined with the sodium silicate solution one day before mixing.

The alkaline solution was added to the fly ash in a Hobart mixer at low speed until the mix became homogeneous, then mixed for another 10 min on high speed with an additional 50 mL of water to improve the workability. This produced a geopolymer matrix of molar composition of SiO_2/Al_2O_3 = 4.16, Na_2O/SiO_2 = 0.37, and H_2O/Na_2O = 11.43.

Table 1 Structure and physical properties of the flax fabric

Fabric thickness (mm)	0.6
Fabric geometry	Woven (plain weave)
Yarn nature	Bundle
Bundle diameter (mm)	0.6 (see Fig. 2(a))
Filament size (mm)	0.01–0.02 (see Fig. 2(b))
Opening size (mm)	2–4
Fabric density (g/cm^3)	1.5
Modulus of elasticity (GPa)	39.5
Tensile strength (MPa)	660

Table 2 Chemical composition of fly ash (Unit: wt%)

SiO_2	Al_2O_3	CaO	Fe_2O_3	K_2O	MgO	Na_2O	P_2O_5	SO_3	TiO_2	MnO	BaO	LOI
63.13	24.88	2.58	3.07	2.01	0.61	0.71	0.17	0.18	0.96	0.05	0.07	1.45

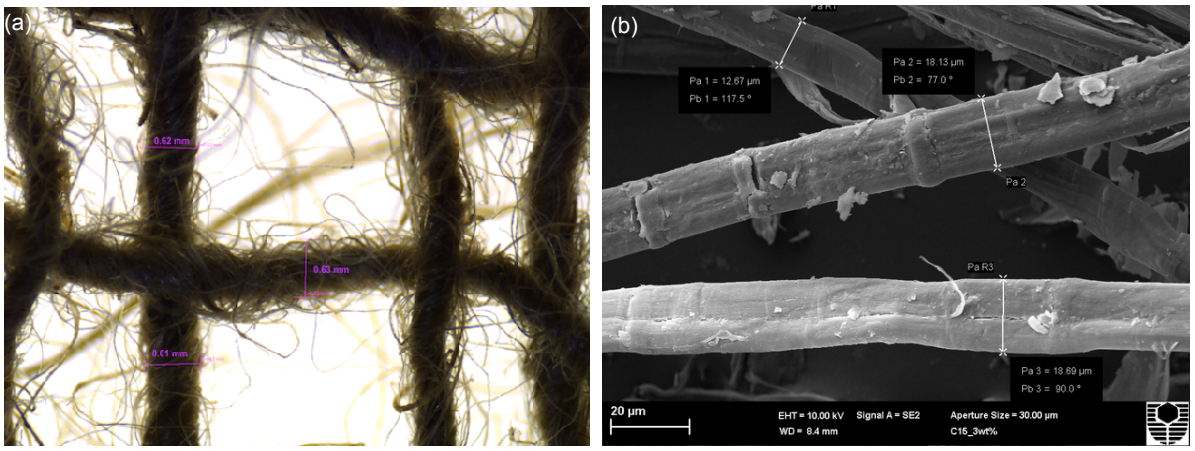

Fig. 2 Diameters of the (a) flax bundle and (b) flax fibres.

Three samples of geopolymer composites reinforced with 2.4, 3.0, and 4.1 wt% FF were prepared by spreading a thin layer of geopolymer paste in a well greased wooden mould and carefully laying the first layer of FF on top. The fabric was fully saturated with paste by a roller, and the process repeated for the desired number of layers; each specimen contained a different number of layers of FF (see Table 3). For each specimen, the final layer was geopolymer paste. The wooden moulds were then placed on a vibration table for 2 min, then covered with plastic film and cured at 80 ℃ for 24 h in an oven before demoulding. They were then dried under ambient conditions for 28 days. This procedure of preparing geopolymer composites is reported by Alomayri *et al.* [25].

2. 2 Mechanical properties

A LLOYD material testing machine (50 kN capacity) with a displacement rate of 0.5 mm/min was used to perform the mechanical tests. Rectangular bars of 60 mm × 18 mm × 15 mm with a span of 40 mm were cut from the fully cured samples for three-point bend tests to evaluate the mechanical properties. All samples were aligned horizontally to the applied load in all mechanical tests. Ten samples of each composite were used to evaluate the flexural strength and the flexural modulus according to the standard ASTM D790 [28]. The values were recorded and analysed with the machine software (NEXYGENPlus) and average values were calculated. The flexural strength (σ_F) was determined using the equation:

$$\sigma_F = \frac{3}{2}\frac{p_m S}{WD^2} \quad (1)$$

where p_m is the maximum load; S is the span of the sample; D is the specimen width; and W is the specimen thickness.

Flexural modulus (E_F) values were computed using the initial slope of the load displacement curve ($\Delta P / \Delta X$) using the equation [29]:

$$E_F = \frac{S^3}{4WD^3}\left(\frac{\Delta P}{\Delta X}\right) \quad (2)$$

A crack with a length to width ratio (a/W) of 0.4 was introduced into the specimen using a 0.4 mm diamond blade, to evaluate fracture toughness. The fracture toughness (K_{IC}) was calculated using the equation [29]:

$$K_{IC} = \frac{p_m S}{WD^{2/3}} f\left(\frac{a}{W}\right) \quad (3)$$

where a is the crack length, and $f(a/W)$ is the polynomial geometrical correction factor given by [29]:

$$f\left(\frac{a}{W}\right) = 3(a/W)^{1/2}[1.99 - (a/W)(1 - a/W)\times$$

Table 3 Formulation of samples

Sample	Fly ash (g)	NaOH solution (g)	Na_2SiO_3 solution (g)	Fabric layers	FF content (wt%)
1	1000	214.5	535.5	0	0
2	1000	214.5	535.5	5	2.4
3	1000	214.5	535.5	7	3.0
4	1000	214.5	535.5	10	4.1

$$(2.15-3.93a/W+2.7a^2/W^2)]/$$
$$[2(1+2a/W)(1-a/W)^{2/3}] \quad (4)$$

The compressive strength of the geopolymer composites was tested according to ASTM C109 [30], but instead of using the recommended 50 mm cube specimens, 20 mm cubes were used. The compressive strength (C) of the sample was calculated using the following formula:

$$C = P / A \quad (5)$$

where P is maximum load on the sample at failure and A is the surface area of the specimen.

The hardness of geopolymer composites was measured on the Rockwell H scale using an Avery Rockwell hardness tester. Before measurement, five samples were polished with emery paper to achieve flat, smooth surfaces.

2. 3 Characterisation

An FTIR spectrum was performed on a Perkin Elmer Spectrum 100 FTIR spectrometer in the range of 4000–500 cm^{-1} at room temperature. The spectrum was an average of 10 scans at a resolution of 2 cm^{-1}, corrected for background.

The microstructures of geopolymer composites were examined using a Zeiss Neon focused ion beam scanning electron microscope (FIB–SEM). The specimens were mounted on aluminium stubs using carbon tape and then coated with a thin layer of platinum to prevent charging before the observation.

A thermogravimetric analyser (TGA) was used to examine the thermal behaviours of the composites. Solid samples of 25 mg were placed in an alumina crucible and tests were carried out in an argon atmosphere with a heating rate of 10 ℃/min from 25 to 800 ℃.

3 Results and discussion

3. 1 FTIR observation

FTIR spectra of both pure geopolymer and flax/geopolymer composite are shown in Fig. 3. The strong peak at ~1000 cm^{-1} is associated with Al–O and Si–O asymmetric stretching vibrations and is the fingerprint of the geopolymerisation [31]. The FTIR spectra show a broad peak in the region at 3466 cm^{-1} corresponding to the hydroxyl (OH) stretching vibration of free and hydrogen bonded –OH groups [32,33], and

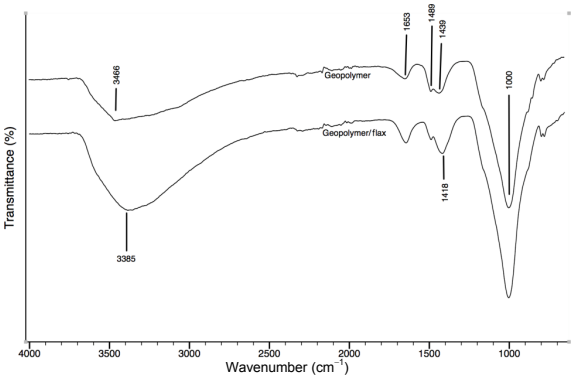

Fig. 3 FTIR spectra of pure geopolymer and flax/geopolymer composite.

the absorbance peak around 1653 cm^{-1} is attributed to the bending vibration of absorbed water [34,35]. The presence of bands in the regions 1440–1490 cm^{-1} is an indicator of the atmospheric carbonation on the surface of the matrix where it reacts with carbon dioxide [34]. The presence of flax fibres in the composites can be recognised by the peak at 1418 cm^{-1}, which is attributed to the CH_3 bending vibration of cellulose [32]. The intensity of the bands at 3385 and 1653 cm^{-1} increases in response to the existence of absorbed water in the cellulose fibres.

3. 2 Flexural strength and modulus

Generally, flexural tests are used to characterise the mechanical properties of layered composites as they provide a simple means of determining the bending response. This provides useful information on the performance of layered fabric based composites [36]. The effect of FF contents on the flexural stress–strain curves of the geopolymer composites is presented in Fig. 4.

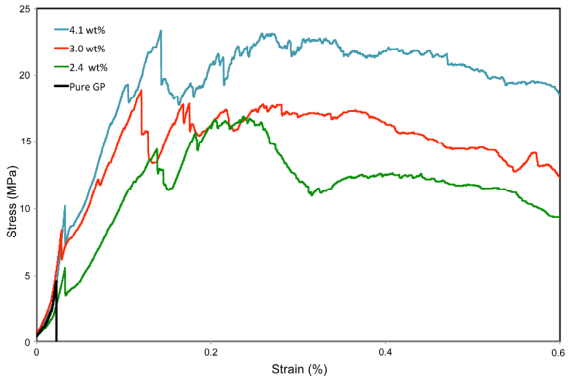

Fig. 4 Typical stress–strain curves of pure geopolymer and geopolymer composites with various FF contents.

It can be seen that, the composite containing 4.1 wt% FF shows the highest flexural strength among all composites. The flexural strength of the composites improves from 4.5 MPa in the pure geopolymer to about 23 MPa with 4.1 wt% FF. This result is comparable with that of short flax fibre reinforced geopolymer composites reported by Alzeer and MacKenzie [27]. Both studies show that increasing the content of flax fibres leads to a significant improvement in the flexural strength of the composite. This can be explained by the fact that the number of reinforcement layers controls the flexural strength. The lower weight of flax fabrics allows multiple layers of fabric in the composite to resist the shear failure and contribute in sustaining the applied load to the composites. This permits greater stress transfer between the matrix and the flax fibres, resulting in improved flexural strength [37].

The flexural modulus of geopolymer composites, shown in Fig. 5, also indicates that the addition of FF to the matrix improves the flexural modulus over that of a pure geopolymer matrix. Flexural modulus is the measure of resistance to deformation of the composite in bending. It was observed that none of the reinforced specimens were completely broken at peak load. This could be attributed to crack bridging of the long continuous flax fibres under load, which makes the flexural modulus higher than that of pure geopolymer. Long fibres are able to withstand a higher load and are capable of supporting multiple cracks throughout the loading process, consequently preventing brittle failure of the geopolymer.

3. 3 Compressive strength

The results presented in Fig. 6 show that the compressive strength of the composites containing FF increases with increase in fibre contents. The increase in compressive strength with fibre loading may be due to the ability of the flax fibres to absorb stress transferred from the matrix. The compressive strength of the neat geopolymer paste increases from 19.4 to 91 MPa after the addition of 4.1 wt% flax fibres. This significant enhancement of compressive strength is due to the fact that the interface between the fabric and the matrix is not exposed to any shear loading, which in turn reduces the possibility of fabric detachments or delamination from the matrix at high loads. Similar remarkable improvements in compressive strength have also been reported by Alomayri *et al*. [38] in the case of cotton fibre reinforced geopolymer composites. They concluded that the increase is due to the ability of horizontally laid cotton fabric to directly absorb and distribute a load uniformly throughout the cross-section.

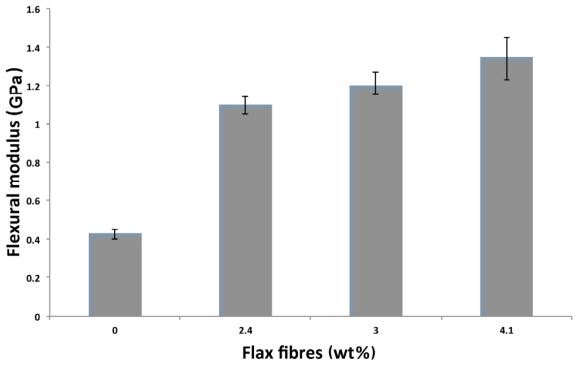

Fig. 5 Flexural modulus of geopolymer composites as a function of fabric content.

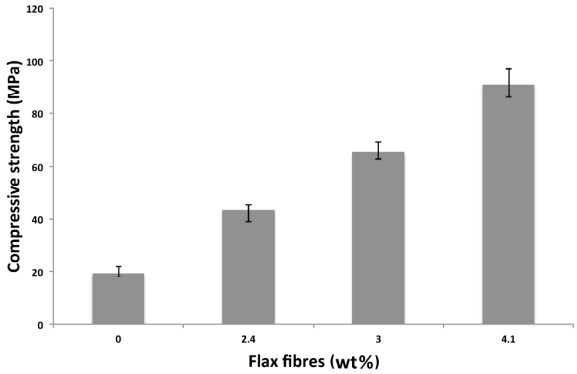

Fig. 6 Compressive strength of geopolymer composites as a function of fabric content.

3. 4 Hardness

Hardness measurement enables the ability of a material to resist plastic deformation under indentation to be determined. The hardness values of FF reinforced geopolymer composites are shown in Fig. 7. The results show that the hardness of composites increases with the addition of high number of flax fabrics to the geopolymer composite. This enhancement in hardness is due to the uniform distribution of the load on the flax fibres, which reduces the penetration of the test ball at the surface of the composite. A similar increase has been reported by other researchers studying natural fibre reinforced geopolymer composites: for instance, Alomayri *et al*. [25] reported that with increasing cotton fibre content, the hardness value of cotton fibre reinforced geopolymer composites increases.

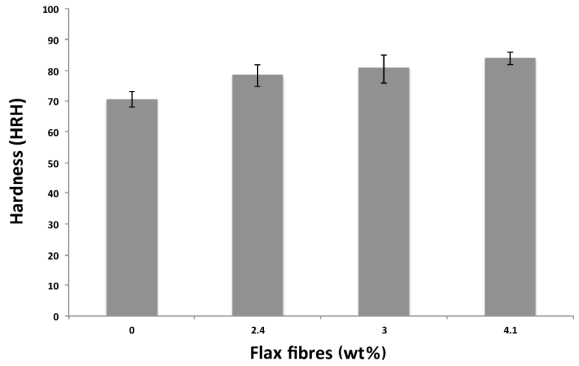

Fig. 7 Hardness of geopolymer composites as a function of fabric content.

3. 5 Fracture toughness

Generally, fibres' ability to resist crack deflection, debonding, and to bridge cracks, slows down crack propagation in fibre reinforced composites and increases the fracture energy [39–42]. Figure 8 shows the influence of FF content on the fracture toughness of geopolymer composites. It can be seen that the composites containing FF show significantly higher fracture toughness than pure geopolymer matrix, and the higher the FF content, the higher is the fracture toughness. The greatest improvement in fracture toughness was obtained from about 0.4 MPa·m$^{1/2}$ in the pure matrix to about 1.8 MPa·m$^{1/2}$ with 4.1 wt% FF reinforcement. This extraordinary enhancement is due to the unique ability of flax fibre to resist fracture resulted in increased energy dissipation from crack-deflection at the fibre–matrix interface, fibre-debonding, fibre-bridging, fibre pull-out and fracture, clearly shown in the SEM images (see Figs. 9(a)–9(f)). It can be seen in these images that small pieces of geopolymer paste attached to the fibre surface of the composites: such retention of the matrix on the fibre surfaces shows good adhesion between fibres and matrix. It was observed that the composites with fibres do not completely break into pieces, as the close spacing of woven FF leads to crack-bridging by fibres and enhancing the resistance to their propagation. The effect of fibre content on the fracture surface can be seen by observing the difference between the matrix region and the fibre region. In Figs. 10(a) and 10(b), composites filled with lower fibre contents (2.4 and 3.0 wt%) show an increase in matrix-rich regions, which means there are insufficient fibres to transfer the load from the matrix. Due to this reason, the geopolymer composites with low fibre content exhibit low fracture toughness and mechanical properties. However, Fig. 10(c) illustrates the fracture surfaces of the geopolymer composites with higher fibre content, which means higher fibre-rich regions of composites with 4.1 wt% of FF. An increase in fibre-rich regions leads to greater stress-transfer from the matrix to the FF thereby resulting in improvement of fracture toughness.

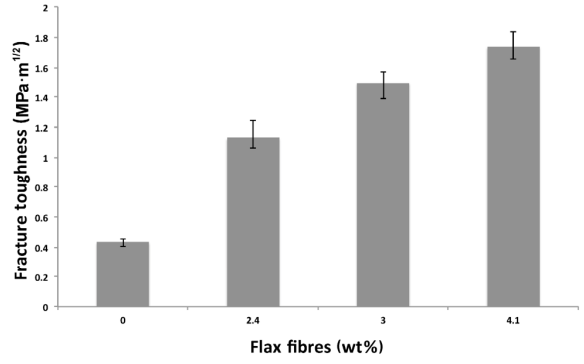

Fig. 8 Fracture toughness of geopolymer composites as a function of fabric content.

3. 6 Thermal stability

The thermal stability of samples was determined using thermogravimetric analysis (TGA). In this test, thermal stability was studied in terms of the weight loss percentage as a function of temperature in argon atmosphere. The thermograms (TGA) of FF, neat geopolymer, and FF reinforced geopolymer composite are shown in Fig. 11.

The thermogram of flax fibres shows degradation in three steps. The first transition occurs from 25 to approximately 240 ℃, with the release of free water evaporation. Then, the largest weight loss occurred between 240 and 365 ℃ is due to the decomposition of cellulose. This result is in agreement with Alzeer and MacKenzie [27], where the highest weight loss of short flax fibres under flowing air is in the range of 240–340 ℃. The final stage occurs above 365 ℃, when the fibres start to decompose but display a lower rate of weight loss, and all volatile substances are dispelled.

The pure geopolymer shows weight loss occurring from 25 to 300 ℃, caused by the evaporation of physically adsorbed water. Above 300 ℃, weight loss is attributed to the dehydroxylation of the chemically bound water. The FF reinforced geopolymer composite shows a weight loss of 10.5% up to about 260 ℃, which is due to the evaporation of physically absorbed water. Above 260 ℃, the composite shows further weight loss because of the degradation of the fibre content in the sample. The porosity of geopolymer matrix allows the

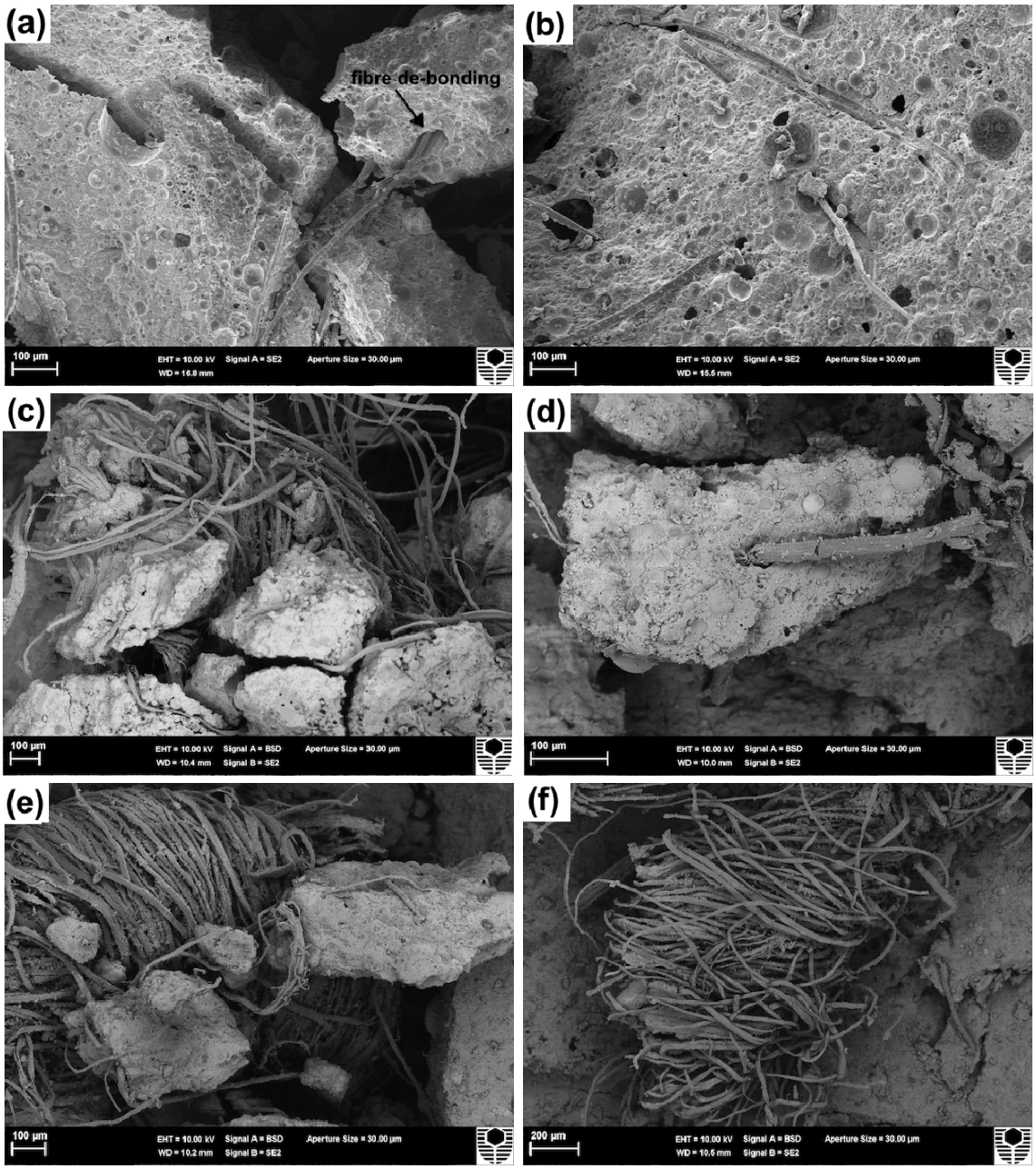

Fig. 9 SEM images of the fracture surface for geopolymer composites reinforced with flax fibres show (a) fibre debonding, (b) fibre imprint and pull-out, (c) fibre bridging cracks ((d) and (e) show the adhesion between fibre and matrix), and (f) fibre fracture.

oxygen to enter and cause degradation of the flax fibres at high temperatures. The composite shows a total weight loss of ~15% at 300 ℃ which indicates further degradation of fibres inside the composite. At this temperature a substantial amount of fibre degradation has occurred. Therefore, it could be concluded that this composite system is only suitable for service below 250 ℃. It is worth mentioning here that the TGA micro-sample is not necessarily representative of the whole composite sample because the distribution of flax fibres is not uniform within the geopolymer matrix. Therefore, the fibre content of the TGA micro-sample will be highly dependent on the position it is taken from the composite sample. However, TGA test can provide a good estimation of the thermal stability of a composite when compared to the thermal stability of its components.

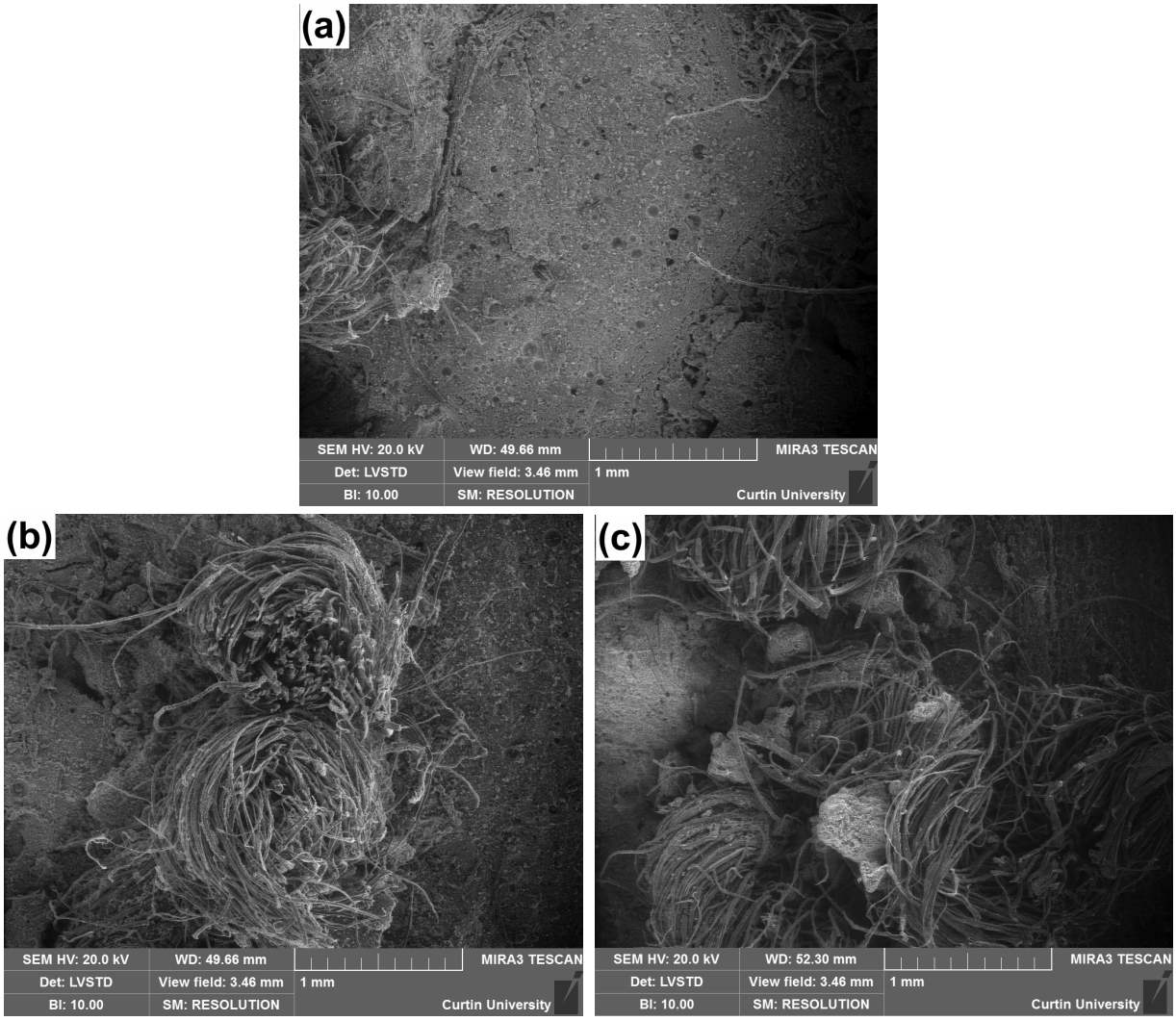

Fig. 10 Low magnification SEM images of the fracture surface for geopolymer composites reinforced with (a) 2.4, (b) 3.0, and (c) 4.1 wt% of flax fibres.

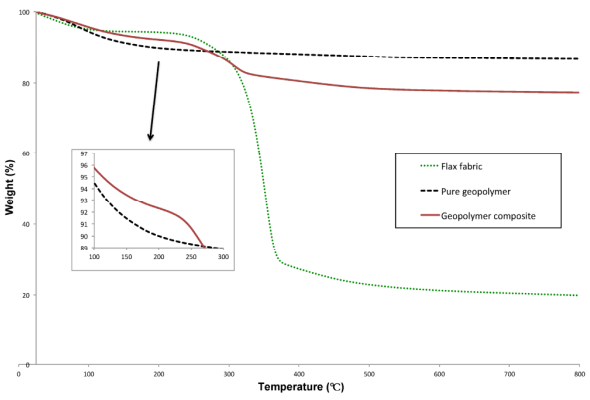

Fig. 11 TGA curves of the flax reinforced geopolymer composite, the matrix, and the flax fibres.

4 Conclusions

This paper presents the mechanical and thermal properties and microstructural characterisation of FF reinforced geopolymer composites. It shows that the presence of FF in geopolymer composites remarkably increases flexural and compressive strength, hardness, and fracture toughness compared to neat geopolymer. These significant enhancements are due to the unique properties of flax fibres in resisting greater bending and fracture forces than the more brittle geopolymer. SEM micrographs show a number of toughening mechanisms that include crack bridging, fibre pull-out, and fibre fracture; these are the major factors contributing to the

enhanced mechanical properties of FF reinforced geopolymer composites. Thermogravimetric analysis of the samples indicates that the FF reinforced geopolymer exhibits higher net weight loss than pure geopolymer due to the degradation of flax fibres.

Acknowledgements

The authors would like to thank Ms. E. Miller from the Department of Applied Physics at Curtin University for her assistance with the SEM. The authors would also thank Mr. Les Vickers of Applied Physics and Mr. Andrew Chan of Chemical Engineering at Curtin University for the help with the TGA.

References

[1] Barbosa VFF, MacKenzie KJD, Thaumaturgo C. Synthesis and characterization of materials based on inorganic polymers of alumina and silica: Sodium polysialate polymers. *Int J Inorg Mater* 2000, **2**: 309–317.

[2] Davidovits J. Geopolymers: Inorganic polymeric new materials. *J Therm Anal* 1991, **37**: 1633–1656.

[3] Duxson P, Fernández-Jiménez A, Provis JL, *et al*. Geopolymer technology: The current state of the art. *J Mater Sci* 2007, **42**: 2917–2933.

[4] Temuujin J, van Riessen A, MacKenzie KJD. Preparation and characterization of fly ash based geopolymer mortars. *Constr Build Mater* 2010, **24**: 1906–1910.

[5] Pernica D, Reis PNB, Ferreira JAM, *et al*. Effect of test conditions on the bending strength of a geopolymer-reinforced composite. *J Mater Sci* 2010, **45**: 744–749.

[6] Kriven WM, Bell JL, Gordon M. Microstructure and microchemistry of fully-reacted geopolymers and geopolymer matrix composites. In *Advances in Ceramic Matrix Composites IX, Volume 153*. Bansal NP, Singh JP, Kriven WM, *et al*. Eds. Hoboken, NJ, USA: John Wiley & Sons, Inc., 2006, DOI: 10.1002/9781118406892.ch15.

[7] Lin T, Jia D, He P, *et al*. Effects of fiber length on mechanical properties and fracture behavior of short carbon fiber reinforced geopolymer matrix composites. *Mat Sci Eng A* 2008, **497**: 181–185.

[8] Hung TD, Pernica D, Kroisová D, *et al*. Composites base on geopolymer matrices: Preliminary fabrication, mechanical properties and future application. *Adv Mat Res* 2008, **55–57**: 477–480.

[9] Rill E, Lowry DR, Kriven WM. Properties of basalt fiber reinforced geopolymer composites. In *Strategic Materials and Computational Design: Ceramic Engineering and Science Proceedings, Volume 31*. Kriven WM, Zhou Y, Radovic M, *et al*. Eds. Hoboken, NJ, USA: John Wiley & Sons, Inc., 2010, DOI: 10.1002/9780470944103.ch6.

[10] Silva FJ, Thaumaturgo C. Fibre reinforcement and fracture response in geopolymeric mortars. *Fatigue Fract Eng M* 2003, **26**: 167–172.

[11] Vijai K, Kumuthaa R, Vishnuram BG. Properties of glass fibre reinforced geopolymer concrete composites. *Asian Journal of Civil Engineering (Building and Housing)* 2012, **13**: 511–520.

[12] Zhao Q, Nair B, Rahimian T, *et al*. Novel geopolymer based composites with enhanced ductility. *J Mater Sci* 2007, **42**: 3131–3137.

[13] Dweib MA, Hu B, O'Donnell A, *et al*. All natural composite sandwich beams for structural applications. *Compos Struct* 2004, **63**: 147–157.

[14] Tanobe VOA, Sydenstricker THD, Munaro M, *et al*. A comprehensive characterization of chemically treated Brazilian sponge-gourds (*luffa cylindrical*). *Polym Test* 2005, **24**: 474–482.

[15] Chandramohan D, Marimuthu K. A review on natural fibers. *IJRRAS* 2011, **8**: 194–206.

[16] Beckwith SW. Natural fibers: Nature providing technology for composites. *SAMPE J* 2008, **44**: 64–65.

[17] Low IM, Schmidt P, Lane J. Synthesis and properties of cellulose-fibre/epoxy laminates. *J Mater Sci Lett* 1995, **14**: 170–172.

[18] Low IM, Somers J, Pang WK. Synthesis and properties of recycled paper-nano-clay-reinforced epoxy eco-composites. *Key Eng Mat* 2007, **334–335**: 609–612.

[19] Zadorecki P, Michell AJ. Future prospects for wood cellulose as reinforcement in organic polymer composites. *Polym Composite* 1989, **10**: 69–77.

[20] McGrath M, Vilaiphand W, Vaihola S, *et al*. Synthesis and properties of clay–ZrO_2–cellulose fibre-reinforced polymeric nano-hybrids. In Proceedings of Structural Integrity and Fracture International Conference, Brisbane, 2004: 265–270.

[21] Panaitescu DM, Vuluga DM, Paven H, *et al*. Properties of polymer composites with cellulose microfibrils. *Mol Cryst Liq Cryst* 2008, **484**: 86–98.

[22] Low IM, Somers J, Kho HS, *et al*. Fabrication and properties of recycled cellulose fibre-reinforced epoxy composites. *Compos Interface* 2009, **16**: 659–669.

[23] Rahman MM, Rashid MH, Hossain MA, *et al*. Performance evaluation of bamboo reinforced concrete beam. *International Journal of Engineering & Technology* 2011, **11**: 113–118.

[24] Lin X, Silsbee MR, Roy DM, *et al*. Approaches to improve the properties of wood fiber reinforced cementitious composites. *Cement Concrete Res* 1994, **24**: 1558–1566.

[25] Alomayri T, Shaikh FUA, Low IM. Effect of fabric orientation on mechanical properties of cotton fabric reinforced geopolymer composites. *Mater Design* 2014, **57**: 360–365.

[26] Alzeer M, MacKenzie KJD. Synthesis and mechanical

properties of new fibre-reinforced composites of inorganic polymers with natural wool fibres. *J Mater Sci* 2012, **47**: 6958–6965.

[27] Alzeer M, MacKenzie K. Synthesis and mechanical properties of novel composites of inorganic polymers (geopolymers) with unidirectional natural flax fibres (*phormium tenax*). *Appl Clay Sci* 2013, **75–76**: 148–152.

[28] ASTM International. ASTM D790, Standard test methods for flexural properties of unreinforced and reinforced plastics and electrical insulating materials. ASTM International, West Conshohocken, PA, USA, 2015.

[29] Low IM, McGrath M, Lawrence D, *et al*. Mechanical and fracture properties of cellulose-fibre-reinforced epoxy laminates. *Composites Part A* 2007, **38**: 963–974.

[30] ASTM International. ASTM C109/C109-12, Standard test method for compressive strength of hydraulic cement mortars (using 2-in. or [50-mm] cube specimens). ASTM International, West Conshohocken, PA, USA, 2013.

[31] Phair JW, Van Deventer JSJ. Effect of the silicate activator pH on the microstructural characteristics of waste-based geopolymers. *Int J Miner Process* 2002, **66**: 121–143.

[32] Karbowiak T, Ferret E, Debeaufort F, *et al*. Investigation of water transfer across thin layer biopolymer films by infrared spectroscopy. *J Membrane Sci* 2011, **370**: 82–90.

[33] Lasagabáster A, Abad MJ, Barral L, *et al*. Application of FTIR spectroscopy to determine transport properties and water–polymer interactions polypropylene(PP)/poly (ethylene-co-vinyl alcohol) (EVOH) blend films: Effect of poly(ethylene-co-vinyl alcohol) content and water activity. *Polymer* 2009, **50**: 2981–2989.

[34] Zaharaki D, Komnitsas K, Perdikatsis V. Use of analytical techniques for identification of inorganic polymer gel composition. *J Mater Sci* 2010, **45**: 2715–2724.

[35] Tserki V, Zafeiropoulos NE, Simon F, *et al*. A study of the effect of acetylation and propionylation surface treatments on natural fibres. *Composites Part A* 2005, **36**: 1110–1118.

[36] Abanilla MA, Karbhari VM, Li Y. Interlaminar and interlaminar durability characterization of wet layup carbon/epoxy used in external strengthening. *Composites Part B* 2006, **37**: 650–661.

[37] Sim J, Park C, Moon DY. Characteristics of basalt fiber as a strengthening material for concrete structures. *Composites Part B* 2005, **36**: 504–512.

[38] Alomayri T, Shaikh FUA, Low IM. Synthesis and mechanical properties of cotton fabric reinforced geopolymer composites. *Composites Part B* 2014, **60**: 36–42.

[39] Reis JML. Fracture and flexural characterization of natural fiber-reinforced polymer concrete. *Constr Build Mater* 2006, **20**: 673–678.

[40] Silva FA, Mobasher B, Filho RDT. Cracking mechanisms in durable sisal fiber reinforced cement composites. *Cement Concrete Comp* 2009, **31**: 721–730.

[41] Silva FA, Filho RDT, Filho JAM, *et al*. Physical and mechanical properties of durable sisal fiber–cement composites. *Constr Build Mater* 2010, **24**: 777–785.

[42] Filho RDT, Ghavami K, England GL, *et al*. Development of vegetable fibre–mortar composites of improved durability. *Cement Concrete Comp* 2003, **25**: 185–196.

3.2 Effect of nano-clay on mechanical and thermal properties of geopolymer

Assaedi, H., Shaikh, F.U.A. and Low, I.M., 2016. Effect of nano-clay on mechanical and thermal properties of geopolymer. *Journal of Asian Ceramic Societies*, *4*(1), pp.19-28.

Journal of Asian Ceramic Societies 4 (2016) 19–28

HOSTED BY

Contents lists available at ScienceDirect

Journal of Asian Ceramic Societies

journal homepage: www.elsevier.com/locate/jascer

Effect of nano-clay on mechanical and thermal properties of geopolymer

H. Assaedi [a], F.U.A. Shaikh [b], I.M. Low [a,*]

[a] Department of Imaging & Applied Physics, Curtin University, GPO Box U1987, Perth, WA 6845, Australia
[b] Department of Civil Engineering, Curtin University, GPO Box U1987, Perth, WA 6845, Australia

ARTICLE INFO

Article history:
Received 18 September 2015
Received in revised form 29 October 2015
Accepted 31 October 2015
Available online 15 December 2015

Keywords:
Geopolymer
Nano-clay
Mechanical properties
Thermal properties

ABSTRACT

The effect of nano-clay platelets (Cloisite 30B) on the mechanical and thermal properties of fly ash geopolymer has been investigated in this paper. The nano-clay platelets are added to reinforce the geopolymer at loadings of 1.0%, 2.0%, and 3.0% by weight. The phase composition and microstructure of geopolymer nano-composites are also investigated using X-ray diffraction (XRD), Fourier transform infrared spectroscopy (FTIR) and scanning electron microscope (SEM) techniques. Results show that the mechanical properties of geopolymer nano-composites are improved due to addition of nano-clay. It is found that the addition of 2.0 wt% nano-clay decreases the porosity and increases the nano-composite's resistance to water absorption significantly. The optimum 2.0 wt% nano-clay addition exhibited the highest flexural and compressive strengths, flexural modulus and hardness. The microstructural analysis results indicate that the nano-clay behaves not only as a filler to improve the microstructure, but also as an activator to facilitate the geopolymeric reaction. The geopolymer nano-composite also exhibited better thermal stability than its counterpart pure geopolymer.

1. Introduction

Geopolymers are synthesized by activating a solid aluminosilicate source with alkaline solutions. They are currently attracting extensive research because of their potential as a high-performance and environmentally friendly alternative to ordinary Portland cement in different applications [1,2]. It has been shown that a wide range of waste aluminosilicate materials can be converted into building materials, as they show excellent physical and chemical properties [3–7]. However, geopolymer pastes suffer from brittle failure mode under applied force. The typical values of the compressive strength of geopolymer-based ceramics are around 45 MPa [8] which are comparable to the strength of Portland cement pastes. However, geopolymer pastes show lower flexural strength ranging between 1.7 MPa and 16.8 MPa [8,9]. Improving the flexural and tensile strengths will promote the application of these materials significantly in construction and building industries.

In recent years, nanotechnology has gained attention in ceramic and polymer research, particularly in forming nano-composites which have superior physical and mechanical properties [5]. In geopolymers, various types of nanoparticles have been incorporated successfully to improve their mechanical properties. Alumina and silica nanoparticles have been used successfully as reinforcements for geopolymer pastes, giving them superior mechanical properties. Nano-alumina and nano-silica not only acted as fillers, but also enhanced the geopolymerization reaction [10]. In another study, it has been found that nano-silica and nano-alumina particles have the ability to reduce the porosity and water absorption of geopolymer matrices [11]. A further study on the effect of adding carbon nanotubes to fly-ash-based geopolymer has shown an increase in the mechanical and electrical properties of geopolymer nano-composites when compared to the control paste [12]. In another study, the addition of calcium carbonate ($CaCO_3$) nanoparticles to high-volume fly-ash concrete improved the flexural and mechanical properties, decreased the porosity and improved the concrete resistance to water absorption [13]. Recently, a study on nano-clay cement nano-composites demonstrated that the nano-clay significantly improved the mechanical and thermal properties of the cement matrix [14]. Hitherto, no research has been conducted to investigate the effect of nano-clay on thermal and mechanical properties of geopolymer. The incorporation of nano-clay in

* Corresponding author. Tel.: +61 8 9266 4759; fax: +61 8 9266 2377.
E-mail address: j.low@curtin.edu.au (I.M. Low).
Peer review under responsibility of The Ceramic Society of Japan and the Korean Ceramic Society.

http://dx.doi.org/10.1016/j.jascer.2015.10.004

Table 1
Chemical composition of fly-ash (wt%).

SiO_2	Al_2O_3	CaO	Fe_2O_3	K_2O	MgO	Na_2O	P_2O_5	SO_3	TiO_2	MnO	BaO	LOI
63.13	24.88	2.58	3.07	2.01	0.61	0.71	0.17	0.18	0.96	0.05	0.07	1.45

geopolymer paste could significantly enhance the matrix in two ways: (a) by adding more silica to the system which reacts with sodium to produce sodium aluminosilicate hydrate (geopolymer gel) [10] and (b) by producing a denser matrix through the pore filling effect [14].

The current study has examined the effect of adding different loadings of nano-clay to the geopolymer paste. Results showed that the addition of nano-clay improved the mechanical and thermal properties of geopolymer. Flexural and compressive tests have been performed to measure the various mechanical properties and thermogravimetric analysis (TGA) has been used to examine the thermal behavior of geopolymer containing nano-clay. In addition, X-ray diffraction, Fourier transform infrared spectroscopy (FTIR) and scanning electron microscopy (SEM) techniques were used to characterize the phase composition and microstructure of geopolymer-nano-clay composites.

2. Experimental procedure

2.1. Materials

Low-calcium fly-ash (ASTM class F), obtained from the Erarring power station in NSW, was used to prepare the geopolymeric nano-composites. The chemical composition of fly-ash is shown in Table 1. The alkaline activator for geopolymerization was a combination of sodium hydroxide solution and sodium silicate grade D solution. Sodium hydroxide flakes with 98% purity were used to prepare the solution. The chemical composition of sodium silicate used was 14.7% Na_2O, 29.4% SiO_2 and 55.9% water by mass. The nano-clay (Cloisite 30B) used in this investigation was based on natural montmorillonite clay which has composition of $(Na,Ca)_{0.33}(Al,Mg)_2(Si_4O_{10})(OH)_2{\cdot}nH_2O$. Cloisite 30B is a natural montmorillonite modified with a quaternary ammonium salt, which was supplied by Southern Clay Products, USA. The specification and physical properties of Cloisite 30B are outlined in Table 2 [15].

2.2. Preparation of geopolymer nano-composites

To prepare the geopolymer pastes, an alkaline solution to fly ash ratio of 0.75 was used and the ratio of sodium silicate solution to sodium hydroxide solution was fixed at 2.5. The concentration of sodium hydroxide solution was 8 M, which is prepared and combined with the sodium silicate solution one day before mixing.

The nano-clay was added to the fly-ash at the loadings of 1.0%, 2.0% and 3.0% by weight. The fly-ash and nano-clay were first dry mixed for 5 min in a Hobart mixer at a low speed and then mixed for another 10 min at high speed until a uniform mixture was achieved.

Table 2
Physical properties of the nano-clay platelets (Cloisite 30B) [13].

Color	Off white
Density (g/cm^3)	1.98
d-Spacing (0 0 1) (nm)	1.85
Aspect ratio	200–1000
Surface area (m^2/g)	750
Typical dry particle sizes	90% volume < 13 μm
	50% volume < 6 μm
	10% volume < 2 μm

The alkaline solution was then added slowly to the fly-ash and nano-clay in the mixer at a low speed until the mix became homogeneous, then further mixed for another 10 min on high speed. The resultant mixture was then poured into wooden molds. The wooden molds were then placed on a vibration table for 2 min before they were covered with a plastic film and cured at 80 °C for 24 h in an oven before demolding. They were then cured under ambient conditions for 28 days. The pure geopolymer, and nano-composites containing 1.0%, 2.0% and 3.0% nano-clay were labeled GP, GPNC-1, GPNC-2 and GPNC-3, respectively. The formulation of samples is given in Table 3.

2.3. Physical properties

Measurements of bulk density and porosity were conducted to define the quality of geopolymer nano-composite. Density of samples (ρ) with volume (V) and dry mass (m_d) was calculated using Eq. (1):

$$\rho = \frac{m_d}{V} \tag{1}$$

The value of apparent porosity (P_a) was determined using Archimedes' principle in accordance with the ASTM Standard (C-20) [16]. Pure geopolymer and nano-composite samples were immersed in clean water, and the apparent porosity (P_a) was calculated using Eq. (2) [17]:

$$P_a = \frac{m_a - m_d}{m_a - m_w} \times 100 \tag{2}$$

where m_a is mass of the saturated samples in air, and m_w is mass of the saturated samples in water.

For the water absorption test, samples of pure geopolymer and geopolymer nano-composites were dried at a temperature of 80 °C until reaching stable mass (m_o). The samples were then submerged in clean water at a temperature of 20 °C for 48 h. After the desired absorption period, the samples were removed and the mass was weighed (m_1) immediately. The water absorption (W_A) of samples was calculated using the equation [18]:

$$W_A = \frac{m_1 - m_0}{m_0} \times 100 \tag{3}$$

2.4. Mechanical properties

A LLOYD Material Testing Machine (50 kN capacity) with a displacement rate of 0.5 mm/min was used to perform the mechanical tests. Rectangular bars of 60 mm × 18 mm × 15 mm were cut from the fully cured samples for three-point bend test with a span of 40 mm to evaluate the flexural strength. Five samples of each group were used to evaluate the flexural strength and flexural modulus of geopolymer composites. The values were recorded and analyzed with the machine software (NEXYGENPlus) and average values

Table 3
Formulation of samples.

Sample	Fly-ash (g)	NaOH solution (g)	Na_2SiO_3 solution (g)	Nano-clay (g)
GP	1000	214.5	535.5	0
GPNC-1	1000	214.5	535.5	10
GPNC-2	1000	214.5	535.5	20
GPNC-3	1000	214.5	535.5	30

were calculated. The flexural strength (σ_F) was determined using the equation [19]:

$$\sigma_F = \frac{3P_mS}{2WD^2} \quad (4)$$

where P_m is the maximum load, S is the span of the sample, D is the specimen width, and W is the specimen thickness.

Values of flexural modulus (E_F) were computed using the initial slope of the load–displacement curve ($\Delta P/\Delta X$) [19]:

$$E_F = \frac{S^3}{4WD^3}\left(\frac{\Delta P}{\Delta X}\right) \quad (5)$$

20 mm cube specimens were used for the determination of compressive strength. The compressive strength of geopolymer composites was tested according to ASTM C109 and calculated using the following formula [20]:

$$C = \frac{P}{A} \quad (6)$$

where P is maximum load on the sample at failure, and A is the surface area of the specimen.

The hardness of geopolymer composites was measured on the Rockwell H scale using an Avery Rockwell hardness tester. Before measurement, five samples of each group were polished with emery paper to achieve flat and smooth surfaces.

2.5. Structural and microstructural characterization

The samples were broken and ground to fine powder. Then, they were scanned using a D8 Advance Diffractometer (Bruker-AXS, Germany) using copper radiation and a LynxEye position sensitive detector. The diffractometer was scanned from 7.5° to 60° using a scanning rate of 0.5°/min. XRD patterns were obtained by using Cu k_α lines (k = 1.5406 Å).

The microstructures of geopolymer composites were examined using Zeiss Neon focused ion beam scanning electron microscope (FIB-SEM). The specimens were mounted on aluminum stubs using carbon tape and then coated with a thin layer of platinum to prevent charging before the observation.

An FTIR analysis was performed on a Perkin Elmer Spectrum 100 FTIR spectrometer in the range of 4000–500 cm^{-1} at room temperature. The spectrum was an average of 10 scans at a resolution of 2 cm^{-1}, corrected for background.

The thermal behavior of samples was studied by thermogravimetric analysis (TGA) and differential thermogravimetry (DTG). A Mettler Toledo TGA/DSC star system analyzer was used for the measurements. Solid samples were placed in an alumina crucible and tests were carried out in Argon atmosphere with a heating rate of 10 °C/min from 25 to 800 °C.

3. Results and discussion

3.1. Density, porosity and water absorption

The results of porosity and water absorption of geopolymer paste and geopolymer nano-composites are shown in Table 4. All geopolymer nano-composites showed higher densities and lower porosities than the control paste. The addition of nano-clay has increased the density and reduced the porosity and the water absorption of geopolymer nano-composites when compared to control geopolymer paste. The optimum addition was found as

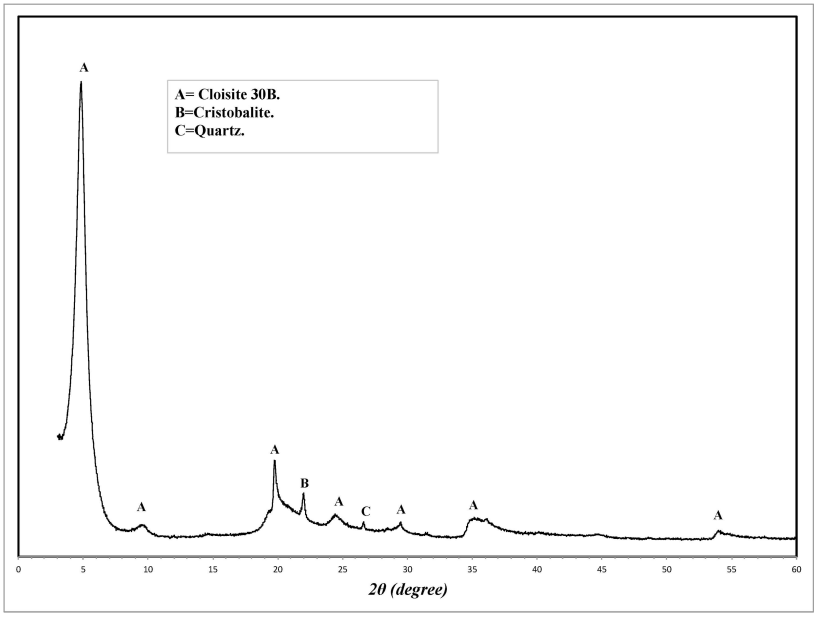

Fig. 1. X-ray diffraction pattern of nano-clay (Cloisite 30B).

Table 4
Porosity and water absorption for pure geopolymer and geopolymer nano-composites.

Sample	Density (gm/cm^3)	Porosity (%)	Water absorption (%)
GP	1.84 ± 0.02	22.2 ± 0.4	12.1 ± 0.2
GPNC-1	1.92 ± 0.02	21.3 ± 0.3	11.1 ± 0.1
GPNC-2	2.05 ± 0.02	20.6 ± 0.3	10.0 ± 0.2
GPNC-3	1.98 ± 0.03	21.0 ± 0.2	10.6 ± 0.2

2.0 wt% of nano-clay, which reduced the porosity by 7.1%, and the water absorption by 17% when compared to the control paste. This implies that nano-clay particles played a pore-filling role to reduce the porosity of geopolymer composites. However, adding excessive amounts of nano-clay increased the porosity and decreased the density of all samples. This result is comparable to that of cement reinforced organo-clay composites whereby the porosity of cement paste is decreased due to addition of an optimum amount of nano-clay to cement paste. However, the porosity is increased when more nanoparticles were added because of the agglomeration effect [14].

3.2. X-ray diffraction (XRD)

The XRD patterns of nano-clay, fly ash, control geopolymer paste, and geopolymer nano-composites containing 1.0, 2.0 and 3.0 wt% of nano-clay are shown in Figs. 1 and 2. The crystalline phases were indexed using Powder Diffraction Files (PDFs) from the Inorganic Crystal Structure Database (ISCD).

Fig. 1 shows the XRD patterns of nano-clay. Three phases have been indexed in the diffraction pattern of nano-clay with the major phase being Cloisite 30B and minor phases of Cristobalite [SiO_2]

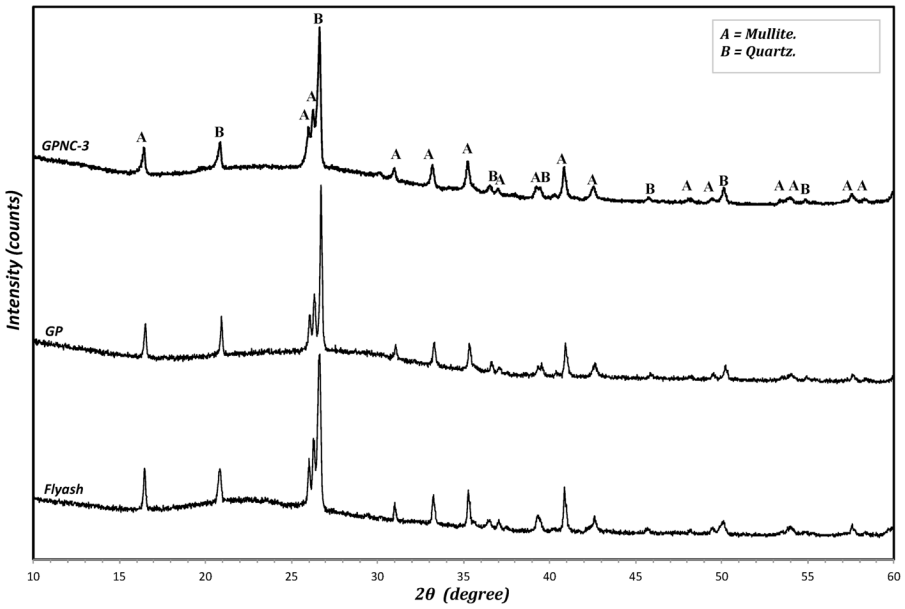

Fig. 2. X-ray diffraction patterns of fly-ash, GP and GPNC-3.

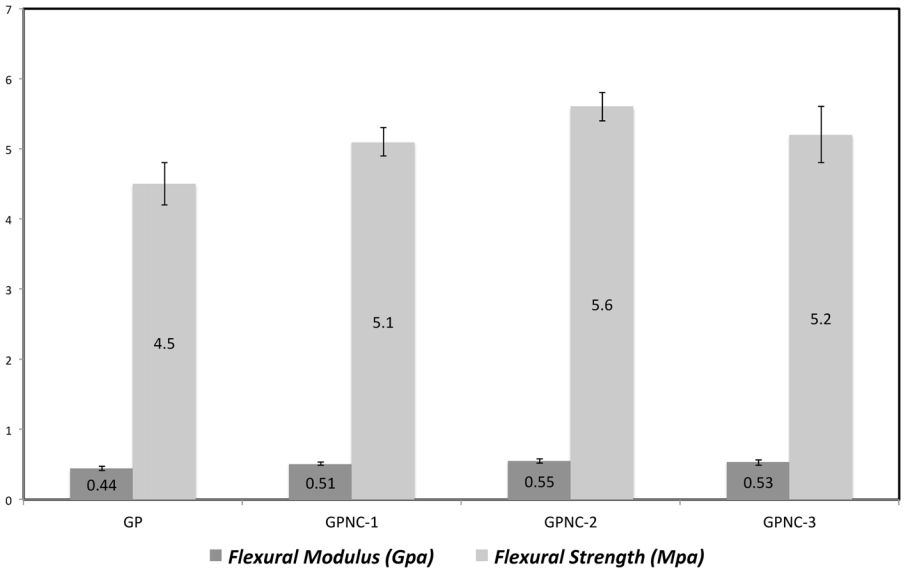

Fig. 3. Flexural strength and flexural modulus of samples GP, GPNC-1, GPNC-2 and GPNC-3.

(PDF-000391425) and Quartz [SiO_2] (PDF-000470718). Cloisite 30B consists of Montmorillonite [$(Ca,Na)_{0.3}Al_2(Si,Al)_4O_{10}(OH)_2{\cdot}xH_2O$] and the quaternary ammonium salt. Montmorillonite has four major peaks in the XRD pattern that correspond to 2θ of 4.84°, 19.74°, 35.12° and 53.98°. The quaternary ammonium salt has four peaks that correspond to 2θ of 4.84°, 9.55°, 24.42° and 29.49°. Note that there was an overlap of peaks at 2θ of 4.84° for Montmorillonite and quaternary ammonium salt. Both Cristobalite and Quartz have a peak that corresponds to 2θ of 21.99° and 26.61° respectively. The broad hump in the diffraction pattern of Cloisite 30B indicates the presence of amorphous content in the nano-clay.

Fig. 2 shows two important phases: quartz [SiO_2] (PDF-010872096) and mullite [$Al_{4.56}Si_{1.44}O_{9.72}$] (PDF-010791458). These crystalline phases are mainly the fly-ash phases, and they are not reactive in the geopolymeric reaction, but they are existing as unreactive and filler particles in the geopolymer paste [21,22]. However, the amorphous aluminosilicate phase generated between $2\theta = 14°$ and 27° is a sign of the activity of geopolymeric reaction, which is the reactive and dissolvable content in alkaline solution throughout the geopolymer formation [23]. This amorphous phase affects the mechanical properties of geopolymer matrix significantly: the higher the content of amorphous phase, the higher the strength exhibited by the geopolymer [24,25].

3.3. Mechanical properties

The flexural tests are often used to characterize the mechanical properties of composites as they provide a simple means of determining the bending response. This provides useful information on the performance of the composites. The effect of

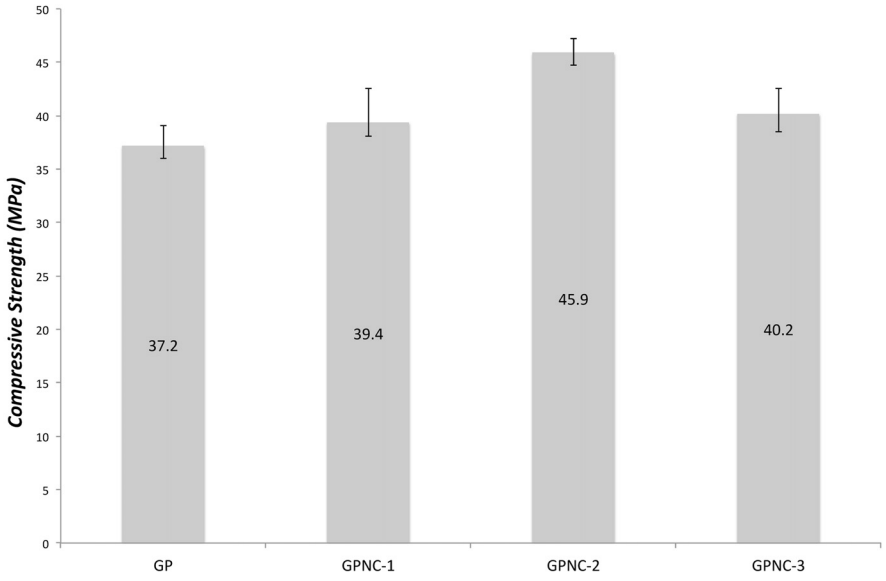

Fig. 4. Compressive strength of samples GP, GPNC-1, GPNC-2 and GPNC-3.

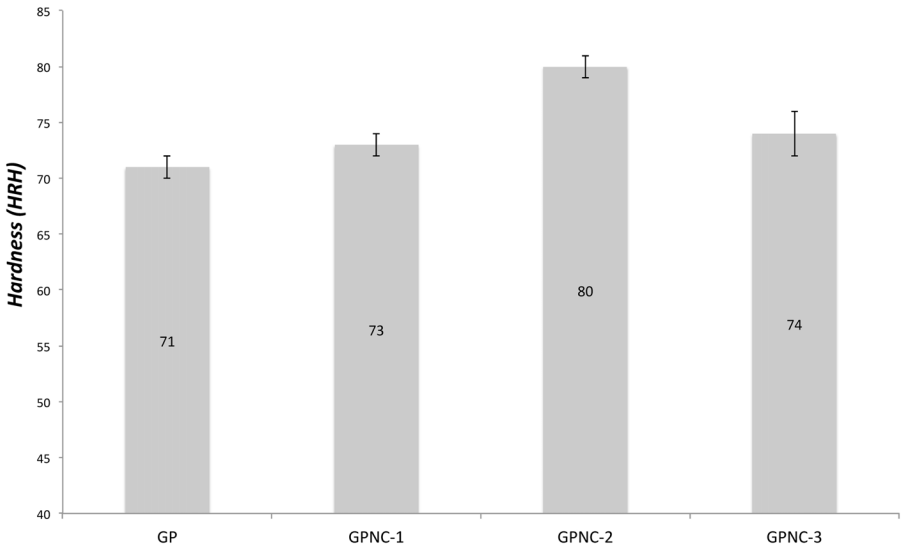

Fig. 5. Hardness of samples GP, GPNC-1, GPNC-2 and GPNC-3.

nano-clay addition on the flexural strength of geopolymer nano-composites is presented in Fig. 3. Experimental results indicate that the flexural strength of samples initially increases with increasing nano-clay content of up to 2.0 wt% but decreases at higher contents. The flexural strength of the nano-composites is improved from 4.5 MPa in the control to about 5.6 MPa with 2.0 wt% nano-clay. This improvement can be attributed to the good dispersion of the nano-particles throughout the matrix, leading to less porosity and denser geopolymer matrix. This result is comparable with that of nano-clay-cement composite reported by Hakamy et al. [14] who found that the optimum addition of nano-clay to cement mix is about 1.0 wt%, which increases the flexural strength of the nano-composites by 31% over the control sample. Both studies imply that increasing the content of nano-clay led to some improvement in flexural strength of the composite. This result can also be ascribed to the nano-particles effect, which improved the matrix through geopolymeric reaction and increased the amorphous content, producing higher content of geopolymer products.

The flexural modulus is a measure of resistance to deformation of the composite in bending. The flexural modulus of control paste and geopolymer nano-composites is shown in Fig. 3 and also indicates that the optimum addition of nano-clay is 2.0 wt% to the geopolymer matrix, and it improved the flexural modulus over a pure geopolymer matrix by 25%.

The compressive strength results of geopolymer and geopolymer nano-composites are shown in Fig. 4, and indicate similar trends to flexural strength and modulus values. Compressive strength is inversely proportional to porosity: specimens with less porosity displayed higher compressive strength. The compressive strength of the neat geopolymer paste is improved from 37.2 to 45.9 MPa after the addition of 2.0 wt% nano-clay, but this trend is reversed, reducing the strength to 40.2 MPa with the addition of 3.0 wt% nano-clay. In a similar study, Phoo-ngernkham et al. [10] reported that the addition of 1.0–2.0 wt% nano-alumina and amorphous nano-silica into geopolymer matrix enhanced the geopolymeric reaction and increased the geopolymer gel, which increased the density and consequently improved the compressive strength of geopolymer matrix. Both studies showed that increasing the compressive strength of geopolymer pastes is corresponded to the reduction in porosity.

The hardness values of the control sample and geopolymer nano-composites are presented in Fig. 5. The results show that there was no significant improvement observed between all samples. However, the geopolymer nano-composite with 2.0 wt% of nano-clay showed slightly higher hardness than other samples. This enhancement could be attributed to the high density of the geopolymer nano-composite paste, which decreased the penetration of the test ball on the surface of the nano-composite matrix and consequently improved the hardness.

3.4. SEM observation

Fig. 6a–d shows the SEM micrographs of fracture surface of nano-composite containing 0, 1.0, 2.0, and 3.0 wt% nano-clay. The pure geopolymer has a less dense matrix with a higher number of non-reacted and partially reacted fly-ash particles embedded in the matrix (Fig. 6a). For the 1–3 wt% nano-clay (Fig. 6b–d) less numbers of fly-ash particles were observed, and the matrix seemed denser than that of the control paste.

Fig. 6e and f displays an observation of the geopolymer matrix that was loaded with 3.0 wt% nano-clay at low magnification. Nano-clay particles are poorly dispersed and agglomerated due to the high content of nano-clay. Fig. 6g and h shows agglomerations of nano-clay platelets at higher magnification.

3.5. FTIR observation

FTIR spectra of both pure geopolymer and geopolymer nano-composite are shown in Fig. 7. The FTIR spectra of all samples show a strong peak at ~1000 cm^{-1} which is associated with Si–O–Si asymmetric stretching vibrations and is the fingerprint of the geopolymerization [26]. A broad peak in the region around 3340 cm^{-1} is corresponding to the hydroxyl (OH) group of physically free water (higher frequencies), and to chemically bounded water through hydrogen bonds (lower frequencies) [27]. The absorbance peak at 1640 cm^{-1} is also attributed to the (OH) bending vibration [28]. The band at 1440 cm^{-1} is an indicator of the presence of sodium carbonate; this was produced because of the atmospheric carbonation on the surface of the matrix where it reacts with carbon dioxide [29]. The level of geopolymerization can be specified by measuring the ratios of the height and the area of the Si–O–Si stretching peaks of the nano-composites to the pure matrix [28]. Table 5 illustrates that all nano-composites had generally higher contents of geopolymer compared to the control paste; however, the addition of 2.0 wt%

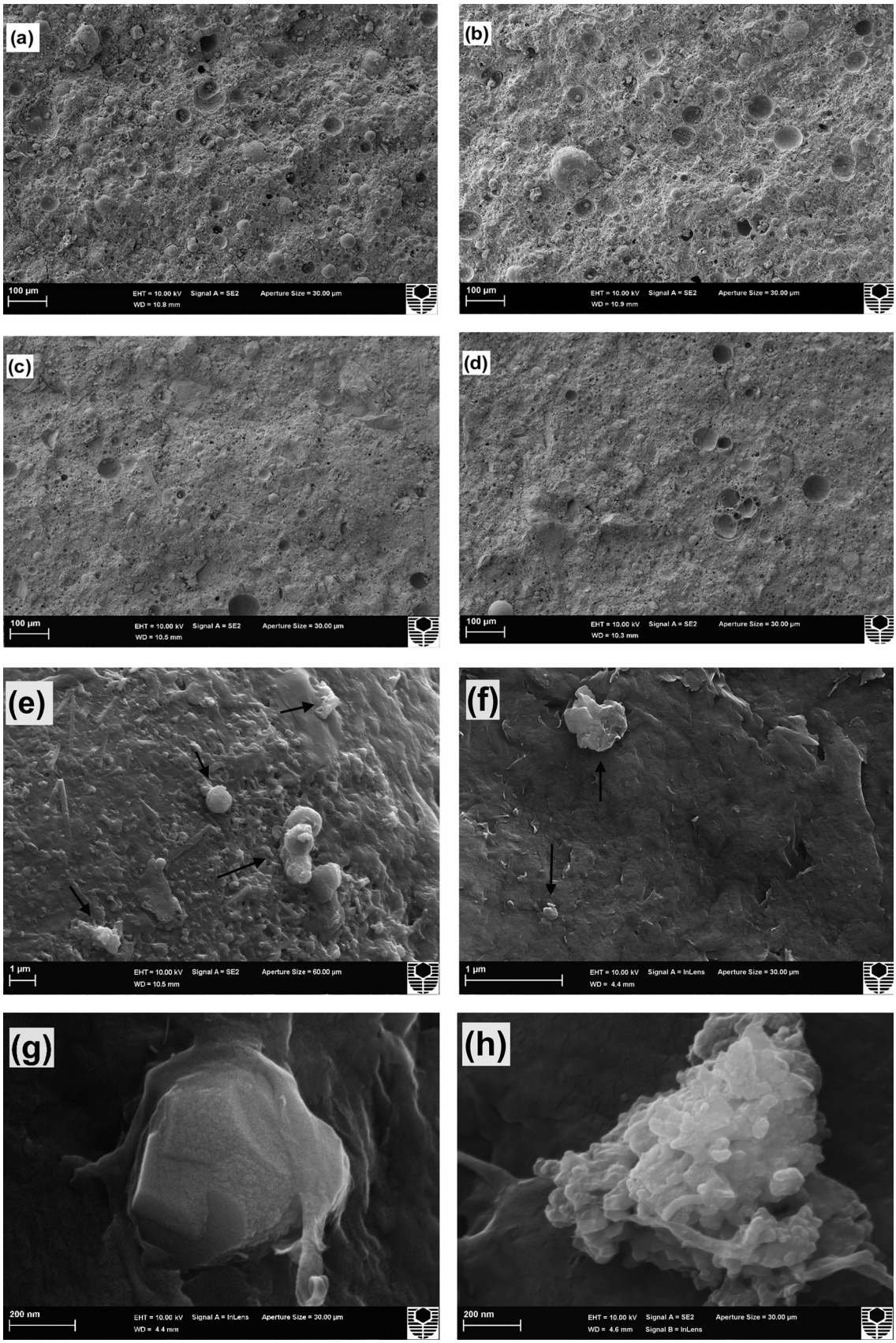

Fig. 6. SEM images of the fracture surface of geopolymer nano-composites with different loadings of nano-clay: (a) pure geopolymer, (b) 1.0 wt%, (c) 2.0 wt%, (d) 3.0 wt%, agglomerated nano-clay particles embedded in the matrix at: (e and f) low magnification and (g and h) higher magnification.

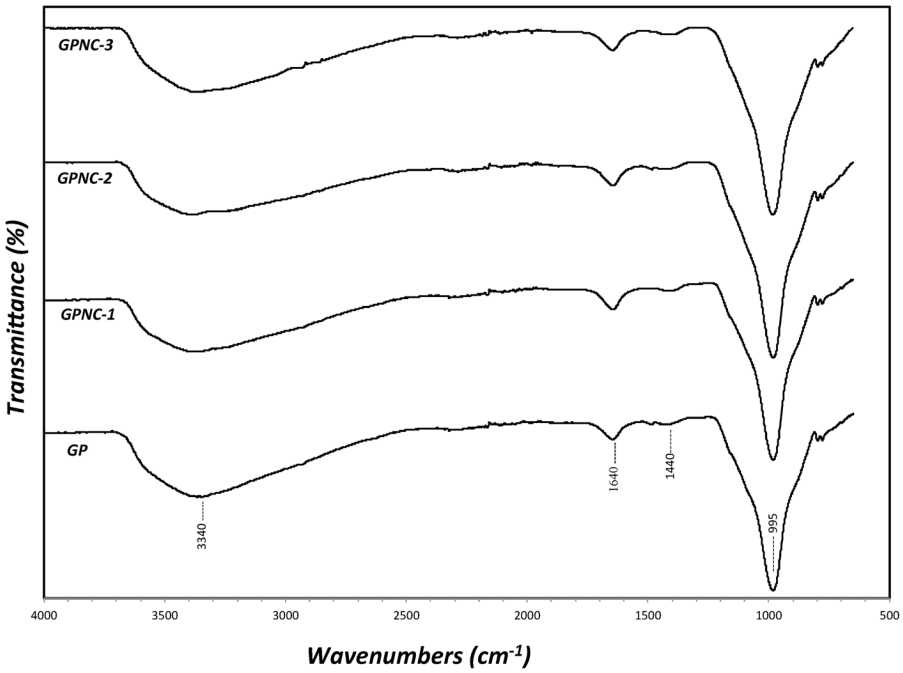

Fig. 7. FTIR spectra of all samples.

of nano-clay had the highest level of geopolymerization among all samples.

3.6. Thermal stability

The thermal stability of samples was determined using thermogravimetric analysis (TGA). In this test, the thermal stability was studied in terms of the weight loss percentage as a function of temperature in Argon atmosphere. The results of thermogravimetric analysis (TGA) and the differential thermogravimetry (DTG) of all samples are shown in Figs. 8 and 9, respectively. The residual mass at different temperatures for nano-clay and all samples are summarized in Table 6.

The residual mass results exhibit the remaining weight percentage of the material after the TGA test, which could be an indicator of the organic/inorganic component of the material [30]. For instance, in the case of nano-clay, TGA showed that about 30 wt% of the component burnt at 800 °C, which is the organic component in the Cloisite 30B. This is equivalent to the loss on ignition wt% of the supplier technical data sheet of the Cloisite 30B.

Fig. 8 shows that the major decomposition region of the nano-clay is between 300 °C and 450 °C, where the weight loss is about 21%. However, there are no noteworthy changes that occurred to the weight loss of the nano-composites curves at the same region, rather they showed almost the same weight loss of the pure geopolymer. This shows that the decomposition of nano-clay did not influence the thermal stability of the nano-composite due to the small wt% nano-clay additions.

Table 5
Peak areas and peak heights ratios of geopolymers at Si–O–Si stretching vibrations from FTIR spectra.

Sample	Wave-number of Si–O–Si peak	Ratio of peak heights	Ratio of peak areas
GP	983	1	1
GPNC-1	983	1.02	1.02
GPNC-2	981	1.19	1.07
GPNC-3	980	1.15	1.03

The TGA of the pure geopolymer and the nano-composites showed a major weight loss from room temperature to 150 °C, due to the evaporation of physically adsorbed water. The neat geopolymer curve is steeper in this region compared to the nano-composites curves, which is clearly shown in DTG graph (Fig. 9) where the peak of pure geopolymer moved to a lower temperature compared to the nano-composite. This is due to the formation of high porosity in the neat geopolymer, which reduces the ability of the sample to retain water. On the other hand, GPNC-2 sample exhibited the highest thermal stability among all geopolymer samples, the peak of the nano-composite containing 2.0 wt% nano-clay shifted slightly to a higher temperature than other samples. This may be attributed to the effect of nano-clay filling the voids, producing denser geopolymer, and/or it may be attributed to the fact that the nano-composite specimens had higher amounts of geopolymer gel and amorphous content. Between 150 °C and 300 °C, the rate of weight loss for all samples started to slow as the physical free water had already evaporated, and the interstitial water [31] started to decompose, and these are the water molecules that were possibly associated with sodium cations [32]. The gradual weight loss between 300 °C and 600 °C is attributed to the de-hydroxylation of the chemically bound silicon-hydroxyl group giving (silicon–oxygen–silicon) bridge with loss of water [32,33].

$$2\text{Si–OH} \rightarrow \text{Si–O–Si} + \text{H}_2\text{O} \uparrow$$

Between 600 °C and 700 °C the weight loss was very slow and attributed to the burning of the remnants of coal in the fly ash [26]. Carbon remnants in the fly ash are 1.45 wt% (Table 1). This is clear particularly above 600 °C in DTG curves where a small hump displayed a small change of the weight loss (Fig. 9).

The presence of 1.0, 2.0, and 3.0 wt% nano-clay decreased the weight loss of geopolymer from 12.4% to 12.1, 11.5 and 11.8% (Table 6), respectively, revealing that the highest enhancement to the thermal stability of geopolymer matrix was 2.0 wt% nano-clay.

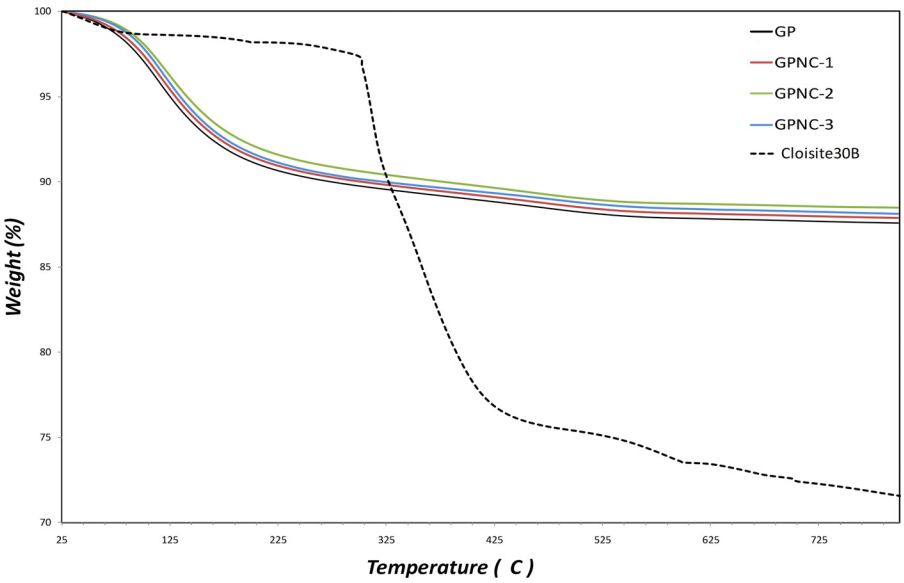

Fig. 8. TGA curves of nano-clay (Cloisite 30B) and all samples.

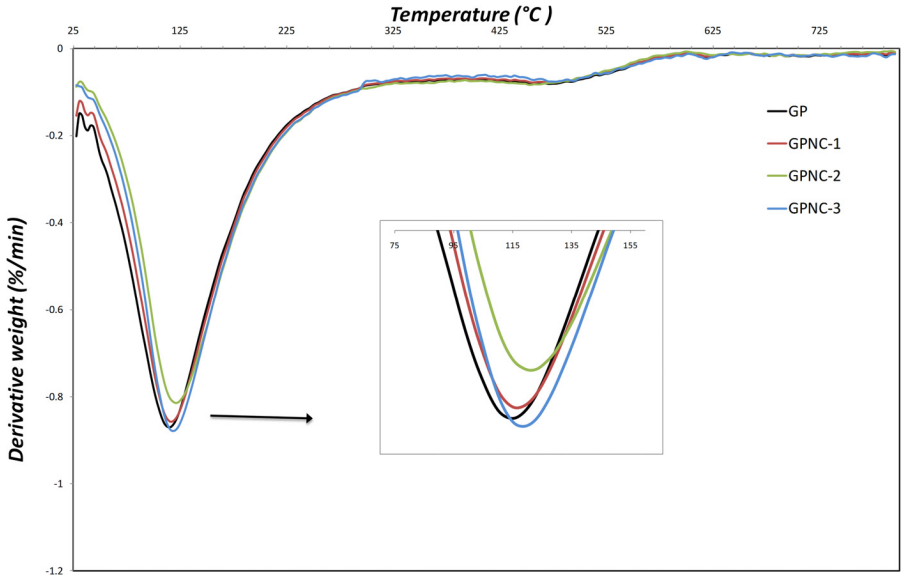

Fig. 9. DTG curves of pure geopolymer and geopolymer nano-composites.

Table 6
Thermal properties of control paste, geopolymer nano-composites and nano-clay (Cloisite 30B).

Sample	Residual mass at different temperatures (%)							
	100 °C	200 °C	300 °C	400 °C	500 °C	600 °C	700 °C	800 °C
GP	97.1	91.1	89.7	89.0	88.6	87.8	87.7	87.5
GPNC-1	97.5	91.4	90.0	89.2	88.5	88.1	88.0	87.8
GPNC-2	98.1	92.1	90.6	89.8	89.0	88.7	88.6	88.4
GPNC-3	97.8	91.6	90.1	89.4	88.8	88.4	88.2	88.1
Nano-clay	98.6	98.2	97.3	78.7	75.4	73.5	72.6	71.5

4. Conclusions

Pure geopolymer and geopolymer nano-clay composites have been synthesized and characterized in terms of mechanical, thermal, and microstructural properties. It has been shown that the addition of 2.0 wt% nano-clay to the geopolymer composites enhanced their flexural strength (by 20%) and compressive strength (by 23%). However, adding more nano-clay showed no further increase in these properties due to agglomeration and poor dispersion of higher amount of nano-clay, which resulted in increased porosity. XRD and FTIR analyses demonstrated an increase in the amorphous phase and geopolymerization after the addition of nano-clay to the geopolymer paste. SEM micrographs showed a denser matrix, and a lower content of unreacted fly-ash particles after the addition of nano-clay. TGA and DTG investigations of these nano-composites indicated that the sample loaded with optimum

addition of nano-clay has lower content of moisture, which confirm the results of previous measurements.

Acknowledgment

The authors would like to thank Ms. E. Miller from the Department of Applied Physics at Curtin University for the assistance with SEM.

References

[1] B.C. McLellan, R.P. Williams, J. Lay, A.V. Riessen and G.D. Corder, J. Clean. Prod., 19, 1080–1090 (2011).
[2] F. Pacheco-Torgal, Z. Abdollahnejad, A.F. Camoes, M. Jamshidi and Y. Ding, Constr. Build. Mater., 30, 400–405 (2012).
[3] J. Davidovits, J. Therm. Anal., 37, 1633–1656 (1991).
[4] P.N. Lemougna, K. MacKenzie and U.F.C. Melo, Ceram. Int., 37, 3011–3018 (2011).
[5] D.D. Higgins, Cem. Concr. Compos., 25, 913–919 (2003).
[6] J.L. Provis, A. Palomo and C. Shi, Cem. Concr. Res., 78, 110–125 (2015).
[7] C. Ferone, B. Liguori, I. Capasso, F. Colangelo, R. Cioffi, E. Cappelletto and R. Di Maggio, Appl. Clay Sci., 107, 195–204 (2015).
[8] W.M. Kriven, J.L. Bell and M. Gordon, Ceram. Trans., 153, 227–250 (2003).
[9] T. Lin, D. Jia, P. He, M. Wang and D. Liang, Mater. Sci. Eng. A, 497, 181–185 (2008).
[10] T. Phoo-ngernkham, P. Chindaprasirt, V. Sata, S. Hanjitsuwan and S. Hatanaka, Mater. Des., 55, 58–65 (2014).
[11] A. Nazari and J.G. Sanjayan, Measurement, 60, 240–246 (2015).
[12] M. Saafi, K. Andrew, P.L. Tang, D. McGhon, S. Taylor, M. Rahman, S. Yang and X. Zhou, Constr. Build. Mater., 49, 46–55 (2013).
[13] F.U.A. Shaikh and S.W.M. Supit, Constr. Build. Mater., 70, 309–321 (2014).
[14] A. Hakamy, F.U.A. Shaikh and I.M. Low, J. Mater. Sci., 49, 1684–1694 (2014).
[15] H. Alamri and I.M. Low, Composites Part A, 44, 23–31 (2013).
[16] ASTM C-20, Standard test methods for apparent porosity, water absorption, apparent specific gravity, and bulk density of burned refractory brick and shapes by boiling water (2010).
[17] T. Alomayri, F.U.A. Shaikh and I.M. Low, Mater. Des., 57, 360–365 (2014).
[18] S.F.U. Ahmed, J. Mater. Civ. Eng., 23, 1311–1319 (2011).
[19] I.M. Low, M. McGrath, D. Lawrence, P. Schmidt, J. Lane, B.A. Latella and K.S. Sim, Composites A, 38, 963–974 (2007).
[20] ASTM C109, Standard test method for compressive strength of hydraulic cement mortars (using 2-in. or [50 mm] cube specimens) (2013).
[21] A. Fernández-Jiménez and A. Palomo, Cem. Concr. Res., 35, 1984–1992 (2005).
[22] T. Alomayri and I.M. Low, J. Asian Ceram. Soc., 30, 223–230 (2013).
[23] N.W. Chen-Tan, A.V. Riessen, V.L.Y. Chi and D.C. Southam, J. Am. Ceram. Soc., 92, 881–887 (2009).
[24] T. Bakharev, Cem. Concr. Res., 36, 1134–1147 (2006).
[25] W.D.A. Rickard, R. Williams, J. Temuujin and A.V. Riessen, Mater. Sci. Eng. A, 528, 3390–3397 (2011).
[26] J.W. Phair and J.S.J. VanDeventer, Int. J. Miner. Process., 66, 121–143 (2002).
[27] H. Alamri and I.M. Low, Composites A, 44, 23–31 (2013).
[28] E.U. Haq, S.K. Padmanabhan and A. Licciulli, Ceram. Int., 40, 2965–2971 (2014).
[29] D. Zaharaki, K. Komnitsas and V. Perdikatsis, J. Mater. Sci., 45, 2715–2724 (2010).
[30] Q. Li, H. Xu, F. Li, P. Li, L. Shen and J. Zhai, Fuel, 97, 366–372 (2012).
[31] C. Ferone, F. Colangelo, G. Roviello, R. Cioffi, C. Menna, D. Asprone, A. Balsamo, A. Prota and G. Manfredi, Materials, 6, 1920–1939 (2013).
[32] D.S. Perera, E.R. Vence, K.S. Finnie, M.G. Blackford, J.V. Hanna and D.J. Cassidy, in Advances in Ceramic Matrix Composites XI, Ed. by N.P. Bansal, J.P. Singh and W.M. Kriven, The American Ceramic Society (2006) pp. 225–236.
[33] C.Y. Lai, A. Groth, S. Gray and M. Duke, Water Res., 57, 56–66 (2014).

3.3 Characterizations of flax fabric reinforced nanoclay-geopolymer composites

Assaedi, H., Shaikh, F.U.A. and Low, I.M., 2016. Characterizations of flax fabric reinforced nanoclay-geopolymer composites. *Composites Part B: Engineering*, *95*, pp.412-422.

Composites Part B 95 (2016) 412–422

Contents lists available at ScienceDirect

Composites Part B

journal homepage: www.elsevier.com/locate/compositesb

Characterizations of flax fabric reinforced nanoclay-geopolymer composites

H. Assaedi [a, b], F.U.A. Shaikh [c], I.M. Low [a, *]

[a] Department of Imaging & Applied Physics, Curtin University, GPO Box U1987, Perth, WA 6845, Australia
[b] Department of Physics, Umm Al-Qura University, P.O. Box 715, Makkah, Saudi Arabia
[c] Department of Civil Engineering, Curtin University, GPO Box U1987, Perth, WA 6845, Australia

ARTICLE INFO

Article history:
Received 8 October 2015
Received in revised form
1 April 2016
Accepted 1 April 2016
Available online 9 April 2016

Keywords:
A. Nano-structures
A. Fibre/matrix bond
B. Physical properties
B. Mechanical properties
B. Thermal properties

ABSTRACT

Geopolymer composites reinforced with flax fabrics (FF) and nanoclay platelets are synthesised and studied in terms of physical and mechanical properties. X-Ray Diffraction (XRD), Fourier transform infrared spectroscopy (FTIR), Scanning Electron Microscope (SEM) techniques are used for phase and microstructure characterisation. The nanoclay platelets are added to reinforce the geopolymer matrices at 1.0%, 2.0%, and 3.0% by weight. It is found that 2.0 wt.% nanoclay enhances the density, decreases the porosity and subsequently improves the flexural strength and toughness. The microstructural analysis results indicate that the nanoclay behaves not only as a filler to improve the microstructure of the binder, but also as an activator to support the geopolymeric reaction producing higher content of geopolymer gel. This enhances the adhesion between geopolymer matrix and flax fibres, which improves the mechanical properties of the geopolymer nanocomposites reinforced with flax fabrics.

1. Introduction

Ordinary Portland cements are widely used in construction applications due to their suitable mechanical and durability properties. Greenhouse emissions from the production of such cement-based materials, however, have necessitated the search for eco-friendly alternatives. Geopolymer is one such alternative. This material, first introduced by Davidovits (1989), exhibit durability, good mechanical performance and fire and acid resistance. The production of geopolymers, being cured at room temperature is considerably more ecologically friendly than the production of Portland cement. It is a process that offers 80–90% reduction in carbon dioxide emission [1–5].

Despite promising characteristics of geopolymers, the material's matrix is one which suffers brittle failure readily under applied force and typically demonstrate poor flexural strength [6,7]. Improving the mechanical properties such as flexural strength and toughness of geopolymers will significantly increase its application in the construction and building industries; and this may be accomplished by two ways [8]: one is to develop 'environmental-friendly materials' through utilizing natural fibres as fibre-reinforced geopolymer composite, and the other is to improve the physical properties of the matrix by adding nanoparticles to the geopolymer paste.

The advantages of using natural fibres in composites include the low density, flexibility and the high modulus [9,10]. Other advantages in addition to good mechanical properties include biodegradable, renewable and recyclable nature of natural fibres [11]. These characteristics have made natural fibres attractive to be utilized as reinforcement in various composites systems. For instance, cellulose extracted from wood materials is used to strengthen polymers and epoxy [12,13]. Bamboo and wood fibres are also used in the strengthening of concrete and known for the flexural advantages [14,15]. Cotton fibres are used to increase the mechanical properties of geopolymer composites [16]. Flax and wool fibres have also shown positive effects when used in geopolymer composites. These fibres improved the fracture and mechanical properties of these composites [17,18].

Researchers of polymers and ceramics have recently become interested in nanotechnology, particularly in developing nanocomposites, which have superior physical and mechanical properties. A number of nano-particles are being added to geopolymers to increase mechanical properties. For instance, nano-alumina and nano-silica have been used effectively as reinforcements for geopolymer pastes, providing outstanding mechanical properties. The nanoparticles not only performed as voids-fillers, but also

* Corresponding author. Tel.: +61 8 9266 7544; fax: +61 8 9266 2377.
E-mail address: j.low@curtin.edu.au (I.M. Low).

http://dx.doi.org/10.1016/j.compositesb.2016.04.007
1359-8368/

enhanced the geopolymer reaction [19]. In another study, it has been found that nano-silica and nano-alumina particles have the ability to reduce the porosity and water absorption of geopolymer matrices [20]. A further study on the effect of addition of carbon nanotubes to fly-ash-based geopolymer has shown an increase in the mechanical and electrical properties of geopolymer nano-composites when compared to the control paste [21]. In another study, the addition of calcium carbonate ($CaCO_3$) nanoparticles to high-volume fly-ash concrete improved the flexural and mechanical properties, decreased the porosity and improved the concrete resistance to water absorption [22]. Finally, in a more recent study of nano-clay cement nano-composites, it was observed that nano-clay not only increased mechanical and physical properties of cement matrices, but also improved thermal properties [23]. However, no research is reported on the effect of nano clay on properties of flax fabric reinforced geopolymer composites.

In this study, the fabrication of eco or "green" nano-composites using nanoclay and flax fibre (FF) as reinforcement of fly ash geopolymer matrices is investigated. Fourier transform infrared spectroscopy (FTIR) and scanning electron microscopy (SEM) are used to investigate the morphology and microstructure of geopolymer/flax nanocomposites. The effect of different nanoclay platelets contents on mechanical properties such as flexural strength and flexural toughness is also evaluated in this paper.

2. Experimental procedures

2.1. Materials and preparation

Low calcium fly ash (ASTM class F), collected from the Eraring power station in NSW, was used as the source material for the geopolymer matrix. The chemical composition of fly ash is shown in Table 1. The alkaline activator for geopolymerisation was a combination of sodium hydroxide and sodium silicate grade D solution. Sodium hydroxide flakes of 98% purity were used to prepare the solution. The chemical composition of sodium silicate used was 14.7% Na_2O, 29.4% SiO_2 and 55.9% water by mass.

Flax fabric (FF) and organo-nanoclay (Cloisite 30B) were used for the reinforcement of geopolymer nanocomposites. The fabric of 30 × 30 cm^2, supplied by Pure Linen Australia, is made up of yarns with a density of 1.5 g/cm^3; the space between the yarns is between 2 and 4 mm, necessary to allow the geopolymer matrix to penetrate. The average diameter of the fibre yarns was about 0.60 mm (Fig. 1a), and the fibres diameter was about 20 μm (Fig. 1b). The physical properties of the flax fibres are presented in Table 2. The nanoclay platelets used in this study was based on natural montmorillonite clay $(Na,Ca)_{0.33}(Al,Mg)_2(Si_4O_{10})(OH)_2.nH_2O$ which was supplied by Southern Clay Products, USA. The description and physical properties of Cloisite 30B are shown in Table 3 [24].

To prepare the geopolymer matrix, an alkaline solution to fly ash ratio of 0.75 was used and the ratio of sodium silicate solution to sodium hydroxide solution was fixed at 2.5. The concentration of sodium hydroxide solution was 8 M, and was prepared and combined with the sodium silicate solution one day before mixing.

The nanoclay was added first to the fly ash at the dosages of 0%, 1.0%, 2.0% and 3.0% by weight. The fly ash and nanoclay were dry mixed for 5 min in a covered mixer at a low speed and then mixed for another 10 min at high speed until homogeneity was achieved. The alkaline

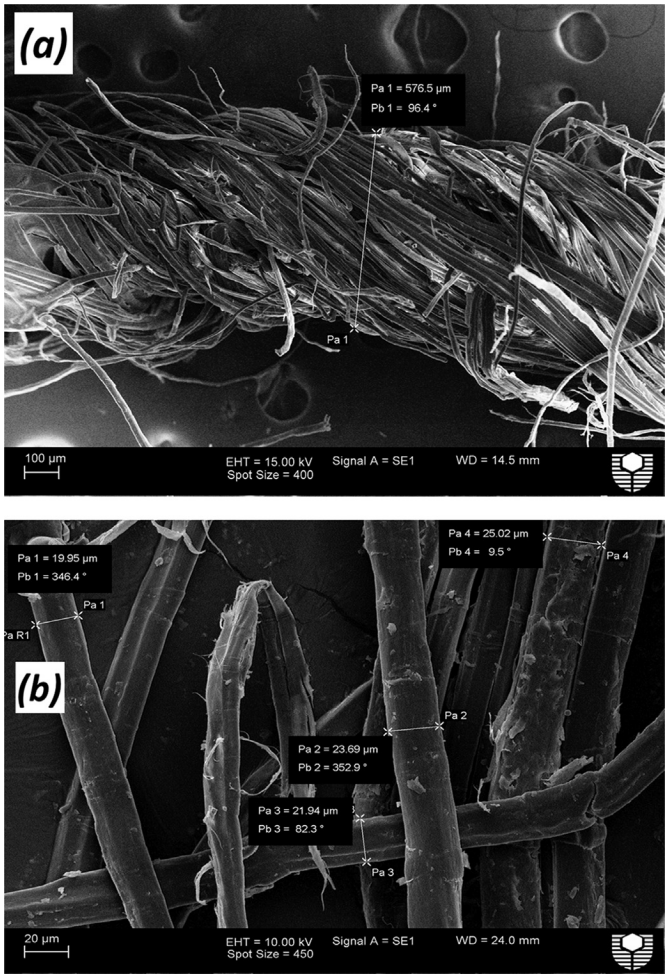

Fig. 1. SEM images showing diameters of the (a) flax bundle, and (b) flax fibres.

Table 2
Structure and physical properties of the flax fabric (Source of reference?).

Fabric thickness (mm)	0.6
Fabric geometry	Woven (plain weave)
Yarn nature	Bundle
Bundle diameter (mm)	0.6 (see Fig. 2a)
Filament size (mm)	0.01–0.02 (see Fig. 2b)
Opening size (mm)	2–4
Fabric density (g/cm^3)	1.5
Modulus of elasticity (GPa)	39.5
Tensile strength (MPa)	660

Table 3
Physical properties of the organo-nanoclay platelets (Cloisite 30B).

Colour	Off white
Density (g/cm^3)	1.98
d-spacing (001) (nm)	1.85
Aspect ratio	200–1000
Surface area (m^2/g)	750

Table 1
Chemical compositions of fly ash (wt%).

SiO_2	Al_2O_3	CaO	Fe_2O_3	K_2O	MgO	Na_2O	P_2O_5	SO_3	TiO_2	MnO	BaO	LOI
63.13	24.88	2.58	3.07	2.01	0.61	0.71	0.17	0.18	0.96	0.05	0.07	1.45

solution was then added slowly to the fly ash/nanoclay in the mixer at a low speed until the mix became homogeneous, then further mixed for another 10 min on high speed. The resultant mixture was then poured into wooden moulds and placed on a vibration table for 2 min.

Similar mixtures were prepared to produce the nanocomposites reinforced with FF. Four samples of geopolymer pastes reinforced with 4.1 wt% FF were prepared by spreading a thin layer of geopolymer paste in a well-greased wooden mould and carefully placing the first layer of FF on it. The fabric was fully saturated with paste by a roller, and the process repeated for ten layers; each specimen contained a different weight percentage of nanoclay. The samples then were left under heavy weight for 1 h to reduce entrapped air inside the samples. All samples were covered with plastic film and cured at 80 C for 24 h in an oven before demoulding. They were then dried under ambient conditions for 28 days. The pure geopolymer, and nanocomposites containing 1.0%, 2.0% and 3.0% nanoclay were labelled as GP, GPNC-1, GPNC-2 and GPNC-3, respectively. Also, the composites reinforced with a combination of FF and the same weight percentages of nanoclay were denoted as GPFNC-0, GPFNC-1, GPFNC-2 and GPFNC-3, respectively (see Table 4).

2.2. Mechanical properties

A LLOYD Material Testing Machine (50 kN capacity) with a displacement rate of 1 mm/min was used to perform the mechanical tests. Rectangular bars of 60 × 18 × 15 mm^3 with a span of 40 mm were cut from the fully cured samples for three-point bend tests to evaluate the mechanical properties. All samples were aligned horizontally to the applied load in all mechanical tests. Five samples of each composite were used to evaluate the flexural strength

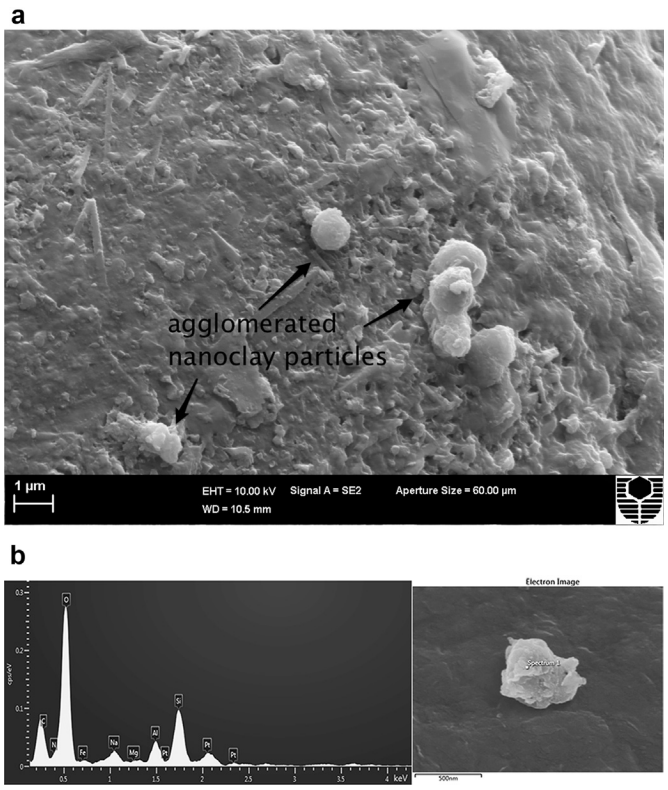

Fig. 3. (a) SEM image of agglomerated nanoclay particles on the fracture surface of GPNC-3, (b) with EDS analysis.

Table 4
Formulation of samples.

Sample name	Fly-ash (g)	NaOH solution (g)	Na_2SiO_3 solution (g)	Nanoclay (g)	FF content (wt%)
GP	1000	214.5	535.5	0	0
GPNC-1	1000	214.5	535.5	10	0
GPNC-2	1000	214.5	535.5	20	0
GPNC-3	1000	214.5	535.5	30	0
GPFNC-0	1000	214.5	535.5	0	4.1
GPFNC-1	1000	214.5	535.5	10	4.1
GPFNC-2	1000	214.5	535.5	20	4.1
GPFNC-3	1000	214.5	535.5	30	4.1

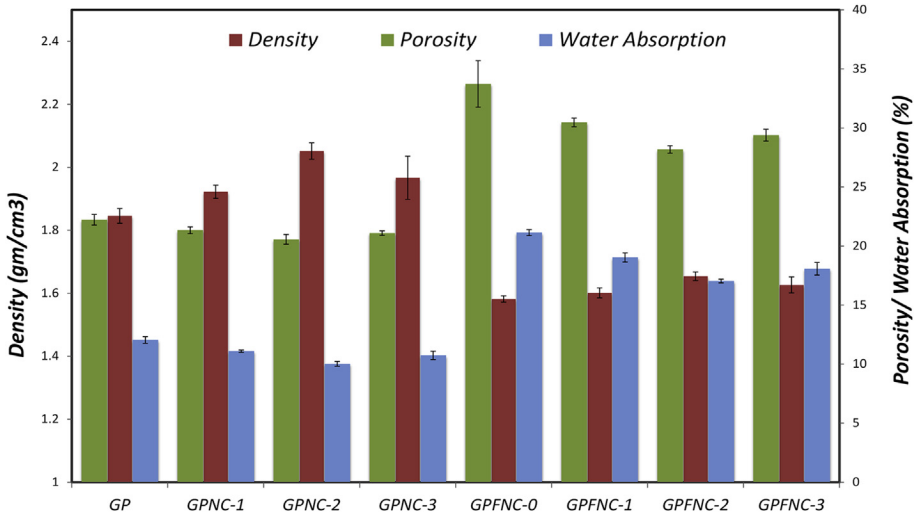

Fig. 2. Density, porosity and water absorption values for all samples.

according to the standard ASTM D790 [25]. The values were recorded and analysed with the machine software (NEXYGENPlus) and average values were calculated. The flexural toughness of the composites containing FF were characterised by the toughness indices I_5, I_{10} and $I_{failure}$ as defined by ASTM C1018 [26].

2.3. Characterisation

The samples were measured on a D8 Advance Diffractometer (Bruker-AXS) using copper radiation and a LynxEye position sensitive detector. The diffractometer were scanned from 7° to 60° (2θ)

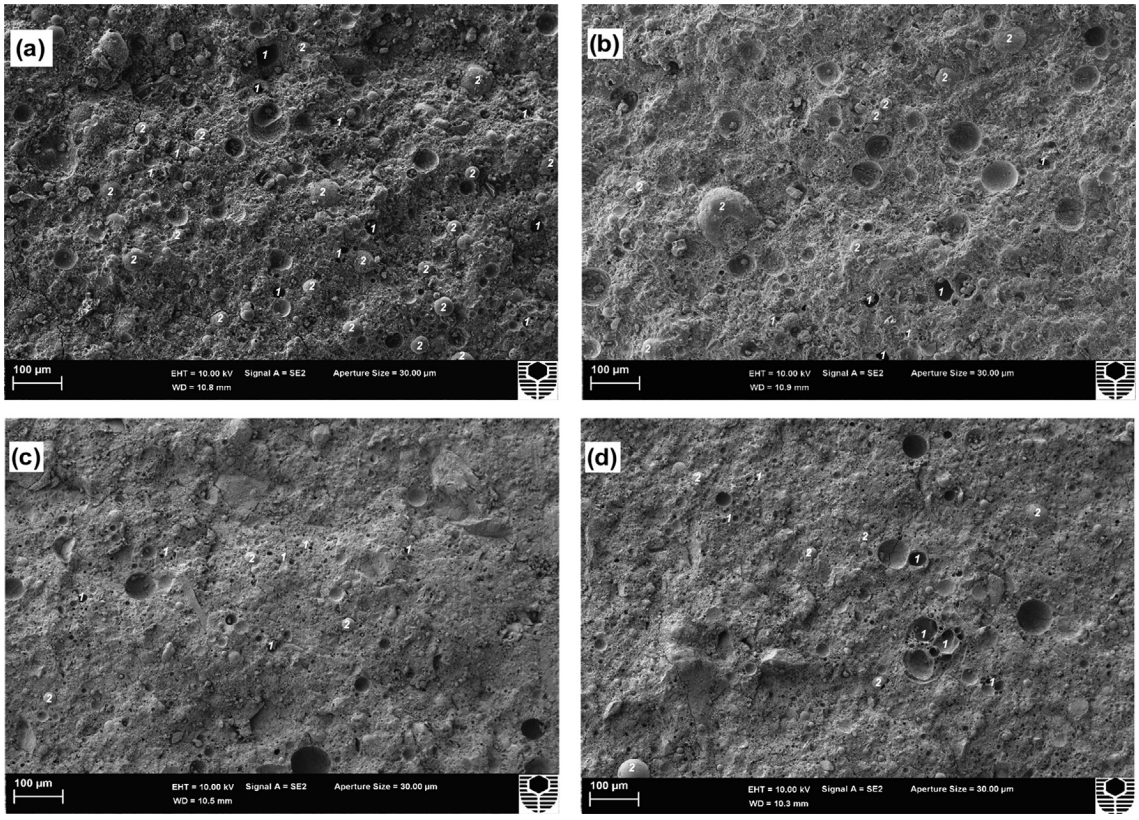

Fig. 4. SEM images of the fracture surface of geopolymer nanocomposites with different loadings of nano-clay (a) pure geopolymer, (b) 1.0 wt%, (c) 2.0 wt% and (d) 3.0 wt%. [Legend: 1. Pores and 2. Unreacted flyash particles].

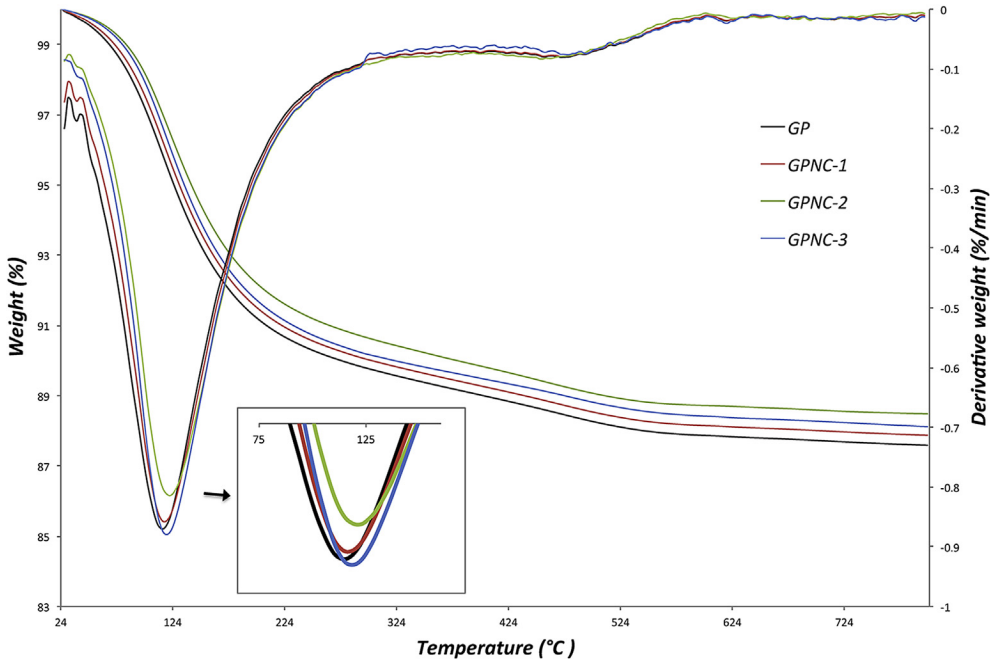

Fig. 5. TGA/DTG curves of pure geopolymer and geopolymer nanocomposites.

in steps of 0.015° using a scanning rate of 0.5°/min. XRD patterns were obtained by using Cu K_α lines ($\lambda = 1.5406$ Å).

An FTIR spectrum was performed on a Perkin Elmer Spectrum 100 FTIR spectrometer in the range of 4000–500 cm^1 at room temperature. The spectrum was an average of 10 scans at a resolution of 2 cm^{-1}, corrected for background.

The microstructures of geopolymer composites were examined using a Zeiss Neon focused ion beam scanning electron microscope (FIB–SEM), equipped with energy dispersive spectroscopy (EDS). The specimens were mounted on aluminium stubs using carbon tape and then coated with a thin layer of platinum to prevent charging before the observation.

3. Results and discussion

3.1. Physical properties

The results of porosity and water absorption of all samples are shown in Fig. 2. It can be seen in general that the composites containing FF have higher porosity and water absorption than those composites without FF. This is because of the hydrophilic nature of cellulose fibres, which creates voids in the interfacial region between the flax fibres and the matrices [27].

All geopolymer nanocomposites displayed higher densities and lower porosities than the control paste. This indicates that nanoclay

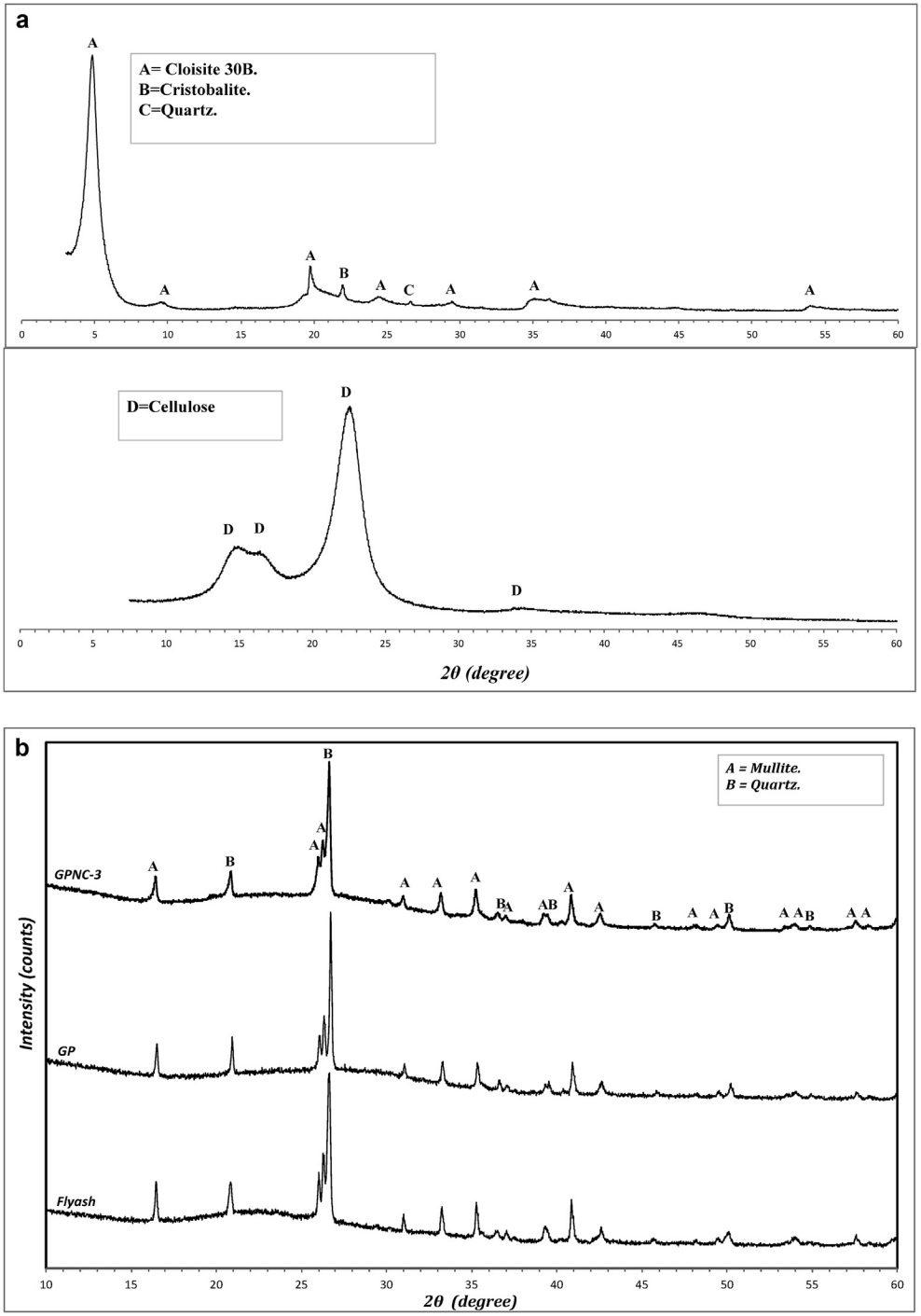

Fig. 6. X-ray diffraction patterns of: (a) nano-clay platelets and flax fibres, (b) fly-ash, GP and GPNC-3.

particles played a pore-filling role to reduce the porosity of the geopolymer composites, producing dense geopolymer paste. As a consequence of this, the geopolymer nanocomposites exhibited lower water absorption. The optimum addition was found as 2.0 wt % of nanoclay, which reduced the porosity by 7.1%, and the water absorption by 17% when compared to the pure geopolymer matrix. However, the addition of excessive amounts of nanoclay increased the porosity and water absorption, and decreased the density of the nanocomposite sample due to the poor dispersion and agglomeration of nanoparticles [28]. This is a common phenomenon for nanoparticles due to small sizes, and high surface area to volume ratio of nanoparticles (van der Waal's force) [29]. Fig. 3 (a and b) shows SEM images of agglomerated nanoclay particles in GPNC-3 sample with Energy Dispersive Spectroscopy (EDS) spectra (Fig. 3b), ammonium salt in the nanoclay is identified by carbon and nitrogen elements. The nitrogen element is not detected clearly in the spectra because the nitrogen content is very low. However, the carbon content is clearly detected at 0.25 KeV. This result is comparable with physical properties where the porosity of cement paste is decreased due to addition of 1.0 wt% of nanoclay to cement paste. Nevertheless, after the addition of more nanoclay to the paste, values of porosities and water absorption have increased because of the effect of nanoparticles agglomeration [30]. Fig. 4a–d show the SEM micrographs of the surface of neat geopolymer and nanocomposites containing 1.0, 2.0, and 3.0 wt% nano-clay. The pure geopolymer matrix has a porous structure with a higher number of non-reacted and partially reacted fly ash particles embedded in the matrix (Fig. 4a). For the 1–3 wt% nano-clay (Fig. 4b–d) less fly ash particles were observed, and the matrix seemed denser when compared to the matrix of the control sample.

In the case of FF reinforced nanocomposites, the physical properties show similar trends to that of the nanocomposites trends. The optimum loading of nanoclay to the composites was found as 2.0 wt% in the case of GPFNC-2, which decreased the value of porosity by 16.3% and water absorption by 19.4% lower than the sample GPFNC-0.

3.2. Thermal behaviour

The thermal stability of neat geopolymer and geopolymer nanocomposites was analysed using thermogravimetric analysis (TGA) and derivative thermograms (DTG). In this investigation, the thermal stability was studied in terms of the weight-loss percentage as a function of temperature in Argon atmosphere. The results are shown in Fig. 5.

The thermograms of the pure geopolymer and the nanocomposites samples display a weight loss from 25 to 225 °C due to the evaporation of absorbed water [31]. The neat geopolymer curve shows sharp decrease in this region compared to the nanocomposites curves, which is clearly shown in DTG graph (Fig. 5), where the peak of nanocomposites shifted to higher temperatures compared to the neat geopolymer. GPNC-2 shows the lowest reduction of rate of he weight loss indicating that geopolymer containing 2.0 wt.% nanoclay has the lowest water content compared to the tested samples. This may be attributed to the effect of nanoclay filling the voids, producing denser matrices. Between 225 °C and 525 °C, the rate of weight loss for all samples was slow as the physical free water was evaporated. This gradual weight loss is recognized as the de-hydroxylation of the chemically bound silicon-hydroxyl group giving silicon-oxygen group and evaporated water [32].

$$2Si-OH \rightarrow Si-O-Si + H_2O\uparrow$$

Between 500 °C and 700 °C the weight loss was slow and attributed to the burning of the remaining coal of fly ash [33]. This is clear specifically above 600 °C in DTG curves where a small hump displaying a small change of the weight loss.

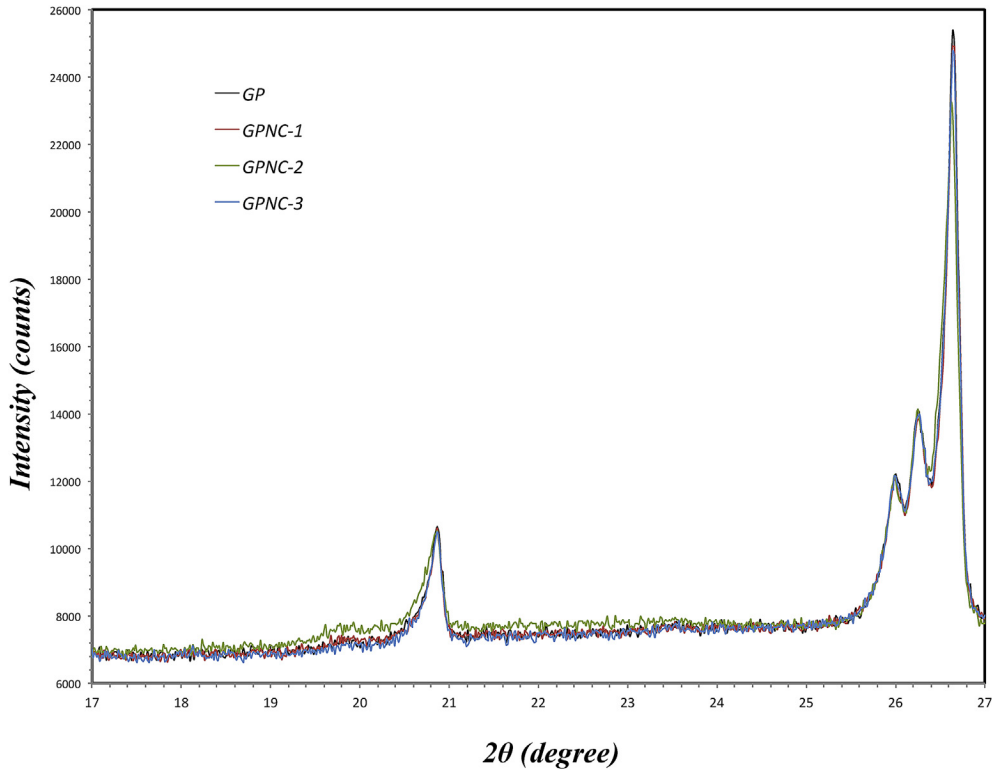

Fig. 7. An overlay of the amorphous phases of XRD patterns for pure geopolymer, GPNC-1, GPNC-2 and GPNC-3.

The presence of 1.0, 2.0, and 3.0 wt% nanoclay reduced the weight loss of geopolymer from 12.4% to 12.1, 11.5 and 11.8%, respectively, revealing that the highest improvement to thermal stability of geopolymer matrix was 2.0 wt% loading of nanoclay. Note that composites reinforced with flax fibres have not been investigated. This is because that TGA technique is very sensitive to the fibre/matrix ratio, which cannot be fixed for all composites containing FF, considering the small weight of the TGA micro-

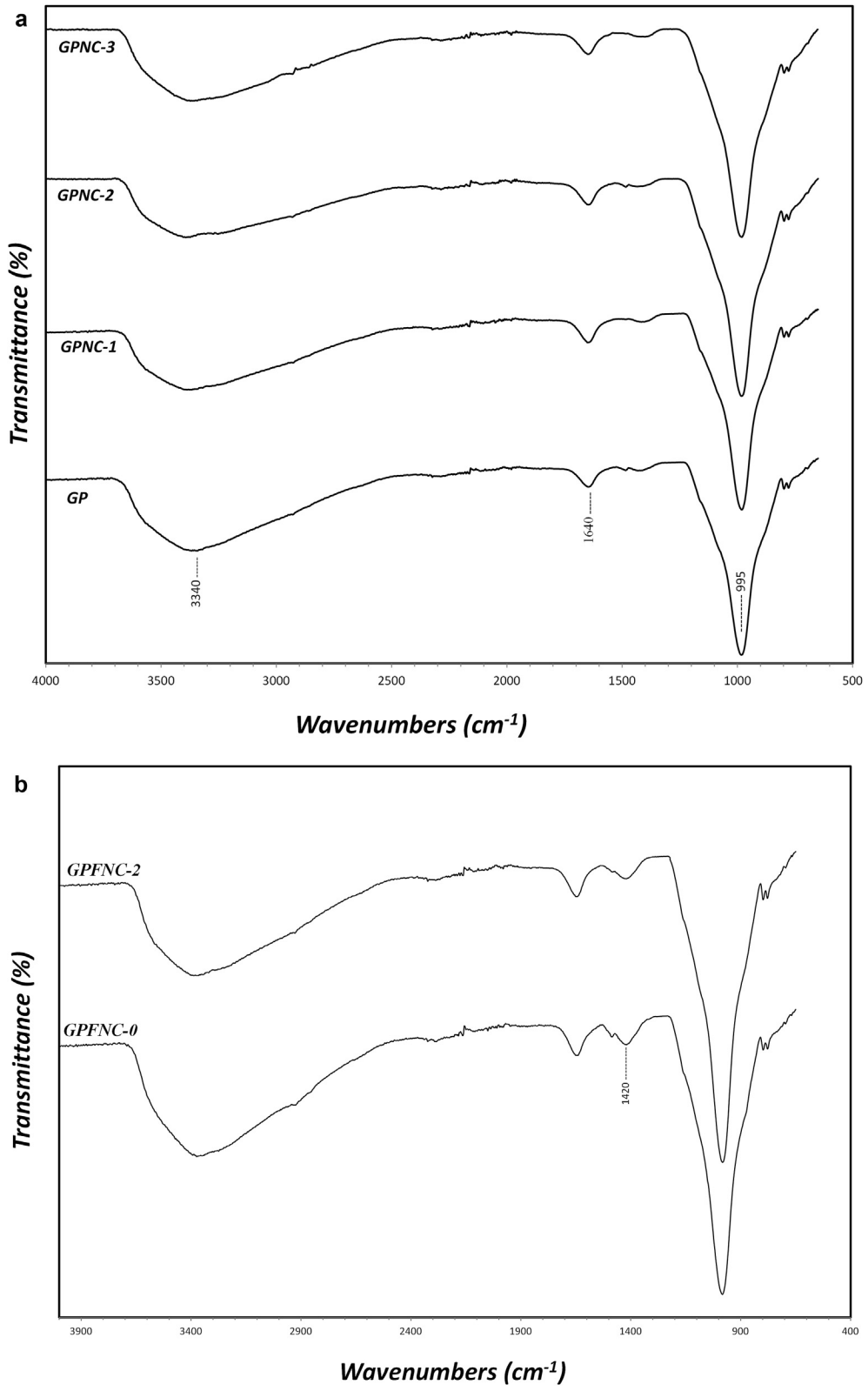

Fig. 8. (a) FTIR spectra of pure geopolymer and the nanocomposites GPNC-1, GPNC-2 and GPNC-3, (b) FTIR spectra of the FF-reinforced geopolymer composite GPFNC-0 and GPFNC-2.

samples and the flax fibres size. However, the main objective of this study is to determine the effect of nanoclay on the physical structure of the geopolymer/nanocomposites matrices.

3.3. X-ray diffraction (XRD)

The XRD spectra obtained for nanoclay, flax fibres, fly ash, GPNC-0 and GPNC-3 specimens are presented in Fig. 6a–b. The crystalline phases were indexed using Powder Diffraction Files (PDFs) from the Inorganic Crystal Structure Database (ISCD).

Fig. 6a shows the diffraction patterns of nanoclay and flax fibres. Three phases have been indexed in the diffraction pattern of nanoclay with the major phase being Cloisite30B [34], and minor phases of Cristobalite [SiO_2] (PDF 00-039-1425) and Quartz [SiO_2](PDF 00-047-0718). Cloisite30B consists of Montmorillonite [$(Ca,Na)_{0.3}Al_2(Si,Al)_4O_{10}(OH)_2 \cdot xH_2O$] and the quaternary ammonium salt. Montmorillonite has four major peaks in the XRD pattern, which correspond to 2θ of 4.84°, 19.74°, 35.12° and 53.98°. The quaternary ammonium salt has four peaks at 2θ of 4.84°, 9.55°, 24.42° and 29.49°. Note that there is an overlap of peaks at 2θ of 4.84° for Montmorillonite and quaternary ammonium salt. Both Cristobalite and Quartz has a peak that corresponds to 2θ of 21.99° and 26.61°, respectively. The diffraction pattern of flax fibres shows typical peaks of cellulose (PDF 00-060-1502).

For fly ash, GP and GPNC-3 samples, two major phases are identified clearly: quartz [SiO_2] (PDF 00-046-1045) and mullite [$Al_{1.272}\ Si_{0.278}\ O_{4.864}$] (PDF 01-083-1881) (Fig. 6b). As the crystalline phases of quartz and mullite are also the fly ash phases they are insensitive to geopolymetric reactions, and their role is limited in geopolymer paste as filler particles [35,36]. However, the amorphous aluminosilicate phase that created between $2\theta = 14°$ and 27° is an active indication of geopolymer reaction, which is the reactive and dissolvable content in alkaline solution throughout the geopolymer formation [37]. The geopolymer matrix mechanical properties are noticeably affected through the amorphous phase. When the amorphous phase is higher, the strength of the geopolymer is likewise higher [38,39]. Fig. 7 shows overlays of the amorphous hump under the quartz phase of nanocomposites samples. It can be seen that GPNC-2 has the highest amorphous phase over all nanocomposites. Also, it can be noticed that GPNC-2 displays less intensity of quartz peak compared to other samples, which demonstrates that the reaction of geopolymer is activated by the optimum addition of nanoclay and higher content of quartz is dissolved, resulting in more geopolymer gel. This improves the mechanical properties of the geopolymer nanocomposites by improving the physical properties of the matrix, besides improving the adhesion between the reinforcement flax fibres and the matrix. However, the more addition of nanoclay is inactive and resulted in almost the same amount of amorphous content as GPNC-1.

3.4. FTIR observation

FTIR spectra of pure geopolymer, nanocomposites, GPF and GPFNC-2 are shown in Fig. 8a and b. The strong peak at ~1000 cm^{-1} in all samples is associated with Si-O-T (T: Si or Al) asymmetric stretching vibrations and is the special mark of the geopolymerisation [40]. The level of geopolymerization can be identified quantitatively by comparing the height and the area under the geopolymer stretching peaks of the nanocomposites to the pure matrix peak [33]. Considering the size of the geopolymer peak, it can be seen that all nanocomposites had generally higher contents of geopolymer compared to the control paste (Fig. 8a); however, the addition of 2.0 wt.% of nanoclay had the highest level of geopolymerization among all samples. The areas under the geopolymer peak for the nanocomposites when compared to the pure matrix have enlarged by 2.0%, 7.0% and 3.0%, while the peak's heights have expanded by 2.0%, 19% and 15% for GPNC-1, GPNC-2 and GPNC-3, respectively. This result is in agreement with the XRD results that discussed above. A broad peak at the region of 3200–3600 cm^{-1} is corresponding to the stretching vibration of the hydroxyl (OH) group of physically free water (higher frequencies), and to chemically bounded water to the inorganic polymer through hydrogen bonds (lower frequencies) [24,41]. The peak around 1640 cm^{-1} is also due to the (OH) bending vibration of absorbed water [33].

Fig. 8b shows the FTIR scan for GPFNC-0 and GPFNC-2. The presence of flax fibres in the samples can be recognised in the peak at 1420 cm^1, which is attributed to the CH_2 bending vibration of

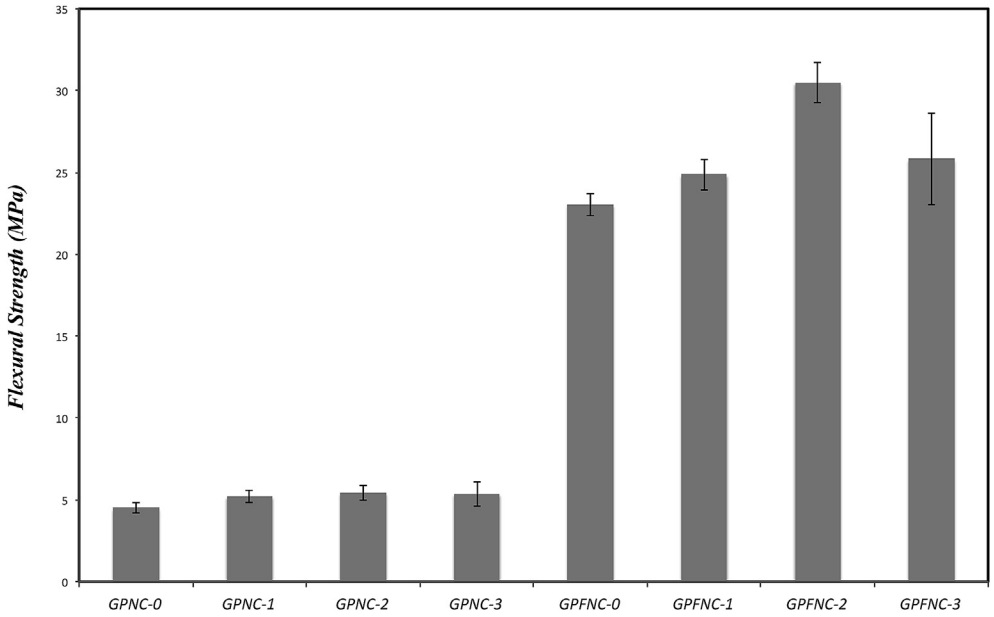

Fig. 9. Flexural strength of all samples.

cellulose [24]. The intensity of the band between 3200 and 3600 cm^{-1} is a sign to the samples water uptake. Samples reinforced with FF have higher water uptake because of the hydrophilic nature of cellulose fibres; however, GPFNC-2 has lower content of water compared to GPFNC-0 due to the barrier property of the nanocomposites against moisture uptake.

3.5. Mechanical properties

Flexural tests are used to characterise the mechanical properties of layered composites as they provide a simple means of determining the bending response. This provides useful information on the performance of layered fabric-based composites. The effect of nanoclay contents on the flexural strength of the geopolymer FF-composites is presented in Fig. 9. It can be seen clearly that all composites reinforced with FF showed higher flexural strength than the pure geopolymer and nanocomposites samples. The flexural strength of the composites improved from 4.5 MPa in the control sample to about 23 MPa in GPFNC-0. This result is comparable with that of short flax fibre-reinforced geopolymer composites reported by Alzeer and MacKenzie [17]. This can be explained by the fact that flax fabrics bridge the cracks of geopolymer matrix develop during bending and resisted the failure through frictional deboning of fabric in the matrix. This permits

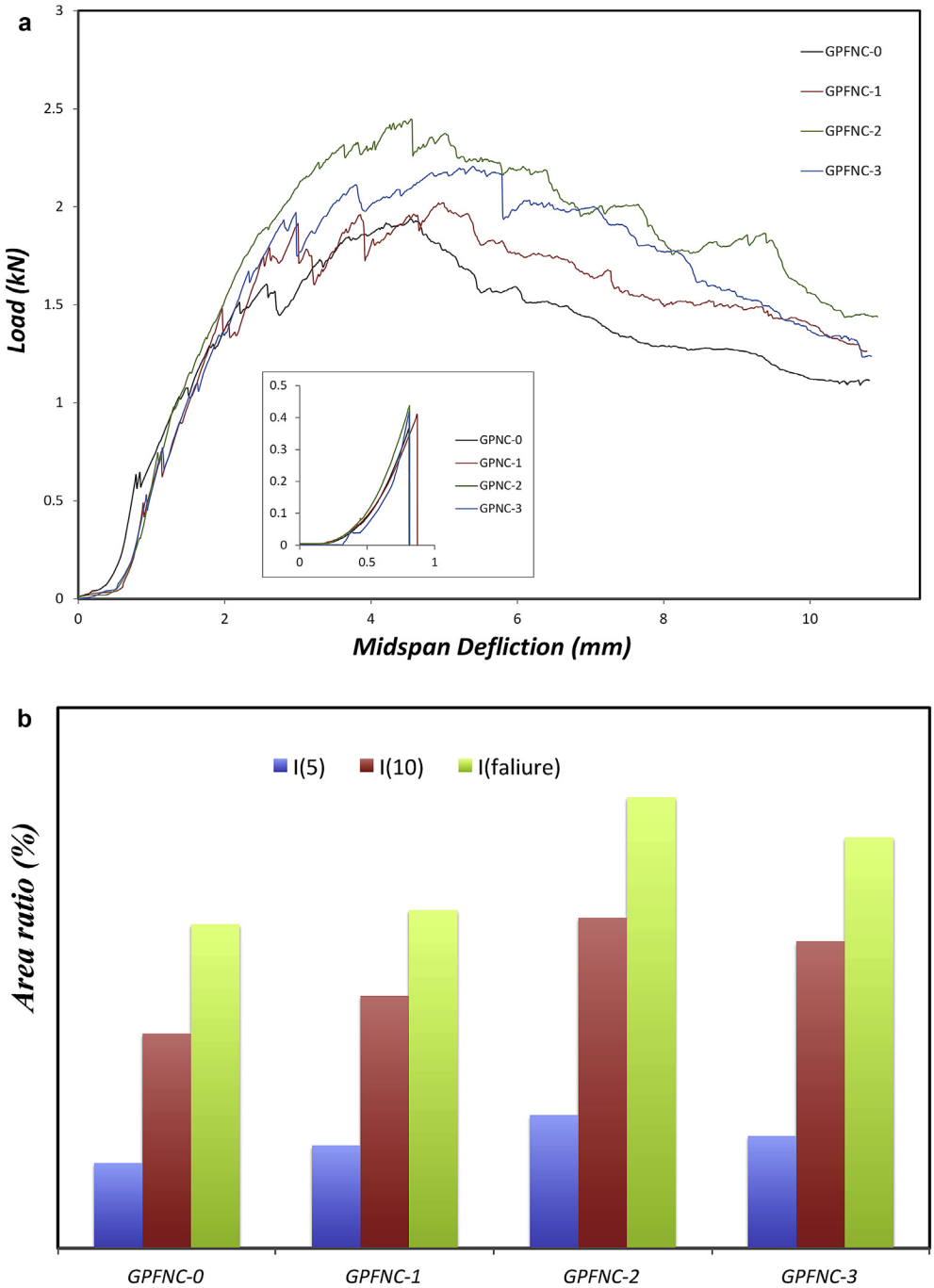

Fig. 10. (a) Typical load-midspan deflection curves of all composites, (b) Toughness indices I_5, I_{10} and $I_{failure}$ for FF/reinforced geopolymer samples.

more stress transfer between the matrix and the flax fibres, resulting in greater flexural strength [42].

The addition of nanoclay, however, enhanced the adhesion force between the matrix and fibres creating composites with higher flexural strength. Fig. 9 shows that GPFNC-2 had the highest flexural strength among all samples, which means that the optimum addition that improved the flexural strength was 2.0 wt% of nanoclay. The loading of 2.0 wt% not only enhanced the bond between the matrix and the fibre, but also created a denser geopolymer paste with higher contents of geopolymer products.

This result is also confirmed by studying the flexural toughness indices I_5, I_{10} and $I_{failure}$ of the composites (Fig. 10a). According to the standard used, I_5 is defined as the ratio obtained by dividing the area up to a deflection of three times the first-crack deflection by the area up to first crack, while I_{10} is the ratio between the area up to a deflection of 5.5 times the first-crack deflection by the area up to the first crack. For the failure deflection, $I_{failure}$ is calculated at 11.4 mm deflection for all samples reinforced with FF.

Pure geopolymer and geopolymer nanocomposites had zero values of toughness because of the brittleness of the geopolymer. However, FF-reinforced composites exhibited high flexural toughness due to the ability of long fibres to withstand a higher load and to support multiple cracks throughout the loading process, which prevented the brittle failure of geopolymer.

Fig. 10b presents values of toughness indices of FF-reinforced composites, the sample reinforced with the optimum loading of nanoclay showed higher toughness indices than GPFNC-0 by 58%, 54% and 39% for I_5, I_{10} and $I_{failure}$, respectively. The rate of improvement of the toughness indices decreased with deflection. While I_5 has enhanced by 58% after the addition of 2.0 wt% of nanoclay, $I_{failure}$ has only improved by 39%. This may be attributed to the effect of fibre pull-out that occurred more extensively in GPFNC-0 than in GPFNC-2. The bond between the matrix and flax fibres has improved due to the high content of geopolymer gel, which caused more fibres fracture than the pull-out in GPFNC-2. This can be considered clearly in Fig. 10a, where the slope of GPFNC-2 curve has sharper decrease in load with increasing deflection in the region between 9 and 11 mm than other curves.

SEM images of the fracture surface of FF-reinforced geopolymer composite and FF-reinforced nanocomposites after flexural toughness test are shown in Fig. 11. A range of toughness mechanisms such as fibre de-bonding, fibre pull-out and rupture and matrix fracture can be clearly seen. The examination of fracture surface of FF reinforced geopolymer composite shows high porous structure and number of unreacted fly ash, which caused poor adhesion between fibres and the matrix (Fig. 11a). FF-reinforced nanocomposites containing 1.0 and 3.0 wt% nanoclay displays relatively denser matrices with lower number of unreacted fly ash particles embedded in the matrices (Fig. 11b and d). However, in FF-reinforced geopolymer nanocomposite containing 2.0 wt% nanoclay, a smaller amount of unreacted fly ash particles was observed, and higher content of geopolymer gel can be clearly seen, which provided better adhesion between the flax fibres and the matrix. A significant amount of fibre fracture was also observed (Fig. 11c) by virtue of this enhanced interfacial fibre-matrix bonding.

3.6. Conclusions

The investigation of FF-reinforced geopolymer nanocomposites and the effects of nanoclay through physical and mechanical testing presented a number of findings. Analysis using FTIR and XRD show that nanocomposites of geopolymer with the optimum amount of

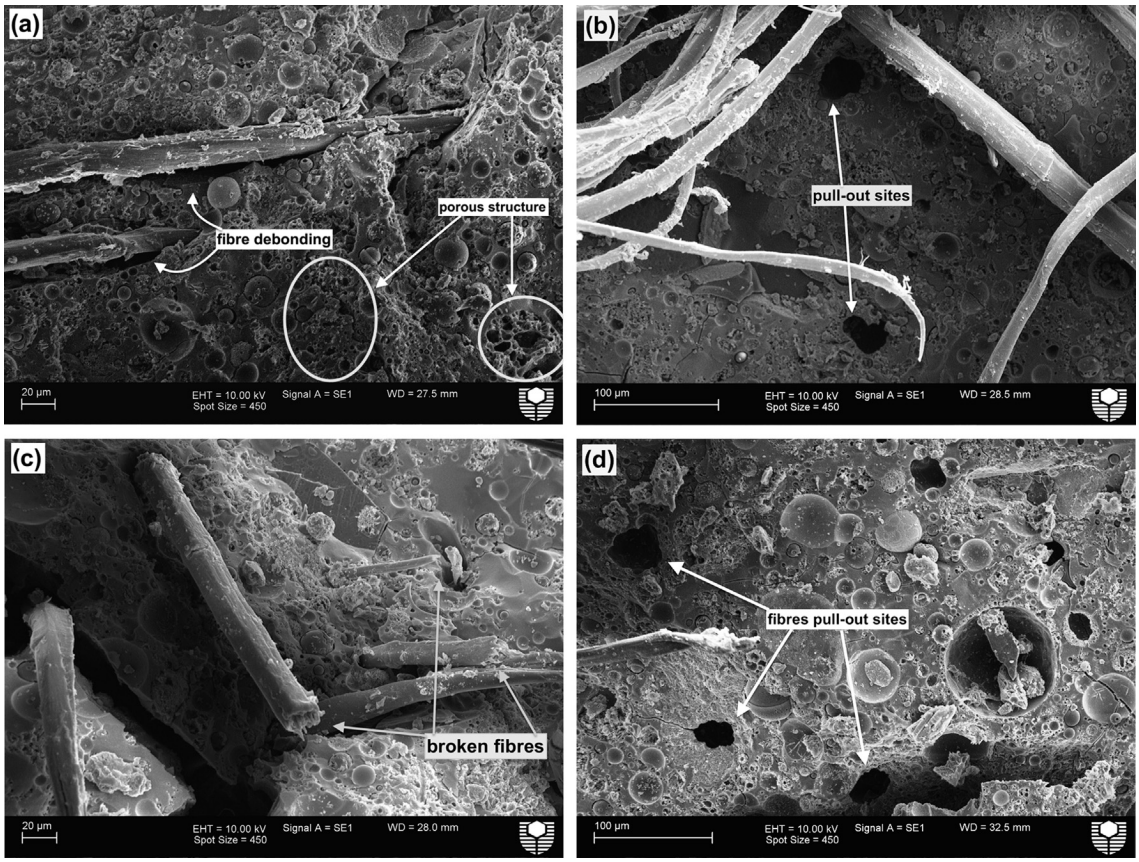

Fig. 11. SEM images of a fracture surface of FF-reinforced samples; (a) GPFNC-0, (b) GPFNC-1, (c) GPFNC-2 (d) GPFNC-3.

nanoclay produce higher amounts of geopolymer gel. The nanoclay added to nanocomposites at 2.0 wt% provides a denser microstructure, and has better adhesion bond between the matrix and the flax fibres. It was also observed that the loading of 2.0 wt% nanoclay to the nanocomposites reduced the porosity and increased the density; this caused an improvement in flexural strength and toughness. However, adverse physical and mechanical properties are observed when the FF-reinforced geopolymer contains nanoclay loadings that exceeded the 2.0 wt%.

Acknowledgements

The authors would like to thank Ms E. Miller from the Department of Applied Physics at Curtin University for her assistance with SEM. The author (HA) is grateful to the Physics Department of Umm Al-Qura University (4290371) for the financial support in the form of a PhD scholarship.

References

[1] Barbosa VFF, MacKenzie KJD, Thaumaturgo C. Synthesis and characterisation of materials based on inorganic polymers of alumina and silica: sodium polysialate polymers. Inter J Inorg Mater 2000;2(4):309–17.
[2] van-Jaarsveld JGS, van-Deventer JSJ, Lorenzen L. Factors affecting the immobilization of metals in geopolymerized flyash. Metal Mater Trans 1998;29B(291).
[3] Davidovits J. Geopolymers and geopolymeric materials. J Therm Anal 1989;35(2):429–41.
[4] Duxson P, Fernández-Jiménez A, Provis JL, Lukey GC, Palomo A, Deventer JSJ. Geopolymer technology: the current state of the art. J Mater Sci 2007;42(9):2917–33.
[5] Pernica D, Reis PNB, Ferreira JAM, Louda P. Effect of test conditions on the bending strength of a geopolymer- reinforced composite. J Mater Sci 2010;45(3):744–9.
[6] Lin T, Jia D, He P, Wang M, Liang D. Effects of fiber length on mechanical properties and fracture behavior of short carbon fiber reinforced geopolymer matrix composites. Mater Sci Eng A 2008;497(1–2):181–5.
[7] Alomayri T, Shaikh FUA, Low IM. Synthesis and mechanical properties of cotton fabric reinforced geopolymer composites. Compos Part B 2014;60:36–42.
[8] Bernal SA, Bejarano J, Garzón C, Mejía de Gutiérrez R, Delvasto S, Rodríguez ED. Performance of refractory aluminosilicate particle/fiber-reinforced geopolymer composites. Compos Part B 2012;43(4):1919–28.
[9] Herrera-Franco PJ, Valadez-González A. A study of the mechanical properties of short natural-fiber reinforced composites. Compos Part B 2005;36(8):597–608.
[10] Bohlooli H, Nazari A, Khalaj G, Kaykha MM, Riahi S. Experimental investigations and fuzzy logic modeling of compressive strength of geopolymers with seeded fly ash and rice husk bark ash. Compos Part B 2012;43(3):1293–301.
[11] Low IM, Somers J, Pang WK. Synthesis and properties of recycled paper-nanoclay-reinforced epoxy eco-composites. Key Eng Mater 2007;334:609–12.
[12] Zadorecki P, Michell A. Future-prospect for wood cellulose as reinforcment in otganic polymer composites. Polym Compos 1989;10(2):69–77.
[13] Low IM, Somers J, Kho HS, Davies IJ, Latella BA. Fabrication and properties of recycled cellulose fibre-reinforced epoxy composites. Compos Interfaces 2009;16(7–9):659–69.
[14] Rahman MM, Rashid MH, Hossain MA, Hasan MT, Hasan MK. Performance evaluation of bamboo reinforced concrete beam. Int J Eng Tech 2011;11(04):142–6.
[15] Lin X, Silsbee MR, Roy DM, Kessler K, Blankenhorn PR. Approaches to improve the properties of wood fiber reinforced cementitious composites. Cem Concr Res 1994;24(8):1558–66.
[16] Alomayri T, Shaikh FUA, Low IM. Characterisation of cotton fibre-reinforced geopolymer composites. Compos Part B 2013;50:1–6.
[17] Alzeer M, MacKenzie K. Synthesis and mechanical properties of novel composites of inorganic polymers (geopolymers) with unidirectional natural flax fibres (phormium tenax). Appl Clay Sci 2013;75–76:148–52.
[18] Alzeer M, MacKenzie KD. Synthesis and mechanical properties of new fibre-reinforced composites of inorganic polymers with natural wool fibres. J Mater Sci 2012;47(19):6958–65.
[19] Phoo-ngernkham T, Chindaprasirt P, Sata V, Hanjitsuwan S, Hatanaka S. The effect of adding nano-SiO2 and nano-Al2O3 on properties of high calcium fly ash geopolymer cured at ambient temperature. Mater Des 2014;55:58–65.
[20] Nazari A, Sanjayan JG. Hybrid effects of alumina and silica nanoparticles on water absorption of geopolymers: application of Taguchi approach. Measurement 2015;60:240–6.
[21] Saafi M, Andrew K, Tang PL, McGhon D, Taylor S, Rahman M, et al. Multifunctional properties of carbon nanotube/fly ash geopolymeric nanocomposites. Constr Build Mater 2013;49:46–55.
[22] Shaikh FUA, Supit SWM. Mechanical and durability properties of high volume fly ash (HVFA) concrete containing calcium carbonate (CaCO3) nanoparticles. Constr Build Mater 2014;70:309–21.
[23] Hakamy A, Shaikh FUA, Low IM. Characteristics of nanoclay and calcined nanoclay-cement nanocomposites. Compos Part B 2015;78:174–84.
[24] Alamri H, Low IM. Effect of water absorption on the mechanical properties of nanoclay filled recycled cellulose fibre reinforced epoxy hybrid nanocomposites. Compos Part A 2013;44:23–31.
[25] ASTM. Standard test methods for flexural properties of unreinforced and reinforced plastics and electrical insulating materials. 2010.
[26] ASTM. Standard test method for flexural toughness and first-crack strength of fiber-reinforced concrete (using beam with third-point loading). 1998.
[27] Alomayri T, Assaedi H, Shaikh FUA, Low IM. Effect of water absorption on the mechanical properties of cotton fabric-reinforced geopolymer composites. J Asian Ceram Soc 2014;2:223–30.
[28] Alamri H, Low IM, Alothman Z. Mechanical, thermal and microstructural characteristics of cellulose fibre reinforced epoxy/organoclay nanocomposites. Compos Part B 2012;43(7):2762–71.
[29] Shaikh F, Supit S, Sarker P. A study on the effect of nano silica on compressive strength of high volume fly ash mortars and concretes. Mater Des 2014;60:433–42.
[30] Hakamy A, Shaikh FUA, Low IM. Thermal and mechanical properties of hemp fabric-reinforced nanoclay-cement nanocomposites. J Mater Sci 2013;49:1684–94.
[31] Zivica V, Palou MT, Bage TIL. High strength metahalloysite based geopolymer. Compos Part B 2014;57:155–65.
[32] Li Q, Xu H, Li F, Li P, Shen L, Zhai J. Synthesis of geopolymer composites from blends of CFBC fly and bottom ashes. Fuel 2012;97:366–72.
[33] ul-Haq E, Kunjalukkal Padmanabhan S, Licciulli A. Synthesis and characteristics of fly ash and bottom ash based geopolymers–A comparative study. Ceram Int 2014;40(2):2965–71.
[34] Ebadi-Dehaghani H, Khonakdar HA, Barikani M, Jafari SH. Experimental and theoretical analyses of mechanical properties of PP/PLA/clay nanocomposites. Compos Part B 2015;69:133–44.
[35] Fernandez-Jimenez A, Palomo A. Composition and microstructure of alkali activated fly ash binder: effect of the activator. Cem Concr Res 2005;35(10):1984–92.
[36] Alomayri T, Low IM. Synthesis and characterization of mechanical properties in cotton fiber-reinforced geopolymer composites. J Asian Ceram Soc 2013;1(1):30–4.
[37] Chen-Tanw N, van-Riessen A. Determining the reactivity of a fly ash for production of geopolymer. J Am Ceram Soc 2009;92:881–7.
[38] Bakharev T. Thermal behaviour of geopolymers prepared using class F fly ash and elevated temperature curing. Cem Concr Res 2006;36(6):1134–47.
[39] Rickard WDA, Williams R, Temuujin J, van Riessen A. Assessing the suitability of three Australian fly ashes as an aluminosilicate source for geopolymers in high temperature applications. Mater Sci Eng A 2011;528(9):3390–7.
[40] Phair JW, van-Deventer JSJ. Effect of the silicate activator pH on the microstructural characteristics of waste-based geopolymers. Int J Min Process 2002;66(1–4):121–43.
[41] Kanny K, Mohan TP. Resin infusion analysis of nanoclay filled glass fiber laminates. Compos Part B 2014;58:328–34.
[42] Sim J, Park C, Moon DY. Characteristics of basalt fiber as a strengthening material for concrete structures. Compos Part B 2005;36(6–7):504–12.

3.4 Influence of mixing methods of nano-silica on the microstructural and mechanical properties of flax fabric reinforced geopolymer composites

Assaedi, H., Shaikh, F.U.A. and Low, I.M., 2016. Influence of mixing methods of nano-silica on the microstructural and mechanical properties of flax fabric reinforced geopolymer composites. *Construction and Building Materials*, *123*, pp.541-552.

Construction and Building Materials 123 (2016) 541–552

Contents lists available at ScienceDirect

Construction and Building Materials

journal homepage: www.elsevier.com/locate/conbuildmat

Influence of mixing methods of nano silica on the microstructural and mechanical properties of flax fabric reinforced geopolymer composites

H. Assaedi [a], F.U.A. Shaikh [b], I.M. Low [a,*]

[a] Department of Imaging & Applied Physics, Curtin University, GPO Box U1987, Perth, WA 6845, Australia
[b] Department of Civil Engineering, Curtin University, GPO Box U1987, Perth, WA 6845, Australia

HIGHLIGHTS

- Geopolymers are prepared using the wet-mix and dry-mix methods.
- Nanosilica improves the microstructure of geopolymer.
- Flexural and compressive strengths of samples are improved by nanosilica.
- Samples prepared by dry-mixing have better physical and mechanical properties.

ARTICLE INFO

Article history:
Received 15 March 2016
Received in revised form 23 June 2016
Accepted 15 July 2016
Available online 21 July 2016

Keywords:
Geopolymer
Nano-silica
Mixing procedure
Flax fabric
Mechanical properties

ABSTRACT

This paper presents the effects of two mixing methods of nanosilica on physical and mechanical properties of flyash-based geopolymer matrices containing nanosilica (NS) at 0.5, 1.0, 2.0, and 3.0 wt%. Comparison is made with conventional mechanical dry-mix of NS with fly-ash and wet-mix of NS in alkaline solutions. The influence of NS on the flexural toughness of flax fabric (FF) reinforced geopolymer nanocomposites has also been reported. Physical and microstructural properties are investigated using X-ray diffraction, scanning electron microscopy and energy dispersive X-ray spectroscopy. Results show that generally the addition of NS particles improves the microstructure and increases flexural and compressive strengths of geopolymer nanocomposites. However, samples prepared using the dry-mix approach demonstrate better physical and mechanical properties when compared to wet-mix samples.

1. Introduction

Geopolymers are synthesized by activating a solid aluminosilicate source with alkaline solutions, which forms amorphous networks of tetrahedral SiO_4 and AlO_4 connected by sharing oxygen atoms. Molecular geopolymeric network units can be formed depending on the Si:Al ratio. The fundamental geopolymeric chemical networks are poly-sialate (SiO_4-AlO_4), poly-sialate-siloxo (SiO_4-AlO_4-SiO_4) and poly-sialate-disiloxo (SiO_4-AlO_4-SiO_4-SiO_4), which represent the Si:Al ratios of 1, 2 and 3, respectively [1]. One of the most important parameters that influence the physical and mechanical properties of geopolymer matrices is the chemical content of silicon and aluminum elements. The molar chemical ratio Si:Al has been studied extensively and is considered a critical factor that controls the compressive strengths of geopolymers [2]. The optimum mechanical properties exhibited in geopolymers have Si:Al ranging between 1.8 and 2.5 [2–4]. However, these ratios of the aluminosilicate composition must be identified for the reactive geopolymer gel or the amorphous phase, since the crystalline phases are unreactive in the geopolymeric reaction [5,6].

Improving the mechanical properties such as flexural and compressive strengths, and flexural toughness of geopolymers will significantly increase their applications in the construction industry; and this may be accomplished by two ways: one is through enhancement of physical structure of geopolymer matrices by incorporating nanoparticles in the system, and the other is through improving the toughness behavior of the material by adding fibres as fibre-reinforced geopolymer composite. Currently, nanotechnology has several applications in polymer and ceramic research, especially in producing nanocomposites that exhibit superior physical properties [5]. In geopolymers, the incorporation of nanoparticles is a relatively novel field; however, some types of nanoparticle have been added efficiently to geopolymer pastes to improve their mechanical properties. In a previous study, the effect of nano-clay (Cloisite 30B) on the mechanical and thermal properties of geopolymer composites is investigated [7]. Nanoclay

* Corresponding author.
E-mail address: j.low@curtin.edu.au (I.M. Low).

http://dx.doi.org/10.1016/j.conbuildmat.2016.07.049
0950-0618/

particles were found to improve the physical structure of geopolymer matrices, producing geopolymer with superior mechanical performance. Also, nano-alumina and nano-silica particles have been integrated successfully into geopolymer matrices, resulting in higher mechanical properties. The alumina and silica acted positively in two ways: physically as a nano-filler and chemically by activating the geopolymeric reaction [8]. In another study, it has been reported that the silica and alumina nano-particles have the ability to reduce the porosity and water absorption of geopolymer matrices [9]. A further study on the effect of adding carbon nanotubes to fly-ash-based geopolymer has demonstrated a significant improvement in the mechanical and electrical properties of geopolymer nano-composites when compared to the control paste [10]. A critical factor, however, that limits the addition of nanoparticles is the good dispersion of the nanoparticles in the matrix. Poor dispersion of nanoparticles could lead to the agglomeration of nano particles, which adversely affects the physical and mechanical properties of geopolymers [11]. Yet, modifying the preparation procedure including the way of mixing nanoparticles could change the nanoparticles level of dispersion in the matrices, which consequently influences the composite's physical properties [12].

Geopolymers like other ceramics also suffer from brittle cracking under mechanical loads. This limitation may be readily overcome with fibre reinforcement as in high performance polymer-matrix composites. Natural fibres have revealed desirable effect on the mechanical properties of geopolymers. For example, wool and flax fibres have been successfully used in reinforcing geopolymer composites with concomitant improvements in mechanical and fracture properties [13,14]. Furthermore, it has been found that cotton fibres enhanced the strength and toughness of geopolymer [15]. In our previous work, fly-ash based geopolymer has been reinforced with flax fabrics, resulting in significant improvement on the mechanical properties of the eco-composites [16]. Flax fibres offer advantages such as low density, low cost, availability, specified properties and low energy consumption throughout the extraction process. Flax fibre (FF) is a main natural fibre that made up of 64.1% cellulose, 16.7% hemicelluloses, 1.8% pectin and 2% lignin. FF also contains minor amounts of waxes, bound water and inorganic component material [17].

In this study, the effects of dry mixing of nano-silica (NS) with fly-ash before adding alkaline solutions and of the dispersion of NS in alkaline solution on the physical and mechanical properties of geopolymers are investigated. XRD analysis and EDS are used to explore the morphology and microstructure of geopolymer nanocomposites. Besides, the effect of different amounts of NS on the flexural toughness of FF-reinforced geopolymer nanocomposites is also evaluated. To the best knowledge of authors, no study has been reported on reinforcing geopolymer with a combination of both NS and FF.

2. Experimental procedure

2.1. Raw materials

Low calcium fly ash (ASTM class F), collected from the Eraring power station in NSW of Australia, and was used as the source material for the geopolymer matrix. The chemical composition of fly ash is shown in Table 1. Nanosilica is obtained from Nanostructured and Amorphous Materials, Inc. of USA with average particle diameter of 18–25 nm (Fig. 1). The alkaline activator for geopolymerisation was a combination of sodium hydroxide and sodium silicate grade D solution. Sodium hydroxide flakes of 98% purity were used to prepare the solution. The chemical composition of sodium silicate used was 14.7% Na_2O, 29.4% SiO_2 and 55.9% water by mass.

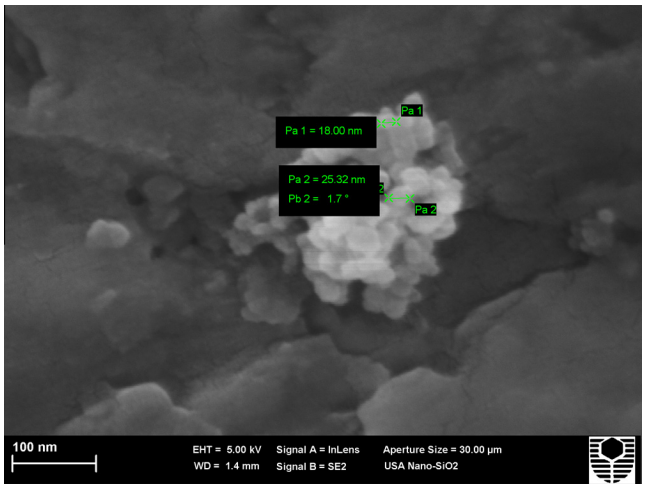

Fig. 1. SEM image of nanosilica (NS) particles.

2.2. Preparation of geopolymer nano-composites

To prepare the geopolymer matrix, an alkaline solution to fly ash ratio of 0.75 was used and the ratio of sodium silicate solution to sodium hydroxide solution was fixed at 2.5. The concentration of sodium hydroxide solution was 8 M, and it was prepared and combined with the sodium silicate solution one day before mixing.

The geopolymer pastes were prepared by two methods, a dry and wet process (Fig. 2). For dry-mix process, the NS was added first to the fly-ash at the dosages of 0.5, 1.0, 2.0 and 3.0% by weight (Table 2). The fly-ash and NS were dry-mixed for 5 min in a covered mixer at a low speed and then mixed for another 10 min at high speed until homogeneity was achieved. The alkaline solution was then added slowly to the fly-ash/NS powders in the Hobart mixer at a low speed until the mixes became homogeneous, then further mixed for another 10 min on high speed. Similar mixtures dosages were prepared to produce the wet-mix paste. However, the NS powder was first wet-mixed with the alkaline solution mechanically until the dissolution of the NS powder was achieved. Then, the solutions, with different dosages of silica, were mixed with fly ash in the Hobart mixer at the same period of time of the dry-mix process. The resultant mixtures, dry/wet-mixes, were then poured into coated wooden moulds and placed on a vibration table for two minutes to remove any entrapped air inside the pastes.

Similar mixtures were prepared to produce the FF-composites and nanocomposites. The samples prepared by spreading a thin layer of geopolymer paste in a well-greased wooden mould and carefully placing the first layer of FF on it. The fabric was fully saturated with paste by a roller, and the process repeated for ten layers; each specimen contained a different weight percentage of NS. The samples then were left under heavy weight (20 kg) for 1 h to reduce entrapped air inside the samples. All samples (see

Table 1
Chemical composition of fly-ash (wt%).

SiO_2	Al_2O_3	CaO	Fe_2O_3	K_2O	MgO	Na_2O	P_2O_5	SO_3	TiO_2	MnO	BaO	LOI
63.13	24.88	2.58	3.07	2.01	0.61	0.71	0.17	0.18	0.96	0.05	0.07	1.45

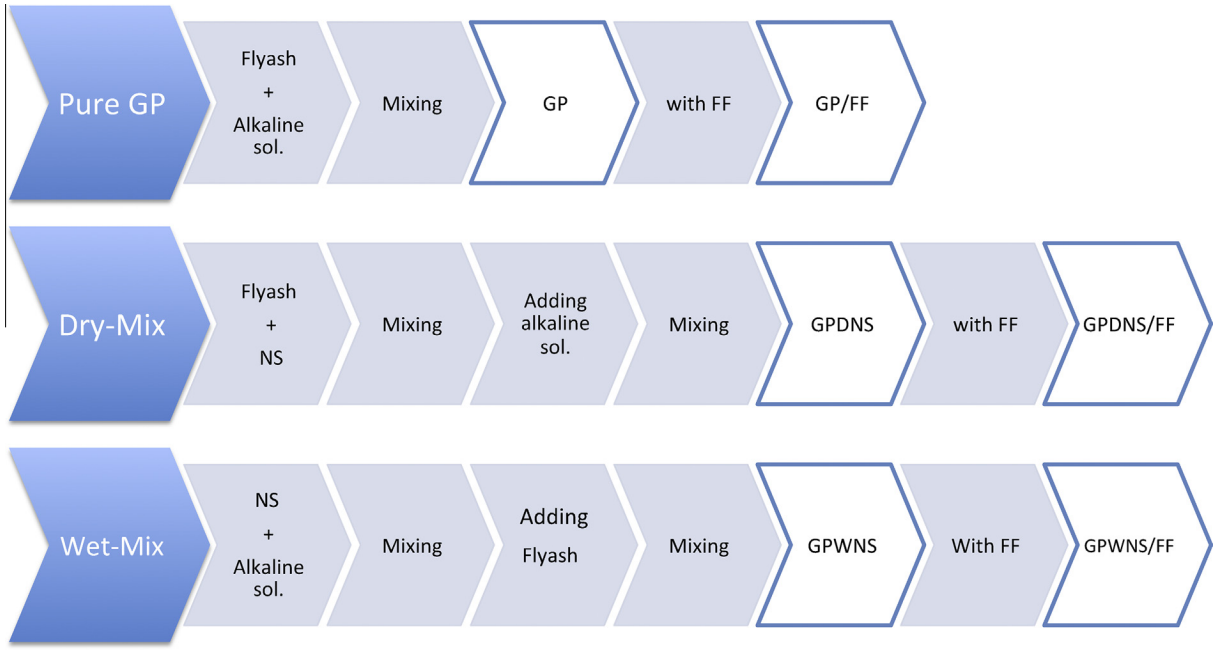

Fig. 2. Schematic showing the preparation of geopolymer; geopolymer nanocomposites and FF-reinforced geopolymer nanocomposites in dry/wet mix procedures.

Table 2
Formulation and composition of samples prepared using dry and wet mix procedures. Mass ratio: (SiO_2/Na_2O) of sodium silicate = 2.0; (Na_2O/fly ash) = 0.079.

Sample	Fly-ash (g)	NaOH (g)	Na_2SiO_3 (g)	Water (g)	Nanosilica (g)
GP	1000	214.5	535.5	50	0
GPNS-0.5	1000	214.5	535.5	50	5
GPNS-1.0	1000	214.5	535.5	50	10
GPNS-2.0	1000	214.5	535.5	50	20
GPNS-3.0	1000	214.5	535.5	50	30

Table 2) were covered with plastic film and cured at 80 °C for 24 h in an oven before demoulding. They were then cured under ambient conditions to be tested after 28 days. The total content of FF in each specimen was about 4.1 wt%. This procedure of preparing FF-reinforced geopolymer composites was reported by the authors in previous study [16].

2.3. Structural and microstructural characterization

The samples were broken and ground to fine powder. Then, they were scanned using a D8 Advance Diffractometer (Bruker-AXS, Germany) using copper radiation and a LynxEye position sensitive detector. The diffractometer were scanned from 7.5° to 60° using a scanning rate of 0.5°/min. XRD patterns were obtained by using Cu k_α lines (k = 1.5406 Å). The Quantitative X-ray Diffraction Analysis (QXDA) with Rietveld refinement was done using *MAUD* V2.44 software. A fluorite [CaF_2] was chosen to serve as an internal standard [6]. The samples for QXDA were prepared by mixing a dry weight of 3.0 g of geopolymer paste or geopolymer nanocomposite paste with 0.33 g of fluorite. The weight percentage of each crystalline phase W_{Cr} was determined by Rietveld refined parameters using Eq. (1) [18]:

$$W_{Cr} = \left[W_{std}\frac{S_{Cr}(ZMV)_{Cr}}{S_{std}(ZMV)_{std}}\right] \times \left[\frac{1}{1-W_{std}}\right] \quad (1)$$

where the standard (fluorite) weight percent is W_{std}. M and V are the mas and volume of unit cells, Z is the number of formula units per unit cell, S_{Cr} and S_{std} are the scale factors for the crystalline phases and the standard, respectively.

The amorphous weight content W_{Am} is then found using [18]:

$$W_{Am} = 1 - \sum_{i=1}^{n} W_n \quad (2)$$

where n is the number of crystalline phases refined.

Scanning electron microscopy imaging was obtained using EVO 40XVP (Zeiss, Germany), equipped with energy dispersive spectroscopy (EDS). Quantitative EDS analysis was undertaken using the INCA software package (Oxford Instruments, England). Samples were polished and coated with platinum for analysis. The accelerating voltage for secondary electrons was fixed at 20 kV.

2.4. Physical and mechanical properties

Measurements of bulk density and porosity were conducted to define the quality of geopolymer nanocomposite. Density of samples (ρ) with volume (V) and dry mass (m_d) was calculated using Eq. (3):

$$\rho = \frac{m_d}{V} \quad (3)$$

Pure geopolymer and geopolymer nanocomposite were immersed in clean water, and the value of apparent porosity (P_a) was determined using Archimedes' principle in accordance with the ASTM (C-20) [19].

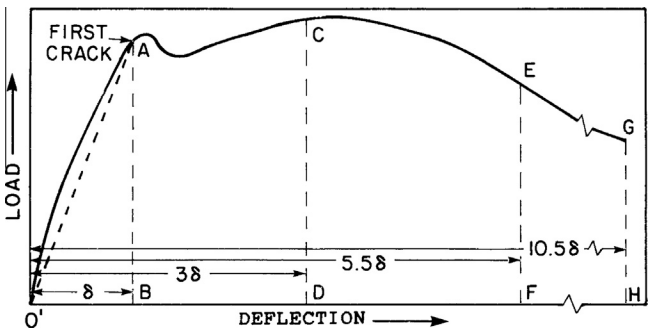

Fig. 3. Definition of ASTM toughness indices [22].

A LLOYD Material Testing Machine (50 kN capacity) with a displacement rate of 1 mm/min was used to perform the mechanical tests. Five rectangular bars of $60 \times 18 \times 15\ mm^3$ with a span of 40 mm were cut from the fully-cured samples for three-point bend tests to evaluate the flexural strength. All samples were aligned horizontally to the applied load in the mechanical test. Flexural strength was evaluated according to ASTM D790 [20]. The values were recorded and analysed with the machine software (NEXYGENPlus) and average values were calculated. The compressive strength of geopolymer composites was tested according to ASTM C109 [21]. The flexural toughness of FF-reinforced nanocomposites was characterised and evaluated using toughness indices I_5, I_{10} and $I_{failure}$ as defined by ASTM C1018 [22], Standard Test Method for Flexural Toughness and First-Crack Strength of Fibre-Reinforced Concrete (Using Beam With Third-Point Loading). According to the Standard, I_5 is defined as the ratio obtained by dividing the area up to a deflection of three times the first-crack deflection by the area up to first crack deflection, while I_{10} is the ratio of the area up to a deflection of 5.5 times the first-crack deflection to the area up to the first crack (see Fig. 3). Thus, it could be written as:

$$I_5 = \frac{(Area)_{OACDO}}{(Area)_{OABO}} \tag{4}$$

$$I_{10} = \frac{(Area)_{OAEFO}}{(Area)_{OABO}} \tag{5}$$

Similarly, $I_{failure}$ can be evaluated for the failure deflection of 11.4 mm in this study as most of the specimens lost their load carrying capacity significantly at that deflection.

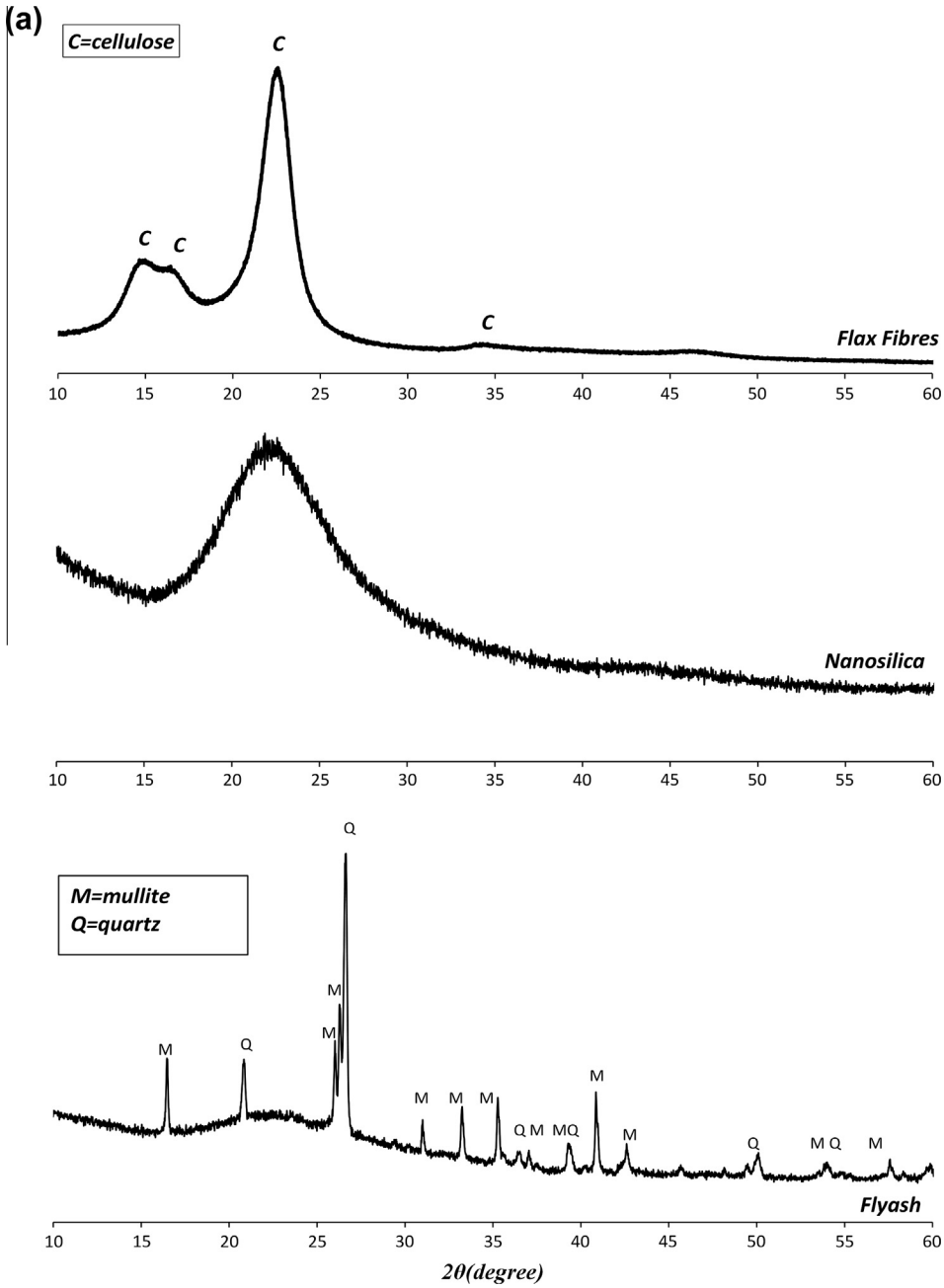

Fig. 4. XRD patterns of: (a) flax fibres, nanosilica and flyash. (b) Geopolymer nanocomposites prepared by dry-mix procedure. (c) Geopolymer nanocomposites prepared by wet-mix procedure. [Legend: M = Mullite, Q = Quartz and F = Fluorite].

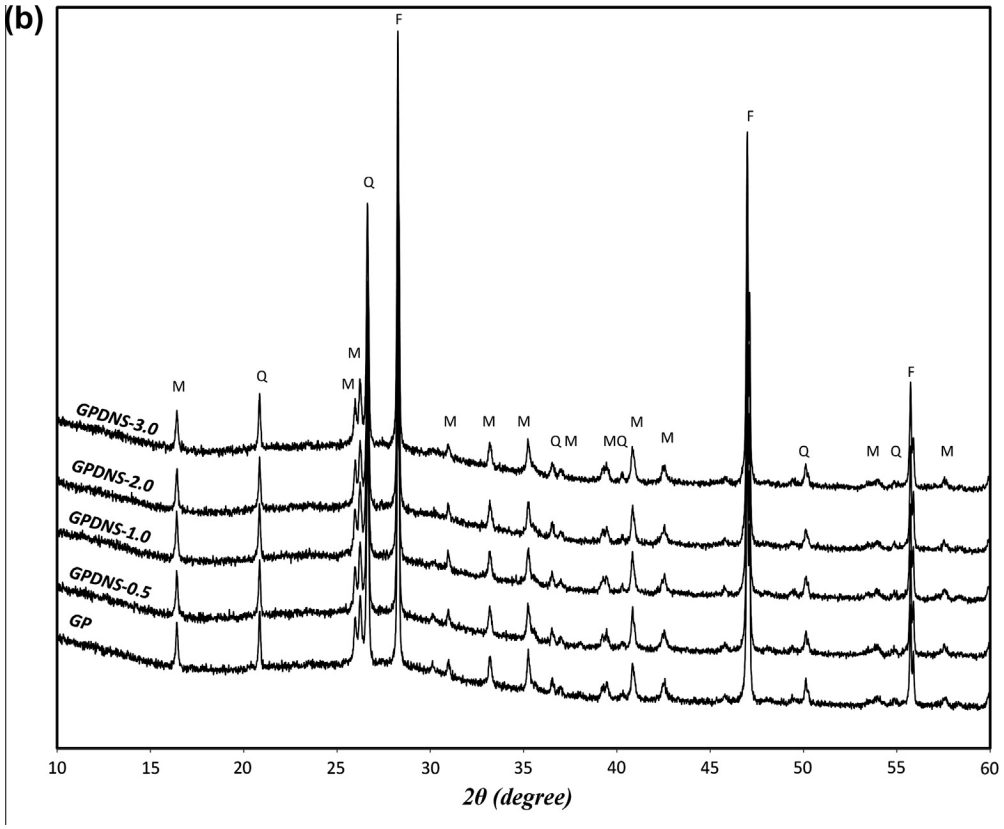

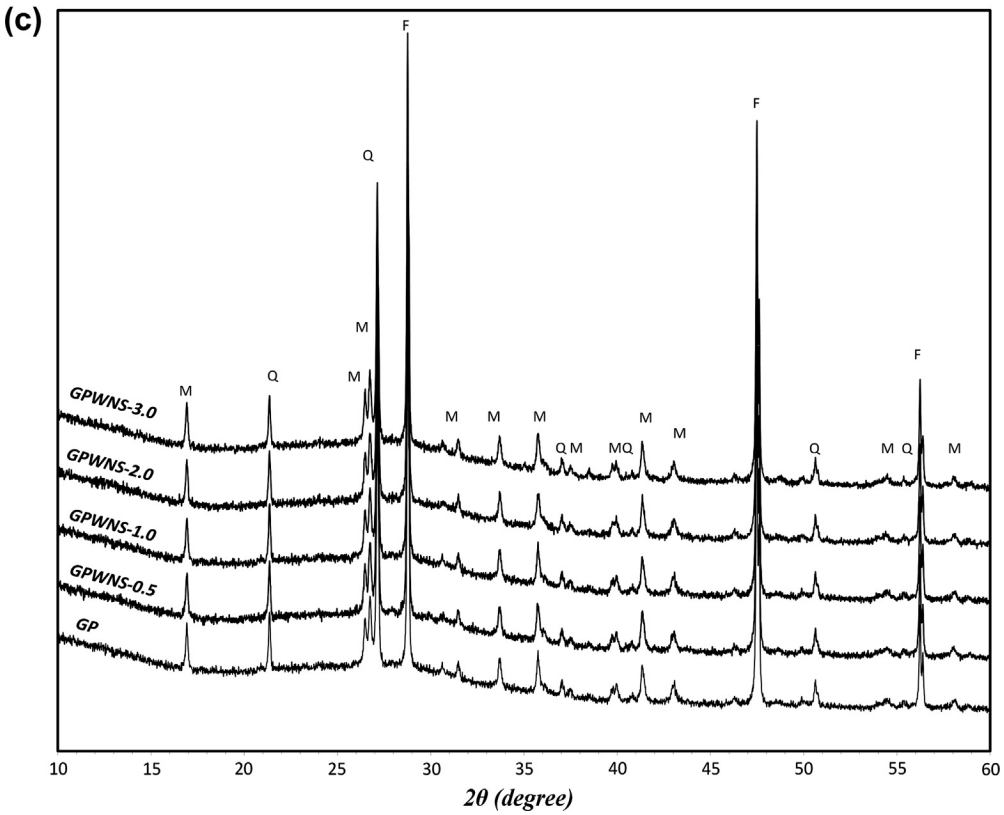

Fig. 4 (*continued*)

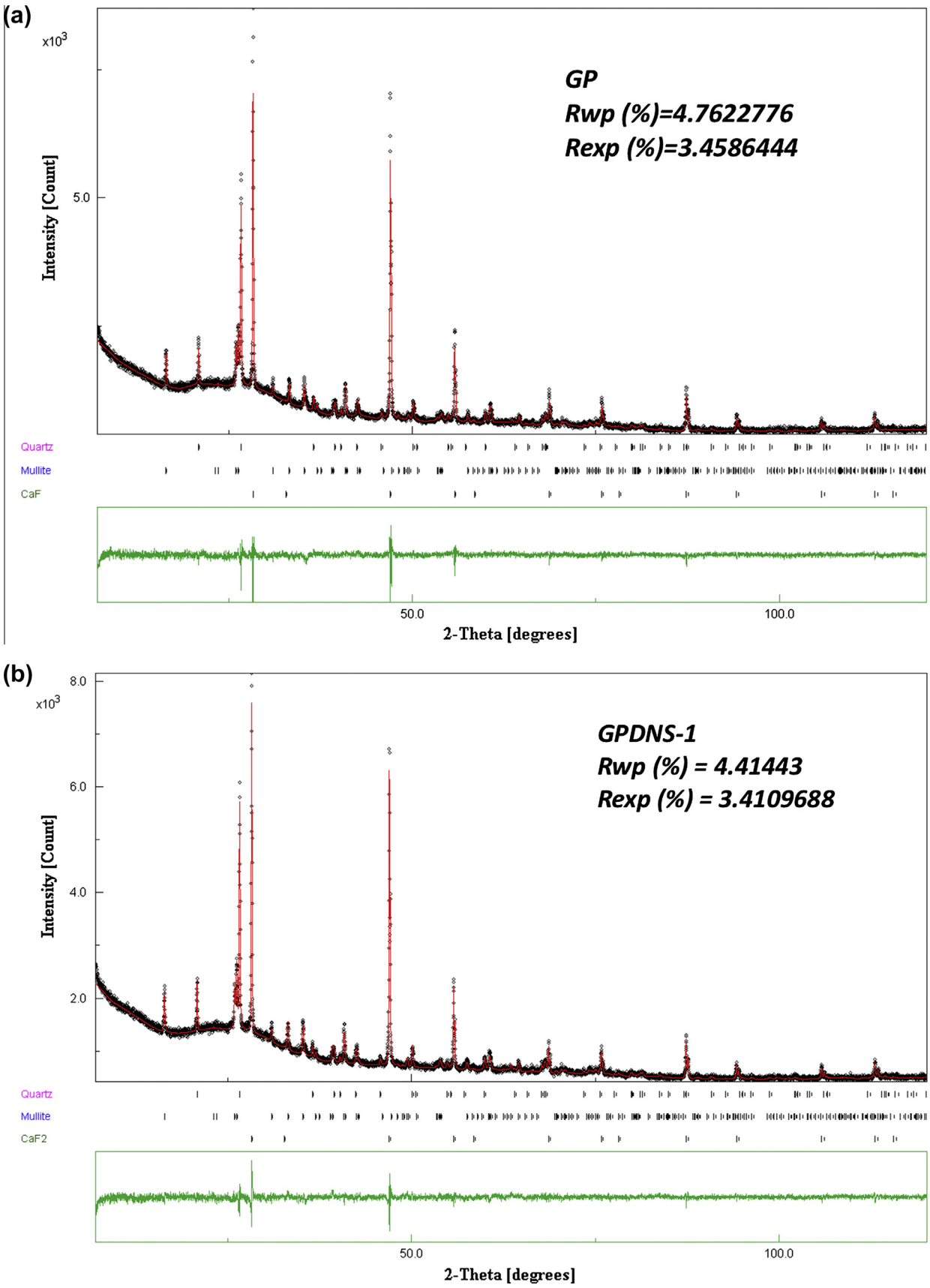

Fig. 5. XRD Rietveld plots for: (a) GP; and (b) GPDNS-1. Measured patterns are indicated by black points, and calculated patterns by solid red lines. The green residual plot shows the difference between the calculated and the measured patterns.

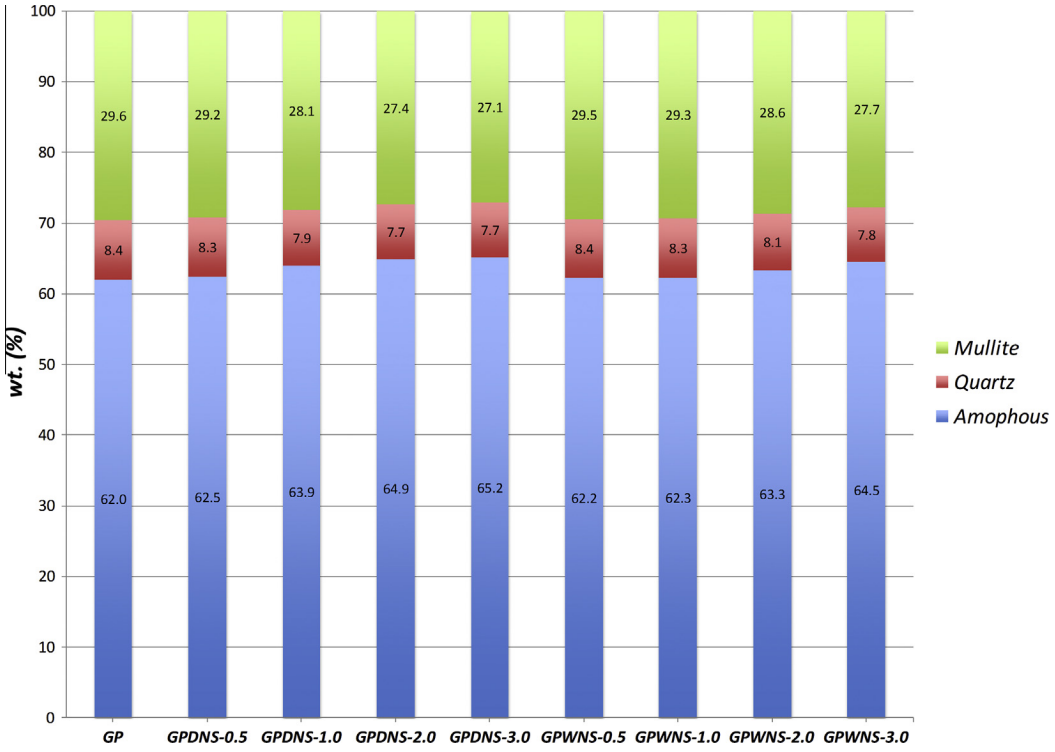

Fig. 6. Amorphous and crystalline phase compositions of pure geopolymer and geopolymer nanocomposites.

Table 3
Geopolymer pastes with different silica contents as calculated and measured experimentally using QEDS technique. Uncertainties are indicated in brackets.

Sample	$(Si:Al)_{calc}$	$(Si:Al)_{exp}$
GP	2.69	2.29 (0.2)
GPDNS-0.5	2.69	2.66 (0.3)
GPDNS-1.0	2.72	3.02 (0.2)
GPDNS-2.0	2.76	3.41 (0.2)
GPDNS-3.0	2.79	3.57 (0.3)
GPWNS-0.5	2.69	2.75 (0.2)
GPWNS-1.0	2.72	3.63 (0.2)
GPWNS-2.0	2.76	3.91 (0.2)
GPWNS-3.0	2.79	4.10 (0.4)

3. Results and discussion

3.1. X-ray diffraction analysis (XRD) and quantitative energy dispersive X-ray spectrometer (QEDS)

The XRD spectra obtained for NS, flax fibres, fly ash and all nanocomposite samples are given in Fig. 4a–c. The crystalline phases were indexed using Powder Diffraction Files (PDFs) from the Inorganic Crystal Structure Database (ICSD). The diffraction pattern of NS, FF and fly ash are shown in Fig. 4a. The diffraction pattern of flax fibres shows typical peaks of cellulose (PDF 00-060-1502), whereas the NS powder displays a complete amorphous (glass) phase. In the case of fly ash, two main phases are indexed distinctly: quartz [SiO_2] (PDF 00-046-1045) and mullite [$Al_{2.32}Si_{0.68}O_{4.84}$] (PDF 04-016-1588). Quartz and mullite are the major crystalline phases of the Eraring fly-ash [7,23]. Therefore, they are unreactive in the geopolymeric reaction, and act as filler in geopolymer matrices [21,22]. Nevertheless, the amorphous aluminosilicate broad hump produced between $2\theta = 14°$ and 27° characterizes the reactive and dissolvable content in alkaline solution during the geopolymer development, which determines the activity of geopolymeric reaction [24–26]. The degree of amorphous fly ash is recognized as one of the most important factors that influence the physical and mechanical properties of fly ash geopolymers: the higher the amount of amorphous phase, the greater the strength exhibited by the geopolymer [24,25]. Fig. 4b and c show the XRD spectra of pure geopolymer and geopolymer nanocomposites prepared by dry and wet mix preparation procedures. All samples have the main crystalline phases, quartz and Mullite, besides the fluorite [CaF_2] (PDF 04-002-2191). Fluorite is the standard used to determine the weight percentage of each crystalline phase. The phase abundance of crystalline phases in each sample was determined using Rietveld refinement, and the amorphous contents were calculated using Eq. (2). Fig. 5a and b show Rietveld refinement of the diffraction pattern of pure geopolymer and GPDNS-1, respectively. In general, the addition of 0.5, 1.0, 2.0 and 3.0 wt% NS into the geopolymer matrix has resulted in slight changes to the crystalline and amorphous contents in the samples. As can be seen from Fig. 6, the addition of 3.0 wt% NS increased the amorphous content in both dry and wet mix samples by 3.2% and 2.5%, respectively compared to the pure geopolymer paste. As a consequence of this, the relative amounts of crystalline phases for the dry and wet mix nanocomposites were reduced. The growth of the amorphous content in the nanocomposite samples could be attributed to two reasons. First, the amorphous nature of the unreacted NS contributes to the total amorphous contents in the nanocomposites. This effect is believed to occur more in the case of dry-mix samples since a part of the NS particles perform as a filler in the matrices. Secondly, the addition of NS to the system promotes geopolymeric reaction producing higher amorphous amount of geopolymer gel in the nanocomposite.

The silicon-to-aluminum (Si/Al) ratio has a significant impact on the physical and mechanical properties of geopolymers [2,4]. Table 3 shows the Si/Al ratio as prepared and calculated theoretically in all samples, and the Si/Al ratios as determined experimentally using QEDS analysis. The theoretical ratios are similar in dry and wet mix nanocomposites as the amounts of silica added to

the system are the same in both cases. However, preparation and mixing approaches could control the way the nanoparticles disperse in matrices, which produce samples with different ratios depending on the mixing methods. EDS analysis was conducted to determine the experimental ratios of Si/Al. EDS investigation was restricted to just the geopolymer gel areas in both dry and wet mix samples. Five spots at different location from the geopolymer gel are detected and averaged. The results are presented in Table 3 and denoted as $(Si/Al)_{exp.}$ Generally, the Si/Al ratios increased with the addition of NS particles in all samples due to the silica added to the system. The ratio started from 2.29% at pure geopolymer and rose up to 3.57% in dry-mix samples and 4.10% in samples prepared using wet-mix procedure. It can be seen that, all wet-mix samples exhibited higher ratios of Si/Al compared to their counterpart dry-mix samples. This is because the whole amount of silica particles dissolved in the case of wet-mix approach increasing the silicon contents of geopolymer pastes, while in the dry-mix preparation method a part of the NS particles did not dissolve and played a filler role in geopolymer matrices. Fig. 7a–c show SEM images of pure geopolymer and geopolymer nanocomposites containing 3.0 wt% NS in wet and dry mix samples, respectively. High amount of unreacted and partially reacted fly ash particles can be clearly seen in the case of pure geopolymer (Fig. 7a). However, after the addition of NS higher amount of geopolymer gel, and fewer amount of unreacted flyash particles appeared in the wet and dry mix samples (Fig. 7b and c).

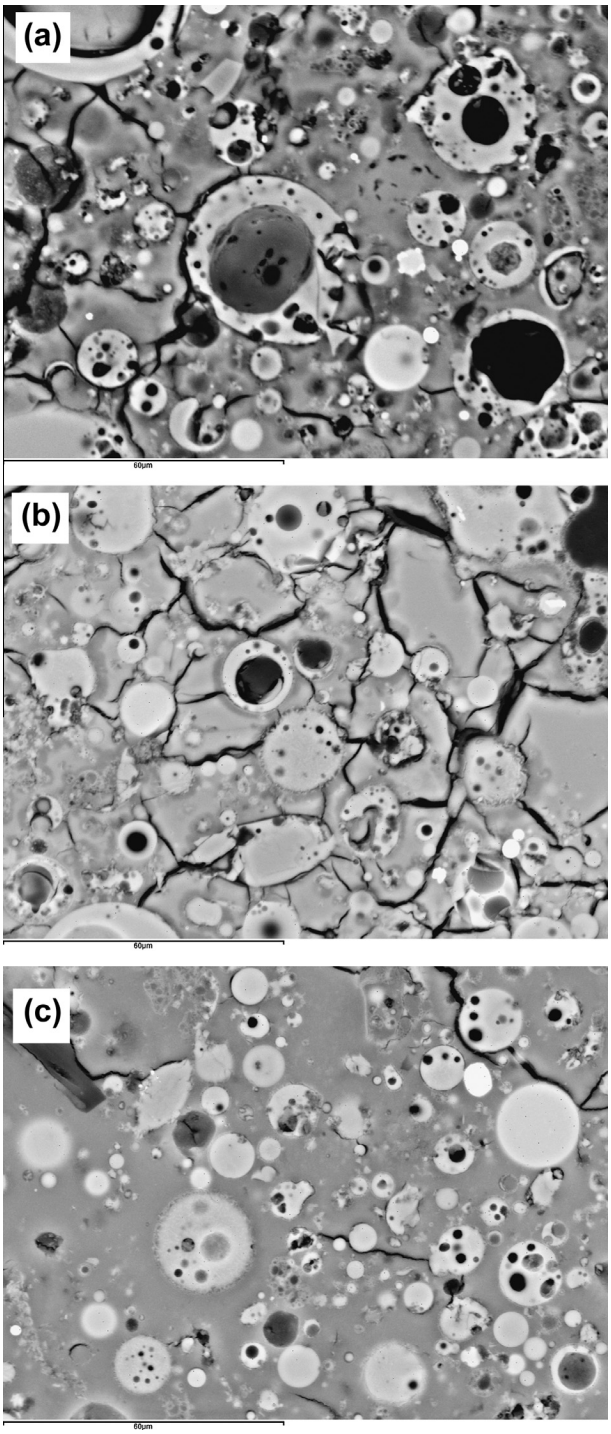

Fig. 7. SEM images showing (a) Pure geopolymer. Geopolymer nanocomposites containing 3.0 wt% NS prepared by (b) wet-mix procedure, and (c) dry mix procedure.

3.2. Physical properties

The density, porosity and water absorption of geopolymer paste and that containing NS are shown in Fig. 8. It is observed that the addition of NS decreases the porosity and water absorption of all geopolymer nanocomposites when compared to control geopolymer paste. In the wet-mix samples, the density is improved by 7.6%, while the porosity and water absorption are decreased by 16.2% and 21.5%, respectively. However, in the case of dry mix preparation method, the optimum loading was found as 1.0 wt% of NS, which improved the density by 15%, and reduced the porosity and water absorption by 27% and 35%, respectively, when compared to the control paste.

This development could be attributed to two factors. First, the addition of amorphous silica to the system in the form of NS particles has enhanced the geopolymeric reaction producing more geopolymer gel and denser matrices [8]. Secondly, the NS particles acted as pore-filler reducing the porosity of all dry-mix samples. This enhancement reveals that geopolymer nanocomposite with the optimum supplement of NS synthesized using dry and wet mix preparation methods yields consolidated dense microstructure. The current results are in agreement with the work done by Jo et al. [27] where the porosity of cement mortar is reduced by the addition of NS particles. In another study, Supit and Shaikh reported that the addition of 2.0 wt% NS notably reduced the porosity of high volume fly ash concrete [28]. However, the further addition of NS leads to an increase in porosity and water absorption and a drop in density. This could be attributed to the poor dispersion and agglomerations of the high NS contents, which creates more voids in the matrix [7,29]. Agglomeration and poor dispersion are common phenomena in nanoparticles. The high ratio of surface area to the volumes of the nanoparticles increases the adhesion forces between the particles resulting in agglomerated nanoparticles.

3.3. Flexural and compressive strengths of geopolymer nanocomposites

The effect of NS on the flexural and compressive strengths of geopolymer nano-composites is presented in Fig. 9a and b. Overall, the incorporation of NS into geopolymer matrices led to noticeable enhancement in the flexural and compressive strength of geopolymer nanocomposites in the two mix approaches. The flexural strength of dry-mix nanocomposites containing 0.5, 1.0, 2.0 and 3.0 wt% NS is increased by 20.0, 28.8, 24.4 and 15.5%, respectively. While the flexural strength of wet-mix samples is increased by 8.8, 15.5, 22.2 and 13.3%, respectively, when compared to the control

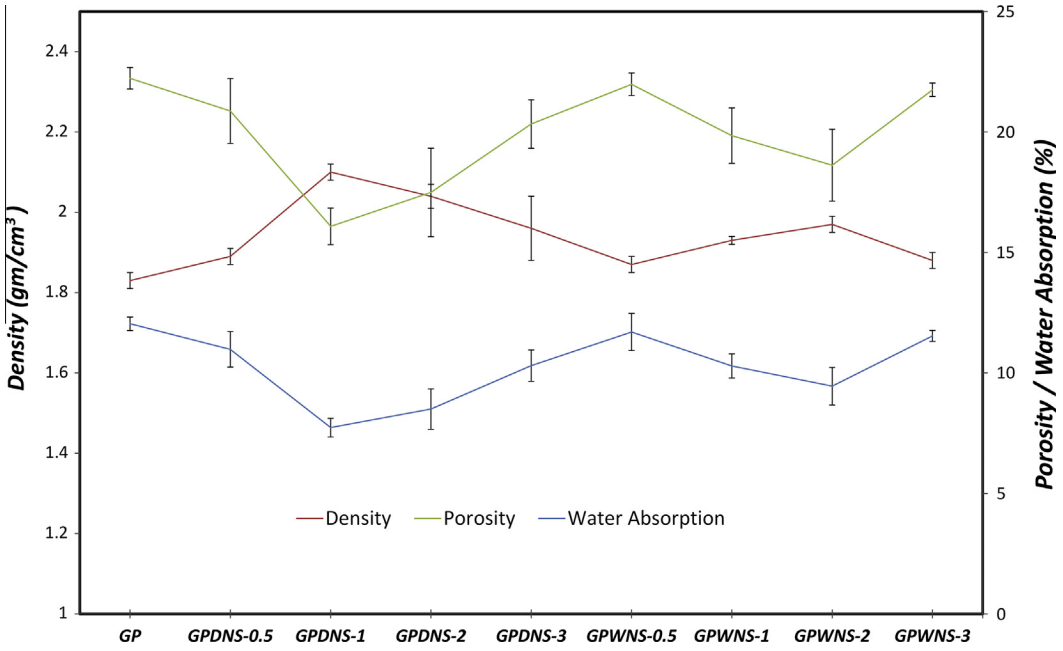

Fig. 8. Density, porosity and water absorption of pure geopolymer and geopolymer nanocomposites.

sample. The compressive strength results of geopolymer nanocomposites prepared by both dry and wet mix procedures imply comparable trends to the flexural strength results. The compressive strength of geopolymer paste improved from 37.2 to 47.3 MPa and 44.9 MPa after the addition of 1.0 and 2.0 wt% NS in dry and wet mix samples, respectively. It can be noticed that the physical structure of geopolymer pastes has significant impacts on the mechanical behavior of geopolymer nanocomposites as the mechanical tests results followed similar trends to the densities of all samples. Flexural and compressive strengths are directly proportional to the nanocomposites densities and inversely proportional to the porosities: denser specimens exhibited higher flexural and compressive strengths.

This improvement clearly indicates the efficiency of NS in improving the mechanical behavior in two ways: first, chemically by promoting the geopolymer reaction due to addition of nano silica to the system and forming additional sodium aluminosilicate hydrate or geopolymer gel [8]. This process occurs in both preparation methods; however, higher rates of silica was detected in the wet-mix process since the whole amounts of NS particles was dissolved in the alkaline solution, which accordingly produces geopolymer gel with higher content of silica. Secondly, NS particles could act as nano-fillers that fill the pores in geopolymer matrices [30]. Therefore, the enhanced physical structure of geopolymer nanocomposite exhibited superior mechanical performance when compared to the control paste, particularly in the case of dry-mix procedure, where the nanoparticles could play both functions, filling the voids of the matrix beside the chemical role.

The flexural strength is related linearly to the square root of the compressive strength (Fig. 9c) in both dry-mix (Eq. (6)) and wet-mix (Eq. (7)) samples as follow:

$$\sigma_F = 1.65\sqrt{C} - 5.58 \quad (6)$$

$$\sigma_F = 1.35\sqrt{C} - 3.58 \quad (7)$$

where σ_F is the flexural strength and C is the compressive strength of the samples. A similar trend that represents similar relationship of NS-reinforced geopolymer composite reported by Phoongernkham et al. [8] was also shown in the same figure for comparison, and indicate comparable results. They found that the addition of 2.0 wt% NS to geopolymer pastes has improved the flexural and compressive strengths by 44.8% and 31.4%, respectively. In another study, Qing et al. [30] reported the influence of 3.0 wt% nano-SiO_2 addition on the properties of cement paste, and observed that the flexural strength increased by about 72% compared to control cement matrix. The results were attributed this enhancement to the pozzolanic and filler effects of nano-SiO_2 particles. In a further research, the influence of NS on the mechanical properties of cement mortar at 28 days with water/binder ratio of 0.4 has been studied [31]. It has been found that the addition of 1.0 wt% NS improved the flexural strength from 7.0 to 9.3 MPa, and the compressive strength from 50.1 to 56.7 MPa, about 33% and 13% increase, respectively. Furthermore, the effect of nanoclay (Cloisite 30B) on the physical and mechanical properties of fly ash based geopolymer has been reported in previous study [7], and found that 2.0 wt% loading of nanoclay has improved the flexural and compressive strength by 20% and 23%, respectively.

The trends, however, are reversed after addition of high amounts of NS in both cases. The reduction in mechanical properties of wet-mix samples containing high amount of NS is due to the excessive amounts of silica dissolved in the system, which led to an inadequate OH^- ions that fully dissolve the aluminum ions (Al^{3+}), leaving unreacted flyash in the sample [2]. While the reduction in the mechanical properties of dry-mix samples containing high amount of NS could be attributed to the relatively poor dispersion and agglomerations of NS particles in geopolymer matrices at higher NS contents, which create weak zones in the form of micro-pores [7,32,33]. Nevertheless, the addition of NS improved the mechanical strength of geopolymer nanocomposite when compared to the control geopolymer paste regardless of the mixing method and the amount of NS added to the pastes. Though the flexural and compressive strengths of geopolymer nanocomposite with high content of NS are decreased compared to the nanocomposite with the optimum loading in dry/wet-mixing approaches, they are still higher than the pure geopolymer matrix.

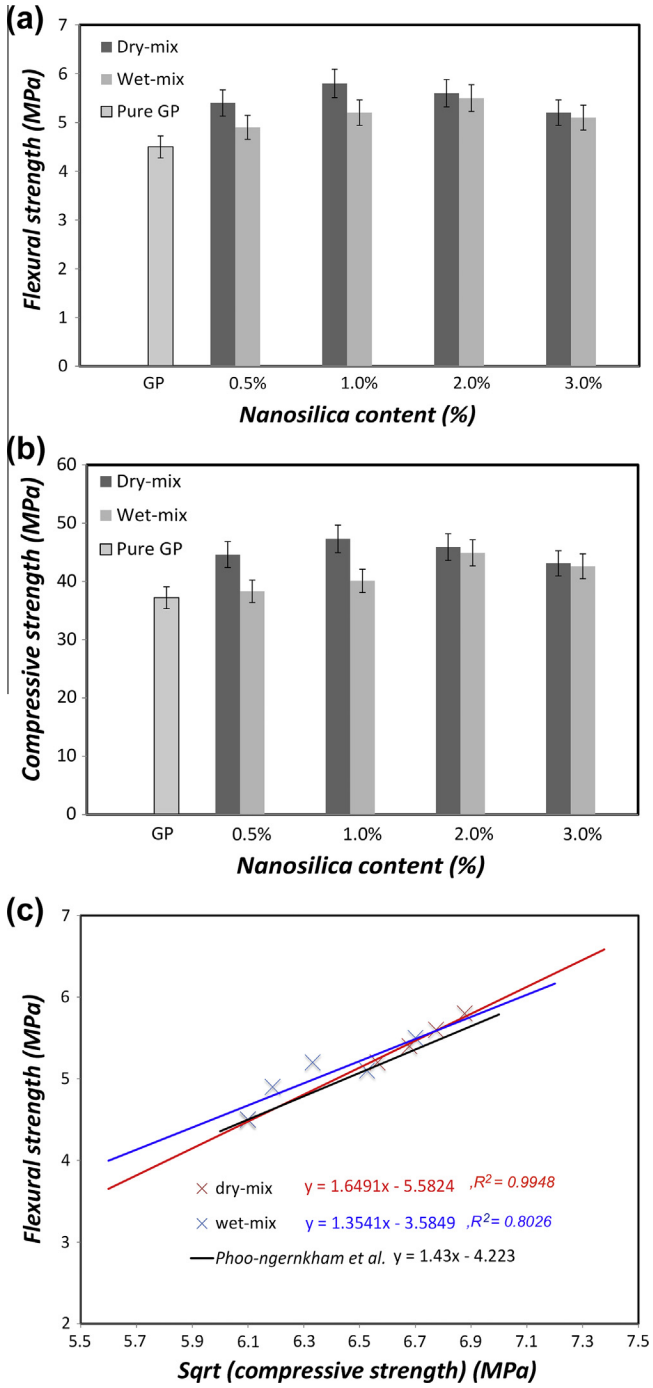

Fig. 9. Mechanical properties of geopolymer and geopolymer nanocomposites: (a) Flexural strength, (b) Compressive strength, and (c) Linear relationships between flexural strength and the square root of compressive strength of all samples.

3.4. Flexural toughness indices of FF-reinforced geopolymer nanocomposites

Pure Geopolymer matrices and geopolymer nanocomposite are brittle in nature and crack easily under applied forces; thus, they do not exhibit any toughness. To improve the capability of load capacity at strains greater than that at the initial crack, it is essential to reinforce the matrix using fibres such as FF. In previous study, pure geopolymer pastes have been reinforced with various weight contents of FF, which exhibited higher toughness as the natural fibres content increased [16]. Composites reinforced with high amount of FF demonstrated greater flexural toughness because of the capability of FF to bear the higher loads and to support the multiple cracks during the loading process, which avoided the brittle failure of geopolymers. In the current study, flexural toughness of hybrid composites containing a combination of NS and FF are studied.

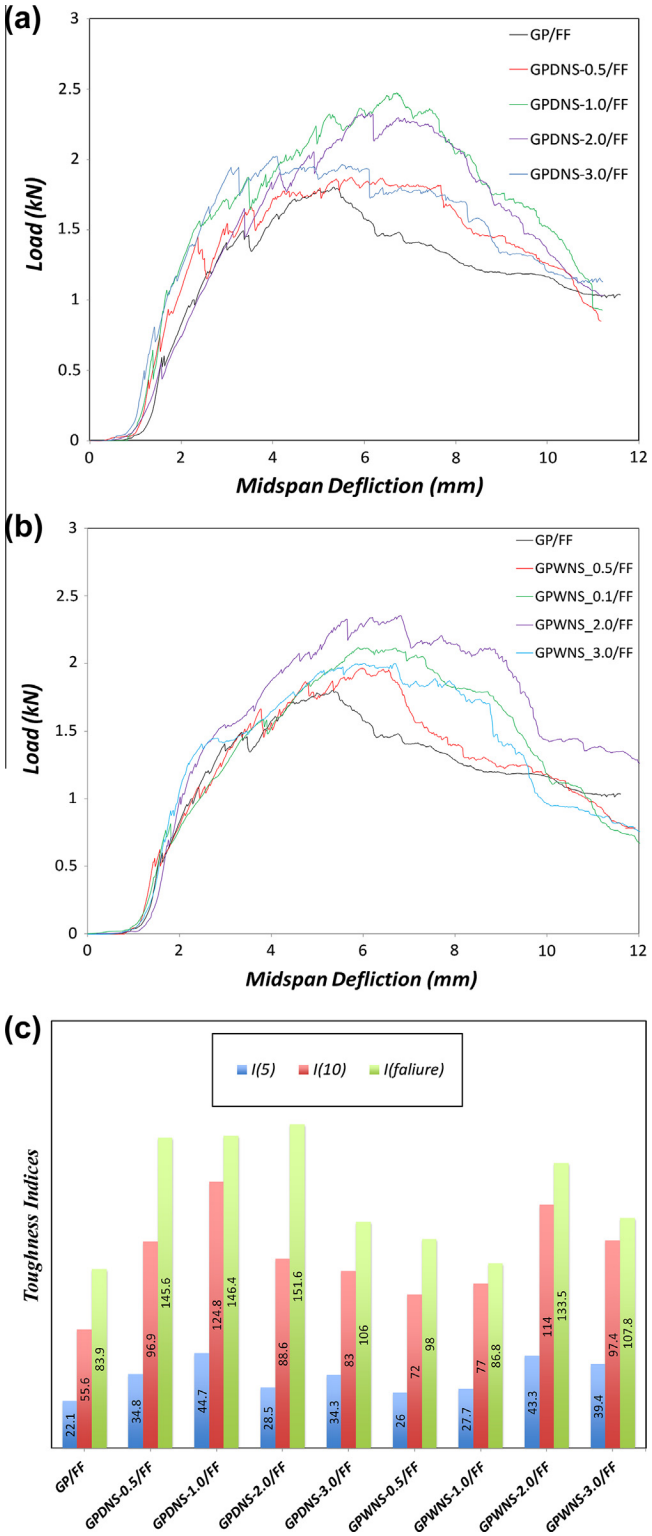

Fig. 10. Typical load-midspan deflection curves of: (a) FF-reinforced geopolymer nanocomposites prepared by dry-mix approach, (b) FF-reinforced geopolymer nanocomposites prepared by wet-mix approach (c) Toughness indices I_5, I_{10} and $I_{failure}$ for all FF-reinforced geopolymer samples.

The ability of FF-reinforced geopolymer nanocomposites to absorb energy is identified by studying the flexural toughness indices I_5, I_{10} and $I_{failure}$. For the failure deflection, $I_{failure}$ is calculated at 11.4 mm deflection for geopolymer composites and nanocomposites reinforced with FF. Fig. 10a and b display the load versus midspan deflection curves of FF-reinforced geopolymer composites and nanocomposites. FF-reinforced nanocomposite with the optimum loading of NS in both groups showed likewise optimum flexural toughness. Fig. 10c presents the toughness indices of FF-reinforced composites. In the dry-mix samples, the FF-reinforced nanocomposite loaded with 1.0 wt% showed the highest toughness indices of 44, 125 and 146 while the toughness indices of wet-mix sample loaded with 2.0 wt% NS were 43, 114 and 133 for I_5, I_{10} and $I_{failure}$, respectively. This improvement could be ascribed as the bond between the matrix and FF has improved due to the high content of geopolymer gel. The addition of NS particles enhanced the geopolymer matrix and improved the fibre-matrix adhesion, increasing the flexural toughness samples loaded with the optimum addition of NS particles. On the other hand, FF-reinforced pure geopolymer composite, which was rich of unreacted fly ash particle and high in porosity, influenced the bond strength of fibre–matrix adhesion negatively.

SEM images of the fracture surface of FF-reinforced geopolymer composite/nanocomposites after flexural toughness test are shown in Fig. 11. A range of toughness mechanisms such as fibre debonding, fibre pull-out and fibre rupture can be clearly seen. The examination of fracture surface of FF reinforced pure geopolymer composite displays a high porous structure and number of voids and unreacted fly ash particles embedded in the matrices. This reduced the bond between fibres and the matrix, and caused the fibres to de-bound and pull out from the matrix as shown in Fig. 11a. FF-reinforced geopolymer nanocomposites containing 1.0 wt% NS (dry-mix) and 2.0 wt% NS (wet-mix) displays relatively denser matrices with lower amount of unreacted fly ash particles as shown in Fig. 11b and c. This provided better adhesion between the FF and the matrices, increasing the flexural toughness values of all nanocomposites. Because of the strong fibre-matrices bonds, fibres fracture has been seen in the fracture surfaces of the nanocomposites.

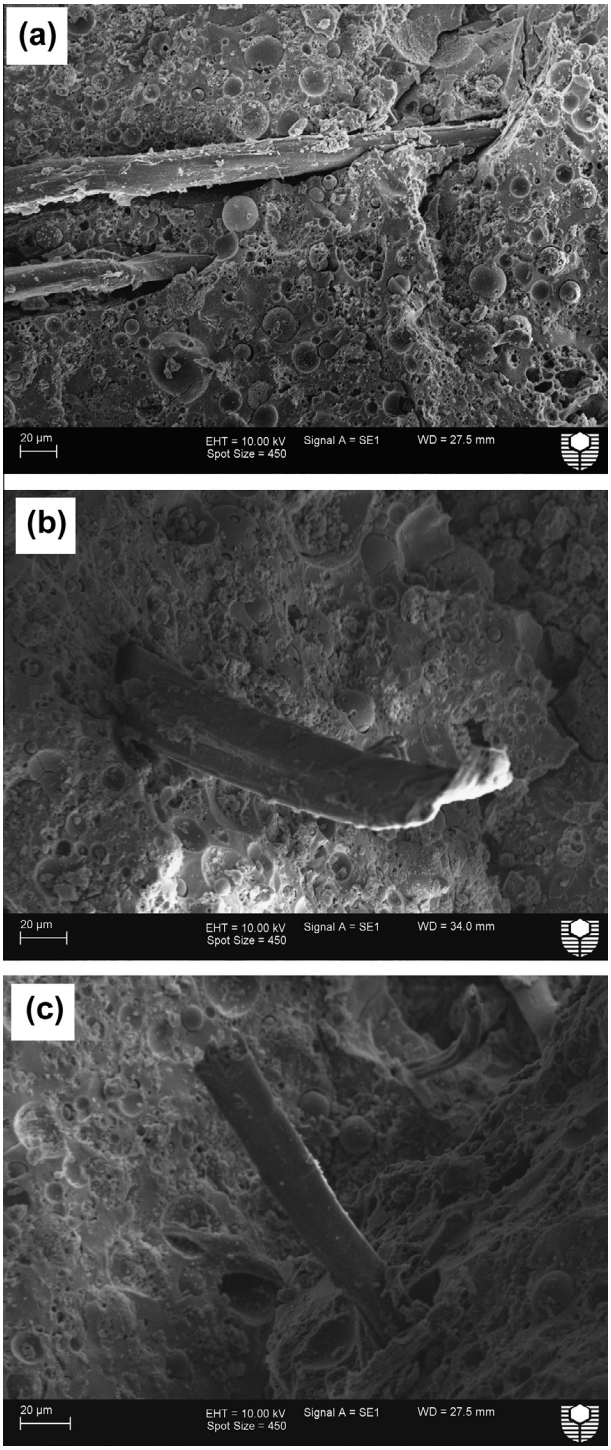

Fig. 11. SEM images showing the fracture surfaces of FF-reinforced samples; (a) GP/FF, (b) GPDNS-1/FF, and (c) GPWNS/FF-2.

4. Conclusions

Geopolymer-nanosilica composites have been synthesized using two different mixing methods, and characterized in terms of microstructural, physical and mechanical properties. Results of QXDA indicate that NS particles increased the amorphous content and supported the geopolymeric reaction in both preparation methods at different percent, and the QEDS technique revealed that the mixing method affected the Si/Al ratio of the nanocomposites. It has been shown that samples produced through the dry-mix approach displayed superior physical and mechanical properties when compared to the wet-mix samples. The dry-mix geopolymer nanocomposite containing 1.0 wt% NS reduced the porosity (by 27%) and water absorption (by 35%) and increased the density (by 15%), compressive strength (by 27%) and flexural strength (by 28.8%). However, the addition of NS beyond 1.0 and 2.0 wt% in the dry and wet-mix, respectively, affected the physical and mechanical properties adversely. This improvement has been clearly recognized in the flexural toughness test of FF-reinforced geopolymer nanocomposites. The higher amount of geopolymer gel and the enhanced density in geopolymer nanocomposites increased the adhesion bond between FF and the nanomatrices, resulting in higher toughness results.

Acknowledgments

The authors would like to thank Ms. E. Miller from the Department of Applied Physics at Curtin University for the assistance with SEM and QEDS techniques. We also thank Miss Kelly Merigot of the John de Laeter Centre of Excellence in Mass Spectrometry for assistance with sample preparation for QEDS.

References

[1] J. Davidovits, Geopolymers – inorganic polymeric new materials, J. Therm. Anal. 37 (8) (1991) 1633–1656.
[2] M. Rowles, B. O'Connor, Chemical optimisation of the compressive strength of aluminosilicate geopolymers synthesised by sodium silicate activation of metakaolinite, J. Mater. Chem. 13 (5) (2003) 1161–1165.
[3] R.P. Williams, R.D. Hart, A. van Riessen, Quantification of the extent of reaction of metakaolin-based geopolymers using X-ray diffraction, scanning electron microscopy, and energy-dispersive spectroscopy, J. Am. Ceram. Soc. 94 (8) (2011) 2663–2670.
[4] P. Duxson, S.W. Mallicoat, G.C. Lukey, W.M. Kriven, J.S.J. van Deventer, The effect of alkali and Si/Al ratio on the development of mechanical properties of metakaolin-based geopolymers, Colloids Surf. A 292 (1) (2007) 8–20.
[5] A. Fernandez-Jimenez, A. Palomo, Composition and microstructure of alkali activated fly ash binder: effect of the activator, Cem. Concr. Res. 35 (10) (2005) 1984–1992.
[6] W.D.A. Rickard, R. Williams, J. Temuujin, A. van Riessen, Assessing the suitability of three Australian fly ashes as an aluminosilicate source for geopolymers in high temperature applications, Mater. Sci. Eng., A 528 (9) (2011) 3390–3397.
[7] H. Assaedi, F.U.A. Shaikh, I.M. Low, Effect of nano-clay on mechanical and thermal properties of geopolymer, J. Asian Cer. Soc. (2015).
[8] T. Phoo-ngernkham, P. Chindaprasirt, V. Sata, S. Hanjitsuwan, S. Hatanaka, The effect of adding nano-SiO_2 and nano-Al_2O_3 on properties of high calcium fly ash geopolymer cured at ambient temperature, Mater. Des. 55 (2014) 58–65.
[9] A. Nazari, J.G. Sanjayan, Hybrid effects of alumina and silica nanoparticles on water absorption of geopolymers: application of Taguchi approach, Measurement 60 (2015) 240–246.
[10] M. Saafi, K. Andrew, P.L. Tang, D. McGhon, S. Taylor, M. Rahman, et al., Multifunctional properties of carbon nanotube/fly ash geopolymeric nanocomposites, Constr. Build. Mater. 49 (2013) 46–55.
[11] A. Hakamy, F.U.A. Shaikh, I.M. Low, Thermal and mechanical properties of hemp fabric-reinforced nanoclay–cement nanocomposites, J. Mater. Sci. 49 (4) (2013) 1684–1694.
[12] D. Wei, R. Dave, R. Pfeffer, Mixing and characterization of nanosized powders: an assessment of different techniques, J. Nanopart. Res. 4 (1) (2002) 21–41.
[13] M. Alzeer, K. MacKenzie, Synthesis and mechanical properties of novel composites of inorganic polymers (geopolymers) with unidirectional natural flax fibres (phormium tenax), Appl. Clay Sci. 75–76 (2013) 148–152.
[14] M. Alzeer, K.J.D. MacKenzie, Synthesis and mechanical properties of new fibre-reinforced composites of inorganic polymers with natural wool fibres, J. Mater. Sci. 47 (19) (2012) 6958–6965.
[15] T. Alomayri, F.U.A. Shaikh, I.M. Low, Synthesis and mechanical properties of cotton fabric reinforced geopolymer composites, Compos. B Eng. 60 (2014) 36–42.
[16] H. Assaedi, T. Alomayri, F.U.A. Shaikh, I.-M. Low, Characterisation of mechanical and thermal properties in flax fabric reinforced geopolymer composites, J. Adv. Ceram. 4 (4) (2015) 272–281.
[17] C. Baley, Analysis of the flax fibres tensile behaviour and analysis of the tensile stiffness increase, Compos. A 33 (2002) 939–948.
[18] N.W. Chen-tan, A. Van Riessen, C.V. Ly, D.C. Southam, Determining the reactivity of a fly ash for production of geopolymer, J. Am. Ceram. Soc. 92 (4) (2009) 881–887.
[19] Standard Test Methods for Apparent Porosity, Water Absorption, Apparent Specific Gravity, and Bulk Density of Burned Refractory Brick and Shapes by Boiling Water1. 2010.
[20] ASTM, Standard Test Methods for Flexural Properties of Unreinforced and Reinforced Plastics and Electrical Insulating Materials, 2010.
[21] ASTM, Standard Test Method for Compressive Strength of Hydraulic Cement Mortars (Using 2-in. or [50-mm] Cube Specimens), 2013.
[22] ASTM, Standard Test Method for Flexural Toughness and First-Crack Strength of Fiber-Reinforced Concrete (Using Beam With Third-Point Loading), 1998.
[23] W.D.A. Rickard, C.S. Kealley, A. van Riessen, J. Biernaki, Thermally induced microstructural changes in fly ash geopolymers: experimental results and proposed model, J. Am. Ceram. Soc. 98 (3) (2015) 929–939.
[24] E. ul Haq, S. Kunjalukkal Padmanabhan, A. Licciulli, Synthesis and characteristics of fly ash and bottom ash based geopolymers–A comparative study, Ceram. Int. 40 (2) (2014) 2965–2971.
[25] Y. Jun, J. Oh, Use of gypsum as a preventive measure for strength deterioration during curing in class F fly ash geopolymer system, Materials 8 (6) (2015) 3053–3067.
[26] C. Ferone, F. Colangelo, G. Roviello, D. Asprone, C. Menna, A. Balsamo, et al., Application-oriented chemical optimization of a metakaolin based geopolymer, Materials 6 (5) (2013) 1920–1939.
[27] B.-W. Jo, C.-H. Kim, G.-H. Tae, J.-B. Park, Characteristics of cement mortar with nano-SiO_2 particles, Constr. Build. Mater. 21 (6) (2007) 1351–1355.
[28] S.W.M. Supit, F.U.A. Shaikh, Durability properties of high volume fly ash concrete containing nano-silica, Mater. Struct. 48 (8) (2014) 2431–2445.
[29] L. Senff, D.M. Tobaldi, S. Lucas, D. Hotza, V.M. Ferreira, J.A. Labrincha, Formulation of mortars with nano-SiO_2 and nano-TiO_2 for degradation of pollutants in buildings, Compos. B Eng. 44 (1) (2013) 40–47.
[30] Y. Qing, Z. Zenan, K. Deyu, C. Rongshen, Influence of nano-SiO_2 addition on properties of hardened cement paste as compared with silica fume, Constr. Build. Mater. 21 (3) (2007) 539–545.
[31] P. Hosseini, R. Hosseinpourpia, A. Pajum, M.M. Khodavirdi, H. Izadi, A. Vaezi, Effect of nano-particles and aminosilane interaction on the performances of cement-based composites: an experimental study, Constr. Build. Mater. 66 (2014) 113–124.
[32] A. Naji Givi, S. Abdul Rashid, F.N.A. Aziz, M.A.M. Salleh, Experimental investigation of the size effects of SiO_2 nano-particles on the mechanical properties of binary blended concrete, Compos. B Eng. 41 (8) (2010) 673–677.
[33] A. Hakamy, F.U.A. Shaikh, I.M. Low, Thermal and mechanical properties of hemp fabric-reinforced nanoclay–cement nanocomposites, J. Mater. Sci. (2013).

3.5 Effect of nanoclay on durability and mechanical properties of flax fabric reinforced geopolymer composites

Assaedi, H., Shaikh, F.U.A. and Low, I.M., 2017. Effect of nanoclay on durability and mechanical properties of flax fabric reinforced geopolymer composites. *Journal of Asian Ceramic Societies*, *5(1)*, pp.62-70.

Journal of Asian Ceramic Societies 5 (2017) 62–70

Contents lists available at ScienceDirect

Journal of Asian Ceramic Societies

journal homepage: www.elsevier.com/locate/jascer

Full Length Article

Effect of nanoclay on durability and mechanical properties of flax fabric reinforced geopolymer composites

H. Assaedi[a,b], F.U.A. Shaikh[c], I.M. Low[a,*]

[a] Department of Imaging & Applied Physics, Curtin University, GPO Box U1987, Perth, WA 6845, Australia
[b] Department of Physics, Umm Al-Qura University, P.O. Box 715, Makkah, Saudi Arabia
[c] Department of Civil Engineering, Curtin University, GPO Box U1987, Perth, WA 6845, Australia

ARTICLE INFO

Article history:
Received 12 August 2016
Received in revised form
15 November 2016
Accepted 10 January 2017
Available online 13 February 2017

Keywords:
Geopolymer
Nanoclay
Mechanical properties
Flax fibres
Durability

ABSTRACT

The main concern of using natural fibres as reinforcement in geopolymer composites is the durability of the fibres. Geopolymers are alkaline in nature because of the alkaline solution that is required for activating the geopolymer reaction. The alkalinity of the matrix, however, is the key reason of the degradation of natural fibres. The purpose of this study is to determine the effect of nanoclay (NC) loading on the mechanical properties and durability of flax fabric (FF) reinforced geopolymer composites. The durability of composites after 4 and 32 weeks at ambient temperature is presented. The microstructure of geopolymer matrices was investigated using X-ray diffraction (XRD), Fourier transform infrared spectroscopy (FTIR) and scanning electron microscopy (SEM). The results showed that the incorporation of NC has a positive impact on the physical properties, mechanical performance, and durability of FF reinforced geopolymer composites. The presence of NC has a positive impact through accelerating the geopolymerization, reducing the alkalinity of the system and increasing the geopolymer gel.

1. Introduction

Ordinary Portland Cement (OPC) is believed to be responsible of generating 5% of the global carbon dioxide emission [1]. One of the most attractive alternatives of OPC is geopolymer binder due to its comparable mechanical properties to the OPC. The development of geopolymer concrete is not only important because they are environmental friendly materials, but also due to their wide range of raw waste materials to produce worthy construction matrices, resulting in low cost material with similar mechanical properties to that of cement concrete [2]. Geopolymers are produced by activating a solid aluminosilicate source such as coal derived fly-ash, meta-kaolin and slag with alkaline solutions, amorphous networks of tetrahedral SiO_4 and AlO_4 connected by sharing oxygen atoms [3]. The formation of geopolymer gel can be described by Eq. (1) [3].

$$n(Si_2O_5, Al_2O_2) + 2nSiO_2 + 4nH_2O + NaOH \rightarrow Na^+ + n(OH)_3 - Si - O - \underset{\underset{(OH)_2}{|}}{Al^-} - O - Si - (OH)_3 \quad (1)$$

Hitherto, nanomaterials have received increased attention in geopolymer and cement research; especially in producing nanocomposites that possess superior mechanical properties [4–6]. Several kinds of nanomaterials have been incorporated efficiently in geopolymer pastes. For instance, it has been found that nano-silica and nano-alumina particles have the ability to reduce the porosity and water absorption of geopolymer matrices [6]. In another study [7], nano-alumina and nano-silica particles have been incorporated in geopolymer matrices giving them higher mechanical performance. The nanoparticles are not only acting as fillers, but also enhancing the geopolymeric reaction. A further study on the effect of adding carbon nanotubes (CNT) to flyash-based geopolymer has shown an increase in the mechanical and electrical properties of geopolymer nano-composites when compared to the control paste [8]. Wei and Meyer reported the properties of cement/nanoclay composites, where the nanoparticles reduce the porosity of cement matrices, as well as improve the strength of cement matrix through pozzolanic reactions [9].

* Corresponding author. Fax: +61 8 9266 2377.
E-mail address: j.low@curtin.edu.au (I.M. Low).

http://dx.doi.org/10.1016/j.jascer.2017.01.003

Farzadnia et al. [10] reported that incorporation of 3 wt% halloysite nanoclay into cement mortars increased the compressive strength by up to 24% compared to the control sample. In a previous study, we investigated the effect of nanoclay (Cloisite 30B) on the mechanical and thermal properties of geopolymer composites [11]. Nanoclay particles were found to help developing denser geopolymer matrices, thereby producing geopolymer with superior mechanical performance.

Despite the potential improvement of properties of geopolymers, the geopolymer matrix still suffers from brittle failure readily under applied force and generally exhibits low mechanical strength [12,13]. One way to resolve this limitation is through utilizing natural fibres to fabricate fibre-reinforced geopolymer composites. The advantages of using natural fibres in composites include the low density, flexibility and the high specific modulus [14,15]. Cotton fibres and fabrics have been used to improve the fracture toughness and mechanical performance of geopolymer composites [16,17]. Also, flax and wool fibres have presented positive effects when incorporated in geopolymer matrices; they significantly improved the mechanical properties of the natural fibre reinforced geopolymer composites [1,18]. In our previous work, geopolymer composites were reinforced with woven flax fabric and tested for mechanical properties such as flexural strength, flexural modulus, compressive strength, hardness, and fracture toughness. The results showed that all mechanical properties were improved by increasing the flax fibre contents, and showed superior mechanical properties over the pure geopolymer matrix [19]. In a further study, geopolymer matrices were reinforced with a combination of nanoclay (NC) and flax fabrics (FF) and it was found that the addition of NC to geopolymers improved the adhesion between the natural fibres and the matrices due to the high amount of geopolymer gel formed, resulting in higher mechanical results [20].

However, there are concerns in utilizing natural fibres in alkali-based matrices. The main concern is regarding the long-term durability of natural fibre reinforced composites. Natural fibres can be degraded and damaged in high-alkaline environment; thereby adversely affecting the mechanical properties and durability of the composites [21–23]. Natural fibre degradations in alkaline environments was studied by Gram [24] and he described the degradation mechanism as the decomposition of hemicellulose and linen which leads to the splitting of natural fibres into micro-fibrils [24]. This effect has been observed using SEM in the case of jute fibres in cement matrix, where the natural fibres split-up and fibrillised resulting in reduction in the tensile strength of jute fibres by 76% [25]. To reduce the degradation impact, nanoparticles can play an important role. The effect of nanoclay particles on the durability of flax fibres reinforced cement composites at 28 days and after 50 wet/dry cycles has been investigated by Aly et al. [21]. Samples loaded with 2.5 wt% nanoclay particles showed lower deterioration in the flexural strength when compared to its counterpart control samples. This was attributed to the effect of nanoparticles in reducing the degradation of flax fibres.

According to the best of knowledge of authors, no study has been reported on the durability of natural fibres in geopolymer matrices. The presence of nanoclay particles is anticipated to reduce the degradation of natural fibres by consuming certain amounts of alkaline solution, which reduces the alkalinity of the medium. Nanoclay is also expected to produce higher amount of geopolymer gel, increases in matrix density, fibre-matrix adhesion, and the concomitant improvement in mechanical properties. In this paper, in order to improve the durability and reduce the degradation of flax fabric (FF) in geopolymer composites, geopolymer matrices were modified by the addition of nanoclay (NC) particles. This study presented the effect of different loadings of nanoparticles on the durability and mechanical properties of FF-reinforced geopolymer nanocomposites. The medium to long term durability of all samples has been discussed in terms of flexural strength obtained at 4 and 32 weeks. The microstructure was investigated using X-ray diffraction, Fourier transform infrared spectroscopy (FTIR) and scanning electron microscopy (SEM).

Table 1
Formulation of samples. Each samples is a mix of: 1.0 kg Eraring flyash, 214.5 g sodium hydroxide (8 M) and 535.5 g sodium silicate.

Sample	NC (g)	FF (layers)
GP	0	0
GPNC-1	10	0
GPNC-2	20	0
GPNC-3	30	0
GP/FF	0	10
GPNC-1/FF	10	10
GPNC-2/FF	20	10
GPNC-3/FF	30	10

2. Experimental procedure

2.1. Materials

Low-calcium flyash (ASTM class F) with specific gravity 2.1 obtained from the Eraring power station in NSW was used to prepare the geopolymeric nano-composites. The alkaline activator for geopolymerisation was a combination of sodium hydroxide solution and sodium silicate grade D solution. Sodium hydroxide flakes with 98% purity were used to prepare the solution. The chemical composition of sodium silicate used was 14.7% Na_2O, 29.4% SiO_2 and 55.9% water by mass.

Flax fabric (FF) and nanoclay (Cloisite 30B) were used for the reinforcement of geopolymer composites. The fabric, supplied by Pure Linen Australia, is made up of yarns with a density of 1.5 g/cm^2. The nanoclay (NC) with specific gravity of 1.98 has been provided by Southern Clay Products, USA.

To prepare the geopolymer pastes, an alkaline solution to fly ash ratio of 0.75 was used and the ratio of sodium silicate solution to sodium hydroxide solution was fixed at 2.5. The concentration of sodium hydroxide solution was 8 M, which was prepared and combined with the sodium silicate solution one day before mixing.

2.2. Preparation of geopolymer nanocomposites

The nano-clay particles (NC) were added to the flyash at the loadings of 1.0, 2.0 and 3.0% by weight. The flyash and nanoparticles were first dry mixed for 5 min in a covered mixer at low speed and then mixed for another 10 min at high speed until homogeneity was achieved. The alkaline solution was then added slowly to the flyash/nanoparticles mixture in a Hobart mixer at a low speed until the mixture became homogeneous, followed by further mixing for another 10 min on high speed. The resultant mixture was then poured into wooden moulds. The wooden moulds were then placed on a vibration table for 2 min before they were covered with a plastic film and cured at 80°C for 24 h in an oven before demolding.

2.3. Preparation of FF-composite and nanocomposites

Similar mixtures were prepared to produce the FF-nanocomposites. Four samples of geopolymer pastes reinforced with ten layers of FF (see Table 1) were prepared by spreading a thin layer of the paste in a well-greased wooden mould and carefully placing the first layers of FF on it. The fabric was fully saturated with the paste by a roller, and the process repeated for ten layers; each specimen contained a different weight percentage of nanoclay particles. The samples were then left under heavy weight (20 kg) for 1 h to reduce entrapped air inside the samples.

All samples were covered with plastic film and cured at 80°C for 24 h in an oven before demoulding. They were then dried under ambient conditions for 28 days.

All samples were then categorized in two series. In the first series, samples were cured under ambient conditions to be tested after 4 weeks, and the samples of second series were stored in the same condition for 32 weeks. The formulation of samples is given in Table 1.

2.4. Characterization

The samples were crushed and ground to fine powder. They were then measured on a D8 Advance Diffractometer (Bruker-AXS, Germany) using copper radiation and a LynxEye position sensitive detector. The diffractometer were scanned from 7.5° to 60° using a scanning rate of 0.5°/min. XRD patterns were obtained by using Cu k_α lines (k = 1.5406 Å). Crystalline phases were identified using software EVA version 11. The chemical compositions of NC were analyzed using X-ray fluorescence (XRF). XRF was outsourced to a commercial laboratory (Bureau Veritas, Perth). An FTIR scan was performed on a Perkin Elmer Spectrum 100 FTIR spectrometer in the range of 4000–500 cm^{-1} at room temperature. The spectrum was an average of 32 scans at a resolution of 2 cm^{-1}, corrected for background. The microstructures of geopolymer composites were examined using Zeiss Neon focused ion beam scanning electron microscope (FIB-SEM). The specimens were mounted on aluminium stubs using carbon tape and then coated with a thin layer of platinum to prevent charging before observation.

2.5. Physical and mechanical properties

Measurements of bulk density and porosity were conducted to define the quality of geopolymer nanocomposite. Density of samples (ρ) with volume (V) and dry mass (m_d)was calculated using Eq. (2):

$$\rho = \frac{m_d}{V} \tag{2}$$

The value of apparent porosity (P_a) was determined using Archimedes' principle in accordance with the ASTM Standard (C-20) [26]. Pure geopolymer and nano-composite samples were immersed in clean water, and the apparent porosity (P_a) was calculated using Eq. (3):

$$P_a = \frac{m_a - m_d}{m_a - m_w} \times 100 \tag{3}$$

where m_a is mass of the saturated samples in air, and m_w is mass of the saturated samples in water.

A LLOYD Material Testing Machine (50 kN capacity) with a displacement rate of 0.5 mm/min was used to perform the mechanical tests. Rectangular bars of 60 × 18 × 15 mm^3 were cut from the fully cured samples for three-point bend test with a span of 40 mm to evaluate the flexural strength and modulus. Five samples of each group were used to evaluate the flexural strength and flexural modulus of geopolymer composites. The values were recorded and analyzed with the machine software (NEXYGENPlus) and average values were calculated. The flexural strength (σ_F) was determined using the equation [27]:

$$\sigma_F = \frac{3}{2}\frac{P_m S}{WD^2} \tag{4}$$

where P_m is the maximum load, S is the span of the sample, D is the specimen width, and W is the specimen thickness.

Table 2
Density and porosity for pure geopolymer and geopolymer nano-composites.

Sample	Density (g/cm^3)	Porosity (%)
GP	1.84 ± 0.02	22.2 ± 0.4
GPNC-1	1.92 ± 0.02	21.3 ± 0.3
GPNC-2	2.05 ± 0.02	20.6 ± 0.3
GPNC-3	1.98 ± 0.03	21.0 ± 0.2

Values of flexural modulus (E_f) were computed using the initial slope of the load displacement curve ($\Delta P/\Delta X$) using the equation [27]:

$$E_F = \frac{S^3}{4WD^3}\left(\frac{\Delta P}{\Delta X}\right) \tag{5}$$

3. Results and discussion

3.1. Density and porosity

The results of porosity and water absorption of geopolymer paste and geopolymer nano-composites are shown in Table 2. Geopolymer nanocomposites revealed denser matrices and lower porosities when compared to the control sample. The addition of NC has increased the density and reduced the porosity of geopolymer nano-composites when compared to control geopolymer paste. The optimum addition was found as 2.0 wt% of NC, which increased density by 11.4% and reduced the porosity by 7.2% when compared to the control paste. This implies that the nanoparticles played a pore-filling role to reduce the porosity of geopolymer composites. However, adding excessive amounts of NC increased the porosity and decreased the density of all samples due to agglomeration of NC particles [11]. This finding is comparable with the study where the porosity of cement paste is decreased due to addition of 1.0% wt. of NC to cement paste; however, the porosity is increased because of the agglomeration effect when more nanoparticles were added [28].

3.2. X-ray fluorescence (XRF) and X-ray diffraction (XRD)

The chemical composition and loss on ignition of flyash and NC are shown in Table 3. Flyash and NC contain, in addition to silica and alumina, Fe_2O_3, CaO, K_2O, Na_2O, MgO and TiO_2.

The XRD spectra of pure geopolymer and geopolymer nanocomposites at 4 and 32 weeks are shown in Fig. 1(a–b) , respectively. The crystalline phases were indexed using powder diffraction files (PDFs) from the inorganic crystal structure database (ICSD). The diffraction patterns of the samples demonstrate some crystalline phases that were indexed distinctly: quartz [SiO_2] (PDF 00-046-1045) and mullite [$Al_{2.32}Si_{0.68}O_{4.84}$] (PDF 04-016-1588). Quartz and mullite crystalline phases can be seen in all samples. According to Rickard et al. quartz and mullite are the main crystalline content of the Eraring flyash, and hence they are stable and unreactive in the alkaline environment. At 32 weeks, a new crystalline phase, trona [$Na_3H(Co_3)_2.2H_2O$] (PDF 00-029-1447), appears on the surface of geopolymer aged samples. Trona belongs to soda minerals group, which could be formed by the reaction of sodium hydroxide with water and carbon dioxide according to the chemical reaction [29]:

$$3NaOH + 2CO_2 + 2H_2O \rightarrow Na_3H(CO_3)_2 \cdot 2H_2O \tag{6}$$

The amorphous broad phase generated between 2θ = 17° and 30° for all samples reveals the reactivity of geopolymers. It is known that the amorphicity degree remarkably influences the mechanical properties of geopolymers. When the amorphous content is higher, the strength of geopolymers is similarly higher [30]. In previous study, it has been shown that the addition of nanoclay particles to geopolymer pastes increased the amorphous content of geopoly-

Table 3
Chemical compositions of flyash and nanoclay (wt%).

	SiO_2	Al_2O_3	CaO	Fe_2O_3	K_2O	MgO	Na_2O	P_2O_5	SO_3	TiO_2	MnO	BaO	LOI
Flyash	63.13	24.88	2.58	3.07	2.01	0.61	0.71	0.17	0.18	0.96	0.05	0.07	1.45
NC	47.05	16.24	0.29	3.42	0.03	1.75	0.19	0.01	0.11	0.08	0.00	0.00	30.61

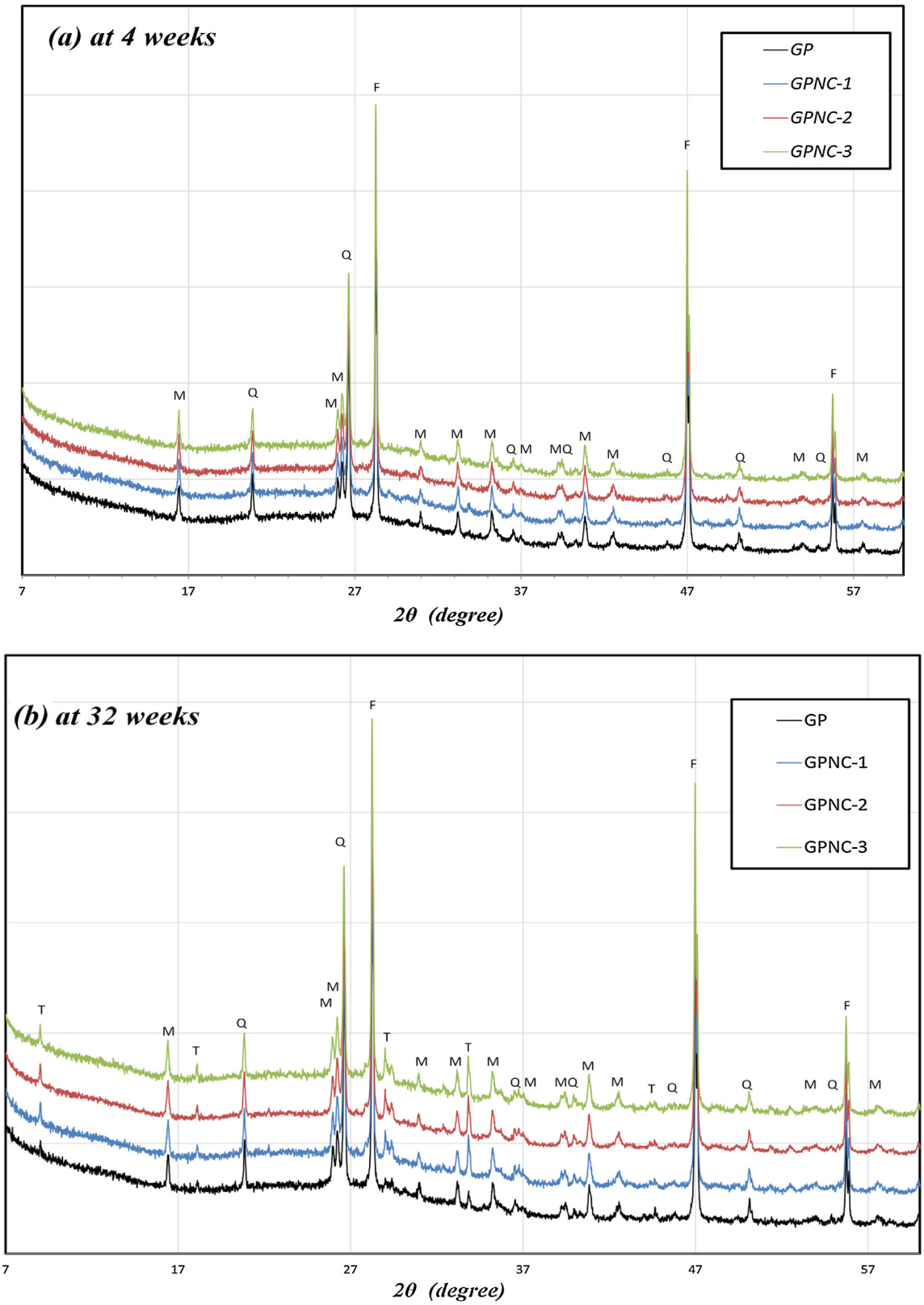

Fig. 1. X-ray diffraction patterns of geopolymer and geopolymer nanocomposites at: (a) 4 weeks; (b) 32 weeks [legend: M = mullite, Q = quartz and T = trona].

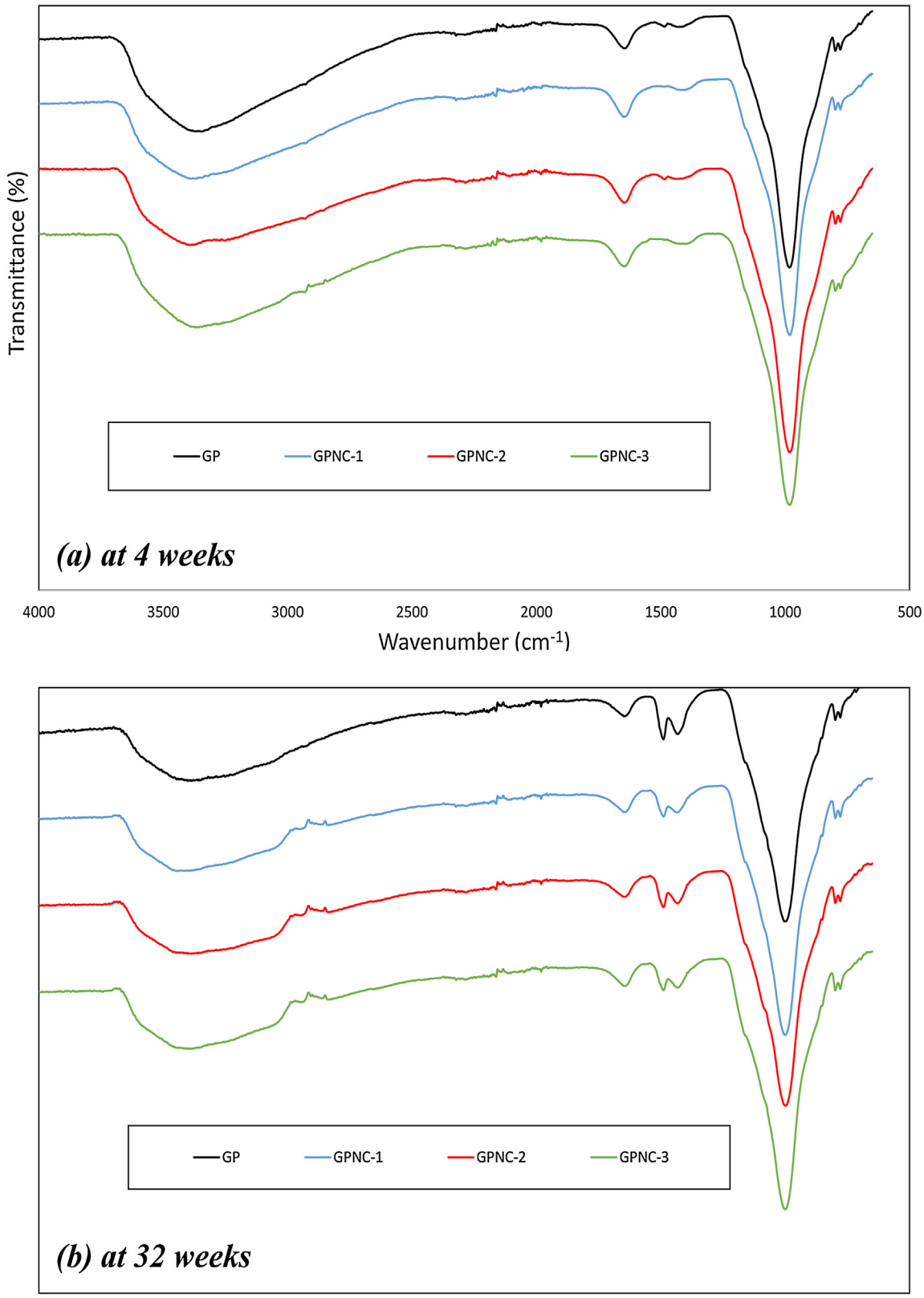

Fig. 2. FTIR spectra of geopolymer and geopolymer nanocomposites at: (a) 4 weeks; (b) 32 weeks.

mer nanocomposites, resulting in denser matrices and superior mechanical performance [11].

3.3. *FTIR observation*

FTIR spectra of pure geopolymer and geopolymer nanocomposite at 4 and 32 weeks are shown in Fig. 2(a–b) . The FTIR spectra of

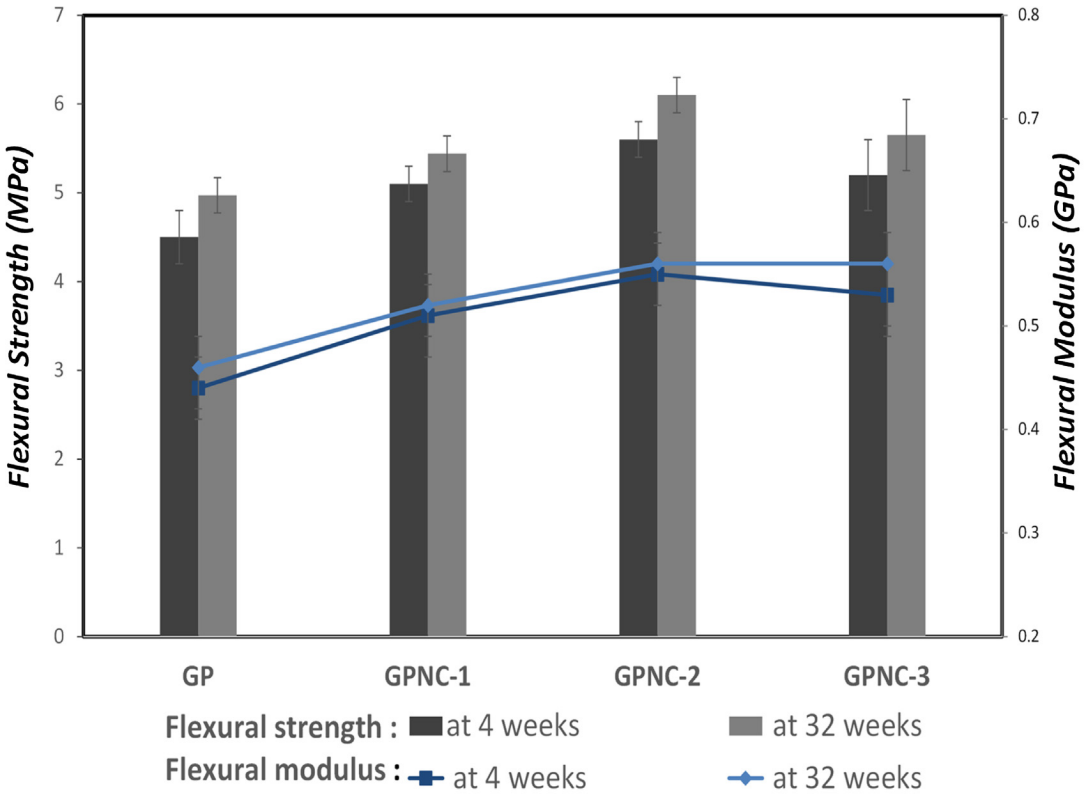

Fig. 3. Flexural strength and modulus of geopolymer and nanocomposites at 4 and 32 weeks.

all samples shows a strong peak at ~1000 cm^{-1} which is attributed to Si—O—Si and Al—O—Si asymmetric stretching vibrations, which is the identification peak of the geopolymerisation [31,32]. A broad peak in the region around 3400 cm^{-1} indicates that the OH group is present attached to different centres (Al, Si) and free water [33,34]. The absorbance peak at 1640 cm^{-1} is also attributed to the (OH) bending vibration [35]. At 32 weeks changes have occurred, two peaks at 1420 and 1480 cm^{-1} appear indicating the presence of sodium carbonate; this was formed due to the atmospheric carbonation on the matrices surfaces which confirms the XRD results [29]. During the ageing period the reaction has carried on at a low rate consuming more OH groups and forming stronger material. The water content decreased to some equilibrium level during this period resulting in lower broad peak at 3400 cm^{-1}.

3.4. Flexural strength of geopolymer nanocomposites

The effect of ageing on the flexural strength and modulus of geopolymer matrices and nanocomposites is shown in Fig. 3. Overall, the incorporation of nanoclay into the geopolymer composite led to noteworthy improvement in the mechanical strength at all ages. At 4 weeks, the flexural strength of geopolymer nanocomposite containing 1.0, 2.0 and 3.0 wt.% NC was increased by 13.3, 24.4 and 15.5% respectively, while the flexural modulus improved by 16, 25 and 20%, respectively compared to the control sample. This enhancement noticeably shows the value of NC in supporting geopolymer reaction and filling the micro pores in the matrix [11–28]. Thus the microstructure of geopolymer nanocomposite is denser than the pure matrix, especially in the case of incorporating 2.0 wt.% NC, which is evident from its higher flexural strength and modulus. However, at 32 weeks, the flexural strength of nanocomposites increased slightly compared to their values at 4 weeks. For instance, the flexural strength of GPNC-2 nanocomposite improved from 5.6 to 6.1 MPa by about 9% increase. This slight improvement in the mechanical performance could be attributed to the slow reaction of free silica and alumina in the presence of Na^+ ions during the ageing period [36,37]. In similar study, Hakamy et al. [23] reported that flexural strength of cement pastes containing 1.0% calcined nanoclay particles improved from 7.2 to 8.2 by about 7% after 236 days compared to its strength at 56 days. SEM images of the microstructure at 32 weeks of geopolymer paste and the geopolymer nanocomposite containing 2.0 wt.% NC are shown in Fig. 4(a–b) . For geopolymer matrix, Fig. 4a displays more pores showing a weak microstructure. On the other hand, Fig. 4b shows the SEM micrograph of GPNC-2 nanocomposite matrix, which is different from that of pure matrix, the microstructure is denser and more compact with fewer pores and more geopolymer gel.

3.5. Flexural strength of flax fabric reinforced geopolymer nanocomposites

The effect of ageing on the flexural strength and modulus of FF-reinforced geopolymer nanocomposites at 4 and 32 weeks is shown in Fig. 5. The incorporation of nanoclay into matrices led to enhancement in the flexural strength of all reinforced nanocomposites. For example, at 4 weeks, the flexural strength and modulus of GPNC-2/FF increased by 32.4% and 5.2%, respectively when compared to GP/FF composite. However, all composite showed reduction in the mechanical strength after 32 weeks. Fig. 6(a–b) shows the effect of ageing on the load-midspan deflection behaviour of GP/FF composites and GPNC-3/FF nanocomposites. The “ductile” behaviour can be observed in both composites with and without NC, with higher load capacity (about 29% increases) in the composite containing NC. It was observed that ductile behaviour is adversely affected and bending stresses are reduced due to degradation process. This decrease was attributed to the lignin and hemicellulose deterioration of flax fibre in matrix by Na^+ ions attack and brittleness of the natural fibres due to the

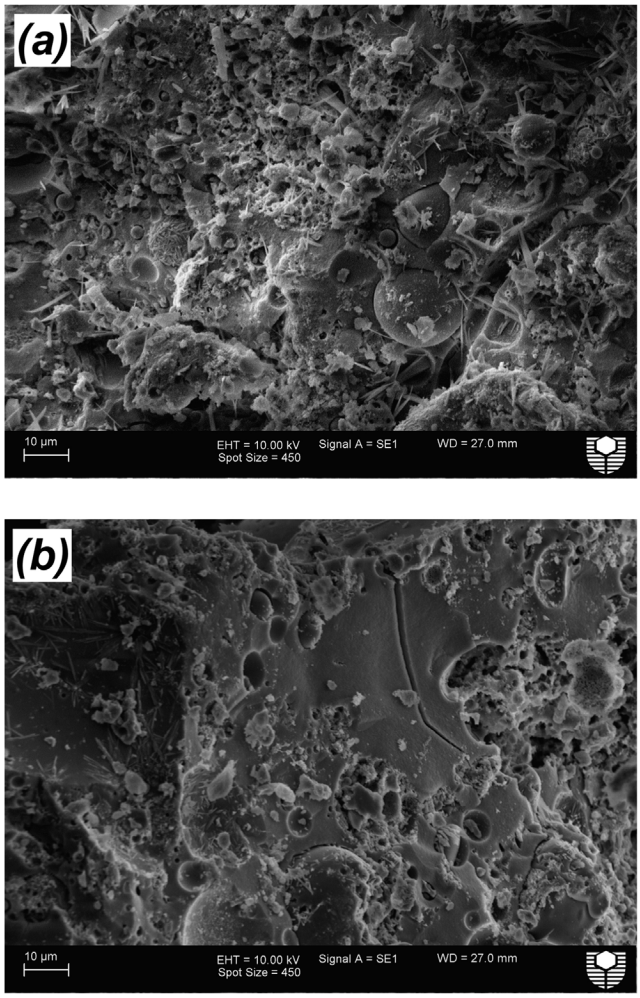

Fig. 4. SEM micrographs at 32 weeks of: (a) geopolymer paste, (b) nanocomposites containing 2.0 wt% NC.

mineralization of fibre cell wall in geopolymer pastes [38–40]. In general, all natural fibres suffer various degree of deterioration when exposed to alkaline environment [41]. This degradation in alkali matrices ultimately led to weaken the fibre–matrix bonding, and consequently reduced the mechanical performance of geopolymer composites. The flexural strength of GP/FF composite dropped to 23.0% of the initial strength at 4 weeks, whereas the flexural strength of GPNC-1/FF, GPNC-2/FF and GPNC-3/FF nanocomposites reduced by about 14.4%, 13.7% and 13.5% compared to its value at 4 weeks. Based on this outcome, it can be concluded that the reduction in the mechanical performance for nanocomposites was less than the reduction of control sample composite after 32 weeks ageing period. This may be attributed to the fact that nanoclay particles consume amounts of the alkaline solution thus reducing the alkalinity of the medium, and producing higher amount of geopolymer gel, which hence enhances the density of the matrices and the fibre–matrix adhesion [20]. In a similar study, the effect of calcined nanoclay on the durability of hemp fabric reinforced cement nanocomposites and the degradation of hemp fibres are reported [23], the nanoparticles were found to improve the durability and reduces the degradation of hemp fibres. In another investigation, Aly et al. [21] reported that the addition of nanoclay and waste glass to cement mortar could improve the durability and mitigate the degradation of flax fibres implemented in the composites by reducing the alkalinity of the matrix. Filho et al. [40] investigated the durability of sisal fibre reinforced mortar with the addition of metakaolin at 28 days and after 25 wet/dry cycles. They observed that the flexural strength of metakaolin composites decreased by 23% when compared to its control composites at 28 days. They reported that 50% metakaolin replacement significantly prevented the sisal fibres from the degradation in cement matrix. In the current investigation, the NC effectively prevented the flax fabric degradation by reducing the alkalinity of the matrix through geopolymer reaction. Thus, the degradation of flax fibres in nanocomposite was mostly reduced and the FF-nanocomposite matrix interfacial bonding was typically improved. Fig. 7(a–b) shows the changes in the fibres surface in GP/FF and GPNC-2/FF at 4 weeks. The fibres look more regular and free of any signs of degradation in both cases. After 32 weeks, however, the fibres extracted from control specimen (Fig. 7c) reveal signs of degradation and the fibrils are clearly splitting up, which influence the flexural strength of the composite, whereas the fibres extracted from GPNC-2/FF after ageing period (Fig. 7d) do not present signs of significant damage.

4. Conclusions

Geopolymer composites and nanocomposites reinforced with flax fabric (FF) and nanoclay (NC) have been fabricated and characterized. The effect of NC on the durability of FF reinforced geopolymer nanocomposites and the degradation of FF is reported. The optimum content of NC was 2.0 wt.%. After 32 weeks, the flexural strength of GP/FF composites decreased by 23.01% whereas flexural strength of GPNC-2/FF nanocomposites

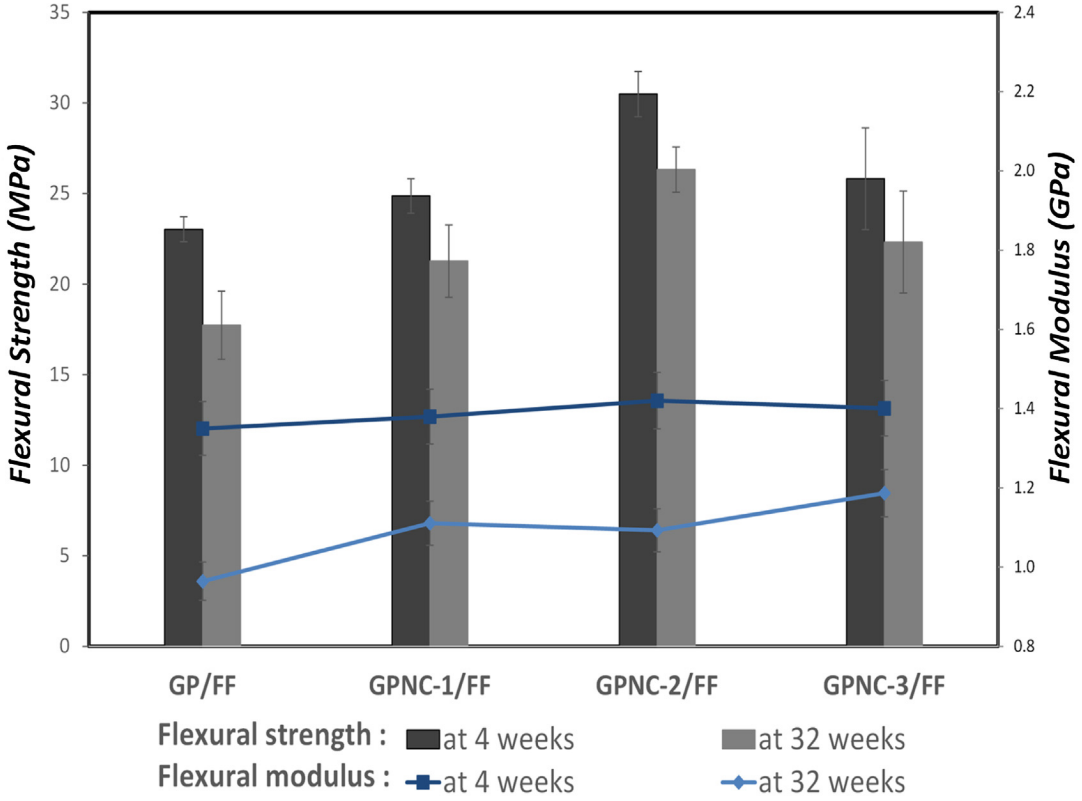

Fig. 5. Flexural strength and modulus of flax fabric reinforced geopolymer composites and nanocomposites at 4 and 32 weeks.

decreased by only 13.7%. SEM micrographs indicated that flax fibres in GP/FF composites suffer more degradation than that in GPNC-2/FF nanocomposites. Based on these observations, the addition of NC has great potential in improving the durability of flax fabric reinforced geopolymer nanocomposites during ageing.

Acknowledgement

The authors would like to thank Ms. E. Miller from the Department of Applied Physics at Curtin University for the assistance with SEM.

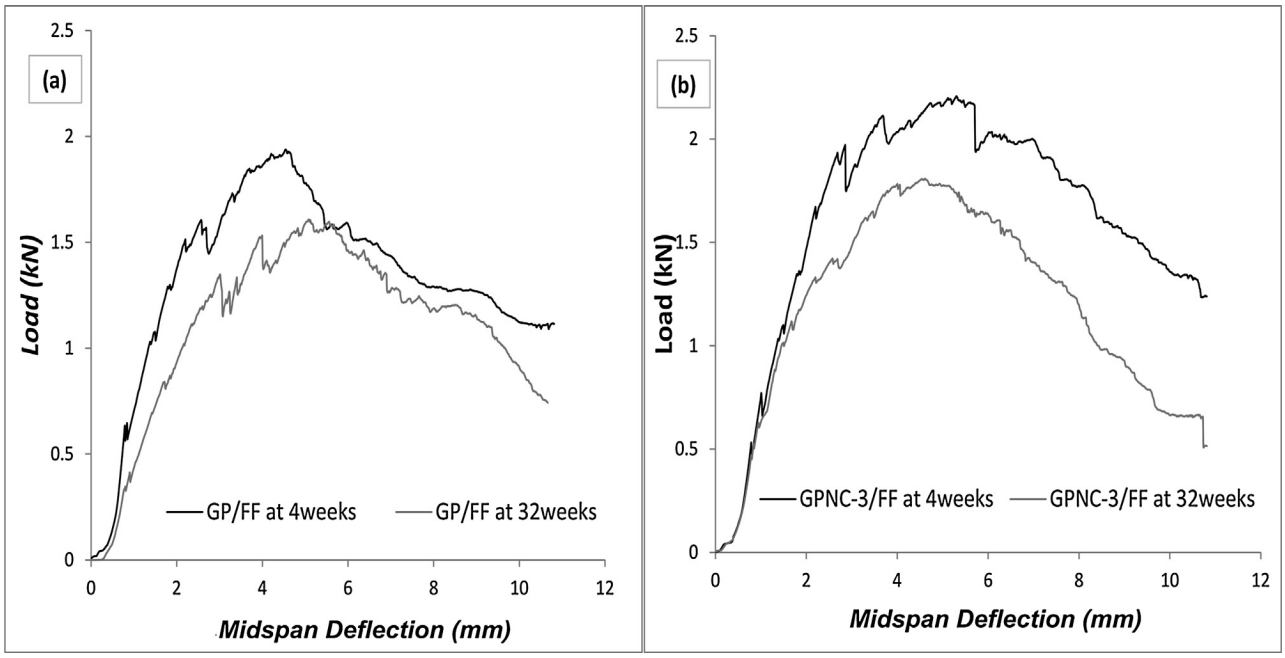

Fig. 6. Load versus mid-span deflection curves at 4 and 32 weeks for: (a) GP/FF composite; and (b) GPNC-3/FF nanocomposites.

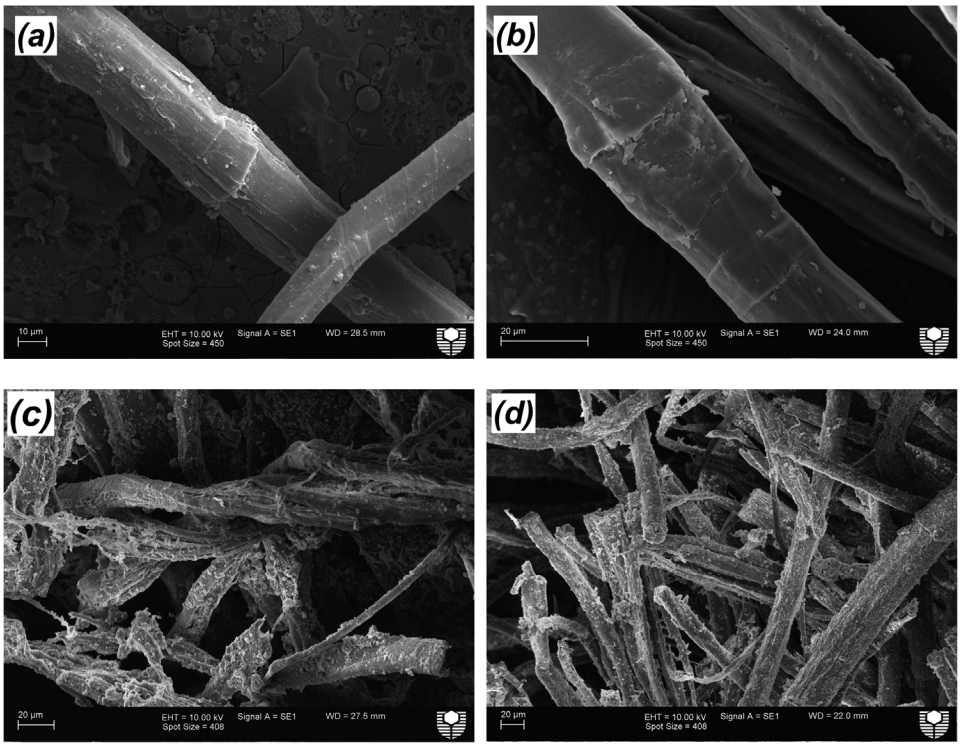

Fig. 7. SEM images of the flax fibres extracted from (a) GP/FF at 4 weeks, (b) GPNC-2/FF at 4 weeks (c) GP/FF at 32 weeks, and (d) GPNC-2/FF at 32 weeks.

References

[1] M. Alzeer and K. MacKenzie, Appl. Clay Sci., 75–76, 148–152 (2013).
[2] V. Zivica, M.T. Palou and T.I. Ľ. Bágel', Composites B, 57, 155–165 (2014).
[3] J. Davidovits, J. Therm. Anal., 37, (8) 1633–1656 (1991).
[4] Y. Qing, Z. Zenan, K. Deyu and C. Rongshen, Constr. Build. Mater., 21, (3) 539–545 (2007).
[5] F.U.A. Shaikh and S.W.M. Supit, Constr. Build. Mater., 70, 309–321 (2014).
[6] A. Nazari and J.G. Sanjayan, Measurement, 60, 240–246 (2015).
[7] T. Phoo-ngernkham, P. Chindaprasirt, V. Sata, S. Hanjitsuwan and S. Hatanaka, Mater. Des., 55, 58–65 (2014).
[8] M. Saafi, K. Andrew, P.L. Tang, D. McGhon, S. Taylor, M. Rahman, S. Yang and X. Zhou, Constr. Build. Mater., 49, 46–55 (2013).
[9] J. Wei and C. Meyer, J. Mater. Sci., 49, (21) 7604–7619 (2014).
[10] N. Farzadnia, A.A. Abang Ali, R. Demirboga and M.P. Anwar, Cem. Concr. Res., 48, 97–104 (2013).
[11] H. Assaedi, F.U.A. Shaikh and I.M. Low, J. Asian Ceram. Soc., 4, 19–28 (2016).
[12] T. Lin, D. Jia, P. He, M. Wang and D. Liang, Mater. Sci. Eng. A, 497, 181–185 (2008).
[13] T. Alomayri, F.U.A. Shaikh and I.M. Low, Composites B, 60, 36–42 (2014).
[14] P.J. Herrera-Franco and A. Valadez-González, Composites B, 36, 597–608 (2005).
[15] H. Bohlooli, A. Nazari, G. Khalaj, M.M. Kaykha and S. Riahi, Composites B, 43, 1293–1301 (2012).
[16] T. Alomayri, F.U.A. Shaikh and I.M. Low, Composites B, 50, 1–6 (2013).
[17] T. Alomayri, F.U.A. Shaikh and I.M. Low, J. Mater. Sci., 48, 6746–6752 (2013).
[18] M. Alzeer and K.D. MacKenzie, J. Mater. Sci., 47, 6958–6965 (2012).
[19] H. Assaedi, T. Alomayri, F.U.A. Shaikh and I.M. Low, J. Adv. Ceram., 4, 272–281 (2015).
[20] H. Assaedi, F.U.A. Shaikh and I.M. Low, Composites B, 95, 412–422 (2016).
[21] M. Aly, M.S.J. Hashmi, A.G. Olabi, M. Messeiry, A.I. Hussain and E.F. Abadir, J. Eng. Appl. Sci., 6, 19–28 (2011).
[22] L. Yan and N. Chouw, Constr. Build. Mater., 99, 118–127 (2015).
[23] A. Hakamy, F.U.A. Shaikh and I.M. Low, Mater. Des., 92, 659–666 (2016).
[24] H.E. Gram, Nordic Concr. Res., 5, 62–71 (1983).
[25] V. Velpari, B.E. Ramachandran, T.A. Bhaskaran, B.C. Pai and N. Balasubramanian, J. Mater. Sci., 15, 1579–1584 (1980).
[26] ASTM C-20, Standard Test Methods for Apparent Porosity, Water Absorption, Apparent Specific Gravity and Bulk Density of Burned Refractory Brick and Shapes by Boiling Water (2010).
[27] I.M. Low, M. McGrath, D. Lawrence, P. Schmidt, J. Lane, B.A. Latella and K.S. Sim, Composites A, 38, 963–974 (2007).
[28] A. Hakamy, F.U.A. Shaikh and I.M. Low, Composites B, 78, 174–184 (2015).
[29] D. Zaharaki, K. Komnitsas and V. Perdikatsis, J. Mater. Sci., 45, 2715–2724 (2010).
[30] T. Bakharev, Cem. Concr. Res., 36, 1134–1147 (2006).
[31] J.W. Phair and J.S.J. Van Deventer, Int. J. Miner. Process., 66, 121–143 (2002).
[32] Q. Li, H. Xu, F. Li, P. Li, L. Shen and J. Zhai, Fuel, 97, 366–372 (2012).
[33] P. Chindaprasirt, C. Jaturapitakkul, W. Chalee and U. Rattanasak, Waste Manage., 29, 539–543 (2009).
[34] U. Rattanasak and P. Chindaprasirt, Miner. Eng., 22, 1073–1078 (2009).
[35] E. ul Haq, S. Kunjalukkal Padmanabhan and A. Licciulli, Ceram. Int., 40, 2965–2971 (2014).
[36] Y.J. Zhang, Y.C. Wang, D.L. Xu and S. Li, Mater. Sci. Eng., 527, 6574–6580 (2010).
[37] M.M. Yadollahi, A. Benli and R. Demirboğa, Constr. Build. Mater., 94, 767–774 (2015).
[38] B.J. Mohr, J.J. Biernacki and K.E. Kurtis, Cem. Concr. Res., 37, 1531–1543 (2007).
[39] F. Pacheco-Torgal and S. Jalali, Constr. Build. Mater., 25, 575–581 (2011).
[40] J.D.A.M. Filho, F.D.A. Silva and R.D. Toledo Filho, Cem. Concr. Compos., 40, 30–39 (2013).
[41] A. Bentur and S. Mindess, Fibre Reinforced Cementitious Composites, 2nd ed., Taylor & Francis, London and New York (2007).

4 CONCLUSIONS AND FUTURE WORK

4.1 Flax fabric-reinforced geopolymer composites (section 3.1).

Geopolymer composites reinforced with different loadings of flax fabric (0 to 4.1 wt. %) were fabricated. The increase in flax fibre content in geopolymer composites was found to improve their mechanical properties. The flexural and compressive strength, flexural modulus, hardness and fracture toughness improved at a maximum fibre content of 4.1 wt. % (i.e., ten layers of flax fabrics). The flexural strength of the composites increased from 4.5 MPa in pure geopolymer to about 23 MPa (about 410% increase), and the compressive strength was found to increase from 19.4 in pure geopolymer to 91 MPa after the incorporation of FF. Slight improvements were also noticed on the flexural modulus and hardness of geopolymer composites as compared to the neat geopolymer.

The fracture toughness of composites was also improved after the addition of FF. For instance, while the fracture toughness of pure geopolymer was measured as 0.4 $MPa.m^{1/2}$, after the addition of 2.4, 3.0 and 4.1 wt.% FF, the fracture toughness was increased to 1.13, 1.5 and 1.8 $MPa.m^{1/2}$, respectively.

Regarding the thermal stability, composites exhibited a total weight loss of ~15% at 300 °C which indicates a degradation of FF inside the composite. A large amount of fibre degradation occurred at this temperature. The open pores within the geopolymer matrices allowed oxygen to diffuse in and cause degradation of the flax fibres at high temperatures. For that reason, it could be concluded that this composite system is only appropriate for service below 250 °C.

4.2 Nanoclay-geopolymer composites (section 3.2).

Nanoclay particles were added to reinforce the geopolymer at loadings of 1.0%, 2.0%, and 3.0% by weight. Results showed that the mechanical properties of all geopolymer nanocomposites were enhanced due to the addition of nanoclay. It is found that the addition of 2.0 wt. % nanoclay decreases the porosity and increases

the nanocomposite's resistance to water absorption significantly. The optimum 2.0 wt.% nanoclay addition exhibited the highest flexural and compressive strengths, flexural modulus and hardness. The geopolymer nanocomposite containing 2.0 wt.% nanoclay reduced the porosity by 7.1% and the water absorption by 17%, but increased the density by 11.4%, flexural strength by 24%, compressive strength by 23%, flexural modules by 25% and Rockwell hardness by 12.6% when compared to the control geopolymer sample.

The results of microstructural analysis indicated that the denser structure of nanoclay-geopolymer was due to the filler effect of the nanoparticles, as well as the high amount of geopolymer gel produced in the nano-matrices. Using the FTIR technique, it was shown that all nanocomposites had generally higher contents of geopolymer gel as compared to the control paste. However, the addition of 2.0 wt. % of nanoclay had the highest level of geopolymerization among all samples. SEM observation confirmed the previous results and showed denser microstructure in the case of nanocomposites. The geopolymer nanocomposite also exhibited better thermal stability than its pure geopolymer counterpart.

This enhancement can be attributed to the pore-filling effect and the activation of geopolymer containing 2.0 wt. % nanoclay in which this nanocomposite had more consolidated microstructure than others. However, the addition of more nanoclay (beyond 2.0 wt%) into geopolymer nanocomposite had an adverse effect on the mechanical and thermal properties. This could be attributed to poor dispersion and agglomerations of the high nanoclay contents which created more voids in the matrix.

4.3 Flax fabric-reinforced nanoclay-geopolymer composites (section 3.3).

Geopolymer composites and nanocompsites were fabricated using flax fabrics and nanoclay particles. The total amount of flax fabric in each sample was about 4.1 wt. % and different contents of nanoclay (1.0, 2.0 and 3.0 wt %) were used. All samples were fabricated and stored for 4 weeks before testing. The effect of nanoclay on

physical and mechanical properties of flax fabric-reinforced geopolymer composites as well as flax fibre-matrix interfaces was investigated.

The results showed that the optimum content of nanoclay was 2.0 wt.%. The flax fabric-reinforced nanocomposite containing 2.0 wt.% nanoclay reduced the porosity and water absorption by 16.3 and 19.4%, respectively, but increased the density by 4.4% and flexural strength by 32.4% when compared to the flax fabric-reinforced geopolymer composite. This finding was also confirmed by the flexural toughness indices of the nanocomposites. The composite reinforced with the optimum loading of 2.0 wt.% nanoclay showed higher toughness indices than the composite without nanoclay by 58%, 54% and 39% for I_{5},I_{10} and $I_{failure}$, respectively.

SEM micrographs of flax fibre-reinforced nanocomposite containing 2.0 wt.% nanoclay also verified its improvement as compared to other composites in terms of better fibre-matrix interface. All nanocomposites displayed denser matrices with lower number of unreacted fly-ash particles embedded in the matrices. However, in the flax fabric geopolymer nanocomposite containing 2.0 wt.% nanoclay, a smaller amount of unreacted fly-ash particles was observed, and higher content of geopolymer gel was clearly seen, which thus provided better adhesion between the flax fibres and the matrix. However, less such enhancement was observed when nanoclay content exceeds the optimum amount. This could be attributed to the increase in porosity which reduced the strength of bonding between fibres and geopolymer matrices, and thus the associated load-transfer capacity. This means that pores and voids in the geopolymer material acted as defects that weaken the composites.

4.4 Nanosilica-geopolymer composites (section 3.4)

The effects of nanosilica particles on the physical, microstructural and mechanical properties of geopolymer matrices containing nanosilica at 0.5, 1.0, 2.0, and 3.0 wt. % were presented. The nanoparticles were mixed with geopolymer in two different methods, namely the dry and the wet-mixing method. All samples were stored for 4 weeks at ambient temperatures before testing. The way of mixing was found to influence the dispersion of nanoparticles, and thus their chemical, physical and

mechanical properties. For example, Si:Al ratios increased with the addition of nanosilica in all pastes due to the amount of silica added to the system. The Si:Al ratio started from 2.29% at the control geopolymer and increased up to 3.57% in dry-mixed nanocomposites and 4.10% in nanocomposites fabricated using the wet-mix technique. All wet-mixed nanocomposites showed higher ratios of Si:Al as compared to their dry-mixed counterpart samples.

It has also been observed that loading nanosilica to geopolymers using both preparation methods improved the density and reduced the porosity and water absorption of geopolymers. In wet-mixed geopolymer samples, the density was enhanced by 7.6%, while the porosity and water absorption were reduced by 16.2% and 21.5%, respectively. However, in the situation of dry-mixing method, the optimum addition was found as 1.0 wt.% of nanosilica, which improved the density by 15%, and reduced the porosity and water absorption by 27% and 35%, respectively, when compared to the control sample.

The physical structure was found to have great impacts on the mechanical behaviour of geopolymer nanocomposites as the results of flexural and compressive strengths followed similar trends to the densities of all nanocomposites. The flexural strength of dry-mixed nanocomposites containing 0.5, 1.0, 2.0 and 3.0 wt. % nanosilica was improved by 20, 28, 24 and 15%, respectively. In contrast, the flexural strength of wet-mixed nanocomposites was improved by 9, 15, 22 and 13%, respectively, as compared to the pure geopolymer sample. The compressive strength results of geopolymer nanocomposites prepared through both dry and wet mix procedures indicate similar trends to that of flexural strength. The compressive strength of geopolymer nanocomposites improved by 21 and 27% after the addition of 1.0 and 2.0 wt.% nanosilica in dry- and wet-mixed samples, respectively. The strengths were found to be directly proportional to the nanocomposites densities but inversely proportional to the porosities; nanocomposites with higher densities demonstrated higher mechanical results.

Results also showed that the addition of nanosilica particles improved the microstructure and the strength of geopolymer nanocomposites regardless of the method of preparation. Nevertheless, nanocomposites prepared using the dry-mix

method demonstrated superior physical and mechanical properties as compared to their wet-mixed counterpart samples. The optimum addition was found as 1.0 wt.% nanosilica when prepared using the dry-mix procedure. Any further addition of nanosilica particles beyond the optimum weight of 1.0 wt.% adversely affected the physical and mechanical properties. This might be attributed to the poor dispersion and agglomerations of the high content of nanoparticles which formed more voids in the matrices.

4.5 Flax fabric-reinforced nanosilica-geopolymer composites (section 3.4)

Flax fabric-reinforced nanosilca-geopolymer composites were fabricated with ten layers of flax fabrics (~ 4.1 wt. %) and similar contents of nanosilca (0.5, 1.0, 2.0 and 3.0 wt.%). The samples were tested at 4 weeks after preparation. The ability of flax fabric-reinforced geopolymer composites and nanocomposites to absorb energy is identified by their flexural properties.

The results generally indicated that the addition of nanosilica into FF-reinforced nanocomposite improved their mechanical flexural properties. Furthermore, the FF-reinforced nanocomposites containing 1.0 wt.% nanosilica achieved the highest improvements. The flexural strength of nanocomposites containing 1.0 wt.% increased from 23.0 to 30.5 MPa, about 32% increase as compared to flax fabric-reinforced composite.

The ability of a composite to absorb energy is identified by their flexural toughness indices I_5, I_{10} and $I_{failure}$. Flax fabric nanocomposite including the optimum addition of nanosilica particles and prepared through dry-mix procedure exhibited the highest flexural toughness. Composites loaded with 1.0 wt. % nanosilica showed the maximum toughness indices of I_5, I_{10} and $I_{failure}$ as follows 44, 125 and 146, respectively. This improvement could be attributed to the enhanced density and the high content of geopolymer gel in the nanocomposites that led to better adhesion bond between the flax fibres and the geopolymer matrices.

SEM micrographs of the fracture surfaces of flax fibre reinforced geopolymer composite revealed poor adhesion bond between the fibres and geopolymer matrices. In contrast, good bonding at the fibre-matrix interface as well as denser microstructure were observed in flax fibre-reinforced nanocomposites containing 1.0 wt.% nanosilca. The improvement in mechanical properties along with fibre-matrice interfaces of the latter was attributed to the fact that the nanoparticles improved the microstructure of matrix through enhanced geopolymeric reaction and pore-filling effect. Therefore, good interfacial bonding between the resulted geopolymer matrices and the flax fibres was achieved.

4.6 Durability of flax fabric reinforced geopolymer nanocomposites (section 3.5).

The effect of different loadings of nanoclay and nanosilica particles on the durability and mechanical properties of geopolymer and flax fabric reinforced geopolymer composites was studied. The medium to long term durability of the composites was investigated in terms of flexural strength obtained at 32 weeks. The composition and microstructure of these composites were investigated using XRD, FTIR and SEM.

XRD revealed a new carbonation phase (Trona) on the surfaces of geopolymer samples at 32 weeks. The carbonation content was confirmed when aged samples were analysed using the FTIR technique. FTIR also showed that the reaction occurred at a low rate in consuming more OH groups and forming tougher material during the ageing period. The water content decreased to some equilibrium level during this period resulting in lower broad peak at 3400 cm^{-1}.

At 32 weeks, the flexural strength of nanocomposites improved slightly when compared to their values at 4 weeks. For example, the flexural strength of geopolymer nanocomposite containing 2.0 wt.% nanoclay increased from 5.6 to 6.1 MPa (i.e.9.0% increase). Whereas in the case of nanosilica, the flexural strength of the optimum addition of 1.0 wt.% nansilica improved the nanocompsite from 5.8 to 6.2 MPa (i.e. 6.8% increase), when compared to their values at 4 weeks. This slight enhancement in the mechanical performance could be attributed to the slow reaction of free silica and alumina in the presence of Na^{+} ions during the 32 weeks.

On the other hand, all flax fabric reinforced geopolymer composites and nanocomposites showed reduction in the mechanical performance after the aging period by varying degrees. After the aging period of 32 weeks, the reduction in the flexural strength of nanocomposites was less than that of control sample composite. The flexural strength of flax fabric reinforced geopolymer composites decreased by 23%, while the strength of flax fabric reinforced nanocomposites containing 2.0 wt.% nanoclay and 1.0 wt. % nanosilica decreased by only 13.7% and 10.3%, respectively. This may be attributed to the fact that the nanoparticles consumed large amounts of the alkaline solution, thus reducing the alkalinity of the matrices, and producing higher amount of geopolymer gel. As a result, both the density of matrices and the strength of fibre-matrix adhesion were improved.

SEM micrographs showed that flax fibres in geopolymer composites suffer more degradation than that in the nanocomposites. Based on these observations, the addition of nanoclay and nanosilica has great potential in improving the durability of flax fabric reinforced geopolymer nanocomposites during ageing.

Finally, it can be concluded that geopolymer matrices modified with both nanoclay and nanosilica particles displayed improved microstructural, physical and mechanical properties. At the same time, the degradation of flax fibres in geopolymer composites was reduced. Both types of nanoparticles showed comparable results but composites reinforced with nanosilica showed slightly better results than those contained nanoclay particles.

4.7 Recommendations for future work

The main aims of this investigation have been achieved. The effect of nanoparticles (nanoclay and nanosilica) and flax fabrics on the microstructural, physical and mechanical properties, as well as the durability of geopolymer nanocomposites and FF-reinforced geopolymer nanocomposites were investigated and discussed. Despite the significant enhancement and improvement in mechanical properties of geopolymer reinforced with both flax fabrics and nanoparticles, a limited improvement was achieved for FF-reinforced geopolymer nanocomposites as compared to the FF-reinforced geopolymer composites. Therefore, there is still a

need to continue investigating the potential of flax fibres and nanoparticles as reinforcement for geopolymers. The following recommendations have been expressed to help guide further work:

- In this investigation, no chemical or physical treatment was used on flax fabrics. Further investigation in treating the natural fibres is required to improve their mechanical and physical properties, as well as to enhance the fibre/geopolymer interfacial bonding.
- In this experimental work, it was found that further loading of nanoparticles beyond the optimum addition into geopolymer nanocomposite matrices adversely affected the mechanical and physical properties of geopolymer nanocomposites and FF-reinforced geopolymer nanocomposites. Further investigation is required to resolve the issue of nanoparticle agglomerations and also to identify the best method of mixing to achieve good dispersion of the nanoparticles at high amounts in geopolymers.
- Since the main concern for the use of natural fibres in geopolymer composites is long-term durability of the fibres and composites, it is suggested that additional studies are necessary to overcome the degradation of natural fibres.
- In this study, the aluminosilicate source (class-F fly ash) and the alkaline solution molarity that were used to prepare geopolymers have been fixed in all geopolymer samples in order to measure the effect of incorporating nanoparticles on the degradation of the flax fibres. Further investigations on the effect of various geopolymer molarity and source materials such as class-C fly ash and metakaolin on the degradation of natural fibres are required to better understand the relationship between the deterioration of natural fibres and the chemistry of geopolymer matrices.
- Flax fibres, nanoclay and nanosilica were used as reinforcement materials in this study. The experimental work can be extended by combining other types of natural fibre and nanoparticle within the geopolymer matrices.
- In this study, the medium to long-term durability of flax fabric reinforced geopolymer composites and nanocomposites was investigated under ambient condition. Other conditions of durability such as long-term durability, dry-

wet cycles and freeze-thaw cycles are needed to confirm the outcomes of this investigation.

- As the fibre-matrix interaction is a main issue in natural fibres reinforced geopolymer composites, it is recommended that further research is required to study the interfacial chemistry between the natural fibres and geopolymer matrices.

APPENDICES

APPENDIX I: Influence of nanosilica particles on the durability of flax fabric reinforced geopolymer composites.

(A journal article was submitted to the journal of Composite Part B on Sep 16, 2016)

Abstract

Natural fibres are currently considered as a suitable alternative to synthetic fibres in geopolymer composites. However, the durability of natural fibres as reinforcement in geopolymer composites is still a concern due to the alkalinity of activators of geopolymer matrices. The alkaline environment is the main reason of the degradation of natural fibres in cementitious matrix. This paper presents the influence of nanosilica (NS) on the mechanical performance and durability of flax fabric (FF) reinforced geopolymer composites. The durability of the composite after 4 and 32 weeks under ambient temperature is also presented. The results showed that the incorporation of NS has a positive impact on the physical properties, mechanical performance and durability of FF-geopolymer nanocomposites. The presence of NS has accelerated the geopolymeric reaction and lowered the alkalinity of the system, thus reducing the degradation of flax fibres.

1. Introduction

Geopolymers are formed by activating a solid aluminosilicate source such as fly-ash, meta-kaolin and slag with alkaline solutions, creating amorphous networks of tetrahedral SiO_4 and AlO_4 connected by sharing oxygen atoms (Davidovits, 1991). Duxson *et al.* (Duxson *et al.*, 2007a) described a model for the geopolymerisation process in few steps. In essence, this process involves the dissolution of aluminosilicate by alkaline solution and the concomitant release of aluminate and silicate species. Then a mixture of the dissolved silicate and aluminate species with the aluminosilicate material is formed in the alkaline environment. This leads to a growth of a gel as the oligomers in the aqueous phase develop networks by condensation and polymerisation. While the chemical reaction is progressing, water

is released and consumed in the dissolution process. Reformation of gel 1 to gel 2 occurs with the release of additional water. Lastly, polymerisation through a condensation and hardening stage occurs. Even though the procedure is exhibited in sequential steps, these phases could occur simultaneously and heterogeneously.

Despite the potential and attractive properties, geopolymers still suffer from brittle failure readily under applied force and exhibit low mechanical strength (Lin *et al.*, 2008, Alomayri *et al.*, 2014b). One way to resolve this limitation is through utilizing natural fibres to fabricate fibre-reinforced geopolymer composites. The advantages of using natural fibres in composites include low density, flexibility and high specific modulus (Herrera-Franco and Valadez-González, 2005, Bohlooli *et al.*, 2012). Several types of natural fibres have been successfully utilized in geopolymer matrices. For instance, cotton fibres and fabrics have been used to improve the fracture toughness and mechanical performance of geopolymer composites (Alomayri *et al.*, 2013a, Alomayri *et al.*, 2013b). Furthermore, flax and wool fibres have presented positive effects when incorporated into geopolymer matrices; where they significantly improved the mechanical properties of the natural fibre reinforced geopolymer composites (Alzeer and MacKenzie, 2013, Alzeer and MacKenzie, 2012). In a another study, geopolymer composites were reinforced with woven flax fabric and tested for mechanical properties such as flexural strength, flexural modulus, compressive strength, hardness, and fracture toughness. The results showed that all mechanical properties were improved by increasing the flax fibre contents, and showed superior mechanical properties over the pure geopolymer matrix (Assaedi *et al.*, 2015a).

However, there are concerns in utilizing natural fibres in alkali-based matrices. The main concern is regarding the long-term durability of natural fibre reinforced composites. Natural fibres can be degraded and damaged in high-alkaline environment; thereby adversely affecting the mechanical properties and durability of the composites (Hakamy *et al.*, 2016, Aly *et al.*, 2011b, Yan and Chouw, 2015). Natural fibre degradations in alkaline environments was studied by Gram (Gram, 1983) and he described the degradation mechanism as the decomposition of hemicellulose and linen which leads to the splitting of natural fibres into micro-fibrils. This effect has been observed using SEM in the case of jute fibres in cement

matrix, where the natural fibres split-up and fibrillised, resulting in reduction of the tensile strength of jute fibres by 76% (Velpari *et al.*, 1980). To reduce the degradation impact, nanoparticles can play an important role. The effect of nanoclay particles on the durability of flax fibre reinforced cement composites at 28 days and after 50 wet/dry cycles has been investigated by Aly and coworkers (Aly *et al.*, 2011b). Samples loaded with 2.5 wt% nanoclay particles showed lower deterioration in the flexural strength when compared to its counterpart control samples. This was attributed to the beneficial effect of nanoparticles in reducing the degradation of flax fibres.

In order to improve the durability of flax fabric (FF) in geopolymer composites, geopolymer matrices were modified by the addition of nanosilica (NS) particles. This study presented the effect of different loadings of NS on the durability and mechanical properties of FF-reinforced geopolymer nanocomposites. The durability of all samples has been discussed in terms of flexural strength obtained at 4 and 32 weeks. The microstructure was investigated using X-ray diffraction, Fourier transform infrared spectroscopy (FTIR) and scanning electron microscopy (SEM).

2. Experimental Procedure

2.1 Materials

Low-calcium fly-ash (ASTM class F), obtained from the Eraring power station of NSW, Australia, was used to prepare the geopolymeric nano-composites. The alkaline activator for geopolymerisation was a combination of sodium hydroxide solution and sodium silicate grade D solution. Sodium hydroxide flakes with 98% purity were used to prepare the solution. The chemical composition of sodium silicate used was 14.7% Na_2O, 29.4% SiO_2 and 55.9% water by mass. Nanosilica was obtained from Nanostructured and Amorphous Materials, Inc. of USA. The average diameter of particles was between 18-25 nm.

To prepare the geopolymer pastes, an alkaline solution to fly-ash ratio of 0.75 was used and the ratio of sodium silicate solution to sodium hydroxide solution was fixed at 2.5. The concentration of sodium hydroxide solution was 8 M, which was prepared and combined with the sodium silicate solution one day before mixing.

2.2 Samples preparation

The preparation process of all samples is summarized in Figure 1. To prepare the pure geopolymer and geopolymer nanocomposites, nanosilica particles were added to the flyash at the loadings of 0.0%, 0.5%, 1.0%, 2.0% and 3.0% by weight. They were first dry mixed for 5 min in a covered mixer at a low speed and then mixed for another 10 min at high speed until homogeneity was achieved. The alkaline solution was then added slowly to the dry mix in a Hobart mixer at a low speed until the mixture became homogeneous, then further mixed for another 10 min in high speed. The resultant mixture was then poured into wooden moulds, which were then placed on a vibration table for 2 min before they were covered with a plastic film and cured at 80° C for 24 h in an oven before demolding. The geopolymer paste without nanosilica particles was identified as the control sample.

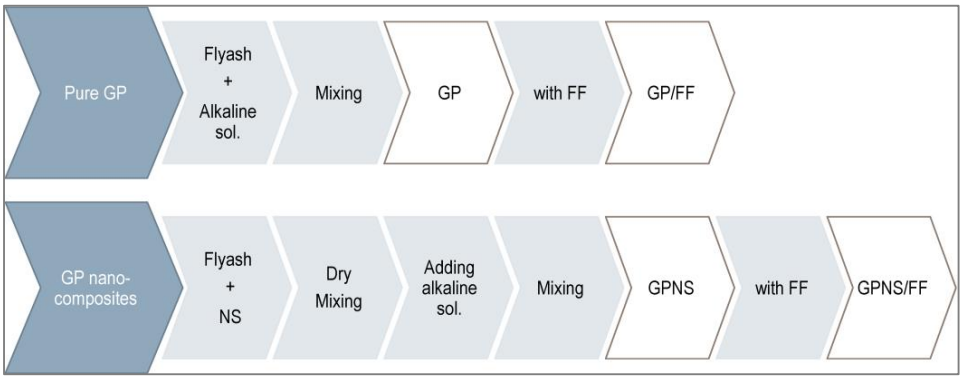

Figure 1: Scheme showing the preparation procedures of geopolymer, geopolymer nanocomposites and FF-reinforced geopolymer nanocomposites.

Similar mixtures were prepared to fabricate FF-reinforced composites and nanocomposites. Four samples of geopolymer pastes reinforced with ten layers of FF were prepared by spreading a thin layer of the paste in a well-greased wooden mould, followed by carefully placing the first layers of FF on it. The fabric was fully saturated with the paste by a roller, and the process repeated for ten layers; each composite contained a different weight percentage of NS particles. The samples were left for curing under a heavy weight (20 kg) for 1 hour to reduce entrapped air inside the samples. All samples were covered with plastic film and cured at 80℃ for 24 hours in an oven before demoulding. They were then dried under ambient conditions for 28 days. The flax fabric reinforced geopolymer matrix without nanosilica particles was considered as the control sample.

All samples were then categorized in two series. The samples of the first series were

cured under ambient conditions for 4 weeks, and the samples of the other series were stored in the same condition for 32 weeks. The formulation of samples is given in Table 1.

Table 1: Mix proportions of samples.

Sample	Fly-ash (g)	Alkaline Solution (g)	NS(g)	Water (g)	FF (wt%)
GP	1000	750	0	50	0
GPNS-0.5	1000	750	5	50	0
GPNS-1.0	1000	750	10	50	0
GPNS-2.0	1000	750	20	50	0
GPNS-3.0	1000	750	30	50	0
GP/FF	1000	750	0	50	4.1
GPNS-0.5/FF	1000	750	5	50	4.1
GPNS-1.0/FF	1000	750	10	50	4.1
GPNS-2.0/FF	1000	750	20	50	4.1
GPNS-3.0/FF	1000	750	30	50	4.1

Note: The alkaline solution is a mix of 214.5g sodium hydroxide (8M) and 535.5g sodium silicate.

2.1 Characterization

Identical pieces were chosen and cut from each sample. They were then crushed and ground to fine powder. The powder samples were measured on a D8 Advance Diffractometer (Bruker-AXS, Germany) using copper radiation and a LynxEye position sensitive detector. The diffractometer was scanned from 7.5° to 60° using a scanning rate of 0.5°/min. XRD patterns were obtained by using Cu k_{α} lines (k = 1.5406 Å). The Quantitative X-ray Diffraction Analysis (QXDA) with Rietveld refinement was done using the *MAUD* V2.44 software. Fluorite [CaF_2] was chosen to serve as an internal standard (Rickard *et al.*, 2011). The samples for QXDA were prepared by mixing a dry weight of 3.0 g of geopolymer paste or geopolymer nanocomposite paste with 0.33 g of fluorite. The weight percentage of each crystalline phase W_{Cr} was determined by Rietveld refined parameters using Eq. 1 (Chen‐Tan *et al.*, 2009):

$$W_{Cr} = \left[W_{std} \frac{S_{Cr}(ZMV)_{Cr}}{S_{std}(ZMV)_{std}} \right] \times \left[\frac{1}{1 - W_{std}} \right] \quad (1)$$

Where W_{std} is the standard (fluorite) weight percent. M and V are the mass and volume of unit cells, Z is the number of formula units per unit cell, S_{Cr} and S_{std} are the scale factors for the crystalline phases and the standard, respectively. The amorphous weight content W_{Am} is then determined using the equation (Chen‐Tan *et al.*, 2009):

$$W_{Am} = 1 - \sum_{i=1}^{n} W_n \tag{2}$$

where n is the number of crystalline phases refined.

The chemical compositions of Eraring fly ash was analyzed using X-ray fluorescence (XRF). An FTIR scan was performed on a Perkin Elmer Spectrum 100 FTIR spectrometer in the range of 4000–500 cm^{-1} at room temperature. The microstructures and the fracture surfaces of samples tested were examined using a Zeiss EVO-40 (Carl-Zeiss, Germany) scanning electron microscope (SEM). Fracture surfaces of geopolymer samples were placed in a vacuum desiccator for 2 days to allow complete out-gassing before being mounted on aluminum stubs and coated with a thin layer of platinum prior to examination.

2.2 Physical and mechanical properties

Measurements of bulk density and porosity were conducted to define the quality of geopolymer nanocomposites. Density of samples (ρ) with volume (V) and dry mass (m_d) was calculated using Eq. 3:

$$\rho = \frac{m_d}{V} \tag{3}$$

The value of apparent porosity (P_a) was determined using Archimedes' principle in accordance with the ASTM Standard (C-20). Pure geopolymer and nano-composite samples were immersed in clean water, and the apparent porosity (P_a) was calculated using Eq. 4:

$$P_a = \frac{m_a - m_d}{m_a - m_w} \times 100 \tag{4}$$

where m_a is mass of the saturated samples in air, and m_w is mass of the saturated samples in water.

A LLOYD Material Testing Machine (50kN capacity) with a displacement rate of

0.5 mm/min was used to perform the mechanical tests. Rectangular bars of 60×18×15 mm^3 were cut from the fully-cured samples for three-point bend test with a span of 40 mm to evaluate the flexural strength. Five samples of each group were used to evaluate the flexural strength of geopolymer composites. The values were recorded and analyzed with the machine software (NEXYGENPlus) and average values were calculated. The flexural strength (σ_F) was determined using the equation (Low *et al.*, 2007a) :

$$\sigma_F = \frac{3}{2}\frac{P_m S}{WD^2} \tag{5}$$

where P_m is the maximum load, S is the span of the sample, D is the specimen width, and W is the specimen thickness.

3. Results and Discussion

3.1 Physical properties

The results of density and porosity of pure geopolymer and those containing nanoparticles are shown in Table 2. Nanocomposite samples exhibited denser matrices and lower porosities when compared to the control sample. The optimum addition was found as 1.0 wt% NS, which increased the density by about 15% and reduced the porosity by 27% when compared to the control matrix. This improvement could be attributed to two reasons. First, the nanoparticles played a pore-filling role that reduced the porosity of geopolymer nanocomposites. Secondly, the additional silica enhanced the geopolymeric reaction, thus creating more geopolymer gel and denser matrices (Phoo-ngernkham *et al.*, 2014). Nevertheless, further loading of NS produced pastes that have slightly lower density due to inadequate dispersion and agglomeration of the nanosilica particles. This result is in agreement with the study done by Supit and Shaikh (Supit and Shaikh, 2014) who reported that the loading of 2.0 wt.% NS considerably reduced the porosity of concrete containing high volume of fly-ash. This finding is similar to the study by Hakamy and coworkers (Hakamy *et al.*, 2015a) where the porosity of cement paste was reduced due to addition of 1.0 wt.% of nanoclay particles to cement matrix. However, the porosity was increased when more nanoparticles were added due to the agglomeration effect. The microstructures of pure geopolymer paste and the

geopolymer nanocomposite containing 3.0 wt.% NS are shown in Figure 2(a–b). Higher number of voids, unreacted and partially reacted fly ash particles can be clearly seen in the case of pure geopolymer (Figure 2a). However, after the addition of NS, higher amount of geopolymer gel, and fewer amount of unreacted flyash particles appeared in the nanocomposite matrix (Figure 2b).

Table 2: Density and porosity for pure geopolymer and geopolymer nano-composites. Uncertaintaintes are indicated in brackets.

Sample	Density (gm/cm^3)	Porosity (%)
GP	1.84 (0.02)	22.20 (0.45)
GPNS-0.5	1.89 (0.02)	20.87 (1.35)
GPNS-1.0	2.10 (0.02)	16.08 (0.76)
GPNS-2.0	2.04 (0.03)	17.49 (1.84)
GPNS-3.0	1.96 (0.08)	20.33 (1.01)

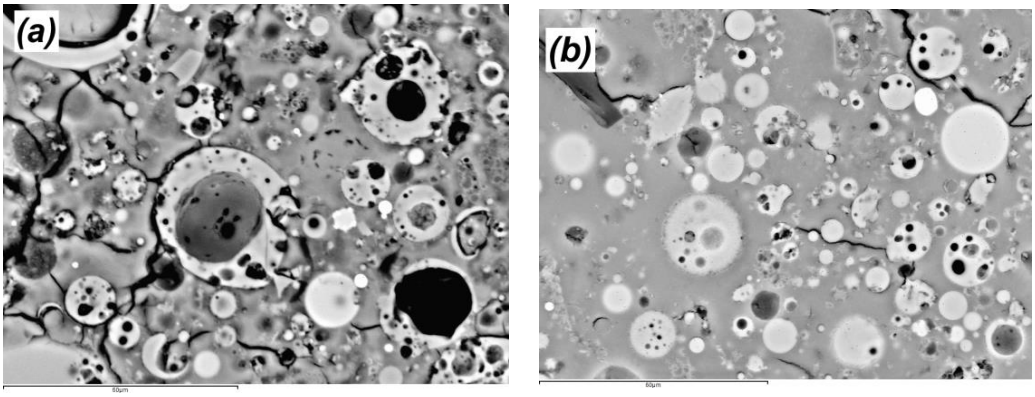

Figures 2: SEM micrographs showing the microstructure of (a) GP and (b) GPNS-3.0.

3.2 Structural properties

The chemical composition and loss on ignition of Eraring flyash are presented in Table 3. The flyash contains, in addition to silica and alumina, Fe_2O_3, CaO, K_2O, Na_2O, MgO and TiO_2. The XRD spectra taken for the pure sample and the nanocomposites at 4 and 32 weeks are shown in Figures. 3(a-b), respectively. Crystalline phases were identified using EVA version 11, and were indexed using

Powder Diffraction Files (PDFs) from the Inorganic Crystal Structure Database (ICSD). Fluorite [CaF_2] (PDF 04-002-2191) was the standard used to determine the weight percentage of each crystalline phase. At 4 weeks, all samples have two crystalline phases, quartz [SiO_2] (PDF 00-046-1045) and mullite [$Al_{2.32}Si_{0.68}O_{4.84}$] (PDF 04-016-1588). Quartz and mullite can be seen in all samples since they are the main crystalline content in the Eraring flyash, and they are unreactive in the alkaline environment (Assaedi *et al.*, 2016).

Table 3: Chemical composition of Eraring flyash (wt. %).

SiO_2	Al_2O_3	CaO	Fe_2O_3	K_2O	MgO	Na_2O	P_2O_5	SO_3	TiO_2	MnO	BaO	LOI
63.13	24.88	2.58	3.07	2.01	0.61	0.71	0.17	0.18	0.96	0.05	0.07	1.45

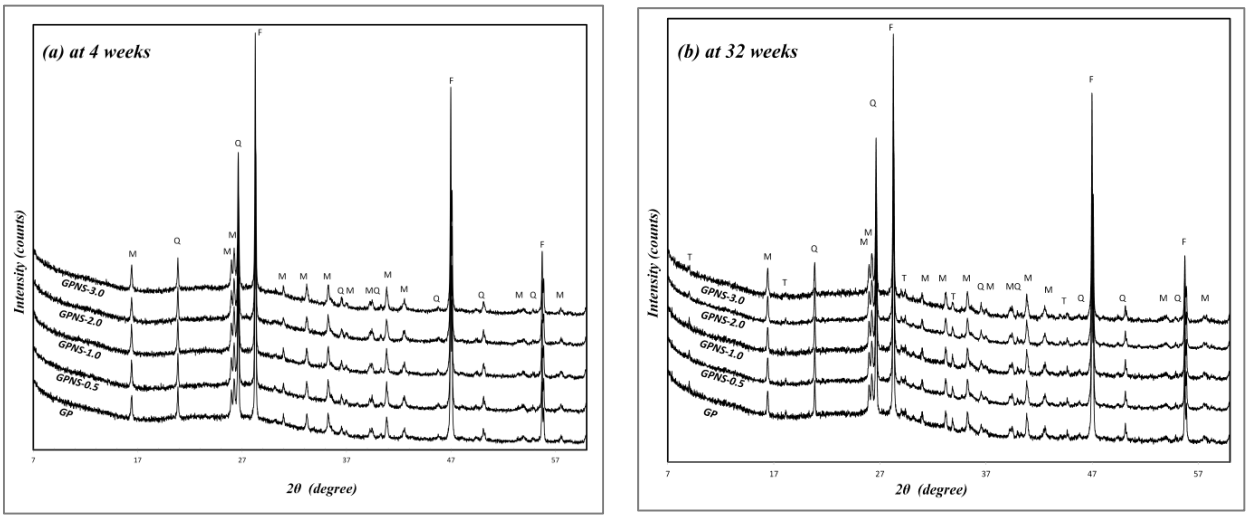

Figures 3: SEM images showing the microstructure of (a) GP and (b) GPNS-3.0.

At 32 weeks, another crystalline phase, trona [$Na_3H(Co_3)_2.2H_2O$] (PDF 00-029-1447), develops on the surface of the pure geopolymer and nancomposites. Trona belongs to soda minerals group, which could be formed by the atmospheric reaction of carbon dioxide with the residual water and sodium hydroxide in the system, according to the chemical formula (Zaharaki *et al.*, 2010):

$$3NaOH + 2CO_2 + 2H_2O \rightarrow Na_3H(CO_3)_2.2H_2O \quad (6)$$

The phase abundance of crystalline phases in each sample was determined using Rietveld refinement, and the amorphous contents were calculated using Eq. 2. Figures. 4(a-b) show the Rietveld refinements of the diffraction pattern of pure geopolymer and geopolymer nanocomposite containing 2.0% NS at 32 weeks, respectively. In general, the addition of amorphous nanosilica into the geopolymer pastes has resulted in slight changes to the crystalline and amorphous contents of all samples. Figure5 presents the amorphous and crystalline phase compositions of pure geopolymer and geopolymer nanocomposites at 4 and 32 weeks. At 4 weeks, the addition of 3.0 wt% NS increased the amorphous content by 3.2%, which caused a concomitant reduction in the crystalline phases contents. The increase of the amorphous content in the nanocomposite samples could be attributed to the amorphous nature of the unreacted NS that was loaded to the pastes and performs as a nano-filler (Nazari and Sanjayan, 2015, Phoo-ngernkham *et al.*, 2014). The active and reacted nanosilica particles could also promote geopolymeric reaction producing higher amorphous amount of geopolymer gel in the nanocomposite (Phoo-ngernkham *et al.*, 2014). At 32 weeks, the amounts of quartz and mullite remained unchanged after the aging period, those crystals are very stable and require high temperatures to be dissolved (Deer *et al.*, 1996, Schneider *et al.*, 2008). Trona crystals formed mainly from the amorphous content in geopolymers and the atmospheric carbon dioxide. This can be noticed by comparing the trona and amorphous content at 4 and 32 weeks. After the aging period, the amorphous amount in geopolymers decreased by about 3% in all samples, which is similar to the amounts of trona that is grown after the aging period. It is worth mentioning here that the carbonation phase content (trona) is highly dependent on the position chosen from each sample since trona formed on the surfaces of geopolymers. However, all samples have been chosen from very similar parts in each composite to ensure they are near identical; hence, the analysis can provide a good estimation of the relative crystalline and amorphous content in each sample.

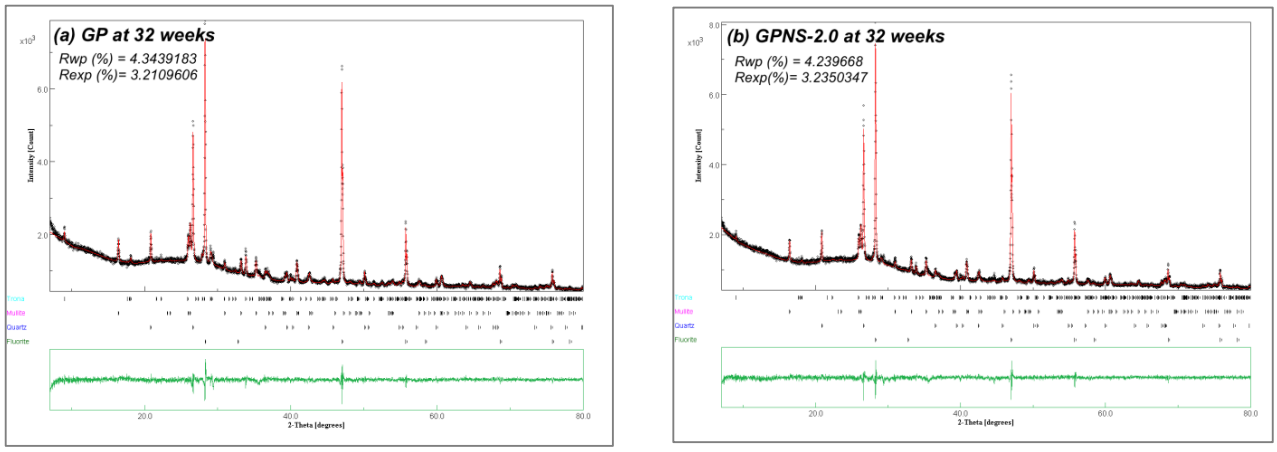

Figures 4: XRD Rietveld plots for: (a) GP and (b) GPNS-1 at 32 weeks. Measured patterns are indicated by black points, and calculated patterns by solid red lines. The green residual plot shows the difference between the calculated and the measured patterns.

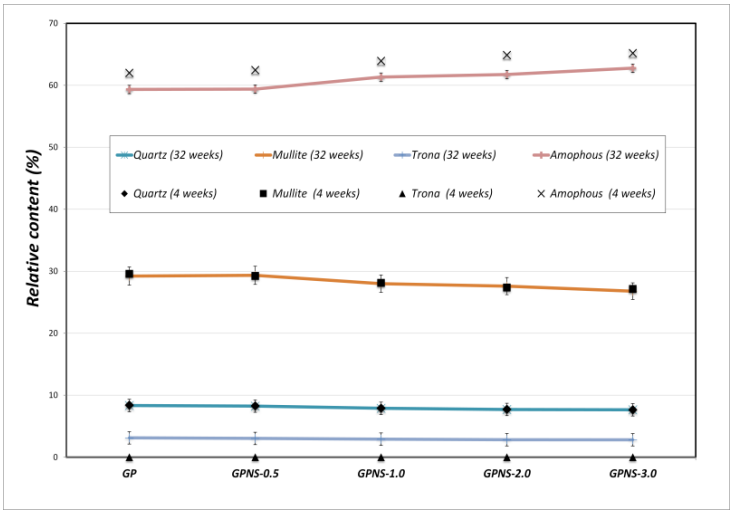

Figure 5: Amorphous and crystalline phase's compositions of pure geopolymer and geopolymer nanocomposites at 4 and 32 weeks.

FTIR spectra of pure geopolymer and geopolymer nanocomposite at 4 and 32 weeks are shown in Figure 6. The FTIR spectra of all samples show a strong peak at ~1000 cm^{-1} which is ascribed as Si-O-Si and Al-O-Si asymmetric stretching vibrations. This peak serves as the identification peak of the geopolymerisation (Phair and Van Deventer, 2002, Li *et al.*, 2012). A broad peak in the region around 3400 cm^{-1} indicates that the OH group is attached to different centers (Al, Si) and free water (Chindaprasirt *et al.*, 2009, Rattanasak and Chindaprasirt, 2009). The absorbance peak at 1640 cm^{-1} is also attributed to the (OH) bending vibration (ul Haq *et al.*, 2014). At 32 weeks changes have occurred, two peaks at 1420 and 1480 cm^{-1} appear

indicating the presence of sodium carbonate; this was formed due to the atmospheric carbonation on the matrice surfaces which thus confirms the XRD results (Zaharaki *et al.*, 2010). During the aging period the reaction has carried on at a low rate consuming more OH groups and forming stronger material. The water content decreased to some equilibrium level during this period resulting in lower broad peak at 3400 cm^{-1}. In addition, the geopolymer band at ~1000 cm^{-1} shifted slightly to higher wavenumbers due to higher polycondensation reaction, thus indicating higher transformation of Gel 1 to Gel 2 (Duxson *et al.*, 2007a, Liew *et al.*, 2016).

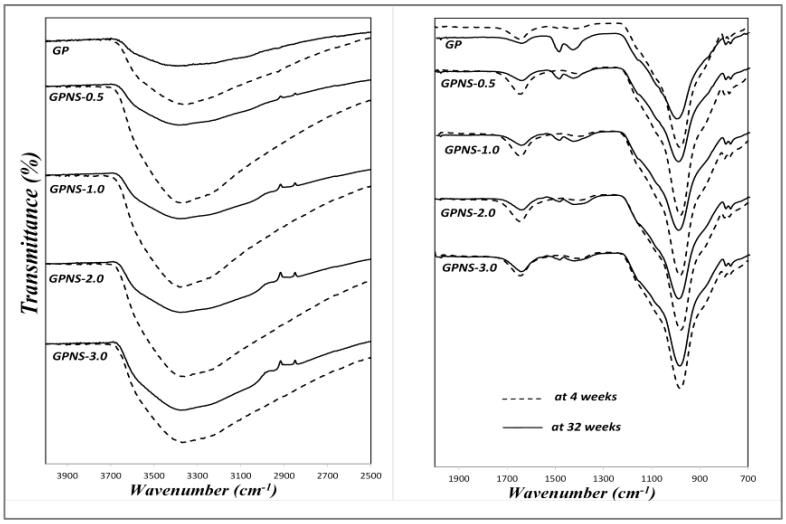

Figure 6: FTIR spectra of geopolymer and geopolymer nanocomposites at 4 and 32 weeks.

3.4 Flexural Strength of geopolymer nanocomposites:

The effect of aging on the flexural strength of pure geopolymer and nanocomposites is presented in Figure 7. Generally, slight improvement in flexural strength was observed at all ages due to the incorporation of nanosilica particles into the geopolymer matix. At 4 weeks, the flexural strength of geopolymer nanocomposite with 0.5, 1.0, 2.0 and 3.0 wt.% NS was increased by about 20%, 28%, 24% and 15%, respectively, when compared to the control paste. This improvement shows the effectiveness of NS in facilitating the geopolymeric reaction and filling of the micro-pores in the matrices (Assaedi *et al.*, 2015b, Assaedi *et al.*, 2016, Hakamy *et al.*, 2015a). Thus, the microstructure of geopolymer nanocomposites was denser than the pure matrix, especially in the case of sample containing 1.0 wt.% NS, which is evident from its higher flexural strength. At 32 weeks, however, the flexural strength of nanocomposites increased slightly compared to their values at 4 weeks. For

instance, the averaged flexural strength of GPNS-1 nanocomposite improved from 5.8 to 6.2 MPa (i.e. 6.8% increase). This slight improvement in the mechanical performance could be attributed to the slow reaction of free silica and alumina in the presence of alkaline environment during the aging period (Yadollahi *et al.*, 2015, Zhang *et al.*, 2010). In a comparable investigation, Rong *et al.* (Rong *et al.*, 2015) studied the effect of 3.0% wt% addition of nanosilica particles on the durability of concrete containing 35% wt% flyash at 28 and 90 days, where they reported an increase in flexural strength of about 11% at 90 days when compared to 28 days. Likewise, Mohamed (Mohamed, 2016) reported that the flexural strength of concrete containing 1.0% wt% nanosilica increased by about 10% after 90 days when compared to its strength at 28 days.

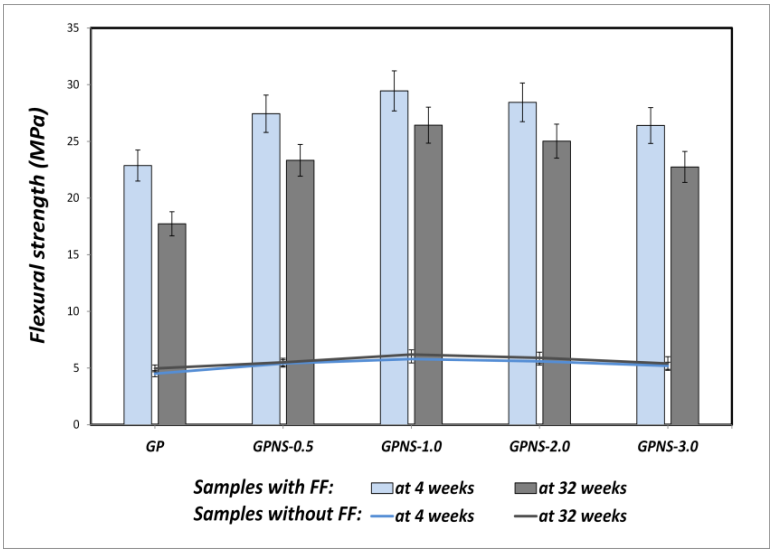

Figure 7: Flexural strength of all samples at 4 and 32 weeks.

3.5 Flexural properties of flax fabric reinforced geopolymer nanocomposites:

Flexural tests are used to describe the mechanical properties of layered composites as they give a simple means of determining the bending response, which provides practical information on the performance of fabric based composites (Abanilla *et al.*, 2006). The effect of aging on the flexural strength of FF-reinforced geopolymer nanocomposites at 4 and 32 weeks is shown in Figure 7. The incorporation of nanosilica particles into matrices led to significant enhancement in flexural strength of all reinforced nanocomposites. For example, at 4 weeks, the flexural strength of GPNS-1/FF increased from 23.0 to 30.5 MPa, which is about 32.4% increase when

compared to GP/FF composite. This improvement could be attributed to the enhanced density of the nanocomposites which led to better adhesion bond between flax fibres and geopolymer nanocomposites. The fracture surfaces of GP/FF and GPNS-0.1/FF after the flexural test at 4 weeks are shown in Figures. 8 (a-c), respectively. The fracture surface of GP/FF composite exhibits a highly porous structure with a number of voids and unreacted fly-ash particles embedded in the matrices. This reduced the bond between the fibres and the matrix, which caused the fibres to de-bound and pull out from the matrix as shown in Figure 8a. However, FF-reinforced geopolymer nanocomposites loaded with 1.0 wt% NS show relatively denser matrices with lower amount of unreacted fly ash particles. Consequently, better adhesion between the fibres and the matrices was observed which caused the fibres to be fractured (Figure 8b-c). In both cases, the fibres seemed quite uniform and did not show any signs of degradation.

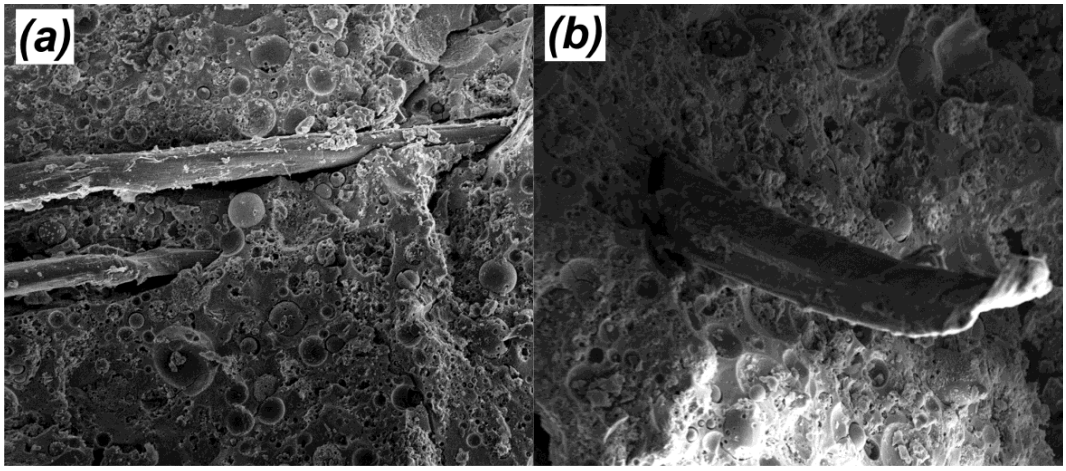

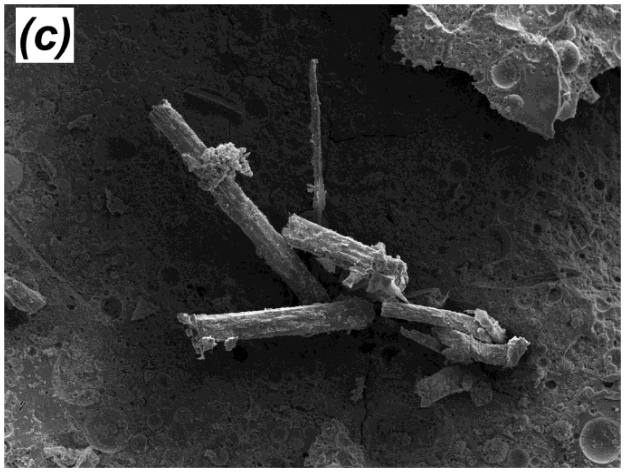

Figures 8: SEM images showing the fracture surfaces of FF-reinforced samples; (a) GP/ FF, and (b-c) GPNS-1/FF.

However, after 32 weeks all composites showed a reduction in their flexural strength. Figures. 9(a–b) show the load-midspan deflection behaviour of GP/FF and GPNS-1/FF composites at 4 and 32 weeks. The "ductile" behavior can be observed in both composites with and without the nanoparticles, with higher load capacity (about 31% increases) in the composite containing NS. It was observed that ductile behavior and bending stress are reduced due to degradation process. In general, all natural fibres suffer several levels of deterioration when exposed to alkaline environment (Bentur and Mindess, 2007). The degradation of natural fibres has been addressed by several studies, and was attributed to the weakening of lignin and hemicellulose due to the attack of alkali ions, and the mineralization of fibre cell walls in geopolymer pastes that led to the fibre brittleness (Pacheco-Torgal and Jalali, 2011, Mohr *et al.*, 2007, Filho *et al.*, 2013). The fibre degradation in alkali matrices eventually led to deterioration of fibre–matrix adhesion, and the concomitant reduction in flexural performance of the composites. The flexural strength of FF reinforced geopolymer composite was reduced by 22.4% of the strength at 4 weeks, while the flexural strength of GPNS-0.5/FF, GPNS-1/FF, GPNS-2/FF and GPNS-3/FF nanocomposites was decreased by about 14.9%, 10.3%, 12.1 and 13.8% when compared to their values at 4 weeks. Based on this outcome, it can be concluded that the reduction in flexural strength for nanocomposites was less than that of the control sample composite after 32 weeks aging period. This may be attributed to the fact that nanosilica consumed large amounts of the alkaline solution, thus reducing the alkalinity of the medium, and producing higher amount of geopolymer gel. As a

result, the density of the matrices and the strength of fibre-matrix adhesion were improved (Assaedi *et al.*, 2016).

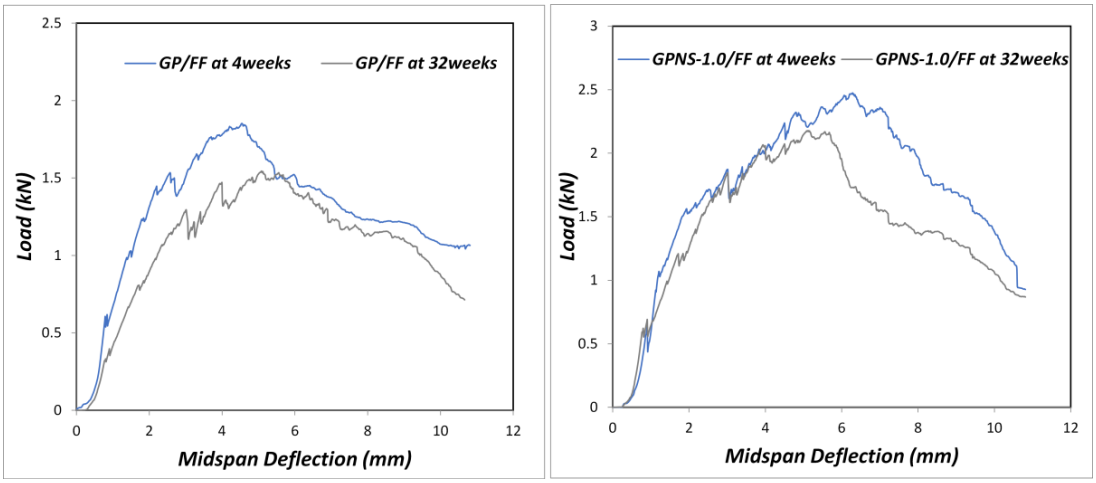

Figures 9: Load versus mid-span deflection curves for GP/FF composite and GPNS-1/FF nanocomposites at 4 and after 32 weeks.

Figures 10(a-d) show the changes on the fibre surfaces in GP/FF, GPNS-1.0/FF and GPNS-3.0/FF at 32 weeks. The fibres in the control sample (Figures. 10a-b) revealed signs of degradation and the fibrils were clearly splitting up, which influenced the flexural strength of the composite. In contrast, the fibres in samples GPNS-1.0/FF and GPNS-3.0/FF did not show any significant signs of damage after the aging period (Figures.10 c-d). In a comparable investigation, Aly *et al.* (Aly *et al.*, 2011b) reported that the addition of nanoclay and waste glass to cement mortar could improve the durability and mitigate the degradation of flax fibres embedded in the composites by reducing the alkalinity of the matrix. In another study, the effect of calcined nanoclay on the durability of hemp fabric reinforced cement nanocomposites and the degradation of hemp fibres were reported (Hakamy *et al.*, 2016), where the nanoparticles were found to improve the durability and reduce the degradation of the natural fibres. In another study, the durability of sisal fibre reinforced mortar with the loading of meta-kaolin at 28 days and after 25 wet/dry cycles was reported (Filho *et al.*, 2013). The flexural strength of the meta-kaolin composites decreased by 23%, when compared to their control composites at 28 days. Additionally, it was found that 50% meta-kaolin replacement significantly prevented the degradation of sisal fibres in cement matrices. In the present study, the degradation of flax fibres in nanocomposite was mostly reduced and the FF-

nanocomposite matrix interfacial bonding was typically improved.

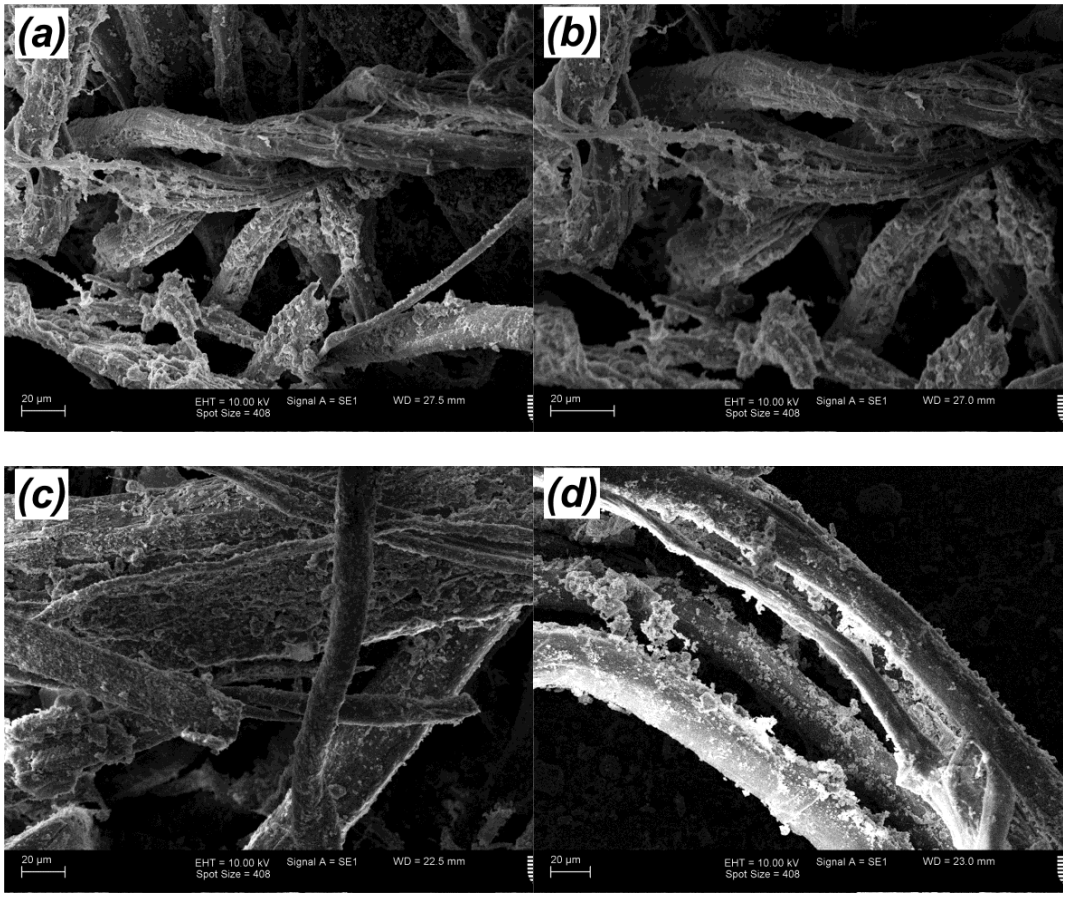

Figures 10: SEM images of the flax fibres at 32 weeks in: (a-b) GP/FF, (c) GPNS-1/FF and (d) GPNS-3/FF.

4. Conclusions

The effect of nanosilica on the durability of flax fibre reinforced geopolymer nanocomposites is reported. The optimum content observed was 1.0 wt.% nanosilica. After 32 weeks, the flexural strength of GP/FF composites decreased by 23.01% whereas the flexural strength of GPNS-1/FF nanocomposites decreased by 10.2%. SEM images showed that flax fibres in GP/FF composites suffer more degradation than that in GPNS-1/FF nanocomposites. Based on these results, the incorporation of NS has significant potential in improving the durability of flax fibres and thus the mechanical properties of flax fabric reinforced geopolymer nanocomposites during the aging period.

APPENDIX II: Advances in geopolymer composites with natural reinforcement

ASSAEDI, H., ALOMAYRI, T. and LOW, I.M. 2017.

(Chapter 19 in *Advances in Ceramic matrix Composites - Second Edition*, Ed. I.M. Low. Elsevier, *In Press)*

Abstract

When compared to their synthetic counterparts, natural fibres represent an environmentally friendly alternative by virtue of several attractive attributes that include low density, lower cost, non-toxicity, and ease in processing, renewability and recyclability. Moreover, the use of natural fibres in polymer matrix composites

has the potential to produce materials with higher specific strength and specific modulus due to their low density. In this chapter, geopolymer matrices reinforced with cotton fabrics (CF) and flax fabrics (FF) have been fabricated and characterized. The thermal stability, physical properties such as density and porosity, and the mechanical properties such as flexural strength, flexural modulus and fracture toughness were evaluated. Results indicated that both FF and CF have significant impact in improving the mechanical properties of geopolymers. However, FF-reinforced geopolymer composites showed better mechanical behaviour as compared to geopolymer reinforced with CF.

1. Introduction

Ordinary Portland cements are widely used in construction applications due to their suitable mechanical and durability properties. Greenhouse emissions from the production of such cement-based materials, however, have necessitated the search for eco-friendly alternatives. Geopolymer is one such alternative. This material, first introduced by Davidovits (1989), exhibit durability, good mechanical performance and fire and acid resistance. The production of geopolymers, being cured at room temperature is considerably more ecologically friendly than the production of Portland cement. It is a process that offers 80-90% reduction in carbon dioxide emission (Barbosa *et al.*, 2000, Van Jaarsveld *et al.*, 1998, Davidovits, 1989, Duxson *et al.*, 2007a).

Despite promising characteristics of geopolymers, the material's matrix is one which suffers brittle failure readily under applied force and typically demonstrates poor flexural strength (Lin *et al.*, 2008, Alomayri *et al.*, 2014b). Improving the mechanical properties such as flexural strength and toughness of geopolymers will significantly increase its application in the construction and building industries; and this may be accomplished by developing ‘environmental-friendly materials’ through utilizing natural fibres as fibre-reinforced geopolymer composite (Bernal *et al.*, 2012).

The advantages of using natural fibres in composites include the low density, flexibility and the high modulus (Herrera-Franco and Valadez-González, 2005, Bohlooli *et al.*, 2012). Other advantages in addition to good mechanical properties

include biodegradable, renewable and recyclable nature of natural fibres (Low *et al.*, 2007b). These characteristics have made natural fibres attractive to be utilized as reinforcement in various composites systems. For instance, cellulose extracted from wood materials is used to strengthen polymers and epoxy (Zadorecki and Michell, 1989, Low *et al.*, 2009). Bamboo and wood fibres are also used in the strengthening of concrete and known for the flexural advantages (Rahman *et al.*, 2011, Lin *et al.*, 1994). Flax and wool fibres have also shown positive effects when used in geopolymer composites. These fibres improved the fracture and mechanical properties of these composites (Alzeer and MacKenzie, 2013, Alzeer and MacKenzie, 2012).

In this chapter, the fabrication of eco or "green" composites using cotton fibres (CF) and flax fibre (FF) as reinforcement of fly ash geopolymer matrices was investigated. Scanning electron microscopy (SEM) was used to investigate microstructure and interface of geopolymer/natural fibres composites. The effect of CF and FF contents on physical, thermal and mechanical properties was evaluated in the study.

2. Experimental Procedures

2.1 Materials and preparation

Low calcium fly-ashes (ASTM class F), collected from the Collie power station in WA (CFA) and the Erraring power station in NSW (EFA), were used as the source material for the geopolymer matrices. The chemical compositions of the fly-ashes are shown in Table 1. The alkaline activator for geopolymerisation was a combination of sodium hydroxide and sodium silicate grade D solution. Sodium hydroxide flakes of 98% purity were used to prepare the solution. The chemical composition of sodium silicate used was 14.7% Na_2O, 29.4% SiO_2 and 55.9% water by mass.

Table 1: Chemical compositions of Erraring and Collie fly-ash (wt%).

	SiO_2	Al_2O_3	CaO	Fe_2O_3	K_2O	MgO	Na_2O	SO_3	LOI
EFA	63.13	24.88	2.58	3.07	2.01	0.61	0.71	0.18	1.45
CFA	50.00	28.25	1.78	13.5	0.46	0.89	0.32	0.38	1.64

Flax fabric (FF) and cotton fabric (CF) were used for the reinforcement of geopolymer composites separately. The description and physical properties of the natural fibres are given in Table. 2. The space between the yarns is essential to allow the geopolymer matrix to penetrate.

Table 2: Structure and physical properties of the flax fabric.

	FF	CF
Fabric thickness (mm)	0.60	0.41
Fabric geometry	Woven (plain weave)	Woven (plain weave)
Yarn nature	Bundle	Bundle
Bundle diameter (mm)	0.6 (see Fig. 1a)	0.23
Filament size (mm)	0.01-0.02 (see Fig. 1b)	0.04
Opening size (mm)	2-4	0.5
Fabric density (g/cm^3)	1.5	1.6
Tensile strength (MPa)	660	400

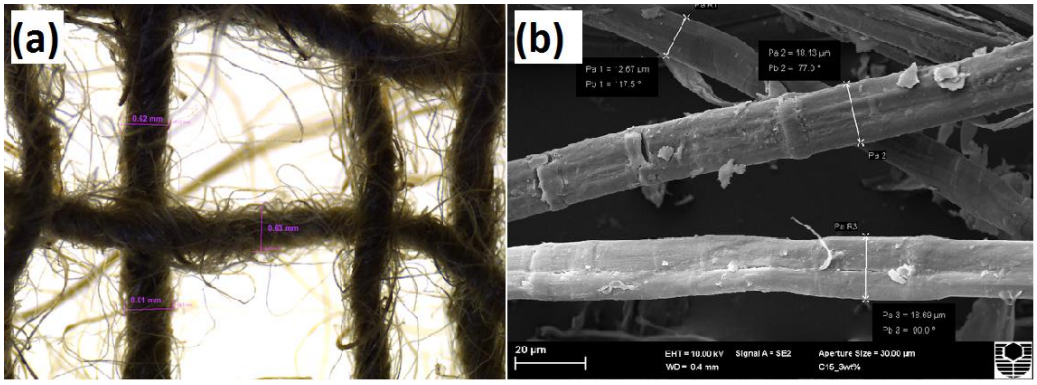

Figure.1: Diameters of the (a) flax bundle and (b) flax fibres.

The amounts of alkaline solutions were varied depending on the fly-ash type in order to produce geopolymer matrices with the highest strength. The alkaline solution to fly-ash ratios were 0.75 and 0.35 in the case of EFA and CFA, respectively. The ratio of sodium silicate solution to sodium hydroxide solution was fixed at 2.5 while the concentration of sodium hydroxide solution was 8 M in both types of fly-ash. The alkaline liquid was prepared and combined with the sodium silicate solution one day before mixing.

The fly-ash and alkaline solution were mixed in a Hobart mixer at a low speed for 5-10 min, and for another 10 min at high speed. To cast the pure geopolymer and composite samples, wooden moulds with open tops were greases to avoid the geopolymer samples sticking during demoulding. A thin layer of geopolymer paste was spread in the wooden mould, and the first layer of the natural fabric (FF or CF) was carefully laid on that layer. The fabric was then covered by another layer of geopolymer paste, and the process repeated for desired number of fabric layers. Each sample contained a different number of FF or CF. For each sample; the final layer was geopolymer material. The geopolymer composites then were left under heavy weight for 1 hour to reduce entrapped air inside the samples. All samples were covered with plastic film and cured in the oven before demoulding. They were then dried under ambient conditions for 28 days. The geopolymer pastes, and composites produced using EFA as source material, and various contents of FF were labelled as EGP, EGPFF-1, EGPFF-2 and EGPFF-3. While, the geopolymer paste produced using CFA and reinforced with different contents of CF were denoted as CGP and CGPCF-1, CGPCF-2, CGPCF-3 and CGPCF-4. The formulations of all geopolymer samples and composites are shown in Table. 3.

Table 3: Formulation of samples.

Sample	EFA (g)	CFA (g)	NaOH solution (g)	Na_2SiO_3 solution (g)	FF		CF	
					Layers	(wt%)	Layers	(wt%)
EGP	1000	0	214.5	535.5	0	0	0	0
EGPFF-1	1000	0	214.5	535.5	5	2.4	0	0
EGPFF -2	1000	0	214.5	535.5	7	3.0	0	0

EGPFF -3	1000	0	214.5	535.5	10	4.1	0	0
CGP	0	1000	100	249.5	0	0	0	0
CGPCF-1	0	1000	100	249.5	0	0	2	1.4
CGPCF-2	0	1000	100	249.5	0	0	3	2.1
CGPCF-3	0	1000	100	249.5	0	0	4	2.8
CGPCF-4	0	1000	100	249.5	0	0	6	4.1

2.2 Physical and Mechanical Properties

Measurements of bulk density and porosity were conducted to define the quality of geopolymer nanocomposite. Density of samples (ρ) with volume (V) and dry mass (m_d) was calculated using Equation 1:

$$\rho = \frac{m_d}{V} \tag{1}$$

The value of apparent porosity (P_a) was determined using Archimedes' principle in accordance with the ASTM Standard (C-20) . Pure geopolymer and nano-composite samples were immersed in clean water, and the apparent porosity (P_a) was calculated using Equation 2:

$$P_a = \frac{m_a - m_d}{m_a - m_w} \times 100 \tag{2}$$

Where m_a is mass of the saturated samples in air, and m_w is mass of the saturated samples in water.

A LLOYD Material Testing Machine (50kN capacity) with a displacement rate of 1 mm/min was used to perform the mechanical tests. Rectangular bars with a span of 40mm were cut from the fully cured samples for three-point bend tests to evaluate the mechanical properties. All samples were aligned horizontally to the applied load in all mechanical tests. Five samples of each composite were used to evaluate the flexural strength according to the standard ASTM D790. The values were recorded and analysed with the machine software (NEXYGENPlus) and average values were calculated. The flexural strength **(σ_F)** was determined using the equation:

$$\sigma_F = \frac{3}{2}\frac{p_m S}{WD^2} \tag{3}$$

Where P_m is the maximum load at crack extension, S is the span of the sample, D is the specimen width and W is the specimen thickness.

Flexural modulus (E_f) values were computed using the initial slope of the load displacement curve **(ΔP/ΔX)** using as follows:

$$E_F = \frac{S^3}{4WD^3}\left(\frac{\Delta P}{\Delta X}\right) \quad (4)$$

A crack with a length to width (a/W) ratio of 0.4 was introduced into the specimen using a 0.4 mm diamond blade to evaluate fracture toughness. The fracture toughness (K_{IC}) was calculated using the equation:

$$K_{IC} = \frac{p_m S}{WD^{2/3}} f\left(\frac{a}{W}\right) \quad (5)$$

Where a is the crack length, and f(a/w) is the polynomial geometrical correction factor given by:

$$f\left(\frac{a}{W}\right) = \frac{3(a/W)^{1/2}\left[1.99 - (a/W)(1 - a/W) \times (2.15 - 3.93a/W + 2.7a^2/W^2)\right]}{2(1 + 2a/W)(1 - a/W)^{2/3}} \quad (6)$$

3. Results and Discussion

3.1 Physical properties

The results of measured density and porosity of all samples are shown in Table 4. It can be seen in general that the composites containing natural fibres have higher porosity and lower density than those samples without natural fibres. This is generally because of the low density of flax and cotton fibres. It may also be attributed to the hydrophilic nature of cellulose fibres, which creates voids in the interfacial region between the natural fibres and the matrices (Alomayri *et al.*, 2014a). The increase in porosity could also be due to voids becoming trapped beneath the natural fibres sheets during casting, creating higher porosity, and thus leading to poor adhesion between the fibre and matrix. It is also worth mentioning here that the pure geopolymer produced using CFA is higher in density than the counterparts EFA geopolymer due to the high content of iron in CFA geopolymer (Rickard *et al.*, 2015, Rickard *et al.*, 2011). After the addition of natural fibres, however, the composites in both geopolymer matrices (EGP and CGP) exhibited comparable physical results.

Table 4: Density and porosity values of all samples.

Sample	Fibre content (wt %)	Density (g/cm3)	Porosity (%)
EGP	0	1.84±0.02	22.2
EGPFF-1	2.4	1.72±0.04	26.7
EGPFF -2	3.0	1.63±0.02	31.2
EGPFF -3	4.1	1.58±0.02	33.7
CGP	0	2.02 ± 0.03	21.1
CGPCF-1	1.4	1.84 ± 0.02	24.8
CGPCF-2	2.1	1.76 ± 0.02	26.2
CGPCF-3	2.8	1.68 ± 0.03	29.6
CGPCF-4	4.1	1.59 ± 0.05	32.6

3.2 Mechanical properties

3.2.1 Flexural strength and flexural modulus:

Flexural tests are used to characterise the mechanical properties of layered composites as they provide a simple means of determining the bending response. This provides useful information on the performance of layered fabric-based composites. The effect of fibre content on the flexural strength of all samples is shown in Fig. 2. In the case of geopolymer composites reinforced with FF, it can be seen that samples containing 4.1 wt% exhibited the highest flexural strength among all composites. The flexural strength of composites improved from 4.5 MPa in EGP to about 23 MPa with 4.1 wt% FF. This result is comparable with that of short flax fibre reinforced geopolymer composites reported by Alzeer and MacKenzie (2013). Both investigations showed that increasing the content of flax fibres leads to a significant improvement in the flexural strength of the composite. This can be explained by the fact that the number of reinforcement layers controls the flexural strength. The lower density of flax fabrics also allows multiple layers of fabric in the composite to resist the shear failure and contribute in sustaining the applied load to the composites. This permits greater stress transfer between the matrix and the flax fibres, resulting in improved flexural strength (Sim *et al.*, 2005). However, in the case of geopolymer reinforced with cotton fabrics, the flexural strength increased with the addition of cotton contents up to 2.1 wt%, and after that the strength of the

composites decreased. The optimum addition of 2.1 wt% CF has provided the highest flexural strength when compared to other composites reinforced with CF. Increasing the amount of cotton fibres to 2.8 and 4.1 wt%, on the contrary, has resulted in a reduction in the flexural strength. This reduction might be caused by misalignment of the cotton fabric, which is due to the procedure of preparation. This imperfection affects the mechanical properties of the composites because the misalignment can lead to the inability of the fibre to support stress transferred from the geopolymer matrix and poor interfacial bonding between the fibre and the matrix. Therefore, the strength of geopolymer composites decreased with the increase in the cotton fabric content beyond 2.1 wt%. The flexural modulus of geopolymer composites as a function of fibre contents is shown in Fig. 3. The results indicate that the addition of CF and FF to the matrices has improved the flexural modulus over that of pure geopolymer materials. Similar trends to that of flexural strength have been observed in the flexural modulus of all samples.

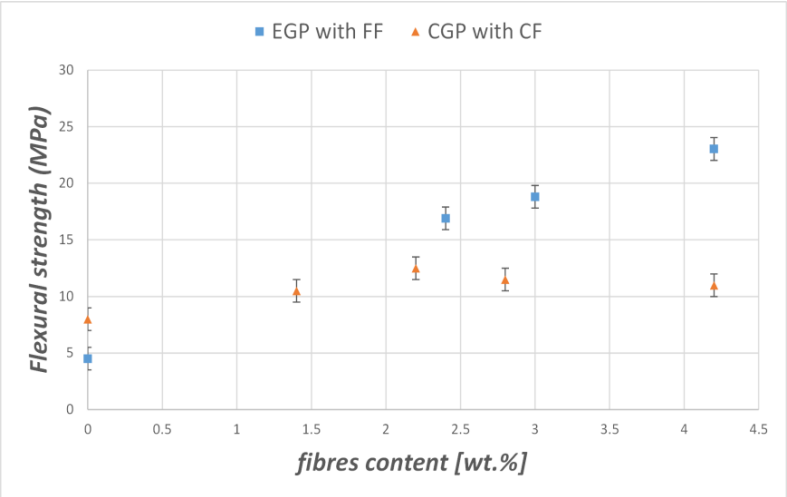

Figure.2: Flexural strength of geopolymer composite as a function of natural fibres content.

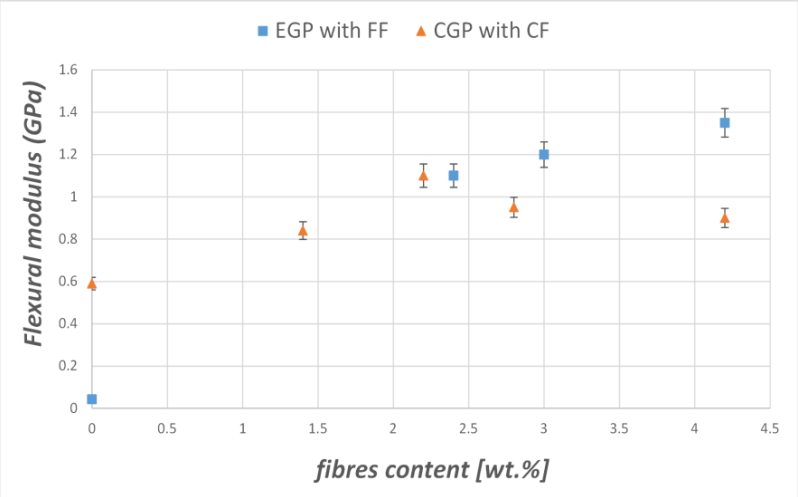

Figure.3: Flexural modulus of geopolymer composite as a function of natural fibres content.

3.2.2 Fracture Toughness:

In general, fibres' ability to resist crack deflection, debonding, and to bridge cracks, slows down crack propagation in fibre reinforced composites and thus increases the fracture energy (Reis, 2006, Silva *et al.*, 2009). Nonetheless, overall the materials are tougher due to the various toughness mechanisms provided by natural fibres. Fig. 4 shows the influence of FF and CF content on the fracture toughness of geopolymer composites. The fracture toughness results in both FF and CF reinforced geopolymer composites displayed an overall improvement due to the various toughness mechanisms mentioned earlier. In the case of FF-reinforced geopolymer composites, the samples showed significantly higher fracture toughness than the pure geopolymer matrix. It has been found that the higher the FF content, the higher is the fracture toughness. The greatest improvement in fracture toughness was obtained from about 0.4 MPa$\cdot$m$^{1/2}$ in EGP to about 1.8 MPa.m$^{1/2}$ with 4.1 wt% FF reinforcement.

While in the case of CF-reinforced geopolymer composites, the higher values of fracture toughness were obtained at lower cotton fibre content (2.1 wt%), as shown in Fig. 4. This enhancement in fracture toughness at 2.1 wt% cotton fibre is due to the embedding of cotton fibre in the geopolymer matrix, which resulted in better adhesion between fibres and the geopolymer paste because the spaces between fibres in the cotton fabric were filled by the geopolymer pastes, thus improved the energy absorption capacity of composites (Pakravan *et al.*, 2011). However, a reduction in

the fracture toughness results occurred when higher contents of CF were incorporated in geopolymer materials. This is thought to be due to the variation in the amount of geopolymer binder that penetrates the openings in the fabric. The penetration of geopolymer binder into the fabric may be maximized when a sufficient amount of the binder holds the fabric together, and gives better adhesion between the fabric and matrix. As the quantity of fabric increased, the amount of binder diminished, and less was available to penetrate through the fabric openings. As a result, the limited amount of binder penetrating the space of the fabric was not sufficient to improve the bonding between the fabric and the matrix. This limitation resulted in a reduction in bonding; fibre pull-out occurs readily and composites exhibit poor toughness results.

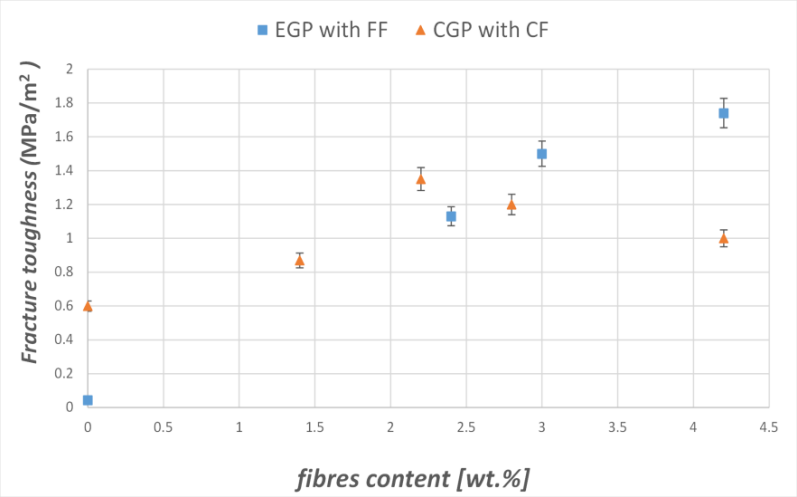

Figure.4: Fracture toughness of geopolymer composite as a function of natural fibres content.

3.3 Microstructure of Geopolymer Composites

The microstructural analyses of fracture surfaces of geopolymer composites are shown in Figs. 5. This extraordinary enhancement was due to the unique ability of the natural fibres to resist fracture resulted in increased energy dissipation from crack-deflection at the fibre–matrix interface, fibre-debonding, fibre-bridging, fibre pull-out and fracture, clearly shown in the SEM images.

The effect of FF content on the fracture surface can be seen by observing the difference between the matrix region and the fibre region. In Figs. 5(a) and 5(b),

composites filled with lower fibre contents (2.4 and 3.0 wt%) showed an increase in matrix-rich regions, which means there were insufficient fibres to transfer the load from the matrices. Due to this reason, the geopolymer composites with low fibre content exhibited low fracture toughness and mechanical properties. However, Fig. 5(c) illustrates the fracture surfaces of the geopolymer composites with higher fibre content, which means higher fibre-rich regions of composites with 4.1 wt% of FF. An increase in fibre-rich regions resulted in greater stress-transfer from the matrix to the FF thereby resulting in improvement of fracture toughness.

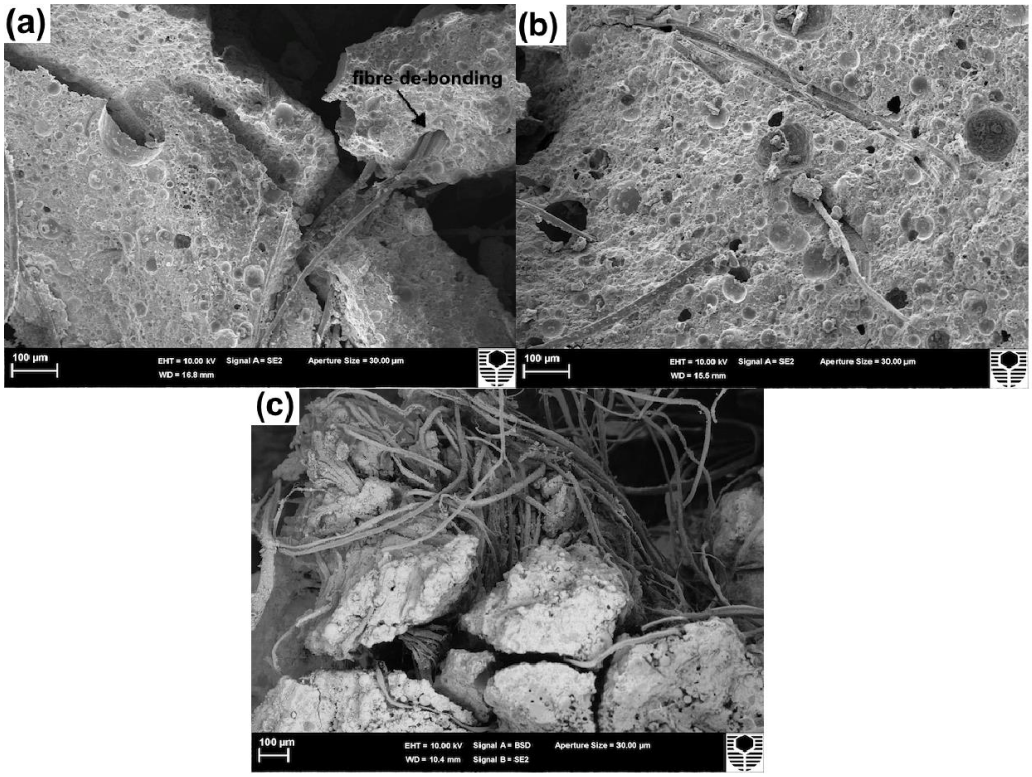

Figure.5: SEM micrographs of the fracture surface of geopolymer composites reinforced with varying contents of FF (a) fibre debonding in EGPFF-1, (b) fibre imprint and pull-out in EGPFF-2 and (c) fibre bridging cracks EGPFF-3.

In the case of CF-reinforced geopolymers, the composites with 1.4 and 2.1 wt% CF show better penetration of the matrix between the fabric openings (see Fig. 6a &b). This leads to enhancement in the interfacial bonding between the fibre and matrix. However, Fig. 6c& d clearly indicated that fibre pull-out is relatively high, and the bonding between cotton fibres and geopolymer matrices was very poor. In addition, micro-cracks can be seen in the fracture surfaces of geopolymer composites with 4.1 wt% cotton fibre, which confirms that fibre–matrix de-bonding has occurred, and

thus strength has been reduced. This is clear evidence that the fibre matrix interfacial adhesion is better for CFGs with 1.4 and 2.1 wt% than for those with 2.8 and 4.1 wt%.

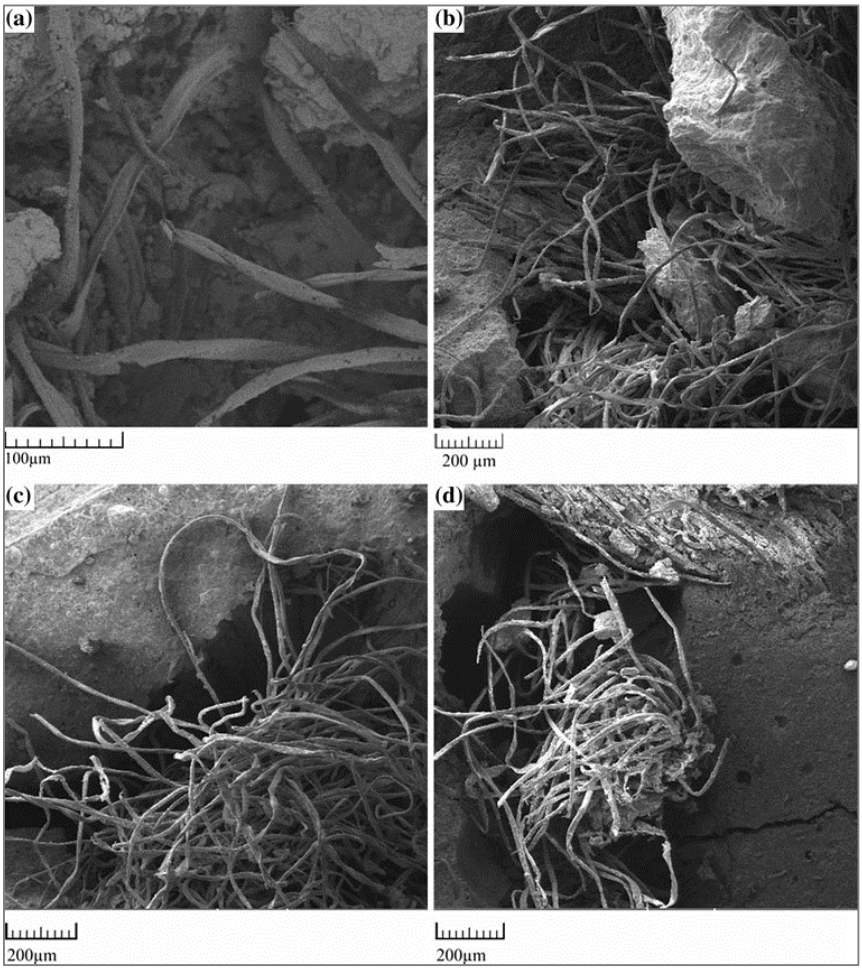

Figure.6: SEM micrographs of the fracture surface of geopolymer composites reinforced with varying contents of CF (a) CGPCF-1, (b) CGPCF-2, (c) CGPCF-3 and (d) CGPCF-4.

3.4 Thermal behaviour:

The thermal behaviour of the natural fibres, geopolymer samples and geopolymer composites were determined using thermogravimetric analysis (TGA). In this test, thermal stability was studied in terms of the weight loss percentage as a function of temperature in argon atmosphere. The TGA test results of FF, EGP, and FF-reinforced geopolymer composite are presented in Fig. 7a, and the results of CF, CGP and CF-reinforced geopolymer composite are presented in Fig. 7b.

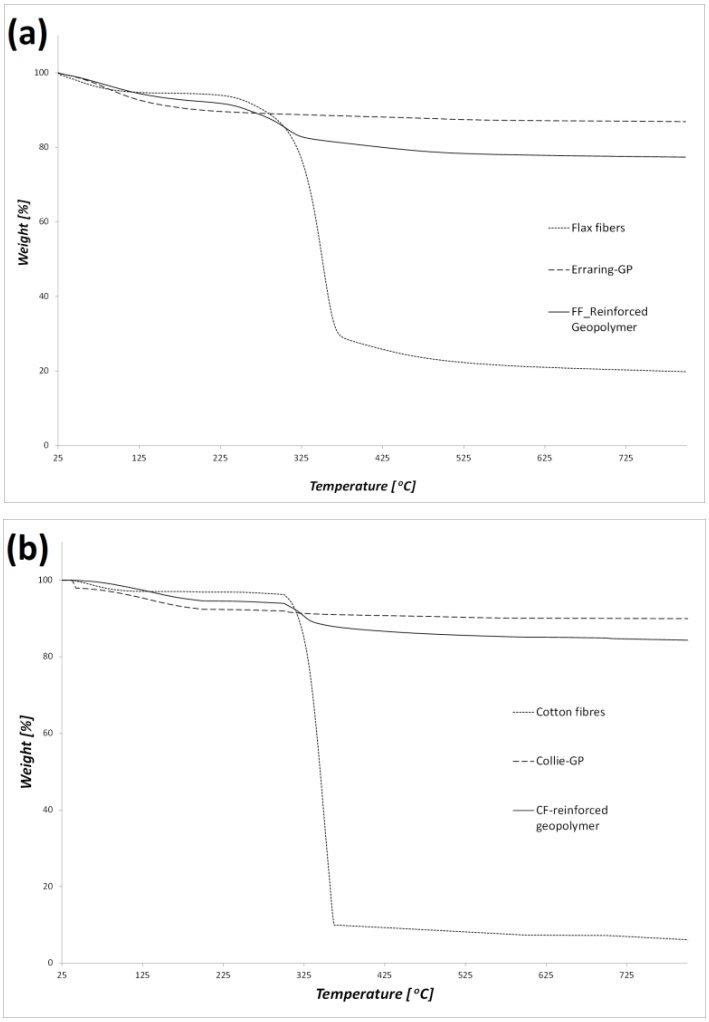

Figure.7: TGA curves of: (a) FF, EGP and EGPFF composite, and (b CF, CGP and CGPCF composite.

The thermogram of FF and CF shows comparable degradation process that can be categorized in three steps. The first transition occurs from 25 to approximately 240°C, with the release of free water evaporation. Then, the largest weight loss occurred between 240 and 370 °C is due to the decomposition of cellulose. This thermal behavior of FF and CF is in agreement with Alzeer and MacKenzie (2013), where the highest weight loss of short flax fibres under flowing air is in the range of 240–340 °C. The final stage occurs above 365-800 °C, when the natural fibres start to decompose but display a lower rate of weight loss, and all volatile substances are dispelled. At 800 °C, FF and CF retained about 20% and 6% of their original weight, respectively. The pure geopolymers (EGP and CGP) showed weight loss occurring from 25 to 300 °C, caused by the evaporation of physically adsorbed water. Above

300 °C, weight loss is attributed to the dehydroxylation of the chemically bound water.

The FF and CF reinforced geopolymer composite showed comparable behavior as well. A weight loss of 10.5% up to about 260 °C, which is due to the evaporation of physically absorbed water. Above 260 °C, the composites shows further weight loss because of the degradation of the natural fibres inside the composites. The porosity of geopolymer matrices allowed the heat to enter and cause degradation of the natural fibres (FF and CF) at high temperatures. The composite showed a total weight loss of 15% and ~10% at 300 °C in the case of EGPFF and CGPCF, respectively, which indicates further degradation of fibres inside the composite. At this temperature a substantial amount of fibre degradation has occurred. The Composite CGPCF was slightly more stable than EGPFF due the lower content of water used in the preparation process of the Collie-geopolymer. Also, the differences on thermal stability at this temperature could be attributed to the difference in physical structures and porosity of the matrices as CGP has lower porosity when compared to EGP matrix. Generally, it could be concluded here that this composite system is only suitable for service below 250°C. It is worth mentioning here that the TGA micro-sample is not necessarily representative of the whole composite sample because the distribution of natural fibres is not uniform within the geopolymer matrices. Consequently, the fibre content of the TGA micro-sample will be highly dependent on the position it is taken from the composite sample. However, TGA test can provide a good estimation of the thermal stability of a composite when compared to the thermal stability of its components.

4. Conclusion

This chapter presents the mechanical and thermal properties as well as microstructural characterisation of geopolymer composites reinforced with flax and cotton fabrics. It shows that the presence of the natural fibres in geopolymer composites significantly increased the flexural strength and modulus, and fracture toughness as compared to the pure geopolymer. The mechanical strength increased at an optimum fibre content of 2.1 wt% in the case of cotton fibres composites. However, increases in cotton fibre content beyond 2.1 wt% caused a reduction in the

mechanical properties due to poor fibre–matrix interfacial bonding. On the other hand, composites reinforced with flax-fibres exhibited higher mechanical strength when compared to those reinforced with cotton fibres. The significant enhancements in FF-composites were due to the unique mechanical properties of flax fibres in resisting greater bending and fracture forces. Thermogravimetric analysis of the composites indicated that natural fibre-geopolymer composites exhibited higher net weight loss than pure geopolymer due to the degradation of the fibres at temperatures higher than 250°C.

APPENDIX III: Statements of Contributions of Others

Statement of Contribution of Others to "Characterisation of Mechanical and Thermal Properties in Flax Fabric Reinforced Geopolymer Composites".

25 March 2017

To Whom It May Concern

I, Prof. I.M. Low, contributed by project supervision and manuscript editing to the paper/publication entitled

Assaedi, H., Alomayri, T., Shaikh, F.U. and Low, I.M., 2015. Characterisation of mechanical and thermal properties in flax fabric reinforced geopolymer composites. *Journal of Advanced Ceramics*, *4*(4), pp.272-281.

Undertaken with Hasan Assaedi

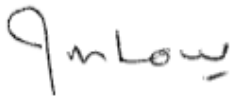

(Signature of Co-Author)
I.M. Low

(Signature of First Author)
Hasan Assaedi

Statement of Contribution of Others to "Characterisation of Mechanical and Thermal Properties in Flax Fabric Reinforced Geopolymer Composites".

25 March 2017

To Whom It May Concern

I, Dr. F.U.A. Shaikh, contributed by project supervision and manuscript editing to the paper/publication entitled

Assaedi, H., Alomayri, T., Shaikh, F.U. and Low, I.M., 2015. Characterisation of mechanical and thermal properties in flax fabric reinforced geopolymer composites. *Journal of Advanced Ceramics*, *4*(4), pp.272-281.

Undertaken with Hasan Assaedi

(Signature of Co-Author)
F. U. A. Shaikh

(Signature of First Author)
Hasan Assaedi

Statement of Contribution of Others to "Characterisation of Mechanical and Thermal Properties in Flax Fabric Reinforced Geopolymer Composites".

25 March 2017

To Whom It May Concern

I, Mr. Thamer Alomayri, provided technical assistance during the preparation and testing of geopolymer composite samples to the paper/publication entitled.

Assaedi, H., Alomayri, T., Shaikh, F.U. and Low, I.M., 2015. Characterisation of mechanical and thermal properties in flax fabric reinforced geopolymer composites. *Journal of Advanced Ceramics*, *4*(4), pp.272-281.

Undertaken with Hasan Assaedi

(Signature of Co-Author)
T. Alomayri

(Signature of First Author)
Hasan Assaedi

Statement of Contribution of Others to "Effect of Nano-clay on Mechanical and Thermal Properties of Geopolymer".

25 March 2017

To Whom It May Concern

I, Prof. I.M. Low, contributed by project supervision and manuscript editing to the paper/publication entitled

Assaedi, H., Shaikh, F.U.A. and Low, I.M., 2016. Effect of nano-clay on mechanical and thermal properties of geopolymer. *Journal of Asian Ceramic Societies*, *4*(1), pp.19-28.

Undertaken with Hasan Assaedi

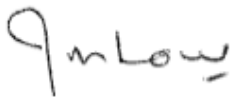

(Signature of Co-Author)
I.M. Low

(Signature of First Author)
Hasan Assaedi

Statement of Contribution of Others to "Effect of Nano-clay on Mechanical and Thermal Properties of Geopolymer"

25 March 2017

To Whom It May Concern

I, Dr. F.U.A. Shaikh, contributed by project supervision and manuscript editing to the paper/publication entitled

Assaedi, H., Shaikh, F.U.A. and Low, I.M., 2016. Effect of nano-clay on mechanical and thermal properties of geopolymer. *Journal of Asian Ceramic Societies*, *4*(1), pp.19-28.

Undertaken with Hasan Assaedi

(Signature of Co-Author)
F. U. A. Shaikh

(Signature of First Author)
Hasan Assaedi

Statement of Contribution of Others to "Characterizations of Flax Fabric Reinforced Nanoclay-Geopolymer Composites".

25 March 2017

To Whom It May Concern

I, Prof. I.M. Low, contributed by project supervision and manuscript editing to the paper/publication entitled

Assaedi, H., Shaikh, F.U.A. and Low, I.M., 2016. Characterizations of flax fabric reinforced nanoclay-geopolymer composites. *Composites Part B: Engineering*, *95*, pp.412-422.

Undertaken with Hasan Assaedi

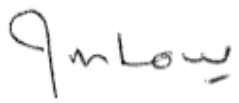

(Signature of Co-Author)
I.M. Low

(Signature of First Author)
Hasan Assaedi

Statement of Contribution of Others to "Characterizations of Flax Fabric Reinforced Nanoclay-Geopolymer Composites"

25 March 2017

To Whom It May Concern

I, Dr. F.U.A. Shaikh, contributed by project supervision and manuscript editing to the paper/publication entitled

Assaedi, H., Shaikh, F.U.A. and Low, I.M., 2016. Characterizations of flax fabric reinforced nanoclay-geopolymer composites. *Composites Part B: Engineering*, *95*, pp.412-422.

Undertaken with Hasan Assaedi

(Signature of Co-Author)
F. U. A. Shaikh

(Signature of First Author)
Hasan Assaedi

Statement of Contribution of Others to "Influence of Mixing Methods of Nano Silica on the Microstructural and Mechanical Properties of Flax Fabric Reinforced Geopolymer Composites".

25 March 2017

To Whom It May Concern

I, Prof. I.M. Low, contributed by project supervision and manuscript editing to the paper/publication entitled

Assaedi, H., Shaikh, F.U.A. and Low, I.M., 2016. Influence of mixing methods of nano silica on the microstructural and mechanical properties of flax fabric reinforced geopolymer composites. *Construction and Building Materials*, *123*, pp.541-552.

Undertaken with Hasan Assaedi

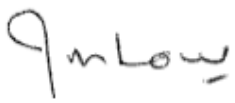

(Signature of Co-Author)
I.M. Low

(Signature of First Author)
Hasan Assaedi

Statement of Contribution of Others to "Influence of Mixing Methods of Nano Silica on the Microstructural and Mechanical Properties of Flax Fabric Reinforced Geopolymer Composites".

25 March 2017

To Whom It May Concern

I, Dr. F.U.A. Shaikh, contributed by project supervision and manuscript editing to the paper/publication entitled

Assaedi, H., Shaikh, F.U.A. and Low, I.M., 2016. Influence of mixing methods of nano silica on the microstructural and mechanical properties of flax fabric reinforced geopolymer composites. *Construction and Building Materials*, *123*, pp.541-552.

Undertaken with Hasan Assaedi

(Signature of Co-Author)
F. U. A. Shaikh

(Signature of First Author)
Hasan Assaedi

Statement of Contribution of Others to "Effect of Nanoclay on the Durability and Mechanical Properties of Geopolymer Composites".

25 March 2017

To Whom It May Concern

I, Prof. I.M. Low, contributed by project supervision and manuscript editing to the paper/publication entitled

Assaedi, H., Shaikh, F.U.A. and Low, I.M., 2017. Effect of nanoclay on durability and mechanical properties of flax fabric reinforced geopolymer composites. *Journal of Asian Ceramic Societies*, *5(1)*, pp.62-70.

Undertaken with Hasan Assaedi

(Signature of Co-Author)
I.M. Low

(Signature of First Author)
Hasan Assaedi

Statement of Contribution of Others to "Effect of Nanoclay on the Durability and Mechanical Properties of Geopolymer Composites".

25 March 2017

To Whom It May Concern

I, Dr. F.U.A. Shaikh, contributed by project supervision and manuscript editing to the paper/publication entitled

Assaedi, H., Shaikh, F.U.A. and Low, I.M., 2017. Effect of nanoclay on durability and mechanical properties of flax fabric reinforced geopolymer composites. *Journal of Asian Ceramic Societies*, *5(1)*, pp.62-70.

Undertaken with Hasan Assaedi

(Signature of Co-Author)
F. U. A. Shaikh

(Signature of First Author)
Hasan Assaedi

APPENDIX IV: Copyright Forms

Appendix IV-2: Copyright information relating to

Assaedi, H., Alomayri, T., Shaikh, F.U. and Low, I.M., 2015. Characterisation of mechanical and thermal properties in flax fabric reinforced geopolymer composites. *Journal of Advanced Ceramics*, *4*(4), pp.272-281.

Copyright Clearance Center

Note: Copyright.com supplies permissions but not the copyrighted content itself.

1 PAYMENT 2 REVIEW 3 CONFIRMATION

Step 3: Order Confirmation

Thank you for your order! A confirmation for your order will be sent to your account email address. If you have questions about your order, you can call us 24 hrs/day, M-F at +1.855.239.3415 Toll Free, or write to us at info@copyright.com. This is not an invoice.

Confirmation Number: 11637882
Order Date: 04/12/2017

If you paid by credit card, your order will be finalized and your card will be charged within 24 hours. If you choose to be invoiced, you can change or cancel your order until the invoice is generated.

Payment Information

Hasan Assaedi
Student
hassaedi@gmail.com
+61 (4)23493904
Payment Method: n/a

Order Details

Journal of Advanced Ceramics

Order detail ID: 70383538
Order License Id: 4086340235252
ISSN: 2226-4108
Publication Type: Journal
Volume:
Issue:
Start page:
Publisher: Springer

Permission Status: Granted
Permission type: Republish or display content
Type of use: Thesis/Dissertation

Requestor type	Author of requested content
Format	Electronic
Portion	chapter/article
Title or numeric reference of the portion(s)	The whole article
Title of the article or chapter the portion is from	Characterisation of mechanical and thermal properties in flax fabric reinforced geopolymer composites
Editor of portion(s)	N/A
Author of portion(s)	Hasan Assaedi
Volume of serial or monograph	4
Issue, if republishing an article from a serial	4

Page range of portion	
Publication date of portion	2015
Rights for	Main product
Duration of use	Current edition and up to 5 years
Creation of copies for the disabled	no
With minor editing privileges	no
For distribution to	Worldwide
In the following language(s)	Original language of publication
With incidental promotional use	no
Lifetime unit quantity of new product	Up to 499
Made available in the following markets	education
The requesting person/organization	Hasan Assaedi
Order reference number	
Author/Editor	Hasan Assaedi
The standard identifier of New Work	Thesis
Title of New Work	Characterization and Development of Flax Fibres Reinforced Geopolymer Nanocomposites
Publisher of New Work	Curtin University
Expected publication date	Apr 2017
Estimated size (pages)	250
Customer Tax ID	6107

Note: This item will be invoiced or charged separately through CCC's **RightsLink** service. More info **$ 0.00**

Appendix IV-2: Copyright information relating to

Assaedi, H., Shaikh, F.U.A. and Low, I.M., 2016. Effect of nano-clay on mechanical and thermal properties of geopolymer. *Journal of Asian Ceramic Societies*, *4*(1), pp.19-28.

PERMISSION TO USE COPYRIGHT MATERIAL AS SPECIFIED BELOW:

Full text of the following article;

Assaedi, H., Shaikh, F.U.A. and Low, I.M., 2016. Effect of nano-clay on mechanical and thermal properties of geopolymer. *Journal of Asian Ceramic Societies*, *4*(1), pp.19-28.

I hereby give permission for Hasan Assaedi to include the abovementioned material in his higher degree thesis for the Curtin University of Technology, and to communicate this material via the Australasian Digital Thesis Program. This permission is granted on a non-exclusive basis and for an indefinite period.

I confirm that I am the copyright owner of the specified material.

Permission to use this material is subject to the following conditions:
*Attribution
*Non-commercial
*No Derivative Works

Signed: Satoru Shimura

Name: Satoru SHIMURA

Position: Secretary General, the Ceramic Society of Japan.

Date: March. 24, 2017

Please email competed copy to: 16892235@student.curtin.edu.au

Appendix IV-3: Copyright information relating to

Assaedi, H., Shaikh, F.U.A. and Low, I.M., 2016. Characterizations of flax fabric reinforced nanoclay-geopolymer composites. *Composites Part B: Engineering*, *95*, pp.412-422.

ELSEVIER LICENSE
TERMS AND CONDITIONS

Aug 11, 2016

This Agreement between Hasan Assaedi ("You") and Elsevier ("Elsevier") consists of your license details and the terms and conditions provided by Elsevier and Copyright Clearance Center.

License Number	3926280626049
License date	Aug 11, 2016
Licensed Content Publisher	Elsevier
Licensed Content Publication	Composites Part B: Engineering
Licensed Content Title	Characterizations of flax fabric reinforced nanoclay-geopolymer composites
Licensed Content Author	H. Assaedi,F.U.A. Shaikh,I.M. Low
Licensed Content Date	15 June 2016
Licensed Content Volume Number	95
Licensed Content Issue Number	n/a
Licensed Content Pages	11
Start Page	412
End Page	422
Type of Use	reuse in a thesis/dissertation
Portion	full article
Format	both print and electronic
Are you the author of this Elsevier article?	Yes
Will you be translating?	No
Order reference number	
Title of your thesis/dissertation	Characterizations and development of flax fabric reinforced geopolymer nanocomposites
Expected completion date	Apr 2017
Estimated size (number of pages)	170
Elsevier VAT number	GB 494 6272 12
Requestor Location	Hasan Assaedi 1/173 Gibbs St. East Cannington, WA 6107 Australia

Appendix IV-4: Copyright information relating to

Assaedi, H., Shaikh, F.U.A. and Low, I.M., 2016. Influence of mixing methods of nano silica on the microstructural and mechanical properties of flax fabric reinforced geopolymer composites. *Construction and Building Materials*, *123*, pp.541-552.

ELSEVIER LICENSE
TERMS AND CONDITIONS

Mar 23, 2017

This Agreement between Hasan Assaedi ("You") and Elsevier ("Elsevier") consists of your license details and the terms and conditions provided by Elsevier and Copyright Clearance Center.

License Number	4075131107938
License date	Mar 23, 2017
Licensed Content Publisher	Elsevier
Licensed Content Publication	Construction and Building Materials
Licensed Content Title	Influence of mixing methods of nano silica on the microstructural and mechanical properties of flax fabric reinforced geopolymer composites
Licensed Content Author	H. Assaedi,F.U.A. Shaikh,I.M. Low
Licensed Content Date	1 October 2016
Licensed Content Volume	123
Licensed Content Issue	n/a
Licensed Content Pages	12
Start Page	541
End Page	552
Type of Use	reuse in a thesis/dissertation
Portion	full article
Format	both print and electronic
Are you the author of this Elsevier article?	Yes
Will you be translating?	No
Order reference number	
Title of your thesis/dissertation	Characterizations and development of flax fabric reinforced geopolymer nanocomposites
Expected completion date	Apr 2017
Estimated size (number of pages)	170
Elsevier VAT number	GB 494 6272 12
Requestor Location	Hasan Assaedi 1/173 Gibbs St. East Cannington, WA 6107 Australia Attn: Hasan Assaedi

APPENDIX IV-5: Copyright information relating to

Assaedi, H., Shaikh, F.U.A. and Low, I.M., 2017. Effect of nanoclay on durability and mechanical properties of flax fabric reinforced geopolymer composites. *Journal of Asian Ceramic Societies*, *5(1)*, pp.62-70.

PERMISSION TO USE COPYRIGHT MATERIAL AS SPECIFIED BELOW:

Full text of the following article;

Assaedi, H., Shaikh, F.U.A. and Low, I.M., 2017. Effect of nanoclay on durability and mechanical properties of flax fabric reinforced geopolymer composites. *Journal of Asian Ceramic Societies*, *5(1)*, pp.62-70.

I hereby give permission for Hasan Assaedi to include the abovementioned material in his higher degree thesis for the Curtin University of Technology, and to communicate this material via the Australasian Digital Thesis Program. This permission is granted on a non-exclusive basis and for an indefinite period.

I confirm that I am the copyright owner of the specified material.

Permission to use this material is subject to the following conditions:
*Attribution
*Non-commercial
*No Derivative Works

Signed:

Name: Satoru SHIMURA

Position: Secretary General, the Ceramic Society of Japan.

Date: March. 24, 2017

Please email competed copy to: 16892235@student.curtin.edu.au

BIBLIOGRAPHY

ABANILLA, M. A., KARBHARI, V. M. & LI, Y. 2006. Interlaminar and intralaminar durability characterization of wet layup carbon/epoxy used in external strengthening. *Composites Part B: Engineering,* 37**,** 650-661.

ABDULLAH, M. M. A. B., HUSSIN, K., BNHUSSAIN, M., ISMAIL, K. N., YAHYA, Z. & ABDUL RAZAK, R. 2012. Fly ash-based geopolymer lightweight concrete using foaming agent. *International Journal of Molecular Sciences,* 13**,** 7186-7198.

ADAK, D., SARKAR, M. & MANDAL, S. 2014. Effect of nano-silica on strength and durability of fly ash based geopolymer mortar. *Construction and Building Materials,* 70**,** 453-459.

AGARWAL, B. D., BROUTMAN, L. J. & CHANDRASHEKHARA, K. 2006. *Analysis and Performance of Fiber Composites*, John Wiley & Sons.

AHMARI, S., REN, X., TOUFIGH, V. & ZHANG, L. 2012. Production of geopolymeric binder from blended waste concrete powder and fly ash. *Construction and Building Materials,* 35**,** 718-729.

AHMARI, S. & ZHANG, L. 2012. Production of eco-friendly bricks from copper mine tailings through geopolymerization. *Construction and Building Materials,* 29**,** 323-331.

AKHTAR, N., GUPTA, K., GOYAL, D. & GOYAL, A. 2015. Recent advances in pretreatment technologies for efficient hydrolysis of lignocellulosic biomass. *Environmental Progress & Sustainable Energy,* 35**,** 489–511.

AL BAKRI, M., MOHD, A., IZZAT, A. M., MUHAMMAD FAHEEM, M., KAMARUDIN, H., KHAIRUL NIZAR, I., BNHUSSAIN, M., RAFIZA, A., ZARINA, Y. & LIYANA, J. 2013. Feasibility of producing wood fibre-reinforced geopolymer composites (WFRGC). *Advanced Materials Research,* 626**,** 918-925.

ALAMRI, H., LOW, I. M. & ALOTHMAN, Z. 2012. Mechanical, thermal and microstructural characteristics of cellulose fibre reinforced epoxy/organoclay nanocomposites. *Composites Part B: Engineering,* 43**,** 2762-2771.

ALDOUSIRI, B., ALAJMI, M. & SHALWAN, A. 2013. Mechanical properties of palm fibre reinforced recycled HDPE. *Advances in Materials Science and Engineering,* 13**,** 1-7.

ALIX, S., MARAIS, S., MORVAN, C. & LEBRUN, L. 2008. Biocomposite materials from flax plants: preparation and properties. *Composites Part A: Applied Science and Manufacturing,* 39**,** 1793-1801.

ALOMAYRI, T. & LOW, I. M. 2013. Synthesis and characterization of mechanical properties in cotton fiber-reinforced geopolymer composites. *Journal of Asian Ceramic Societies,* 1**,** 30-34.

ALOMAYRI, T., SHAIKH, F. U. A. & LOW, I. M. 2013a. Characterisation of cotton fibre-reinforced geopolymer composites. *Composites Part B: Engineering,* 50**,** 1-6.

ALOMAYRI, T., SHAIKH, F. U. A. & LOW, I. M. 2013b. Thermal and mechanical properties of cotton fabric-reinforced geopolymer composites. *Journal of Materials Science,* 48**,** 6746-6752.

ALOMAYRI, T., SHAIKH, F. U. A. & LOW, I. M. 2014a. Effect of fabric orientation on mechanical properties of cotton fabric reinforced geopolymer composites. *Materials and Design,* 57**,** 360-365.

ALOMAYRI, T., SHAIKH, F. U. A. & LOW, I. M. 2014b. Synthesis and mechanical properties of cotton fabric reinforced geopolymer composites. *Composites Part B: Engineering,* 60**,** 36-42.

ALONSO, S. & PALOMO, A. 2001. Alkaline activation of metakaolin and calcium hydroxide mixtures: Influence of temperature, activator concentration and solids ratio. *Materials Letters,* 47**,** 55-62.

ALY, M., HASHMI, M. S. J., OLABI, A. G., MESSEIRY, M. & HUSSAIN, A. I. 2011a. Effect of nano clay particles on mechanical, thermal and physical behaviours of waste-glass cement mortars. *Materials Science and Engineering: A,* 528**,** 7991-7998.

ALY, M., HASHMI, M. S. J., OLABI, A. G., MESSEIRY, M., HUSSAIN, A. I. & ABADIR, E. F. 2011b. Effect of nano-clay and waste glass powder on the properties of flax fibre reinforced mortar. *Journal of Engineering and Applied Sciences,* 6**,** 19-28.

ALZEER, M. & MACKENZIE, K. 2013. Synthesis and mechanical properties of novel composites of inorganic polymers (geopolymers) with unidirectional natural flax fibres (phormium tenax). *Applied Clay Science,* 75-76**,** 148-152.

ALZEER, M. & MACKENZIE, K. J. D. 2012. Synthesis and mechanical properties of new fibre-reinforced composites of inorganic polymers with natural wool fibres. *Journal of Materials Science,* 47**,** 6958-6965.

ARIOZ, E., ARIOZ, O. & KOÇKAR, O. M. 2013. The effect of curing conditions on the properties of geopolymer samples. *International Journal of Chemical Engineering and Applications,* 4**,** 423-426.

ASHORI, A. 2008. Wood–plastic composites as promising green-composites for automotive industries. *Bioresource Technology,* 99**,** 4661-4667.

ASSAEDI, H., ALOMAYRI, T., SHAIKH, F. U. A. & LOW, I. M. 2015a. Characterisation of mechanical and thermal properties in flax fabric reinforced geopolymer composites. *Journal of Advanced Ceramics,* 4**,** 272-281.

ASSAEDI, H., SHAIKH, F. U. A. & LOW, I. M. 2015b. Effect of nano-clay on mechanical and thermal properties of geopolymer. *Journal of Asian Ceramic Societies,* 4**,** 19-28.

ASSAEDI, H., SHAIKH, F. U. A. & LOW, I. M. 2016. Characterizations of flax fabric reinforced nanoclay-geopolymer composites. *Composites Part B: Engineering,* 95**,** 412-422.

AYDIN, S. & BARADAN, B. 2012. Mechanical and microstructural properties of heat cured alkali-activated slag mortars. *Materials and Design,* 35**,** 374-383.

AZWA, Z. N., YOUSIF, B. F., MANALO, A. C. & KARUNASENA, W. 2013. A review on the degradability of polymeric composites based on natural fibres. *Materials and Design,* 47**,** 424-442.

BAKHAREV, T. 2005. Geopolymeric materials prepared using class F fly ash and elevated temperature curing. *Cement and Concrete Research,* 35**,** 1224-1232.

BAKHAREV, T. 2006. Thermal behaviour of geopolymers prepared using class F fly ash and elevated temperature curing. *Cement and Concrete Research,* 36**,** 1134-1147.

BALAGURU, P. N. & SHAH, S. P. 1992. *Fiber-Reinforced Cement Composites,* USA, McGraw-Hill, Inc.

BARBOSA, V. F. F., MACKENZIE, K. J. D. & THAUMATURGO, C. 2000. Synthesis and characterisation of materials based on inorganic polymers of alumina and silica: Sodium polysialate polymers. *International Journal of Inorganic Materials,* 2**,** 309-317.

BAVAN, S. & KUMAR, G. M. 2010. Potential use of natural fiber composite materials in India. *Journal of Reinforced Plastics and Composites,* 29**,** 3600-3613.

BENTUR, A. & MINDESS, S. 2007. *Fibre Reinforced Cementitious Composites,* New York, Taylor & Francis.

BERNAL, S. A., BEJARANO, J., GARZÓN, C., MEJÍA DE GUTIÉRREZ, R., DELVASTO, S. & RODRÍGUEZ, E. D. 2012. Performance of refractory aluminosilicate particle/fiber-reinforced geopolymer composites. *Composites Part B: Engineering,* 43**,** 1919-1928.

BESSADOK, A., MARAIS, S., GOUANVÉ, F., COLASSE, L., ZIMMERLIN, I., ROUDESLI, S. & MÉTAYER, M. 2007. Effect of chemical treatments of Alfa (Stipa tenacissima) fibres on water-sorption properties. *Composites Science and Technology,* 67**,** 685-697.

BIBO, G. & HOGG, P. 1996. The role of reinforcement architecture on impact damage mechanisms and post-impact compression behaviour. *Journal of Materials Science,* 31**,** 1115-1137.

BISMARCK, A., MISHRA, S. & LAMPKE, T. 2005. Plant fibers as reinforcement for green composites. *Natural Fibers, Biopolymers, and Biocomposites.* CRC Press.

BLEDZKI, A. & GASSAN, J. 1999. Composites reinforced with cellulose based fibres. *Progress in Polymer Science,* 24**,** 221-274.

BLEDZKI, A. K., REIHMANE, S. & GASSAN, J. 1996. Properties and modification methods for vegetable fibers for natural fiber composites. *Journal of Applied Polymer Science,* 59**,** 1329-1336.

BOHLOOLI, H., NAZARI, A., KHALAJ, G., KAYKHA, M. M. & RIAHI, S. 2012. Experimental investigations and fuzzy logic modeling of compressive strength of geopolymers with seeded fly ash and rice husk bark ash. *Composites Part B: Engineering,* 43**,** 1293-1301.

BOS, H., VAN DEN OEVER, M. J. & PETERS, O. C. 2002. Tensile and compressive properties of flax fibres for natural fibre reinforced composites. *Journal of Materials Science,* 37**,** 1683-1692.

CALLISTER, W. D. 1991. *Materials Science and Engineering: An Introducton,* New York, John Wiley & Sons.

CÉLINO, A., FRÉOUR, S., JACQUEMIN, F. & CASARI, P. 2013. The hygroscopic behavior of plant fibers: A review. *Frontiers in Chemistry,* 1**,** 1-12.

CHANG, T. P., SHIH, J. Y., YANG, K. M. & HSIAO, T. C. 2007. Material properties of portland cement paste with nano-montmorillonite. *Journal of Materials Science,* 42**,** 7478-7487.

CHEN-TAN, N. W., VAN RIESSEN, A., LY, C. V. & SOUTHAM, D. C. 2009. Determining the reactivity of a fly ash for production of geopolymer. *Journal of the American Ceramic Society,* 92**,** 881-887.

CHEN, R., AHMARI, S. & ZHANG, L. 2014. Utilization of sweet sorghum fiber to reinforce fly ash-based geopolymer. *Journal of Materials Science,* 49**,** 2548-2558.

CHENG, T. & CHIU, J. 2003. Fire-resistant geopolymer produced by granulated blast furnace slag. *Minerals Engineering,* 16**,** 205-210.

CHINDAPRASIRT, P., CHAREERAT, T. & SIRIVIVATNANON, V. 2007. Workability and strength of coarse high calcium fly ash geopolymer. *Cement and Concrete Composites,* 29**,** 224-229.

CHINDAPRASIRT, P., JATURAPITAKKUL, C., CHALEE, W. & RATTANASAK, U. 2009. Comparative study on the characteristics of fly ash and bottom ash geopolymers. *Waste Management,* 29**,** 539-543.

CHINDAPRASIRT, P., RATTANASAK, U. & TAEBUANHUAD, S. 2013. Resistance to acid and sulfate solutions of microwave-assisted high calcium fly ash geopolymer. *Materials and Structures,* 46**,** 375-381.

CIOFFI, R., MAFFUCCI, L. & SANTORO, L. 2003. Optimization of geopolymer synthesis by calcination and polycondensation of a kaolinitic residue. *Resources, Conservation and Recycling,* 40**,** 27-38.

CLEMONS, C. M. & CAUFIELD, D. F. 2005. *Wood Flour. Functional Fillers for Plastics*, Wiley-VCH Verlag GmbH, Weinheim.

CORREIA, E. A. S., TORRES, S. M., DE OLIVEIRA ALEXANDRE, M. E., GOMES, K. C., P BARBOSA, N. & DE BARROS, S. R. 2013. Mechanical performance of natural fibers reinforced geopolymer composites. *Materials Science Forum,* 758**,** 139-145.

CURVELO, A., DE CARVALHO, A. & AGNELLI, J. 2001. Thermoplastic starch–cellulosic fibers composites: preliminary results. *Carbohydrate Polymers,* 45**,** 183-188.

DAVIDOVITS, J. 2002. Years of successes and failures in geopolymer applications. Market trends and potential breakthroughs. Keynote Speech at Geopolymer Conference, Melbourne, Australia.

DAVIDOVITS, J. 1989. Geopolymers and geopolymeric materials. *Journal of Thermal Analysis,* 35**,** 429-441.

DAVIDOVITS, J. 1991. Geopolymers - Inorganic polymeric new materials. *Journal of Thermal Analysis,* 37**,** 1633-1656.

DAVIDOVITS, J. 1994a. Global warming impact on the cement and aggregates industries. *World Resource Review,* 6**,** 263-278.

DAVIDOVITS, J. 1994b. Properties of geopolymer cements. *Proceedings First International Conference.* Saint-Quentin, France. 131-149.

DAVIDOVITS, J. 2008. *Geopolymer Chemistry and Applications,* Saint-Quentin, FR., Geopolymer Institute.

DE, S. & WHITE, J. 1996. *Short Fibre-Polymer Composites*, Elsevier.

DE VARGAS, A. S., DAL MOLIN, D. C. C., VILELA, A. C. F., SILVA, F. J. D., PAVÃO, B. & VEIT, H. 2011. The effects of Na_2O/SiO_2 molar ratio, curing temperature and age on compressive strength, morphology and microstructure of alkali-activated fly ash-based geopolymers. *Cement and Concrete Composites,* 33**,** 653-660.

DEER, W. A., HOWIE, R. A. & ZUSSMAN, J. 1996. *An Introduction to the Rock-Forming Minerals,* England, Essex.

DETPHAN, S. & CHINDAPRASIRT, P. 2009. Preparation of fly ash and rice husk ash geopolymer. *International Journal of Minerals, Metallurgy and Materials,* 16**,** 720-726.

DHAKAL, H., ZHANG, Z. & RICHARDSON, M. 2007. Effect of water absorption on the mechanical properties of hemp fibre reinforced unsaturated polyester composites. *Composites Science and Technology,* 67**,** 1674-1683.

DIMAS, D., GIANNOPOULOU, I. & PANIAS, D. 2009. Polymerization in sodium silicate solutions: A fundamental process in geopolymerization technology. *Journal of Materials Science,* 44**,** 3719-3730.

DITTENBER, D. B. & GANGARAO, H. V. 2012. Critical review of recent publications on use of natural composites in infrastructure. *Composites Part A: Applied Science and Manufacturing,* 43**,** 1419-1429.

DUXSON, P., FERNÁNDEZ-JIMÉNEZ, A., PROVIS, J. L., LUKEY, G. C., PALOMO, A. & VAN DEVENTER, J. S. J. 2007a. Geopolymer technology: The current state of the art. *Journal of Materials Science,* 42**,** 2917-2933.

DUXSON, P., MALLICOAT, S. W., LUKEY, G. C., KRIVEN, W. M. & VAN DEVENTER, J. S. J. 2007b. The effect of alkali and Si/Al ratio on the development of mechanical properties of metakaolin-based geopolymers. *Colloids and Surfaces A: Physicochemical and Engineering Aspects,* 292**,** 8-20.

DWEIB, M., HU, B., O'DONNELL, A., SHENTON, H. & WOOL, R. 2004. All natural composite sandwich beams for structural applications. *Composite Structures,* 63**,** 147-157.

FARZADNIA, N., ABANG ALI, A. A., DEMIRBOGA, R. & ANWAR, M. P. 2013. Effect of halloysite nanoclay on mechanical properties, thermal behavior and microstructure of cement mortars. *Cement and Concrete Research,* 48**,** 97-104.

FERNÁNDEZ-JIMÉNEZ, A., PALOMO, A. & CRIADO, M. 2005. Microstructure development of alkali-activated fly ash cement: a descriptive model. *Cement and Concrete Research,* 35**,** 1204-1209.

FERONE, C., COLANGELO, F., ROVIELLO, G., ASPRONE, D., MENNA, C., BALSAMO, A., PROTA, A., CIOFFI, R. & MANFREDI, G. 2013. Application-oriented chemical optimization of a metakaolin based geopolymer. *Materials,* 6**,** 1920-1939.

FILHO, J. O. D., SILVA, D. A. & TOLEDO, R. D. 2013. Degradation kinetics and aging mechanisms on sisal fiber cement composite systems. *Cement and Concrete Composites,* 40**,** 30-39.

FOWLER, P. A., HUGHES, J. M. & ELIAS, R. M. 2006. Biocomposites: technology, environmental credentials and market forces. *Journal of the Science of Food and Agriculture,* 86**,** 1781-1789.

GAO, K., LIN, K. L., WANG, D., HWANG, C. L., SHIU, H. S., CHANG, Y. M. & CHENG, T. W. 2014. Effects SiO_2/Na_2O molar ratio on mechanical properties and the microstructure of nano-SiO_2 metakaolin-based geopolymers. *Construction and Building Materials,* 53**,** 503-510.

GIASUDDIN, H. M., SANJAYAN, J. G. & RANJITH, P. G. 2013. Strength of geopolymer cured in saline water in ambient conditions. *Fuel,* 107**,** 34-39.

GIVI, A. N., RASHID, S. A., AZIZ, F. N. A. & SALLEH, M. A. M. 2010. Investigations on the development of the permeability properties of binary blended concrete with nano-SiO_2 particles. *Journal of Composite Materials,* 45**,** 1931-1938.

GORHAN, G. & KURKLU, G. 2014. The Influence of the NaOH solution on the properties of the fly ash-based geopolymer mortar cured at different temperatures. *Composites Part B: Engineering,* 58**,** 371-377.

GOURLEY, J. 2003. Geopolymers; opportunities for environmentally friendly construction materials. *Materials Conference: Adaptive Materials for a Modern Society.* Institute of Materials Engineering Australia, Sydney. 15-26.

GRAM, H.-E. 1983. Methods for reducing the tendency towards embrittlement in sisal fibre concrete. *Nordic Concrete Research,* 5**,** 62-71.

GUNASEKARA, M., LAW, D. & SETUNGE, S. 2014. Effect of composition of fly ash on compressive strength of fly ash based geopolymer mortar. *23rd Australasian Conference on the Mechanics of Structures and Materials (ACMSM23).* Southern Cross University, Lismore, NSW. 113-114.

GUO, X., SHI, H. & DICK, W. A. 2010. Compressive strength and microstructural characteristics of class C fly ash geopolymer. *Cement and Concrete Composites,* 32**,** 142-147.

HAKAMY, A., SHAIKH, F. U. A. & LOW, I. M. 2013a. Microstructures and mechanical properties of hemp fabric reinforced organoclay–cement nanocomposites. *Construction and Building Materials,* 49**,** 298-307.

HAKAMY, A., SHAIKH, F. U. A. & LOW, I. M. 2013b. Thermal and mechanical properties of hemp fabric-reinforced nanoclay–cement nanocomposites. *Journal of Materials Science,* 49**,** 1684-1694.

HAKAMY, A., SHAIKH, F. U. A. & LOW, I. M. 2014. Characteristics of hemp fabric reinforced nanoclay–cement nanocomposites. *Cement and Concrete Composites,* 50**,** 27-35.

HAKAMY, A., SHAIKH, F. U. A. & LOW, I. M. 2015a. Characteristics of nanoclay and calcined nanoclay-cement nanocomposites. *Composites Part B: Engineering,* 78**,** 174-184.

HAKAMY, A., SHAIKH, F. U. A. & LOW, I. M. 2015b. Thermal and mechanical properties of NaOH treated hemp fabric and calcined nanoclay-reinforced cement nanocomposites. *Materials and Design,* 80**,** 70-81.

HAKAMY, A., SHAIKH, F. U. A. & LOW, I. M. 2016. Effect of calcined nanoclay on the durability of NaOH treated hemp fabric-reinforced cement nanocomposites. *Materials and Design,* 92**,** 659-666.

HANJITSUWAN, S., HUNPRATUB, S., THONGBAI, P., MAENSIRI, S., SATA, V. & CHINDAPRASIRT, P. 2014. Effects of NaOH concentrations on physical and electrical properties of high calcium fly ash geopolymer paste. *Cement and Concrete Composites,* 45**,** 9-14.

HANUS, M. J. & HARRIS, A. T. 2013. Nanotechnology innovations for the construction industry. *Progress in Materials Science,* 58**,** 1056-1102.

HE, J., JIE, Y., ZHANG, J., YU, Y. & ZHANG, G. 2013. Synthesis and characterization of red mud and rice husk ash-based geopolymer composites. *Cement and Concrete Composites,* 37**,** 108-118.

HE, J., ZHANG, G., ZHANG, J. & YU, Y. 2012. The strength and microstructure of two geopolymers derived from metakaolin and red mud- fly ash admixture: A comparative study. *Construction and Building Materials,* 30**,** 80-91.

HE, X. & SHI, X. 2008. Chloride Permeability and Microstructure of Portland Cement Mortars Incorporating Nanomaterials. *Transportation Research Record: Journal of the Transportation Research Board,* 2070**,** 13-21.

HEAH, C., KAMARUDIN, H., AL BAKRI, A. M., BINHUSSAIN, M., LUQMAN, M., NIZAR, I. K., RUZAIDI, C. & LIEW, Y. 2011. Effect of curing profile on kaolin-based geopolymers. *Physics Procedia,* 22**,** 305-311.

HERRERA-FRANCO, P. J. & VALADEZ-GONZÁLEZ, A. 2005. A study of the mechanical properties of short natural-fiber reinforced composites. *Composites Part B: Engineering,* 36**,** 597-608.

HOLBERY, J. & HOUSTON, D. 2006. Natural-fiber-reinforced polymer composites in automotive applications. *Journal of the Minerals, Metals and Materials Society,* 58**,** 80-86.

HOSSEINI, P., HOSSEINPOURPIA, R., PAJUM, A., KHODAVIRDI, M. M., IZADI, H. & VAEZI, A. 2014. Effect of nano-particles and aminosilane interaction on the performances of cement-based composites: An experimental study. *Construction and Building Materials,* 66**,** 113-124.

HU, M., ZHU, X. & LONG, F. 2009. Alkali-activated fly ash-based geopolymers with zeolite or bentonite as additives. *Cement and Concrete Composites,* 31**,** 762-768.

HUNG, T. D., PERNICA, D., KROISOVÁ, D., BORTNOVSKY, O., LOUDA, P. & RYLICHOVA, V. 2008. Composites base on geopolymer matrices: Preliminary fabrication, mechanical properties and future applications. *Advanced Materials Research,* 55**,** 477-480.

HUSSAIN, F., HOJJATI, M., OKAMOTO, M. & GORGA, R. E. 2006. Review article: Polymer-matrix Nanocomposites, Processing, Manufacturing, and Application: An Overview. *Journal of Composite Materials,* 40**,** 1511-1575.

ISLAM, A., ALENGARAM, U. J., JUMAAT, M. Z. & BASHAR, I. I. 2014. The development of compressive strength of ground granulated blast furnace slag-palm oil fuel ash-fly ash based geopolymer mortar. *Materials and Design,* 56**,** 833-841.

JANSEN, M. S. & CHRISTIANSEN, M. U. Effect of water-solids ratio on the compressive strength and morphology of fly ash-waste glass geopolymer mortars. 2015 World of Coal Ash (WOCA), 2015 Nasvhille, Tennessee. 5-7.

JO, B. W., KIM, C. H., TAE, G. H. & PARK, J. B. 2007. Characteristics of cement mortar with nano-SiO_2 particles. *Construction and Building Materials,* 21**,** 1351-1355.

JOHN, M. J. & THOMAS, S. 2008. Biofibres and biocomposites. *Carbohydrate Polymers,* 71**,** 343-364.

JOHN, S., NILMINI, P., AMANDEEP, S. & HALL, W. 2010. A review of bast fibers and their composites. Part 1: fibers as reinforcement. *Composites Part A: Applied Science and Manufacturing,* 41**,** 1329-1335.

JUN, Y. & OH, J. 2015. Use of gypsum as a preventive measure for strength deterioration during curing in class F fly ash geopolymer system. *Materials,* 8**,** 3053-3067.

KAMSEU, E., NAIT-ALI, B., BIGNOZZI, M., LEONELLI, C., ROSSIGNOL, S. & SMITH, D. 2012. Bulk composition and microstructure dependence of

effective thermal conductivity of porous inorganic polymer cements. *Journal of the European Ceramic Society,* 32**,** 1593-1603.

KANI, E. N. & ALLAHVERDI, A. 2009. Effects of curing time and temperature on strength development of inorganic polymeric binder based on natural pozzolan. *Journal of Materials Science,* 44**,** 3088-3097.

KHALE, D. & CHAUDHARY, R. 2007. Mechanism of geopolymerization and factors influencing its development: A review. *Journal of Materials Science,* 42**,** 729-746.

KHALIL, M. Y. & MERZ, E. 1994. Immobilization of intermediate-level wastes in geopolymers. *Journal of Nuclear Materials,* 211**,** 141-148.

KIM, H. & KIM, Y. 2013. Relationship between compressive strength of geo-polymers and pre-curing conditions. *Applied Microscopy,* 43**,** 155-163.

KOMLJENOVIĆ, M., BAŠČAREVIĆ, Z. & BRADIĆ, V. 2010. Mechanical and microstructural properties of alkali-activated fly ash geopolymers. *Journal of Hazardous Materials,* 181**,** 35-42.

KOMNITSAS, K. & ZAHARAKI, D. 2007. Geopolymerisation: A review and prospects for the minerals industry. *Minerals Engineering,* 20**,** 1261-1277.

KONG, D. L. Y. & SANJAYAN, J. G. 2010. Effect of elevated temperatures on geopolymer paste, mortar and concrete. *Cement and Concrete Research,* 40**,** 334-339.

KONG, D. L. Y., SANJAYAN, J. G. & SAGOE-CRENTSIL, K. 2007. Comparative performance of geopolymers made with metakaolin and fly ash after exposure to elevated temperatures. *Cement and Concrete Research,* 37**,** 1583-1589.

KONG, D. L. Y., SANJAYAN, J. G. & SAGOE-CRENTSIL, K. 2008. Factors affecting the performance of metakaolin geopolymers exposed to elevated temperatures. *Journal of Materials Science,* 43**,** 824-831.

KORNIEJENKO, K., FRĄCZEK, E., PYTLAK, E. & ADAMSKI, M. 2016. Mechanical properties of geopolymer composites reinforced with natural fibers. *Procedia Engineering,* 151**,** 388-393.

KRIVEN, W. M., BELL, J. L. & GORDON, M. 2003. Microstructure and microchemistry of fully-reacted geopolymers and geopolymer matrix composites. *Ceramic Transactions,* 153**,** 227-250.

KUTCHKO, B. G. & KIM, A. G. 2006. Fly ash characterization by SEM–EDS. *Fuel,* 85**,** 2537-2544.

LAI, C. Y., GROTH, A., GRAY, S. & DUKE, M. 2014. Preparation and characterization of poly(vinylidene fluoride)/nanoclay nanocomposite flat sheet membranes for abrasion resistance. *Water Research,* 57**,** 56-66.

LATELLA, B. A., PERERA, D. S., DURCE, D., MEHRTENS, E. G. & DAVIS, J. 2008. Mechanical properties of metakaolin-based geopolymers with molar ratios of Si/Al ≈ 2 and Na/Al ≈ 1. *Journal of Materials Science,* 43**,** 2693-2699.

LAW, D., ADAM, A., MOLYNEAUX, T., PATNAIKUNI, I. & WARDHONO, A. 2014. Long term durability properties of class F fly ash geopolymer concrete. *Materials and Structures,* 48**,** 1-11.

LEE, S. H., DOHERTY, T. V., LINHARDT, R. J. & DORDICK, J. S. 2009. Ionic liquid-mediated selective extraction of lignin from wood leading to enhanced enzymatic cellulose hydrolysis. *Biotechnology and Bioengineering,* 102**,** 1368-1376.

LEE, W. K. W. & VAN DEVENTER, J. S. J. 2002. Structural reorganisation of class F fly ash in alkaline silicate solutions. *Colloids and Surfaces A: Physicochemical and Engineering Aspects,* 211**,** 49-66.

LEMBO, K., LOKUGE, W. & KARUNASENA, W. 2014. Geopolymer concrete with FRP confinement. *23rd Australasian Conference on the Mechanics of Structures and Materials (ACMSM23).* Southern Cross University, Lismore, NSW. 483-84.

LI, G. 2004. Properties of high-volume fly ash concrete incorporating nano-SiO_2. *Cement and Concrete Research,* 34**,** 1043-1049.

LI, Q., XU, H., LI, F., LI, P., SHEN, L. & ZHAI, J. 2012. Synthesis of geopolymer composites from blends of CFBC fly and bottom ashes. *Fuel,* 97**,** 366-372.

LI, W. & XU, J. 2009. Impact characterization of basalt fiber reinforced geopolymeric concrete using a 100-mm-diameter split Hopkinson pressure bar. *Materials Science and Engineering: A,* 513**,** 145-153.

LI, Z., DING, Z. & ZHANG, Y. 2004. Development of sustainable cementitious materials. *Proceedings of the International Workshop on Sustainable Development and Concrete Technology.* Beijing, China. 55-76.

LIEFKE, E. 1999. Industrial applications of foamed inorganic polymers. *Geopolymer '99 Intl. Conf. Proc'.* Saint-Quentin, France. 189-200.

LIEW, Y. M., HEAH, C. Y., MOHD MUSTAFA, A. & KAMARUDIN, H. 2016. Structure and properties of clay-based geopolymer cements: A review. *Progress in Materials Science,* 83**,** 595-629.

LILHOLT, H. & LAWTHER, J. 2000. *Natural Organic Fibers*, Elsevier, Oxford.

LIN, T., JIA, D., HE, P., WANG, M. & LIANG, D. 2008. Effects of fiber length on mechanical properties and fracture behavior of short carbon fiber reinforced geopolymer matrix composites. *Materials Science and Engineering A,* 497**,** 181-185.

LIN, T., JIA, D., WANG, M., HE, P. & LIANG, D. 2009. Effects of fibre content on mechanical properties and fracture behaviour of short carbon fibre reinforced geopolymer matrix composites. *Bulletin of Materials Science,* 32**,** 77-81.

LIN, X., SILSBEE, M. R., ROY, D. M., KESSLER, K. & BLANKENHORN, P. R. 1994. Approaches to improve the properties of wood fiber reinforced cementitious composites. *Cement and Concrete Research,* 24**,** 1558-1566.

LIZCANO, M., GONZALEZ, A., BASU, S., LOZANO, K. & RADOVIC, M. 2012. Effects of water content and chemical composition on structural properties of alkaline activated metakaolin-based geopolymers. *Journal of the American Ceramic Society,* 95**,** 2169-2177.

LOW, I. M., MCGRATH, M., LAWRENCE, D., SCHMIDT, P., LANE, J., LATELLA, B. A. & SIM, K. S. 2007a. Mechanical and fracture properties of cellulose-fibre-reinforced epoxy laminates. *Composites Part A: Applied Science and Manufacturing,* 38**,** 963-974.

LOW, I. M., SCHMIDT, P. & LANE, J. 1995. Synthesis and properties of cellulose-fibre/epoxy laminates. *Journal of Materials Science Letters,* 14**,** 170-172.

LOW, I. M., SOMERS, J., KHO, H. S., DAVIES, I. J. & LATELLA, B. A. 2009. Fabrication and properties of recycled cellulose fibre-reinforced epoxy composites. *Composite Interfaces,* 16**,** 659-669.

LOW, I. M., SOMERS, J. & PANG, W. K. 2007b. Synthesis and properties of recycled paper-nano-clay-reinforced epoxy eco-composites. *Key Engineering Materials,* 334**,** 609-612.

MCLELLAN, B. C., WILLIAMS, R. P., LAY, J., VAN RIESSEN, A. & CORDER, G. D. 2011. Costs and carbon emissions for geopolymer pastes in comparison to ordinary portland cement. *Journal of Cleaner Production,* 19**,** 1080-1090.

MISHRA, A., CHOUDHARY, D., JAIN, N., KUMAR, M., SHARDA, N. & DUTT, D. 2008. Effect of concentration of alkaline liquid and curing time on strength and water absorption of geopolymer concrete. *Journal of Engineering and Applied Science,* 3**,** 14-18.

MOHAMED, A. M. 2016. Influence of nano materials on flexural behavior and compressive strength of concrete. *HBRC Journal,* 12**,** 212-225.

MOHANTY, A., MISRA, M. & DRZAL, L. 2002. Sustainable bio-composites from renewable resources: opportunities and challenges in the green materials world. *Journal of Polymers and the Environment,* 10**,** 19-26.

MOHANTY, A. K., MISRA, M. & DRZAL, L. T. 2005. *Natural Fibers, Biopolymers, and Biocomposites*, CRC Press.

MOHR, B. J., BIERNACKI, J. J. & KURTIS, K. E. 2007. Supplementary cementitious materials for mitigating degradation of kraft pulp fiber-cement composites. *Cement and Concrete Research,* 37**,** 1531-1543.

MOHR, B. J., NANKO, H. & KURTIS, K. E. 2005. Durability of kraft pulp fiber–cement composites to wet/dry cycling. *Cement and Concrete Composites,* 27**,** 435-448.

MORSY, M. S. & AGLAN, H. A. 2007. Development and characterization of nanostructured-perlite-cementitious surface compounds. *Journal of Materials Science,* 42**,** 10188-10195.

MORSY, M. S., AGLAN, H. A. & ABD EL RAZEK, M. M. 2009. Nanostructured zonolite–cementitious surface compounds for thermal insulation. *Construction and Building Materials,* 23**,** 515-521.

MWAIKAMBO, L. Y. & ANSELL, M. P. 2002. Chemical modification of hemp, sisal, jute, and kapok fibers by alkalization. *Journal of Applied Polymer Science,* 84**,** 2222-2234.

NATALI, A., MANZI, S. & BIGNOZZI, M. 2011. Novel fiber-reinforced composite materials based on sustainable geopolymer matrix. *Procedia Engineering,* 21**,** 1124-1131.

NAZARI, A., BAGHERI, A. & RIAHI, S. 2011. Properties of geopolymer with seeded fly ash and rice husk bark ash. *Materials Science and Engineering A,* 528**,** 7395-7401.

NAZARI, A. & SANJAYAN, J. G. 2015. Hybrid effects of alumina and silica nanoparticles on water absorption of geopolymers: Application of Taguchi approach. *Measurement,* 60**,** 240-246.

PACHECO-TORGAL, F., ABDOLLAHNEJAD, Z., MIRALDO, S., BAKLOUTI, S. & DING, Y. 2012. An overview on the potential of geopolymers for concrete infrastructure rehabilitation. *Construction and Building Materials,* 36**,** 1053-1058.

PACHECO-TORGAL, F. & JALALI, S. 2011. Cementitious building materials reinforced with vegetable fibres: A review. *Construction and Building Materials,* 25**,** 575-581.

PAKRAVAN, H., JAMSHIDI, M., LATIFI, M. & NESHASTEHRIZ, M. 2011. Application of polypropylene nonwoven fabrics for cement composites reinforcement. *Asian Journal of Civil Engineering (Building and Housing),* 12**,** 551-562.

PALOMO, A., BLANCO-VARELA, M. T., GRANIZO, M. L., PUERTAS, F., VAZQUEZ, T. & GRUTZECK, M. W. 1999a. Chemical stability of cementitious materials based on metakaolin. *Cement and Concrete Research,* 29**,** 997–1004.

PALOMO, A., GRUTZECK, M. W. & BLANCO, M. T. 1999b. Alkali-activated fly ashes: A cement for the future. *Cement and Concrete Research,* 29**,** 1323-1329.

PAN, Z. & SANJAYAN, J. G. 2010. Stress–strain behaviour and abrupt loss of stiffness of geopolymer at elevated temperatures. *Cement and Concrete Composites,* 32**,** 657-664.

PAN, Z., SANJAYAN, J. G. & RANGAN, B. V. 2011. Fracture properties of geopolymer paste and concrete. *Magazine of Concrete Research,* 63**,** 763-771.

PANGDAENG, S., SATA, V., AGUIAR, J. B., PACHECO-TORGAL, F. & CHINDAPRASIRT, P. 2015. Apatite formation on calcined kaolin-white Portland cement geopolymer. *Materials Science and Engineering C,* 51**,** 1-6.

PART, W. K., RAMLI, M. & CHEAH, C. B. 2015. An overview on the influence of various factors on the properties of geopolymer concrete derived from industrial by-products. *Construction and Building Materials,* 77**,** 370-395.

PERERA, D. S., UCHIDA, O., VANCE, E. R. & FINNIE, K. S. 2007. Influence of curing schedule on the integrity of geopolymers. *Journal of Materials Science,* 42**,** 3099-3106.

PERERA, D. S., VANCE, E. R., FINNIE, K. S., BLACKFORD, M. G., HANNA, J. V. & CASSIDY, D. J. 2005. Disposition of water in metakaolinite based geopolymers. *Advances in Ceramic Matrix Composites XI,* 175**,** 225-236.

PERNÁ, I., HANZLÍČEK, T. & ŠUPOVÁ, M. 2014. The identification of geopolymer affinity in specific cases of clay materials. *Applied Clay Science,* 102**,** 213-219.

PERNICA, D., REIS, P. N. B., FERREIRA, J. A. M. & LOUDA, P. 2010. Effect of test conditions on the bending strength of a geopolymer-reinforced composite. *Journal of Materials Science,* 45**,** 744-749.

PETTERSEN, R. C. 1984. The chemical composition of wood. *Advances in Chemistry,* 207**,** 57-126.

PHAIR, J. W. & VAN DEVENTER, J. S. J. 2002. Effect of the silicate activator pH on the microstructural characteristics of waste-based geopolymers. *International Journal of Mineral Processing,* 66**,** 121-143.

PHOO-NGERNKHAM, T., CHINDAPRASIRT, P., SATA, V., HANJITSUWAN, S. & HATANAKA, S. 2014. The effect of adding nano-SiO_2 and nano-Al_2O_3 on properties of high calcium fly ash geopolymer cured at ambient temperature. *Materials and Design,* 55**,** 58-65.

PICKERING, K. L. 2008. *Properties and Performance of Natural-Fibre Composites,* Boca Raton, CRC Press, Cambridge, England.

PICKERING, K. L., BECKERMANN, G., ALAM, S. & FOREMAN, N. J. 2007. Optimising industrial hemp fibre for composites. *Composites Part A: Applied Science and Manufacturing,* 38**,** 461-468.

PICKERING, K. L., EFENDY, M. A. & LE, T. M. 2016. A review of recent developments in natural fibre composites and their mechanical performance. *Composites Part A: Applied Science and Manufacturing,* 83**,** 98-112.

PIMENTA, S. & PINHO, S. T. 2011. Recycling carbon fibre reinforced polymers for structural applications: Technology review and market outlook. *Waste Management,* 31**,** 378-392.

PUERTAS, F., AMAT, T., FERNÁNDEZ-JIMÉNEZ, A. & VÁZQUEZ, T. 2003. Mechanical and durable behaviour of alkaline cement mortars reinforced with polypropylene fibres. *Cement and Concrete Research,* 33**,** 2031-2036.

QING, Y., ZENAN, Z., DEYU, K. & RONGSHEN, C. 2007. Influence of nano-SiO_2 addition on properties of hardened cement paste as compared with silica fume. *Construction and Building Materials,* 21**,** 539-545.

QUANJI, Z., LOMBOY, G. R. & WANG, K. 2014. Influence of nano-sized highly purified magnesium alumino silicate clay on thixotropic behavior of fresh cement pastes. *Construction and Building Materials,* 69**,** 295-300.

RAHIER, H., SIMONS, W., VAN MELE, B. & BIESEMANS, M. 1997. Low-temperature synthesized aluminosilicate glasses: Part III Influence of the composition of the silicate solution on production, structure and properties. *Journal of Materials Science,* 32**,** 2237-2247.

RAHIER, H., WASTIELS, J., BIESEMANS, M., WILLLEM, R., VAN ASSCHE, G. & VAN MELE, B. 2007. Reaction mechanism, kinetics and high temperature transformations of geopolymers. *Journal of Materials Science,* 42**,** 2982-2996.

RAHMAN, M. M., RASHID, M. H., HOSSAIN, M. A., HASAN, M. T. & HASAN, M. K. 2011. Performance evaluation of bamboo reinforced concrete beam. *International Journal of Engineering & Technology,* 11**,** 142-146.

RATTANASAK, U. & CHINDAPRASIRT, P. 2009. Influence of NaOH solution on the synthesis of fly ash geopolymer. *Minerals Engineering,* 22**,** 1073-1078.

RATTANASAK, U., CHINDAPRASIRT, P. & SUWANVITAYA, P. 2010. Development of high volume rice husk ash alumino silicate composites. *International Journal of Minerals, Metallurgy and Materials,* 17**,** 654-659.

REES, C. A., PROVIS, J. L., LUKEY, G. C. & VAN DEVENTER, J. S. J. 2008. The mechanism of geopolymer gel formation investigated through seeded nucleation. *Colloids and Surfaces A: Physicochemical and Engineering Aspects,* 318**,** 97-105.

REIS, J. M. L. 2006. Fracture and flexural characterization of natural fiber-reinforced polymer concrete. *Construction and Building Materials,* 20**,** 673-678.

RIAHI, S. & NAZARI, A. 2012. The effects of nanoparticles on early age compressive strength of ash-based geopolymers. *Ceramics International,* 38**,** 4467-4476.

RICKARD, W. D. A., KEALLEY, C. S., VAN RIESSEN, A. & BIERNAKI, J. 2015. Thermally induced microstructural changes in fly ash geopolymers: experimental results and proposed model. *Journal of the American Ceramic Society,* 98**,** 929-939.

RICKARD, W. D. A., WILLIAMS, R., TEMUUJIN, J. & VAN RIESSEN, A. 2011. Assessing the suitability of three Australian fly ashes as an aluminosilicate source for geopolymers in high temperature applications. *Materials Science and Engineering: A,* 528**,** 3390-3397.

RIDTIRUD, C., CHINDAPRASIRT, P. & PIMRAKSA, K. 2011. Factors affecting the shrinkage of fly ash geopolymers. *International Journal of Minerals, Metallurgy and Materials,* 18**,** 100-104.

RILL, E., LOWRY, D. R. & KRIVEN, W. M. 2010. Properties of Basalt Fiber Reinforced Geopolymer Composites. *In Strategic Materials and Computational Design.* John Wiley & Sons, Inc.

RONG, Z., SUN, W., XIAO, H. & JIANG, G. 2015. Effects of nano-SiO_2 particles on the mechanical and microstructural properties of ultra-high performance cementitious composites. *Cement and Concrete Composites,* 56**,** 25-31.

RÖSLER, J., HARDERS, H. & BAEKER, M. 2007. *Mechanical Behaviour of Engineering Materials: Metals, Ceramics, Polymers, and Composites*, Springer Science & Business Media.

ROVNANÍK, P. 2010. Effect of curing temperature on the development of hard structure of metakaolin-based geopolymer. *Construction and Building Materials,* 24**,** 1176-1183.

ROWLES, M. & O'CONNOR, B. 2003. Chemical optimisation of the compressive strength of aluminosilicate geopolymers synthesised by sodium silicate activation of metakaolinite. *Journal of Materials Chemistry,* 13**,** 1161-1165.

SAAFI, M., ANDREW, K., TANG, P. L., MCGHON, D., TAYLOR, S., RAHMAN, M., YANG, S. & ZHOU, X. 2013. Multifunctional properties of carbon nanotube/fly ash geopolymeric nanocomposites. *Construction and Building Materials,* 49**,** 46-55.

SALIH, M. A., ABANG ALI, A. A. & FARZADNIA, N. 2014. Characterization of mechanical and microstructural properties of palm oil fuel ash geopolymer cement paste. *Construction and Building Materials,* 65**,** 592-603.

SANCHEZ, F. & SOBOLEV, K. 2010. Nanotechnology in concrete – A review. *Construction and Building Materials,* 24**,** 2060-2071.

SANTOS, S. F. D., TONOLI, G. H. D., MEJIA, J., FIORELLI, J. & SAVASTANO JR, H. 2015. Non-conventional cement-based composites reinforced with vegetable fibers: A review of strategies to improve durability. *Materiales de Construcción,* 65**,** 41-42.

SATHONSAOWAPHAK, A., CHINDAPRASIRT, P. & PIMRAKSA, K. 2009. Workability and strength of lignite bottom ash geopolymer mortar. *Journal of Hazardous Materials,* 168**,** 44-50.

SATYANARAYANA, K., SUKUMARAN, K., MUKHERJEE, P., PAVITHRAN, C. & PILLAI, S. 1990. Natural fibre-polymer composites. *Cement and Concrete Composites,* 12**,** 117-136.

SCHNEIDER, H., SCHREUER, J. & HILDMANN, B. 2008. Structure and properties of mullite—A review. *Journal of the European Ceramic Society,* 28**,** 329-344.

SEDAN, D., PAGNOUX, C., SMITH, A. & CHOTARD, T. 2008. Mechanical properties of hemp fibre reinforced cement: Influence of the fibre/matrix interaction. *Journal of the European Ceramic Society,* 28**,** 183-192.

SENFF, L., TOBALDI, D. M., LUCAS, S., HOTZA, D., FERREIRA, V. M. & LABRINCHA, J. A. 2013. Formulation of mortars with nano-SiO_2 and nano-TiO_2 for degradation of pollutants in buildings. *Composites Part B: Engineering,* 44**,** 40-47.

SHAIKH, F., SUPIT, S. & SARKER, P. 2014. A study on the effect of nano silica on compressive strength of high volume fly ash mortars and concretes. *Materials and Design,* 60**,** 433-442.

SHAIKH, F. U. A. 2013. Review of mechanical properties of short fibre reinforced geopolymer composites. *Construction and Building Materials,* 43**,** 37-49.

SHAIKH, F. U. A. & SUPIT, S. W. M. 2014. Mechanical and durability properties of high volume fly ash (HVFA) concrete containing calcium carbonate ($CaCO_3$) nanoparticles. *Construction and Building Materials,* 70**,** 309-321.

SILVA, F. D. A., MOBASHER, B. & FILHO, R. D. T. 2009. Cracking mechanisms in durable sisal fiber reinforced cement composites. *Cement and Concrete Composites,* 31**,** 721-730.

SILVA, F. D. A., MOBASHER, B., SORANAKOM, C. & FILHO, R. D. T. 2011. Effect of fiber shape and morphology on interfacial bond and cracking behaviors of sisal fiber cement based composites. *Cement and Concrete Composites,* 33**,** 814-823.

SILVA, F. J. & THAUMATURGO, C. 2003. Fibre reinforcement and fracture response in geopolymeric mortars. *Fatigue and Fracture of Engineering Materials and Structures,* 26**,** 167-172.

SIM, J., PARK, C. & MOON, D. Y. 2005. Characteristics of basalt fiber as a strengthening material for concrete structures. *Composites Part B-Engineering,* 36**,** 504-512.

SINGH, L. P., GOEL, A., BHATTACHHARYYA, S. K., AHALAWAT, S., SHARMA, U. & MISHRA, G. 2015. Effect of morphology and dispersibility of silica nanoparticles on the mechanical behaviour of cement mortar. *International Journal of Concrete Structures and Materials,* 9**,** 207-217.

SINGH, L. P., KARADE, S. R., BHATTACHARYYA, S. K., YOUSUF, M. M. & AHALAWAT, S. 2013. Beneficial role of nanosilica in cement based materials – A review. *Construction and Building Materials,* 47**,** 1069-1077.

SOLEIMANI, M., NAGHIZADEH, R., MIRHABIBI, A. & GOLESTANIFARD, F. 2012. Effect of calcination tmperature of the kaolin and molar Na_2O/SiO_2 activator ratio on physical and microstructural properties of metalkaolinbased geopolymers. *Iranian Journal of Materials Science & Engineering,* 9**,** 43-51.

SOMNA, K., JATURAPITAKKUL, C., KAJITVICHYANUKUL, P. & CHINDAPRASIRT, P. 2011. NaOH-activated ground fly ash geopolymer cured at ambient temperature. *Fuel,* 90**,** 2118-2124.

SUKMAK, P., HORPIBULSUK, S. & SHEN, S. L. 2013. Strength development in clay-fly ash geopolymer. *Construction and Building Materials,* 40**,** 566-574.

SUMMERSCALES, J., DISSANAYAKE, N. P., VIRK, A. S. & HALL, W. 2010. A review of bast fibres and their composites. Part 1–Fibres as reinforcements. *Composites Part A: Applied Science and Manufacturing,* 41**,** 1329-1335.

SUPIT, S. W. M. & SHAIKH, F. U. A. 2014. Durability properties of high volume fly ash concrete containing nano-silica. *Materials and Structures,* 48**,** 2431-2445.

TAIB, R. M. 1998. *Cellulose Fiber-Reinforced Thermoplastic Composites: Processing and Product Characteristics.* Doctoral Dissertation, Virginia Polytechnic Institute and State University.

TANOBE, V. O., SYDENSTRICKER, T. H., MUNARO, M. & AMICO, S. C. 2005. A comprehensive characterization of chemically treated Brazilian sponge-gourds (Luffa cylindrica). *Polymer Testing,* 24**,** 474-482.

TCHAKOUTE KOUAMO, H., MBEY, J. A., ELIMBI, A., KENNE DIFFO, B. B. & NJOPWOUO, D. 2013. Synthesis of volcanic ash-based geopolymer mortars by fusion method: Effects of adding metakaolin to fused volcanic ash. *Ceramics International,* 39**,** 1613-1621.

THYGESEN, A., ODDERSHEDE, J., LILHOLT, H., THOMSEN, A. B. & STÅHL, K. 2005. On the determination of crystallinity and cellulose content in plant fibres. *Cellulose,* 12**,** 563.

UL HAQ, E., KUNJALUKKAL PADMANABHAN, S. & LICCIULLI, A. 2014. Synthesis and characteristics of fly ash and bottom ash based geopolymers–A comparative study. *Ceramics International,* 40**,** 2965-2971.

VAN HAZENDONK, J. M., REINERIK, E. J., DE WAARD, P. & VAN DAM, J. E. 1996. Structural analysis of acetylated hemicellulose polysaccharides from fibre flax (Linum usitatissimum L.). *Carbohydrate Research,* 291**,** 141-154.

VAN JAARSVELD, J. & VAN DEVENTER, J. 1999. Effect of the alkali metal activator on the properties of fly ash-based geopolymers. *Industrial & Engineering Chemistry Research,* 38**,** 3932-3941.

VAN JAARSVELD, J., VAN DEVENTER, J. & LORENZEN, L. 1998. Factors affecting the immobilization of metals in geopolymerized flyash. *Metallurgical and Materials Transactions B,* 29**,** 283-291.

VAN JAARSVELD, J., VAN DEVENTER, J. & LUKEY, G. 2002. The effect of composition and temperature on the properties of fly ash-and kaolinite-based geopolymers. *Chemical Engineering Journal,* 89**,** 63-73.

VELPARI, V., RAMACHANDRAN, B. E., BHASKARAN, T. A., PAI, B. C. & BALASUBRAMANIAN, N. 1980. Alkali resistance of fibres in cement. *Journal of Materials Science,* 15**,** 1579-1584.

VINCENT, J. 1990. *Structural Biomaterials*, Princeton University Press.

WALKER, R., PAVIA, S. & MITCHELL, R. 2014. Mechanical properties and durability of hemp-lime concretes. *Construction and Building Materials,* 61**,** 340-348.

WAMBUA, P., IVENS, J. & VERPOEST, I. 2003. Natural fibres: Can they replace glass in fibre reinforced plastics? *Composites Science and Technology,* 63**,** 1259-1264.

WEI, J. & MEYER, C. 2014. Sisal fiber-reinforced cement composite with Portland cement substitution by a combination of metakaolin and nanoclay. *Journal of Materials Science,* 49**,** 7604-7619.

WEI, J. & MEYER, C. 2015. Degradation mechanisms of natural fiber in the matrix of cement composites. *Cement and Concrete Research,* 73**,** 1-16.

WILLIAMS, G. I. & WOOL, R. P. 2000. Composites from natural fibers and soy oil resins. *Applied Composite Materials,* 7**,** 421-432.

WILLIAMS, R. P., HART, R. D. & VAN RIESSEN, A. 2011. Quantification of the extent of reaction of metakaolin-based geopolymers using X-ray diffraction, scanning electron microscopy, and energy-dispersive spectroscopy. *Journal of the American Ceramic Society,* 94**,** 2663-2670.

XU, H. & VAN DEVENTER, J. 2000. The geopolymerisation of alumino-silicate minerals. *International Journal of Mineral Processing,* 59**,** 247-266.

XU, H. & VAN DEVENTER, J. S. J. 2002. Geopolymerisation of multiple minerals. *Minerals Engineering,* 15**,** 1131-1139.

YADOLLAHI, M. M., BENLI, A. & DEMIRBOĞA, R. 2015. The effects of silica modulus and aging on compressive strength of pumice-based geopolymer composites. *Construction and Building Materials,* 94**,** 767-774.

YAN, L. & CHOUW, N. 2015. Effect of water, seawater and alkaline solution ageing on mechanical properties of flax fabric/epoxy composites used for civil engineering applications. *Construction and Building Materials,* 99**,** 118-127.

YAN, S. & SAGOE-CRENTSIL, K. 2012. Properties of wastepaper sludge in geopolymer mortars for masonry applications. *Journal of Environmental Management,* 112**,** 27-32.

YUNSHENG, Z., WEI, S. & ZONGJIN, L. 2006. Impact behavior and microstructural characteristics of PVA fiber reinforced fly ash-geopolymer boards prepared by extrusion technique. *Journal of Materials Science,* 41**,** 2787-2794.

YUNSHENG, Z., WEI, S. & ZONGJIN, L. 2010. Composition design and microstructural characterization of calcined kaolin-based geopolymer cement. *Applied Clay Science,* 47**,** 271-275.

YUNSHENG, Z., WEI, S., ZONGJIN, L., XIANGMING, Z., EDDIE & CHUNGKONG, C. 2008. Impact properties of geopolymer based extrudates

incorporated with fly ash and PVA short fiber. *Construction and Building Materials,* 22**,** 370-383.

YUSUF, M., MEGAT JOHARI, M., AHMAD, Z. & MASLEHUDDIN, M. 2015. Impacts of silica modulus on the early strength of alkaline activated ground slag/ultrafine palm oil fuel ash based concrete. *Materials and Structures,* 48**,** 733-741.

YUSUF, M. O., MEGAT JOHARI, M. A., AHMAD, Z. A. & MASLEHUDDIN, M. 2014. Influence of curing methods and concentration of NaOH on strength of the synthesized alkaline activated ground slag-ultrafine palm oil fuel ash mortar/concrete. *Construction and Building Materials,* 66**,** 541-548.

ZADORECKI, P. & MICHELL, A. 1989. Future-prospect for wood cellulose as reinforcment in otganic polymer composites. *Polymer Composites,* 10**,** 69-77.

ZAHARAKI, D., KOMNITSAS, K. & PERDIKATSIS, V. 2010. Use of analytical techniques for identification of inorganic polymer gel composition. *Journal of Materials Science,* 45**,** 2715-2724.

ZENG, Q., YU, A., LU, G. & PAUL, D. 2005. Clay-based polymer nanocomposites: research and commercial development. *Journal of Nanoscience and Nanotechnology,* 5**,** 1574-1592.

ZHANG, Y. J., WANG, Y. C., XU, D. L. & LI, S. 2010. Mechanical performance and hydration mechanism of geopolymer composite reinforced by resin. *Materials Science and Engineering A,* 527**,** 6574-6580.

ZHANG, Z., PROVIS, J. L., REID, A. & WANG, H. 2014. Geopolymer foam concrete: an emerging material for sustainable construction. *Construction and Building Materials,* 56**,** 113-127.

ZHANG, Z. H., YAO, X., ZHU, H. J., HUA, S. D. & CHEN, Y. 2009. Preparation and mechanical properties of polypropylene fiber reinforced calcined kaolin-fly ash based geopolymer. *Journal of Central South University of Technology,* 16**,** 49-52.

ZHAO, F. Q., ZHAO, J. & LIU, H. J. 2009. Autoclaved brick from low-silicon tailings. *Construction and Building Materials,* 23**,** 538-541.

ZHAO, Q., NAIR, B., RAHIMIAN, T. & BALAGURU, P. 2007. Novel geopolymer based composites with enhanced ductility. *Journal of Materials Science,* 42**,** 3131-3137.

ZHU, J., ZHU, H., NJUGUNA, J. & ABHYANKAR, H. 2013. Recent development of flax fibres and their reinforced composites based on different polymeric matrices. *Materials,* 6**,** 5171-5198.

ZIVICA, V., PALOU, M. T. & BÁGEĽ, T. I. Ľ. 2014. High strength metahalloysite based geopolymer. *Composites Part B: Engineering,* 57**,** 155-165.

ZUHUA, Z., XIAO, Y., HUAJUN, Z. & YUE, C. 2009. Role of water in the synthesis of calcined kaolin-based geopolymer. *Applied Clay Science,* 43**,** 218-223.

"Every reasonable effort has been made to acknowledge the owners of copyright material. I would be pleased to hear from any copyright owner who has been omitted or incorrectly acknowledged"

Hasan Assaedi

14-April-2017